Combining Energy, Indoor Air Quality and Moisture Models for Assessing the Whole Building Performance

by

Seyedmohammadreza HEIBATI

MANUSCRIPT-BASED THESIS PRESENTED TO ÉCOLE DE TECHNOLOGIE SUPÉRIEURE IN PARTIAL FULFILLMENT FOR THE DEGREE OF DOCTOR OF PHILOSOPHY
PH. D.

MONTREAL, 11 OCTOBER 2022

ÉCOLE DE TECHNOLOGIE SUPÉRIEURE
UNIVERSITÉ DU QUÉBEC

BOARD OF EXAMINERS

THIS THESIS HAS BEEN EVALUATED

BY THE FOLLOWING BOARD OF EXAMINERS

Mr. Wahid Maref, Thesis Supervisor
Construction Engineering Department, École de technologie supérieure

Mr. Hamed H. Saber, Thesis Co-supervisor
Mechanical Engineering Department, Jubail University College

Mr. Hakim A. Bouzid, President of the Board of Examiners
Mechanical Engineering Department, École de technologie supérieure

Mrs. Danielle Monfet, Member of the jury
Construction Engineering Department, École de technologie supérieure

Mr. Fitsum Tariku, External Evaluator
Director of the Building Science Centre of Excellence, British Columbia Institute of Technology and Canada Research Chair in Whole-Building Performance, Natural Sciences and Engineering Research Council

THIS THESIS WAS PRESENTED AND DEFENDED

IN THE PRESENCE OF A BOARD OF EXAMINERS AND PUBLIC

2 AUGUST 2022

AT ÉCOLE DE TECHNOLOGIE SUPÉRIEURE

ACKNOWLEDGMENT

I would like to thank first my supervisor, Professor Wahid Maref, and my co-supervisor, Professor Hamed H. Saber, who have responsibly assisted and guided me throughout my Ph.D. and related contributions. Professor Wahid Maref, a passionate researcher in the field of Building Science and in academia that gave the full support on me. He has also played a very important role in improving my scientific and academic path and will continue to do so in the future. In my academic experience with Professor Wahid Maref as well as Professor Hamed H. Saber, I gained a very good experience in research, and I will proudly continue to work with them after graduation as a research team in developing the frontiers of knowledge.

I would also like to thank my wife Caren who has compassionately and patiently helped me through all the stages of my research and doctoral career opportunities.

The road was never easy, but we conquer every trial to give our son Carez Amouri the brightest future. This keeps me motivated to finish this doctoral journey.

I also acknowledge the partial financial contribution of my thesis from the Natural Sciences and Engineering Research Council of Canada (NSERC).

To God be all the Glory

COMBINAISON ÉNERGIE-QUALITÉ DE L'AIR INTÉRIEUR ET MODÉLISATION DE L'HUMIDITÉ POUR L'ENSEMBLE DES PERFORMANCES DU BÂTIMENT

Seyedmohammadreza HEIBATI

RÉSUMÉ

Dans la plupart des études, l'efficacité énergétique, la qualité de l'air intérieur et les mesures de performance en matière d'humidité sont considérées séparément comme un critère de performance du bâtiment. La comparaison des résultats des mesures de l'efficacité énergétique, de la qualité de l'air intérieur et de l'humidité simulées par des outils à modèle unique peut avoir des interactions positives et négatives les unes avec les autres. Pour fournir une solution réaliste et complète qui calcule l'impact des critères d'efficacité énergétique, de qualité de l'air intérieur et d'humidité sur l'ensemble des performances du bâtiment, il est nécessaire d'utiliser un modèle couplé. Par conséquent, dans cette recherche, un nouveau modèle a été développé qui combine les trois modèles simples, par ex. des modèles d'énergie, de qualité de l'air intérieur et d'humidité. L'avantage de ce modèle couplé est qu'en plus de prédire les performances du bâtiment dans les trois domaines de l'énergie, de la qualité de l'air intérieur et de l'humidité, il pourra également considérer l'impact des interactions positives et négatives de ces trois critères sur les résultats de sortie. Par conséquent, dans le modèle couplé, les résultats simulés montrent les performances réelles du bâtiment. L'exactitude du modèle couplé est vérifiée à l'aide de la méthode du test t pour échantillons appariés. Le développement du modèle couplé a été réalisé en trois phases. Dans la première phase, la faisabilité de couplage d'EnergyPlus avec CONTAM a été analysée. Dans la deuxième phase, la faisabilité de couplage de CONTAM avec WUFI a été évaluée, et dans la troisième phase, la faisabilité d'EnergyPlus, CONTAM et WUFI a été conclue. Pour analyser les différences des résultats simulés par les méthodes du modèle couplé et unique, quatre scénarios sont définis pour une étude de cas de maison à trois étages. Ces scénarios incluent : 1- ventilateur hermétique éteint , 2- ventilateur hermétique activé, 3- ventilateur qui fuit éteint et 4- ventilateur qui fuit activé. Pour sélectionner les scénarios optimaux, la norme ASHRAE 90.1 pour l'efficacité énergétique, la norme ASHRAE 62.1 pour la qualité de l'air intérieur, les normes ASHRAE 160 et ASHRAE 55 pour les critères de performance d'humidité et de confort thermique ont été utilisées. Ensuite, les résultats obtenus par les modèles couplés et uniques pour les quatre scénarios sont présentés par les différences de pourcentage avec le niveau acceptable des normes ASHRAE 90.1, 62.1, 160 et 55. La comparaison des résultats simulés pour le modèle couplé avec les modèles uniques a été effectuée pour différents climats de Montréal, Vancouver et Miami. Les résultats de cette recherche montrent que les mesures simulées par le modèle couplé sont différentes des modèles simples. La raison de cette différence est que dans les modèles simples, les débits d'air, les températures et les débits de chauffage/refroidissement sont définis comme des données d'entrée par l'utilisateur, mais dans le modèle couplé, les variables de contrôle des débits d'air, des températures et des débits de chauffage/refroidissement sont échangées de manière cyclique en boucle entre les trois sous-modèles EnergyPlus, CONTAM et WUFI. Étant donné que la précision du modèle couplé a

été validée sur la base de la méthode du test t pour échantillons appariés, il peut être utilisé comme outil de référence pour l'ensemble de l'analyse des performances du bâtiment.

Mots-clés : modèle combiné, Efficacité énergétique, Qualité de l'air intérieur, Performance hygrique

COMBINING ENERGY, INDOOR AIR QUALITY AND MOISTURE MODELS FOR ASSESSING THE WHOLE BUILDING PERFORMANCE

Seyedmohammadreza HEIBATI

ABSTRACT

In most studies, energy efficiency, indoor air quality and moisture performance measures are considered separately as a criterion of the building performance. Comparing the results of the energy efficiency, indoor air quality and moisture performance measures simulated by single model tools can have positive and negative interactions with each other. To provide realistic and comprehensive solution that calculates the impact of energy efficiency, indoor air quality and moisture performance criteria on the whole building performance, it is necessary to use a combined model. Therefore, in this research, a new model has been developed that combines all three e.g. energy, indoor air quality and moisture models. The advantage of this combined model is that in addition to predicting the performances of the building in the three areas of energy, indoor air quality and moisture, it will also be able to consider the impact of positive and negative interactions of these three criteria on the output results. Therefore, in combined model the simulated results show the actual performance of the building. The accuracy of combined model is verified using the paired sample t-test method. The development of the combined model has been performed in three phases. In the first phase, the feasibility of coupling EnergyPlus with CONTAM has been analyzed. In the second phase, the feasibility of coupling CONTAM with WUFI has been evaluated, and in the third phase, the feasibility of combining EnergyPlus, CONTAM and WUFI has been concluded. To analyze the differences of the simulated results by the combined and single models methods, four scenarios are defined for a case study of the three-story house. These scenarios include: 1- airtight fan-off, 2- airtight fan-on, 3- leaky fan-off and 4- leaky fan-on. To select the optimal scenarios, the ASHRAE Standard 90.1 for energy efficiency, ASHRAE Standard 62.1 for indoor air quality, ASHRAE Standard 160 and 55 for moisture performance and thermal comfort criteria have been used. Then, the results simulated by combined and single models for four scenarios are presented in the percentage differences with an acceptable level of ASHRAE Standards 90.1, 62.1, 160 and 55. The comparison of the results for the combined model with the single models have been performed for different climates of Montreal, Vancouver, and Miami. The results of this research show that the simulated measures by the combined model are different from the single models. The reason for this difference is that in single models, airflows, temperatures, and heating/cooling flow are defined as input data by the user but in the combined model, the control variables of airflows, temperatures and heating/cooling flows are exchanged in a cyclic loop between all three sub-models of EnergyPlus, CONTAM and WUFI. Since the accuracy of the combined model has been validated based on the paired sample t-test method, this new model can be used as a benchmark tool for the whole building performance analysis.

Keywords: Combined Model, Energy Efficiency, Indoor Air Quality, Moisture performance

TABLE OF CONTENTS

Page

LIST OF TABLES

LIST OF FIGURES

Page

INTRODUCTION

A high-performance building is a building that, in addition to providing optimal energy consumption while providing a safe place, is defined as having acceptable thermal comfort, adequate moisture and high-quality air without contaminants. There have been many studies and research on the performance of buildings, in most of which the energy efficiency of the building has been considered as a measure of performance. Increasing energy efficiency is one of the most important building performance measures that can play an important role in reducing fossil fuels consumptions, air pollution and greenhouse gases. Alternative energy sources such as solar energy can be another way to increase energy-related performance in buildings. Various methods of using energy efficiency have been performed to evaluate the performance of the building.

Wang et al. (2019) analyzed the impact of building energy efficiency standards (BEES) on reducing energy consumption and increasing the building performance in China. The life cycle cost analysis method has been performed as the optimal selection of windows in Turkey (Yaşar & Kalfa, 2012). According to the report on the global sustainable development goals (SDGs) by 2030, energy performance should be improved enough to significantly reduce greenhouse gas emissions (The Sustainable Development Goals Report (SDGs) 2016). Therefore, it is necessary to increase energy performance in the building sector, which accounts for 35% of the world's final energy consumption (Policy, 2013).

One of the important goals of the Paris Agreement is to reduce greenhouse gas emissions by 2050 in all energy sectors of the world, especially in the construction sector. The international energy agency (IEA) (IEA, 2021), with the help of the world energy model (WEM), predicts that the efficient world scenario (EWS) will reduce energy demand in buildings by 2040 and this improvement, which is the result of energy efficiency measures, should reach 40 ٪ compared to current levels and also predicts a total growth of global building area of 60%, compared to the world population growth of 20% (IEA, 2021; Motherway, 2017; Schiffer, Kober, & Panos, 2018; Zhongming, Wangqiang, & Wei, 2018). These measures to increase

building energy efficiency can include the use of high-efficiency heat pumps instead of the old cooling and heating systems, improving building insulation, increasing building envelope efficiency, increasing high-efficiency equipment, and use of renewable energy sources (IEA, 2021; Motherway, 2017; Schiffer, Kober, & Panos, 2018; Zhongming, Wangqiang, & Wei, 2018).

There are scenarios for increasing energy performance and increasing service-efficiency thermal end-use technologies in buildings that could prevent global warming to reach 1.5 ° C by 2050 (Grubler et al., 2018). Another scenario called the techno-economic potential for energy projects in Chinese buildings has been proposed, in which existing buildings should be 70% more energy efficient by 2050 than at present (Zhou, Khanna, Feng, Ke, & Levine, 2018). The demand for energy in the residential building sector in Los Angeles is changing dramatically to improve energy consumption and the use of efficient technologies (Reyna & Chester, 2017).

A modular-based Green Design Studio (GDS) platform has been developed for a green building design for the whole building performance simulation by providing an easy-to-use and intuitive user interface to assist users without extensive knowledge of building physics (Shen, Krietemeyer, Bartosh, Gao, & Zhang, 2021). In another research, a sustainable and low-emission urban built environment model has been developed for buildings that provide more accurate and realistic microclimate estimation for large-scale building energy dynamic simulation (Ma, Wang, Wang, & Chen, 2021). A tri-objective method has been performed to optimize a solar energy system used in the heating and cooling of a heat pump, an absorption chiller for a two-story building by Bahramian et al. (2021). A method has been developed by e Silva & Calili (2021) based on using parametric simulation models, and the use of genetic algorithms, to measure the impact of window-integrated organic photovoltaic cells on energy demand, with more precise and time-saving process results compared to the regular methods. The artificial neural networks (ANNs) metamodels is another method that has been used in recent years to calculate building performance simulation (BPS) in the field of energy and environment, in which the computational accuracy has increased (Roman, Bre, Fachinotti, &

Lamberts, 2020). New methods have been developed in recent years to improve indoor air quality (IAQ) on an urban or national scale housing stock, which allows reliable prediction of residential indoor pollution concentrations and exposures at various spatial-temporal scales (Abdalla & Chengzhi, 2021). To improve the accuracy of the predictions, the dynamic interaction between heat transfer, intra-regional airflow and internal pollutant transfer has been performed through IAQ-Energy simulation (Abdalla & Chengzhi, 2021). Tagliabue, Cecconi, Rinaldi, & Ciribini (2021) in a study for school educational building eLUX lab, located in the smart campus of the University of Brescia, were able to increase the performance of the building by improving indoor air quality by an integration method using internet-based sensors for heating, ventilation and air conditioning systems (HVAC) as well as opening/closing patterns for windows. Ma, Aviv, Guo, & Braham (2021) have developed a model based on artificial neural networks (ANNs) and reinforcement learning (RL) to calculate building performance in the field of indoor air quality (IAQ) related to health and comfort. This model, as a nonlinear system, dynamically predicts indoor air pollutant control strategies by creating thermal comfort (Ma et al., 2021). To reduce the spread of SARS-CoV-2, the indoor air quality model was developed by Megahed & Ghoneim (2021) based on the integration of engineering controls, design strategies and air disinfection techniques to achieve higher performance in the field of indoor air quality. In a study, a method based on "parametric design modeling – computational simulation – multi-objective optimization – multicriteria decision-making" was developed, which is used to calculate the maximum experiential indoor environmental quality (e-IEQ) over the breathing zone as building performance (Sarkar & Bardhan, 2020).

Building performance is studied in some research based on building envelope design improvements based on controlling the effect of moisture on reducing mold growth risk. Recent studies have developed a variety of simulation tools in building envelope moisture behavior analysis (Chung, Wen, & Lo, 2020). In a study, a tool called HAM-Tools was developed using MATLAB and Simulink computing environments that can analyze the penetration of rain as well as heat and moisture sources in the air layers (Chung et al., 2020). This developed model can simulate the moisture content in the building envelope for a set of common ventilated cladding scenarios over 10 years (Chung et al., 2020). Numerous studies

have been conducted to develop moisture performance models using numerical methods for evaluation of buildings hygrothermal behavior (Cornick, Maref, Abdulghani, & van Reenen, 2003; Cornick, Maref, & Tariku, 2009; Fayad, Maref, & Awad, 2021; Lacasse et al., 2016; Maref, Booth, Lacasse, & Nicholls, 2002; Maref, Cornick, Abdulghani, & van Reenen, 2004; Maref, Lacasse, Kumaran, & Swinton, 2002; Maref, Lacasse, & Booth, 2002; Maref, Lacasse, & Krouglicof, 2001; Maref, Tariku, Di Lenardo, & Gatland, 2009; Saber, 2022; Saber, Hajiah, & Maref, 2020; Saber & Maref, 2015; Saber & Maref, 2019; Saber, Maref, Elmahdy, Swinton, & Glazer, 2012; Saber, Maref, Swinton, & St-Onge, 2011; Saber, Swinton, Kalinger, & Paroli, 2012; Tariku, Maref, Di Lenardo, & Gatland, 2009; Maref, Lacasse, & Rousseau, 2006; Maref & Lacasse, 2010; Maref et al., 2011; Maref et al., 2012). Saber, Maref, & E. Hajiah (2019) calculated moisture performance by using a numerical simulation method for a roofing system in low-rise buildings in Saudi Arabia. They provided indoor conditions according to the ASHRAE Standard 160, and the results of this moisture performance modeling showed that the black and cool roofs did not accumulate moisture from year-to-year after 6 and 7 years, respectively. Also, the highest relative humidity occurs in the black and cool roofs on less than 80% with no risk of condensation and mold grow. In another study, Saber (2022) calculated the moisture performance for black and cool roofs in the two climatic conditions of the Saudi Eastern Province and Kuwait City using a numerical simulation method. The results of numerical simulation showed that installing cool roofs decrease cooling energy loads much greater than heating energy loads compare to the black roofs. So, replacing black roofs with cool roofs in both Saudi Eastern Province and Kuwait City leads to net energy savings. Maref, Lacasse, & Booth (2004) developed an advanced hygrothermal computer model (hygIRC) that can be used to evaluate the hygrothermal response of various components in a wood-frame wall in a nominally steady-state environment. Therefore, this model can be used in the laboratory to analyze hygrothermal properties of materials in small-scale specimens. They compared the results simulated by the hygIRC model with the experimental results to verify the accuracy of the developed model. A stochastic hygrothermal simulation method to evaluate the mold growth risk of a brick veneer-clad wood-frame wall with a drainage cavity under historical and future climatic conditions in Ottawa has been performed by Wang, Defo, Xiao, Ge, & Lacasse (2021). They conclude that under the climatic conditions of Ottawa, limiting

the amount of wind-driven rain can be more effective than improving ventilation for the building envelope to reduce mold growth risk (Wang et al., 2021).

According to recent research, the areas involved in building performance can be categorized into three groups 1-energy efficiency analysis using energy models, 2- indoor air contaminant analysis using indoor air quality models, and 3- building envelope and thermal comfort analysis behavior using moisture performance models. The tools and methods used in the most research related to building performance calculation are presented as single model tools. Each of the measures of energy efficiency, indoor air quality and moisture performance have presented their respective tools separately in this research. The single models' tools of energy efficiency are used for building energy performance, single models' tools of indoor air quality are used for building indoor air quality performance and single models' tools of moisture are used for building moisture performance calculations. Therefore, the values of the simulated results of single model methods cannot be considered as a whole building performance (Heibati, Maref, & Saber, 2021a; Heibati, Maref, & Saber, 2021b). The whole building performance modeling will be real when all three indicators of energy efficiency, indoor air quality and moisture performance are calculated simultaneously as integrated method (Heibati et al., 2021a; Heibati et al., 2021b).

Single model tools do not consider the effects of other measures involved in building performance, so, the simulated results are not real. The reason that all three measures of energy efficiency, indoor air quality and moisture should be considered in the integrated method is related to their positive or negative interactions. Recent research shows the effects of energy efficiency strategies on indoor air quality.

Zender–Swiercz (2021) in his study concluded the negative impact of the reduced outdoor air ventilation rates strategy on increased concentrations of contaminants with indoor sources. He analyzed the unit installed in a façade building, where air supply and exhaust cycles are swapped by proper positioning of dampers. His analysis was performed in the real conditions in an office building and by computational fluid dynamics (CFD) simulation method. He was

able to determine the relationship between the amount of airflow distribution required in a room to supply the required indoor air temperature in the range of 22°C -19.5 °C with CO_2 concentration of less than 1000 ppm. He also concluded that the greatest reduction in CO_2 concentration occurs when the supply/exhaust time is equal to 10 min.

Another study of the negative effect of energy-saving strategies in replacing natural ventilation with the mechanical air conditioning on reducing thermal comfort during the summer by Ahmed, Kumar, & Mottet (2021). In this study, both natural single-sided ventilation and cross ventilation were not able to meet the internal thermal comfort standards. Their only solution to increase thermal comfort in the summer is combining solar chimneys or windcatchers with water evaporation cooling. The use of unfiltered natural ventilation for highly polluted areas can also increase the indoor deposition of harmful particulate matter.

Stamp et al. (2021) analyzed the negative effects of energy saving on increasing high concentrations of NO_2 in a study of five low-energy apartments in London.

SeppĘnen (2008) analyzed the strategies for improving indoor air quality while reducing energy consumption for buildings. He concluded that by observing the aspects of target values and indoor air quality proper design can reduce the negative effects of indoor air quality on energy efficiency in the building. These proper designs include indoor air and climate quality, source control, effective removal of pollutants, proper location of fresh air inlets, cleaning of inlet air, and efficient distribution.

Du, Li, & Yu (2021) have investigated the negative effects of energy efficiency on moisture performance in buildings. Spores such as Cladosporium, Aspergillus and Penicillium are released into the room air, which is facilitated by the increase of room temperature and high humidity, which causes allergies in residents. Energy efficiency strategies such as increasing insulation thickness, improving airtightness and thermal environment can increase mold growth risks, due to lack of sufficient ventilation and accumulation of indoor moisture in the building.

Nowadays, energy policies are geared toward designs that rely on airtight and highly insulated envelopes. However, the high-performance buildings in the field of energy have insufficient indoor air change rates, affecting the indoor air quality and resulting in higher latent loads. Therefore, increasing the internal humidity in buildings that use bio-based materials can lead to mold growth and facilitate indoor organic proliferation, which results in the relationship between the negative effects of energy optimization policies on moisture performance (Brambilla & Sangiorgio, 2020). Damage caused by mold in buildings with high insulation and airtight is 45% in Europe, 40% in the USA, 30% in Canada and 50% in Australia (Brambilla & Sangiorgio, 2020).

Another study showing the negative impact of energy efficiency strategies on moisture performance was conducted by Fedorik, Malaska, Hannila, & Haapala (2015). They concluded that using additional insulation in boreal and arctic climates to improve heat capacity would increase mold growth risk. Increased insulation in concrete-sandwich walls due to elevated temperatures and entrapped humidity can lead to the initiation of mold growth. They also concluded that excess insulation not only negatively affects the structure and material properties of structural elements, but also affects the health of the environment and the comfort of the occupants.

Winkler, Munk, & Woods (2018) analyzed the negative effects of strategies implemented in cooling systems in high-efficiency buildings on the reduction of thermal comfort and indoor air quality. They concluded that in high-efficiency buildings in humid climates, cooling loads operate at a higher fraction of latent loads than in conventional buildings, which increases indoor humidity in high-efficiency buildings. In addition, by reducing the cooling set point, indoor humidity can be reduced, but overcooling leads to a decrease in thermal comfort and indoor air quality.

Some research has shown positive interactions between all three measures of energy efficiency, indoor air quality and moisture performance.

Pekdogan, Tokuç, Ezan, & Başaran (2021) evaluated the positive effect of energy efficiency strategies on indoor air quality. They concluded that the use of natural ventilation was limited due to reduced intrusion loads, increased air pollution, and climatic conditions. Therefore, they used a wall-integrated decentralized ventilation system with heat recovery in the laboratory. The heat recovery system in this study consists of a ceramic block for storing thermal energy. They simulated winter and summer conditions in two rooms with temperature control. They tested the ventilation durations for times of 1, 2, 5, 7.5 and 10 min and finally concluded that 2 minutes of ventilation time was required in the laboratory to provide a comfortable indoor temperature with maximum energy saving for both rooms.

Cho et al. (2021) evaluated a hybrid ventilation system in mechanical and natural conditions by monitoring the temperature, humidity, CO_2 levels, and energy consumption of a multifamily building to generate good indoor air quality with low energy consumption. They concluded that the hybrid ventilation system creates a good level of indoor air quality while maintaining good conditions of energy efficiency.

Woloszyn, Kalamees, Abadie, Steeman, & Kalagasidis (2009) noted the positive relationship between energy efficiency strategy and indoor air quality. They examined the effect of combining a relative-humidity-sensitive (RHS) ventilation system with indoor moisture buffering materials and concluded that in the relative-humidity-sensitive (RHS) ventilation system, the spread between the minimum and maximum values of the relative humidity (RH) in the indoor air reduces and leads to energy savings. In fact, with this combination, the relative humidity (RH) level is maintained in a situation where the risk of condensation is reduced. Therefore, the use of moisture-buffering materials not only reduces the daily moisture variation and keeps the indoor RH at a very stable level but also reduces energy consumption.

The positive effect of moisture performance on indoor air quality has been investigated in a study by Wolkoff (2018). He showed that reducing indoor air humidity could lead to sensory irritation symptoms in the eyes, reduced sleep quality, reduced virus survival and noise

disturbances. He concluded that reducing indoor air humidity is a factor in reducing indoor air quality and increasing indoor air humidity is a positive factor in indoor air quality in the office environment.

The review of the recent studies' results, which are presented, shows that energy efficiency, indoor air quality and moisture performance are considered as the measures in predicting the performance results of the building. But these studies should be highlighted as the main aim of doctoral thesis research for combining energy efficiency, indoor air quality and moisture performance tools for real whole building performance analysis.

The real building performance analysis occurs when the positive or negative interactions of energy efficiency, indoor air quality and moisture performance are considered by a combined method as the main goal of the Ph.D. research plan.

0.1 Research objectives

Recent research studies show that the results of simulations performed by single models in predicting building performance due to not considering the positive and negative interaction of each of the measures of energy, indoor air quality and moisture with each other are not accurate. To solve this problem, a model should be designed that can consider the positive and negative interactions of the three measures of energy efficiency, indoor air quality and moisture performance and calculate the actual performance of the building based on all these indicators. Therefore, the main objective of this research is to develop a new model for calculating whole building performance in which all three measures of energy efficiency, indoor air quality and moisture are predicted simultaneously.

In this new model, the final simulation results are predicted based on the combination of energy efficiency, indoor air quality and moisture performance measures. Therefore, these results are simulated by considering the positive and negative effects on whole building performance measures. The practical objective of this research is that with the help of this combined model,

passive and active systems can be analyzed based on energy efficiency, indoor air quality and moisture performance criteria with the highest accuracy for each type of residential, commercial, office, and hospital buildings. This developed model can be used by engineers, architects and building designer researchers, as a reliable tool with high capability and accuracy in designing a high-performance building. The application of this combined model is designed for all international climate zones defined according to ASHRAE Standard 90.1. These zones include very hot, hot, warm, mixed, cool, cold, very cold and subarctic in dry, marine and humid conditions. This combined model can lead to the development of thermal control systems, ventilation, humidifiers, and dehumidifiers for buildings needed for the highest performances of energy, indoor air quality and moisture.

The most widely used single models in recent research to design a high-performance building in the fields of energy-efficient, indoor air quality and moisture include EnergyPlus, CONTAM and WUFI, respectively (Ansari & Patil, 2021; Banfill, 2021; Borkowska, 2021; Chen, Zheng, Yang, & Yoon, 2021; D'Amico et al., 2021; Ding & Zhou, 2020; Fu et al., 2021; Gan, Wang, Chan, Weerasuriya, & Cheng, 2022; Gholami, Barbaresi, Tassinari, Bovo, & Torreggiani, 2020; Jiang, Hao, & De Carli, 2021; Libralato et al., 2021; Lim, Seo, Song, Yoon, & Kim, 2020; McPherson-Hathaway, 2021; Ratnasari, MT, & MT, 2020; Shen et al., 2021; Shrestha, DeGraw, Zhang, & Liu, 2021; Shrestha & DeGraw, 2021; Tian, Fine, & Touchie, 2020; Junxue Zhang, 2020).

Therefore, in single models, due to the lack of connections between the equations of energy balance, contaminant balance and moisture balance, their simulation results are not accurate enough (Heibati et al., 2021a; Heibati et al., 2021b).

The innovation of this developed model is that with the help of co-simulation and coupling methods, three models of EnergyPlus in the field of energy, CONTAM in the field of indoor air quality and WUFI in the field of moisture were combined for high-performance building applications. The accuracy of this combined model in comparison with other single models has been investigated and evaluated in this research.

The application of this combined model to a three-story house in the three cities of Montreal, Vancouver and Miami has been analyzed. The combined model applications can lead to the development of technologies for heat, ventilation and moisture control systems and can be proven by the capabilities of the combined model in comparison with the existing single models. In this combined model, it is possible to predict the indoor air temperature, indoor airflow and indoor relative humidity in the acceptable level of ASHRAE Standard criteria for building HAVC system control. The criteria in this modeling are ASHRAE Standards 90.1, 62.1, 160 for energy saving, indoor air quality, moisture performance, and thermal comfort, respectively. The combined model can predict the parameters of energy and ventilation based on ASHRAE Standards along with the appropriate relative humidity for advanced control systems. It can be concluded that the application of this combined model in the construction sector and design of high-performance buildings is necessary for the industries such as consulting companies, contracting companies and even factories manufacturing construction equipment. This tool can design the building based on ASHRAE Standard range and led to the development of technologies related to control systems, mechanical and passive and active construction equipment. Other applied research that is involved in the development of building technologies is the 1-development of active and passive technologies for high performance building condition , 2- development of mechanical technologies ventilation systems in buildings based on combined energy efficiency, reduction of indoor air particles, indoor CO_2, indoor VOCs, other indoor contaminants and control relative humidity based on the ASHRAE Standards 3- development of technologies for ventilation systems and air conditioning systems along with filter upgrading to remove airborne particles and infectious micro-droplets released as a result of a cough, sneezing and breathing of patients having respiratory diseases, especially carriers of coronavirus. A reduction of survival time by controlling temperature and relative humidity in the range of deactivating the virus in hospital settings.

0.2 Overview of the Ph.D. Thesis

Recent research has shown that most building performance calculations have been performed in the field of energy efficiency by EnergyPlus, indoor air quality by COANTAM and moisture performance by WUFI. This research shows how important to predict accurately the building performance of a whole building, using solving simultaneously governing equations of energy efficiency, indoor air quality and moisture performance. This can only be established if there is a combined approach to solving the governing equations tools in all three areas of energy, indoor air quality and moisture performance. The innovation of this research was the combination of all three tools EnergyPlus, CONTAM and WUFI using the co-simulation method. To develop this model, temperature, airflow, heating, and cooling flows control variables as the key variables based on the co-simulation method between all three sub-models of EnergyPlus, CONTAM and WUFI are combined.

The novelty of this method is that possibility of exchange control variables of temperatures, airflows, heating, and cooling flows between all three tools of EnergyPlus, CONTAM and WUFI in a combined way, and the possibility of alternating control variables to meet ASHRAE Standard's criteria. The exchange of control variables has been performed in a cyclic loop between EnergyPlus, CONTAM and WUFI, so for sub-models, input data are used as the simulated output data of the previous sub-models, and if the loop is completed, then the combined model has been created. Therefore, each of the sub-models of EnergyPlus, CONTAM and WUFI will be able to use simulated control variables as the input data.

In mathematical point of view, control variables are exchanged between all three equations of energy flow balance, contaminant flow balance and moisture flow balance as the governing equations of EnergyPlus, CONTAM and WUFI and these equations are solved simultaneously.

The most important objectives of the co-simulation method in developing a combined model compared to single models include the following items:

- All simulated results are predicted in full detail by the combined model for the whole building performance.

- The energy simulated results by the combined model are different from the simulated results by EnergyPlus. The reason for this difference is that in the EnergyPlus, the amounts of infiltration and design air handling system airflow are defined as airflows input data by the users but in the combined model, the airflow variables are exchanged by the combination mechanism for EnergyPlus, CONTAM, and WUFI.

- The indoor air quality simulated results by the combined model, are different from the simulated results by CONTAM. The reason for this difference is that in the CONTAM, the amounts of effective leakage area and exhaust fan airflow, as airflows input data and amounts of the junction and default zone temperature as temperatures input data have been defined by the users. But the airflows and temperatures in the combined model method are exchanged by the combination mechanism for EnergyPlus, CONTAM, and WUFI.

- The moisture performance simulated results by the combined model, are different from the simulated results by WUFI. The reason for this difference can be described as in the WUFI model method, amounts of infiltration and mechanical ventilation as airflows input data, amounts of minimal and maximal zone temperature as temperatures input data and amounts of space heating and cooling capacity as heating/cooling flows input data are defined by the users. In the combined model method for the airflows, temperatures, and heating/cooling flows are exchanged by the combination mechanism for EnergyPlus, CONTAM, and WUFI.

The development of a combined model using the co-simulation method for all three sub-models of EnergyPlus, CONTAM and WUFI has been performed in three phases:

1- In the first phase, the feasibility of combining the two EnergyPlus and CONTAM models has been evaluated using the co-simulation method in the development of a new model, and finally, the results predicted by the coupled model have been compared and analyzed with the results simulated by every single model.

2- In the second phase, the feasibility of combining the two CONTAM and WUFI has been evaluated using the co-simulation method for the development of coupled new model. In addition, as in the previous phase, the results of simulated measures in indoor air quality and moisture performance between both single and coupled model is compared with each other, and the differences are analyzed.

3- In the third phase, the feasibility of combining all three EnergyPlus, CONTAM and WUFI has been evaluated using the co-simulation method for the development of a fully combined model. At this phase, both fully combined and single models are compared and analyzed based on the simulated results in the fields of energy, indoor air quality and moisture performance.

Each of the developed models in all three phases are verified using paired sample t-tests method. In the paired sample t-test method, three samples in energy, indoor air quality and moisture fields have been chosen. For these samples, the differences between the simulated and actual values are analyzed for one-year results. This method consists of two steps (1) paired samples difference and (2) paired samples correlation. In paired samples difference method, the differences between the actual and simulated data samples are tested and if this step is passed, the second step of the paired samples correlation is tested for more validation.

Ph.D. thesis contributions for all three phases of the combined model development have been published as three scientific papers in Energies-MDPI as ISI-WOS, Q1 scientific journal. Therefore, the papers extracted from the first, second and third phases of the development of the combined model are entitled:

1- Assessing the Energy and Indoor Air Quality Performance for a Three-Story Building Using an Integrated Model, Part One: The Need for Integration, https://doi.org/10.3390/en12244775

2- Assessing the Energy, Indoor Air Quality, and Moisture Performance for a Three-Story Building Using an Integrated Model, Part Two: Integrating the Indoor Air Quality, Moisture, and Thermal Comfort, https://doi.org/10.3390/en14164915

3- Assessing the Energy, Indoor Air Quality, and Moisture Performance for a Three-Story Building Using an Integrated Model, Part Three: Development of Integrated Model and Applications, https://doi.org/10.3390/en14185648

Since the main purpose of this research is to develop a combined model, so to assess the difference of the combined model compared to single models for all three phases of model development, four scenarios are defined. These scenarios include 1- airtight fan-off, 2- airtight fan-on, 3-leaky fan-off, and 4-leaky fan-on. For each of the four scenarios, the results simulated by the combined model are compared with the results simulated by the single models.

The simulated results are presented as the measures of energy, indoor air quality and moisture performance for combined and single models outputs. The hourly space heating/cooling energy consumptions have been assumed as energy measures, the daily indoor CO_2, $PM_{2.5}$ and volatile organic compounds (VOCs) concentrations, have been assumed as indoor air quality measures and the hourly indoor relative humidity (RH), predicted percentage of dissatisfied (PPD) and predicted mean vote (PMV) have been assumed as moisture performance measures, in this research. ASHRAE 90.1 as energy efficiency, ASHRAE 62.1 as indoor air quality, ASHRAE 160 and 55 as moisture performance and thermal comfort criteria, have been used for comparing simulated results by combine and single models. For this comparison purpose, the percentage difference method is used to compare the simulated results with the acceptable level of the ASHRAE Standards. The simulated results of energy, indoor air quality and moisture

performance obtained by combined and those obtained by single models in three different climatic zones of Montreal, Vancouver and Miami are compared.

CHAPITRE 1

CRITICAL REVIEW OF EXISTING LITERATURE

1.1 Overview of energy tools applications

Building performance simulation tools have been established around since the 1960s and 1970s, but their capabilities are based more on energy analysis (Clarke, 2007; Kusuda, 1999).

Morton, Pyo, & Choi (1992) used CADD (computer aided design and drafting) software packages as an interface to automate data transfer to BLAST (building load analysis and thermodynamic analysis program) for evaluating building energy performance analysis.

Liu, Wittchen, & Heiselberg (2014) used the BSim simulation tool to simulate the energy performance and indoor environment of a Danish building office room with an intelligent glazed facade under different control conditions. In addition, they compared simulated results of energy and comfort performance by BSim with the simplified method and concluded that the simplified method is a less time-consuming tool with acceptable accuracy compared to BSim method.

Feng, Wang, Li, Zhang, & Li (2022) used Designer's Simulation Toolkit (DeST) and Transient System Simulation Program with the help of the dynamic co-simulation method to optimize the solar collectors, collector inclination, tank volume, and electromagnetic energy heating unit power as key parameters of solar heating systems (SHSs) in detached buildings of rural areas. They facilitated low carbon designing by co-simulation method with Designer's Simulation Toolkit (DeST) and Transient System Simulation Program for rural buildings in northern China.

In a study Tahmasebinia et al. (2022) created a geometric model of the building using Autodesk Revit and performed energy simulations for Autodesk Green Building Studio (GBS) using the DOE 2.2 engine. Then, with the Monte Carlo simulation method, they performed to predict precise energy consumption and concluded that single-variable linear regression models are highly accurate.

Amani, Sabamehr, & Palmero Iglesias (2022) used ECOTEC to develop strategies that led to overall reductions in energy consumption in residential buildings. They have used the capabilities of ECOTEC for the simulation of daylight, solar radiation, thermal analysis and shading for energy management and conservation for residential buildings.

Muhammad & Karinka (2022) used eQUEST (The Quick Energy Simulation Tool) software to simulate energy in a laboratory with Galvanized Iron sheet roofing and concrete walls at Nitte, India to investigate passive strategies (using non-energy strategies) to achieve energy-efficient buildings. They improved thermal comfort to an acceptable standard by using the economic thickness of insulation and low emissivity glass windows.

Wieprzkowicz, Heim, & Knera (2022) developed a novel energy-activated thermal insulation composite system using ESP-r software. They compared two different methods of phase change material (PCM) simulation with ESP-r software and then validated the proposed model with experimental data.

In a study, the precise design of the HVAC system was performed by Nadeem et al. (2022) for a workshop building of a power plant located in Karachi, Pakistan. They designed an all-air variable volume system as the HVAC system for the workshop building with two floors by cooling load temperature difference (CLTD) method and the Hourly Analysis Program (HAP) software method. The cooling loads were 190.7 kW and 195.2 kW, obtained by CLTD and HAP software methods, respectively. They concluded that the variation in cooling loads

obtained by two of these methods is about 2%, which helps the engineers to design cost-effective HVAC systems.

Ener-Win software has been used as a tool for simulating hourly, annual and monthly energy consumption in buildings, peak heating and cooling loads, peak demand charges, daylighting contributions, life-cycle cost analysis and solar heating fraction through glazing, to design low-energy buildings by Soebarto & Degelman (1998). They analyzed new and retrofit projects by Ener-Win software and discussed retrofitting strategies for low-energy buildings.

Using the Energy Express (EE) software, Rahman, Rasul, & Khan (2006) performed an energy simulation on a three-story library building of Central Queensland University. In Energy Express (EE) software, it is possible to couple a dynamic multi-zone heat transfer model with an integrated HVAC model and provides graphic geometry input data with the ability to edit and multiple report viewing. They verified the results simulated by Energy Express (EE) software with an energy audit and on-site metered data. They concluded by replacing the existing constant air volume (CAV) system with a variable air volume (VAV) system, 12% energy savings were achieved as an energy retrofitting option.

In the research Attia (2011), ENERGY-10, IES-VE-Ware, e-Quest, BEopt, Vasari, Solar Shoebox, DesignBuilder, Open Studio Plug-in, HEED and ECOTECT were compared for the design of net zero energy buildings (NZEBs). They analyzed the five measures of accuracy, optimization, design process integration, interoperability, and usability of the tools for building performance simulation. There are limitations and major requirements in ENERGY-10, IES-VE-Ware, e-Quest, BEopt, Vasari, Solar Shoebox, DesignBuilder, Open Studio Plug-in, HEED and ECOTECT, that are not able to satisfy the NZEB objectives. These limitations include a lack of focus on carbon besides energy, the impossibility of better, citable, queryable and searchable resources databases, lack of simulation passive design strategies, minimum efficiency, base cases and code compliance calculations, and the impossibility of providing more comprehensive results, the impossibility of designing and optimizing the renewable

energy potential of a site versus whole energy systems and the impossibility of the simulation for innovative systems design solutions and technologies.

Badura, Martina, & Müller (2022) used IDA-ICE for optimizing the using solar radiation during the hot season and increasing the removal of excess heat during the hot season of the year based on parameters such as outdoor and indoor temperatures and desired levels of thermal comfort. In addition, by using IDA-ICE software, it is possible to simulate and explore different adaptive envelope scenarios and calculate heat flows through the walls. They concluded that how accumulated heat can be released during the night by removing the wall insulation layers.

Freire, Abadie, & Mendes (2009) were able to validate several cross and single-sided natural ventilation models implemented by PowerDomus software. They compared airflow rates obtained from the cross and single-sided natural ventilation models with measurements performed in a single-room house located in a wind tunnel facility and another in a real three-storey building. PowerDomus is software capable of a whole-building simulation tool for thermal comfort and energy use and has been developed based on the heat and moisture coupled models. PowerDomus can calculate the temperature and moisture content profiles for multi-layer walls in each time step and temperature and relative humidity. The results of this research showed that more accurate experimental models are needed to evaluate the air change rate by the cross and single-sided natural ventilation.

Elzafraney, Soroushian, & Deru (2005) analyzed the thermal and energy performances of two similar retail buildings located in Lansing, Michigan by SUNREL. SUNREL is an hourly building energy simulation program for designing energy-efficient buildings based on dynamic interactions between the building's envelope, occupants, and the environment. In this software, infiltration and natural ventilation for simplified multizone are calculated based on nodal airflow algorithm and only models idealized HVAC systems. With the help of SUNREL, the user can make optimal windows with a fixed U-value and fixed surface coefficients for thermal modeling of windows. In this research, the simulated results were validated with experimental

data by SUNREL. One of these buildings has normal concrete and the other has a high content of recycled mixed plastics. The results showed that recycled plastic concrete has higher levels of energy efficiency and comfort compared to building with normal concrete. Because recycled plastic concrete in combination with energy-efficient building design techniques reduces cooling and heating loads and enhances the comfort level of the buildings.

Bahadori-Jahromi, Salem, Mylona, Hasan, & Zhang (2022) used the Tas software to simulate the dynamic thermal analysis performance of seven different UK single-family houses. Tas software is simulated based on integrated natural and forced airflow and has a CAD link as a 3D graphics-based geometry input. Also, this software can simulate HVAC systems and total energy demand based on automatic calculation of airflow and plant sizing. Bahadori-Jahromi et al. (2022) compared the simulated results with the actual energy demand. The simulated results showed that the heating setpoint has the greatest effect on the simulated energy demand and by using window opening schemes controlling the heating schedule and the setpoint temperature, the energy demand can be reduced.

Trace 700 software consists of design, systems, equipment, and economics phases. This software was created according to ASHRAE Standard 90.1–2007 and 2010 Appendix G for evaluation performance rating and leadership in energy and environmental design (LEED) analysis, and it is also designed based on ASHRAE Standard 140–2011 and 2014 for whole building dynamic energy consumption simulation (Kim, Bande, Tabet Aoul, & Altan, 2021).

Adesanya et al. (2022) used transient system simulation software (TRNSYS) to model the thermal performance as a building energy simulation (BES) tool. The indoor temperature of the greenhouse and the heating demand in TRNSYS is calculated based on the solution of the transient heat transfer processes. Adesanya et al. (2022) modeled the temperature and the heating demand of two multi-span glass greenhouses of concave and convex shapes. They investigated the effect of different building energy simulation, longwave radiation models, on the indoor temperature of the greenhouse in different zones and the heating demand of a conditioned zone and compared the standard hourly results simulated by TRNSYS with

experimental data. The results showed that the monthly heating demand predicted by the simple and standard radiation modes in concave were matched the experimental measurements and the monthly heating demand predicted by the simple, standard, and detailed radiation modes in convex were like experimental measurements.

Crawley, Hand, Kummert, & Griffith (2008) have compared more than 20 capabilities of popular building performance simulation tools in the field of energy in the building, including BLAST, BSim, DeST, DOE-2.1E, ECOTECT, Ener-Win, Energy Express, Energy-10, eQUEST, ESP-r, IDA ICE, IES / VES, HAP, HEED, PowerDomus, SUNREL, Tas, TRACE and TRNSYS. Categories of these popular building performance simulation tools are included: general modeling features; zone loads; building envelope and daylighting and solar; infiltration ventilation and multizone airflow, renewable energy systems; electrical systems and equipment; HVAC systems, HVAC equipment, environmental emissions, economic evaluation, climate data availability results reporting, validation; and user interface, links to other programs, and availability. Crawley et al. (2001) concluded that EnergyPlus has advantages over other energy modeling tools.

EnergyPlus has been one of the most widely used single-performance model building tools in the field of energy efficiency in recent years.

Grillone, Mor, Danov, Cipriano, & Sumper (2021) used EnergyPlus and a new data-driven method to measure and validate energy efficiency for commercial buildings and facilities. They extracted typical consumption profile patterns using the clustering technique. They also used an innovative technique to assess the building's climate dependence to design a model to accurately estimate the dynamic energy savings in a building. Their method was compared with the time-of-week-and-temperature (TOWT) model and showed a 10% improvement. They also calculated the median estimated savings error of EnergyPlus as lower than 3% of the total reporting period consumption.

In another study using EnergyPlus, Zhang, Diao, Lei, Wang, & Zheng (2021) simulated and tested the energy-saving effects of different enclosure structures for typical single residential buildings in the Wenzhou area. They evaluated ceramist concrete composite blocks, non-clay sintered thermal insulation and foam concrete blocks for choosing the best energy-saving effect type in the wall area. They also evaluated the plant height of 0.1 m and plant height of 0.5 m, leaf area index of 0.3 and leaf area index of 1.0, leaf reflectance of 0.85, the thickness of 0.1 m and 0.051 m, soil electrical conductivity of 0.7 and soil electrical conductivity of 0.4 and 0.7, soil-specific heat of 1500 J / (kg℃) and 501 J / (kg℃) and soil density of 2000 kg/m^3 as the best energy-saving effect for the roof area.

Emil & Diab (2021) used EnergyPlus to model its energy in a study to transform a building in the department of mechanical engineering at the faculty of engineering campus of Ain Shams University in Egypt into a nearly zero-energy building. Using EnergyPlus, they performed several energy-saving techniques and retrofitting strategies for the building and were able to save more than 20% by retrofitting the building walls and combining various building envelope retrofitting strategies by more than 36%.

Brito, Silva, Teixeira, & Teixeira (2021) used EnergyPlus and TRACE700 in a study to evaluate the energy performance of a service building with 30 people and a floor area of 2,000 m^2 in Portugal. Consumption sources in this research are electricity, natural gas, and solar energy. EnergyPlus capability compared to TRACE700 in dynamic simulation of this building is performed by uploading the weather file and then analyzing construction, illumination, interior equipment, and HVAC systems. In this study, they compared the simulation results of both EnergyPlus and TRACE700 and predicted the deviation rate with actual energy consumption values of 2% for EnergyPlus and 0.5% for TRACE700, respectively. They eventually concluded that EnergyPlus and TRACE700 software are great tools for predicting the energy consumption of a services building.

He (2021) evaluated the compound effect of green building design on the waterfront in Wuhan using EnergyPlus, they examined the limitations of roof greening and the application of roof greening in the water-energy relationship.

Singh & Das (2021) in their study used EnergyPlus simulations. The electrical and thermodynamic performance of a triple-hybrid vapor absorption-assisted air-conditioning system was compared and analyzed with a typical system for a small office building. The heat source for this system has been air conditioning, biomass, and solar energy. In this comparison, they concluded that in the hybrid vapor absorption-assisted air-conditioning system, a maximum of 34.1% electrical energy savings can be ensured at a 500 m^2 collector area with 70°C generator temperature, also the absorption system can be dependent on renewable energy.

The innovative simulation features in EnergyPlus studied by Crawley et al. (2001), include:

1- user-configurable modular systems,
2- the possibility of integration with a heat and mass balance-based zone,
3- the possibility of interface development,
4- input and output data structures tailored to facilitate third-party module,
5- the possibility of simulating multizone airflow, electric power, solar thermal and photovoltaic.

According to the critical reviews of the past and recent research results related to energy efficiency tools, and the possibility of a combination of EnergyPlus with CONTAM software (Alonso, Dols, & Mathisen, 2022) it can be concluded that EnergyPlus can be the best choice as the part of this research.

1.2 Overview of indoor air quality tools applications

The number of indoor air quality simulation tools is very small compared to the building energy simulation tools. CONTAM, COMIS, BREEZE software are the most important indoor air quality tools in the field of multizone airflow and contaminant transport models (Walton & Dols, 2006).

The COMIS model is multizone airflow modeling that can be used as a stand-alone airflow model with input and output features and can also be used as an infiltration module in thermal building simulation programs. This model can simulate indoor contaminants, heat flow natural ventilation, flow through openings and crack, and single-side and cross ventilation. COMIS was developed in 12 months in 1988-1989 at Lawrence Berkeley National Laboratory (Feustel, 1999).

Blomsterberg, Carlsson, & Svensson (1996) calculated variation in ventilation rates as a result of variation in climate and variation in performance of the ventilation system in the Swedish housing stock. They used tracer gas sprays to monitor ventilation rate, passive techniques for monthly averaging and constant concentration for hourly averaging. (Blomsterberg et al., 1996) simulated ventilation rates by using COMIS software as a multi-zone airflow network model and then compared simulated and measured average total outdoor ventilation rates. The results showed that despite the disagreement between hourly rates and individual rooms, the average simulated and measured outdoor ventilation rates were matched.

Walton (1989) developed AIRNET model with the ability to the simulation of air pollutant concentrations, heat flow, and various types of airflows through cracks, openings, ducts and fans. This model can also calculate the effect of wind on air infiltration by considering wind pressure coefficients. Airflow elements are calculated based on nonlinear and linear

correlations. The mass balance equations as a nonlinear equations system are solved by iteration (Haghighat & Megri, 1996).

CBSAIR is a program developed by Haghighat & Rao (1991) to verify the multi-zone airflow model. CBSAIR can be implemented based on MATLAB and considers the buildings as nodes connected by openings. Its applicable model is limited to power law equations, but there are arbitrary flow equations in its theoretical model. In the CBSAIR model, there is the possibility of MATLAB programming, sensitivity analysis of the procedure for airflow. The results and data in CBSAIR are displayed and manipulated easily.

BUS is designed as a ventilation system model by a network. In this model, the nodes are connected by one-dimensional flow elements. Mass balance and momentum equations are linearized and iteratively solved based on the fully implicit method (Haghighat & Megri, 1996). The simulated results of the BUS model for calculations of mass balance and momentum equations have been verified based on the simple test case (Haghighat & Megri, 1996; Tuomaala, 1993).

Walker, Hayes, & White (1996) simulated the behavior of natural ventilation by BREEZE and Passive Tracer Gas technique to understand the aging of the air entering the multiroomed office buildings in two situations, one when the air enters the building from the lower level and rises to the upper level due to the stack effect, and the other when the air enters the windward face due to the blowing of the wind and if it passes through the multiroomed office buildings to the downwind. The simulated results showed that the simple ventilation flow rates can not indicate the true "freshness", and the effective ventilation can be less than the current minimum requirement of the occupants.

In another study by Plathner & Ross (2003), a moisture admittance model (MAM) as the simulator for the behavior of moisture in dwellings was integrated with the BREEZE computer model as a simulator of air and contaminant flows. The results simulated by the integrated MAM-BREEZE model were compared with the results predicted by Louden model. There was

reasonable agreement between the simulated results in Louden and MAM-BREEZE models. Also, the effect of sorption on the domestic ventilation system performance was investigated by both Louden and MAM-BREEZE models, so it can be concluded that because the Louden model did not consider sorption, so, using the Louden model in the design of the ventilation system will lead to over-ventilation and reduce energy efficiency.

Li (2002) have been validated COMIS, CONTAM and ESP-r software as three computer simulation models to predict air and contaminant flows for the whole house with the garage through cracks and gaps on exterior walls and roof. Three levels of validation have been performed for COMIS, CONTAM and ESP-r. In the first level, the fundamental comparison has been performed for three models. In the second level, the validation has been performed with experimental data tested in the laboratory, and in the third level, the validation has been done based on the data measured in two single-family houses in Ottawa. The results showed that there are good agreements between the predictions made by COMIS, CONTAM and ESP-r, and the prediction results simulated by COMIS and CONTAM showed that the airtightness of the garage/house interface wall has a significant effect on contaminant dispersion in the room.

Steven J Emmerich (2001) studied analytical verification and inter-model comparisons of multi-zone indoor air quality (IAQ) models in residential buildings. He concluded that in the most of these studies, the experimental data were compared with the predictions results of only one model, usually the COMIS or CONTAM models and there is good agreement between CONTAM, COMIS, AIRNET, CBSAIR, BUS, MZAP and BREEZE (Haghighat & Megri, 1996; Roulet, Fürbringer, & Romano, 1996).

Ng, Dols, & Emmerich (2021) in a study to reduce infiltration in commercial buildings concluded that more airflow should be provided than return and exhaust to provide pressurize conditions in the building. They used airflow simulation using CONTAM multizone airflow software to predict reduced infiltration because of pressurization. They also used the

infiltration rates predicted by CONTAM to calculate the coefficient of input data to EnergyPlus, and finally concluded that the effect of infiltration on HVAC energy use is very important and should be optimized with CONTAM to reduce energy consumption for the whole building.

In Canada and the United States, because pressurized corridor ventilation systems are old and most of them are poor performance, Fine & Touchie (2021) compared six ventilation systems to the pressurized corridor, including various decentralized and direct-to-suite ducted configurations, using a CONTAM airflow model. This modeling has been performed with the help of field data from a representative 24-storey post-World War II MURB in Toronto, Canada, along with field data from the literature. Simulations were performed for each system under cold (−16.1°C, 3°F) and warm (29.0 °C, 84.2 °F) outdoor conditions. The extracted recommendations lead to increased penetration/exit from the outer wall by up to 230% in cold conditions. They also recommended reducing indirect inter-suite flow and avoiding door undercuts and automated ducted supply terminal flow control.

In another study by Tian et al. (2020), because of the poor performance of most pressurized corridor ventilation systems in high-rise multi-family buildings, they used CONTAM, three ventilation strategies that include a traditional pressurized corridor ventilation system, a direct-to-suite ducted ventilation system, and a suite-based heat recovery ventilation system under both summer and winter conditions. Their results showed that the suite-based heat recovery ventilation system strategy has a good performance to provide the required airflow in both winter and summer. In other strategies, there is an uneven airflow distribution in the suites at the top and bottom, which is more noticeable in the winter.

Qi, Cheng, Katal, Wang, & Athienitis (2020) developed a simple hybrid ventilation model based on a multizone airflow network for a 17-storey institutional high-rise building and modeled it using CONTAM. For the model simulated by CONTAM, 5 stacked three-storey atriums have been considered and all floors except the first and seventeenth floors have no

natural valves. The results of the simulated model were compared with the real results and the developed model was validated.

Sowa & Mijakowski (2020) simulated the feasibility of humidity-sensitive, demand-controlled ventilation systems for the entire summer season based on the Warsaw climate in a CONTAM study. In their research, they studied two ventilation systems, including one standard and one hybrid system with additional roof fans. They concluded that the application of humidity-sensitive, demand-controlled ventilation in multiunit residential buildings in a continental climate result in significant energy savings of up to 11.64 kWh/m^2 of primary energy. The use of this technology in the units located in the upper part of the building also leads to a 32% reduction in carbon dioxide concentrations.

The most of existing indoor air quality tools such as CONTAM, COMIS, AIRNET, CBSAIR, BUS, MZAP and BREEZE (Haghighat & Megri, 1996; Roulet, Fürbringer, & Romano, 1996) are very similar, and they can solve airflow and contaminants flow in a multi-zone, linear or non-linear manner (Dols & Polidoro, 2015; Feustel, 1999; Plathner & Woloszyn, 2002). Also, most of the research has compared the capabilities of CONTAM and COMIS with other existing indoor air quality tools. COMIS (Provata & Kolokotsa), developed by the International Energy Agency (IEA) Annex program, has powerful features but has not been used in this research due to model complexities. CONTAM is superior to other indoor air quality simulation tools for the following reasons:

1- relatively easy to use with straightforward,
2- graphic user interface (GUI),
3- simple geometric features and,
4- enough geometrical features (Haghighat & Megri, 1996).

According to the results obtained by reviewing the past and recent research on building indoor air quality tools, CONTAM tool has been selected as the desired tool in part of this research in the field of indoor air quality.

1.3 Overview of moisture performance tools applications

Jirgensone (2022) has been analyzed the thermal inertia and moisture transfer for a building of the Botanical Garden at the University of Latvia with a multi-layer insulation envelope with hempcrete. He used a one-dimensional approach with the help of WUFI software and compared the simulated results with experimental data. Then, he developed an ANSYS-CFX model, as two and three-dimensional methods, for analysis of the transport of moisture and heat indoors for the case study. The comparison results simulated by WUFI and ANSYS-CFX showed good agreement with the experimental data.

Vyas, Johns, Richman, & Liao (2023) developed a novel 1D heat, air and moisture (HAM) numerical modeling tools to analyze the impact of adhesive layers on air and moisture transfer in cross-laminated timber (CLT). To validate the 1D heat, air and moisture (HAM) numerical modeling tool and its methodology, they used WUFI software to compare the simulated results of CLT without adhesive layers. The results showed that adhesive layers reduce the moisture transfer rate in wood layers bounded by adhesives. They concluded that for further validation, analysis of the hygrothermal impact of adhesive layers in CLT should be conducted in the future using laboratory and field tests in specific weather conditions.

Kang & Kim (2021) used WUFI Pro and ANSYS Fluent software to analyze the hygrothermal behavior of building exterior and interior walls, floor, ceiling walls, and interior spaces. They used WUFI Pro to analyze the heat and moisture transfer in the walls of the building with a wooden frame and used ANSYS Fluent for indoor thermal and humidity environment analysis based on the imported flux of the WUFI calculation result. The simulation results of WUFI and ANSYS Fluent showed that the hygrothermal behavior of the building walls in one

dimension was significantly affected by the outdoor climate conditions, so that the surface heat flux can be shown the pattern like the indoor climate conditions that are controlled by certain conditions. They concluded that it is possible to analyze the hygrothermal performance according to the building materials of the walls with two different simulations of WUFI Pro and ANSYS Fluent software.

Asphaug, Andenæs, Geving, Time, & Kvande (2022) used WUFI®Pro and COMSOL Multiphysics® for one- and two-dimensional hygrothermal simulations in studying the use of vapor-permeable thermal insulation and the effect of air gaps behind dimpled membranes for outward drying of concrete basement walls. By using WUFI®Pro and COMSOL Multiphysics®, they simulated outward drying of concrete wall segments and then simulated long-term moisture performance of concrete basement walls. They compared two types of Expanded Polystyrene (EPS) and two dimpled membrane positions with an emphasis on the airflow through the air gap behind the membrane and concluded that when the dimpled membrane is placed between concrete and exterior EPS, the bottom of the concrete segments dries faster than the top, and when the dimpled membrane is placed on the exterior side, the concrete dries uniformly along the height. Therefore, optimum drying occurs when the thickness of interior insulation decreases.

DELPHIN, WUFI, hygIRC and COMSOL as hygrothermal tools have been used by Defo, Lacasse, & Laouadi (2022) for comparing the hygrothermal responses and moisture performance of four wood-frame walls including fibreboard, vinyl, stucco and brick, in three climate conditions of Ottawa, Vancouver and Calgary for two years. In this study temperature, and relative humidity of the outer layer of oriented strand board (OSB) sheathing, simulated by DELPHIN, WUFI, hygIRC and COMSOL were compared with each other. The highest discrepancies among the four tools related to stucco cladding were differences as high as 20% from time to time. Temperature profiles for the outer layer of the OSB showed good agreement for four simulation tools. Predicted mold growth measures of the outer layer of the OSB sheathing were similar for the four simulation tools, but there were differences in some cases. They concluded that these discrepancies among hygrothermal tools are related to material

property processing, calculation of the quantity of wind-driven rain absorbed at the cladding surface and other implementation details. Despite these differences in the simulated results, DELPHIN, WUFI, hygIRC and COMSOL generally yielded consistent results and can be used to compare the effects of different designs on the risk of premature deterioration and assessing the relative effects of climate change on a wall assembly design.

Hejazi, Sakiyama, Frick, & Garrecht (2019) compared WUFI Pro 4.2 and DELPHIN (Version 5) as hygrothermal software to evaluate their differences, identify limitations and potentialities. They considered three types of materials by DELPHIN and WUFI. The results of external, center, and internal temperatures, external and internal humidity and total water content simulated by DELPHIN and WUFI were compared. The results of comparing the two methods of DELPHIN and WUFI showed that the two software are very close to each other except for the total water content during the wetting period, and the results of the constant inside climate method were better than the sinusoid inside climate method.

Nusser & Teibinger (2012) show how the physical approaches used in WUFI were implemented in COMSOL Multiphysics using the Partial Differential Equation interface for a 1-D model. They compared the moisture content of the softwood and the total roof construction for two versions of a flat roof with vapor-tight sealing and wooden cladding at the exterior side, simulated by both models. They concluded that COMSOL and WUFI results are nearly identical in version 1 but in version 2 there are slight deviations between COMSOL and WUFI. They concluded that COMSOL and WUFI results can be close to each other only slight deviation can be occurred if the moisture load on the construction is too high.

Delgado, Ramos, Barreira, & De Freitas (2010) compared hygrothermal modeling tools of 1D-HAM, BSim2000, DELPHIN 5, EMPTIED, GLASTA, hygIRC-1D, HAMLab, HAM-Tools, IDA-ICE, MATCH, MOIST, MOIST-EXPERT, UMIDUS and WUFI. The physical parameters involved in hygrothermal modeling in the fields' material properties and inside-outside boundary conditions were compared. The most important physical parameters that have been considered include ambient temperature, ambient relative humidity, cloud index,

wind velocity, solar direct, wind orientation and horizontal rain precipitation. the results showed that in UMIDUS there was no weather data file for other cities or countries, in MOIST there was no possibility of further development and technical support, in GLASTA it was only suitable for checking condensation and simulating drying, and in EMPTIED there was no ability to consider the influence of wind, rain and sun. Also, the only hygrothermal tools that could evaluate undercooling phenomena include BSim2000, HAMLab, HAM-Tools, hygIRC and WUFI. MOIST-EXPERT completely similar to WUFI. Considering that WUFI and hygIRC did not reflect a specific approach and were easier to use than other tools, these two tools were selected for further comparison in the laboratory. They compared the accumulated degrees of condensation simulated by WUFI and hygIRC for different months in Braganca and Beja. The results showed that the most pronounced condensation for Braganca and Beja simulated by WUFI and hygIRC occurs on different months and considering that the WUFI model uses the explicit radiation balance method, the simulation results of WUFI are more accurate compared to hygIRC.

Lengsfeld & Holm (2007) considered the WUFI as a hygrothermal simulation tool to be a viable alternative to complex and expensive laboratory methods for building estimating indoor environmental conditions. They also validated WUFI tool in the context of the IEA-Annex 41 project "Moist-Eng." and described WUFI simulation results in their research. WUFI has been used as a reliable hygrothermal simulation tool in recent years to predict the results of moisture performance in buildings.

Ghazaryan & Tariku (2021) used WUFI as a hygrothermal analysis computer simulation tool. They compare and analyze the hygrothermal performance of natural cork insulation used in split wall assemblies against similar walls with mineral wool and expanded polystyrene (EPS) in three different Canadian climates. Their simulation results showed that cork assemblies have less advantage in performance than EPS assemblies when the amount of moisture affecting the assemblies is high, and mineral wool assemblies have better performance than cork and EPS insulation.

Jiang et al. (2021) in a study evaluated the hygrothermal and mechanical performance of concrete by WUFI tools because most buildings in the world are made of concrete in whole or in part and concrete are the second most widely used source in the world after water. For this purpose, the density, porosity, specific heat capacity, and thermal conductivity of different sustainable concrete mix designs have been analyzed. They concluded that the hygrothermal performance of concrete could be enhanced without diminishing the value of its mechanical properties, in which case CO_2 emissions would be reduced at the same time. They also found that the use of recycled aggregates coupled with supplementary cementitious materials could increase the strength of concrete with lower environmental impacts.

Kazemi & Courard (2021) simulated hygrothermal conditions of green roofs with unsaturated substrate and drainage layers incorporating coarse recycled materials using WUFI software. They concluded that coarse recycled materials provide sufficient thermal resistance, like soil particles for the substrate layer. They also calculated the optimum design for green roof systems, for drainage layers with coarse aggregates and an unsaturated substrate layer, and a drainage layer of 6 cm and 18 cm, respectively. Finally, an 18 cm unsaturated substrate layer was predicted as the best design for roofing systems.

Considering that WUFI is the most widely used tool , easier to use and more accurate than other hygrothermal tools (Delgado et al., 2010), therefore, in this research it has been used to develop a combined model.

1.4 Overview of energy, indoor air quality and moisture performance combined tools applications

Dols, Milando, Ng, Emmerich, & Teo (2021) developed a set of coupled reference model of building for assessment of the co-simulation method between EnergyPlus and CONTAM. They used an original EnergyPlus prototype model, stand-alone CONTAM simulations, the

original model with NIST-based infiltration correlations and co-simulation between EnergyPlus and CONTAM for evaluating the co-simulation advantage to address the effects of changes in building typology and ventilation system performance on contaminant transport outcomes while utilizing whole building energy analysis capabilities will be explored.

Walker, Clark, et al. (2021) evaluated the use of smart control strategies for ventilation in four different California climates. They evaluate using the co-simulation method for EnergyPlus as a building energy model, CONTAM as an indoor air quality model and an automated Python-based parametric for analysis of control variables, annual operation of multiple control strategies of 24-compliant prototype homes in California. In all these simulations, a single well-mixed zone and the equivalent ventilation method outlined in ASHRAE Standard 62.2-2016 has been performed. Control strategies which included optimization based on sensing outdoor air temperature as the best strategies and control strategies based solely on occupancy as the worst strategy were predicted.

Mokhtari & Jahangir (2021), considering the direct relationship between occupant density and COVID-19 infection risk in a study using the co-simulation method between EnergyPlus and MATLAB, optimized occupant distribution patterns to reduce the number of infected people and minimum energy consumption for a university building located presented in Tehran-Iran. To present these optimum occupant distribution patterns, they defined a multi-objective optimization problem, with the objective functions of energy consumption and COVID-19-infected people, which is solved based on an algorithm developed by co-simulation developed between EnergyPlus and MATLAB. Air exchange rates, class duration, and working hours of the university as COVID-19 controlling approaches have been studied. Results of optimum occupant distribution patterns included 56% reduction in infected people and 32% reduction in energy consumption.

In another study, Walker, Less, Lorenzetti, & Sohn (2021) examined the use of zoned ventilation systems using a coupled CONTAM / EnergyPlus model for new California

dwellings. They performed several intelligent control systems with a target of halving ventilation-related energy use, by reducing dwelling ventilation rates based on zone occupancy. These controls are evaluated based on annual energy consumption relative to non-regional mechanical ventilation systems and compliant with code-compliant mechanical ventilation systems. They also used the CONTAM / EnergyPlus model to compare the annual personal concentration of a contaminant for a control strategy with the personal concentration that would have occurred using a continuously operating, non-zoned system. The contaminants they considered include moisture, CO_2, particles, and a generic contaminant. Reduction in outside airflow leads to reductions in ventilation-related energy of 10% to 30% for zonal control compared to 7% savings from unzone control.

Given that in Poland, more than 25% of the final energy is consumed in the home sector and residents are dissatisfied with the thermal conditions in the summer months, Ferdyn-Grygierek et al. (2021) in a study looking for passive and energy-efficient solutions to improve thermal comfort in Polish dwellings. They selected a five-story, multi-family building as a case study and performed simulations of current and future climatic conditions using EnergyPlus (for thermal calculations) and CONTAM (for air exchange calculations). They considered the stochastic behavior of the occupants when opening the windows as well as the automatic control systems to supply the building with outside air. Finally, they eventually concluded that opening windows could increase heating demand, but that thermal discomfort hours by over 90% would decrease. They proposed a mechanical source of outside air controlled by indoor and outdoor temperatures.

Moujalled et al. (2018) in a study experimentally and numerically study the hygrothermal behavior of a real building envelope using the co-simulation method between MATLAB and WUFI and evaluated the hygrothermal performance of a hemp lime concrete building from an experimental and numerical point of view. The main purpose of this study was to investigate the realistic thermal and hygric behavior of hemp concrete under real climatic conditions. In this study, they concluded that hemp-lime concrete has excellent moisture buffer performance

and comparing numerical and experimental results highlights the effect of temperature on the sorption process.

In another study by Pazold, Burhenne, Radon, Herkel, & Antretter (2012), using the coupling procedure, WUFI as the building model and Modelica as the HVAC model. Their coupling procedure mechanism is based on the implementation of the Modelica HVAC model as a standardized Functional Mock-up Interface (FMI) by importing in Functional Mock-up units (FMU) as a new solver for the WUFI building model. The procedure coupling between the Modelica HVAC model and the WUFI building model has been performed in two iterative approaches and a co-simulation approach. In the iterative approach, there are repeat time steps within the FMU, but in the co-simulation method, the WUFI building envelope model and the Modelica HVAC model operate as the ping-pong method. They concluded that the co-simulation approach has reasonable results so exported FMUs can act as sub-models in the WUFI building envelope model.

Burhenne, Wystrcil, Elci, Narmsara, & Herkel (2013) introduced the coupling method between the Modelica model as an HVAC system model and WUFI®Plus as a building performance simulation model in hygrothermal envelope-level calculation. They conclude that since building envelope and HVAC system influence are intertwined, if each of the Modelica and WUFI®Plus models is simulated separately, the results will be inaccurate, so it is necessary to combine the two models in a co-simulation. They found the functional mock-up interface (FMI) tool for co-simulation as the best way to include the Modelica model into WUFI®Plus.

In a research, the HVAC model was developed with the software of Dymola (Dassault Systèmes AB, 2011) and then with the export of C-code, from the source code generation section to WUFI®plus, the possibility of integration between both building and HVAC models has been provided. Due to coupling between the HVAC model and WUFI®plus and modification of input and output variables in the integrated model, reliable results are predicted (Burhenne, Radon, Pazold, Herkel, & Antretter, 2011).

By considering the literature review in the recent and past research for all three single models of EnergyPlus, CONTAM and WUFI and their coupling feasibility of the existing models, the following general conclusions can be categorized:

- EnergyPlus in energy efficiency, CONTAM in indoor air quality and WUFI in moisture performance have been most used as the functional tools in building performance simulations.

- The possibility of the coupling between EnergyPlus with CONTAM as well as WUFI with other HVAC models have been investigated and coupling mechanisms or co-simulations have been provided for them.

- Analysis of the simulated results by single models in comparison with the simulated results by coupling models shows that the simulation in coupling models is concluded with higher accuracy than in single models.

- The general conclusion that can be drawn from this critical literature review is a necessity to combine all three single models of EnergyPlus, CONTAM and WUFI into a comprehensive and combined model.

- A combined model that has all three capabilities of energy efficiency, indoor air quality and moisture performance has not been found in the critical literature review, so the need to develop a combined model in this study is the main goal that will be taken.

CHAPITRE 2

APPROACH AND ORGANIZATION OF THE DOCUMENT

2.1 Description of the combined model development approach

The development of a combined model for the whole building performance assessment in the doctoral thesis, has been performed according to the flowchart steps in Figure 2.1.

STEP 1: At this step, various building energy tools are analyzed. All energy tools are identified, and their capabilities are compared. Energy tools that have comprehensive and dynamic capabilities are selected. At the same time, various types of indoor air quality (IAQ) tools are identified. After comparing indoor air quality tools, the most capable tool has been selected. The selection criteria are the ability to import and export data between both types of tools. The next important part of this first step is the feasibility of coupling method for indoor air quality (IAQ) and energy tools as a coupled model.

STEP 2: In this step hygrothermal tools are identified and the capabilities of hygrothermal tools are compared. Then a tool with high capabilities is selected. The feasibility of the export and import of variables in required formats between hygrothermal tools is considered. coupling feasibility study between the selected indoor air quality (IAQ) tools with the selected hygrothermal tool is investigated. Finally, the coupling result of both tools is evaluated for a case study.

STEP 3: The method of energy and indoor air quality (IAQ) coupled model should be verified. If the verification in this step is not confirmed, then energy and indoor air quality (IAQ) tools should be changed to find the best match tools to satisfy the verification method criteria.

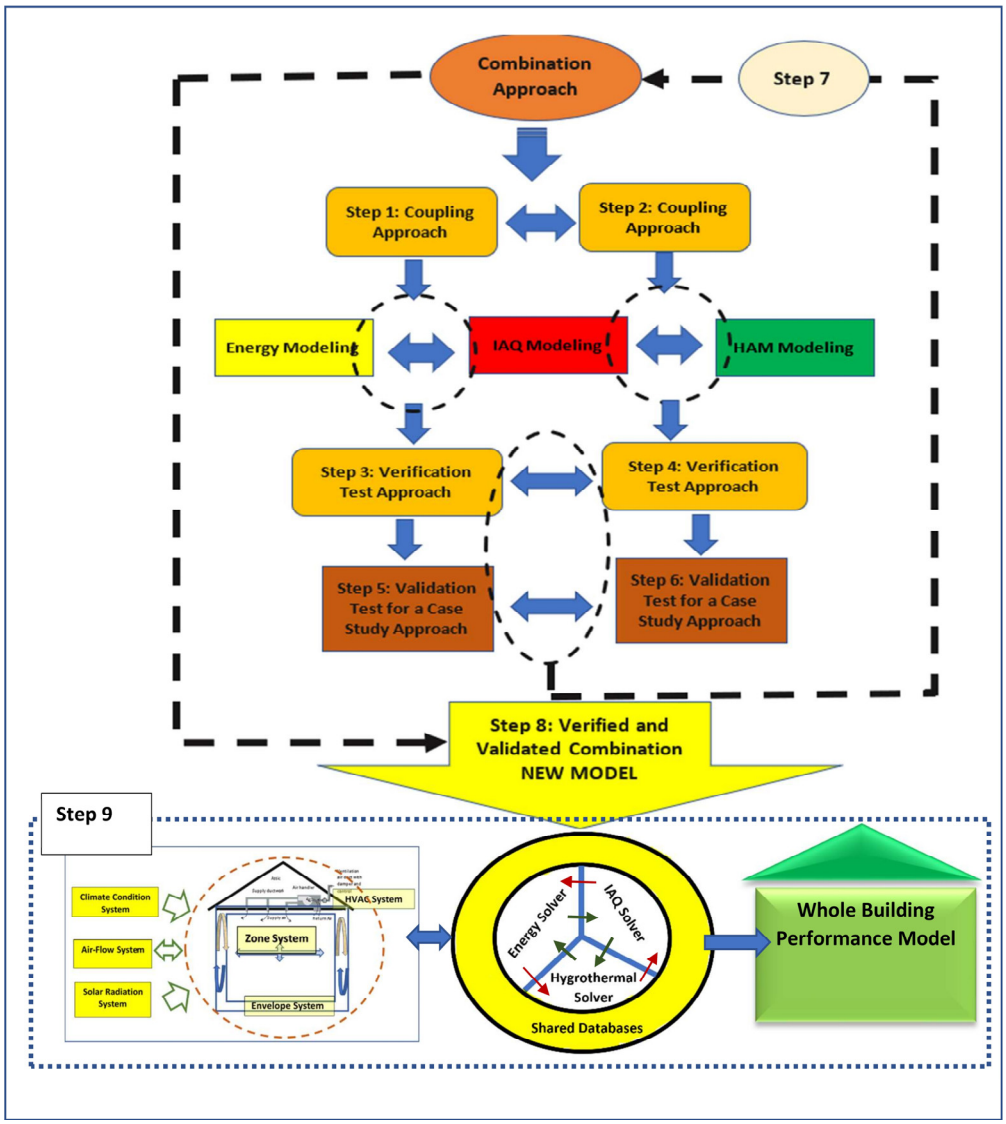

Figure 2.1 Steps to develop a combined model for whole building performance assessment in doctoral thesis research

STEP 4: Verification for the indoor air quality (IAQ) and hygrothermal coupled model should be performed. If indoor air quality (IAQ) and hygrothermal coupled model is not verified, then the new indoor air quality (IAQ) tool should be found and replaced to meet the verification criteria.

STEP 5: At this stage, the simulated results of energy - indoor air quality (IAQ) coupled model should be validated for a case study based on the ASHRAE Standards criteria and compared with the results simulated by single models.

STEP 6: Results simulated by indoor air quality (IAQ) and hygrothermal coupled model should be validated based on the ASHRAE Standards criteria like step 5 and then compared with results simulated by single models.

STEP 7: Given that the main goal of this research is to combine all three energy, indoor air quality (IAQ) and hygrothermal models, the outputs of coupled model should have the ability to exchange. Exchange data should be converted into acceptable formats into any sub-model set. The data should have the ability to exchange between all three energy, indoor air quality (IAQ) and hygrothermal models.

STEP 8: The results simulated by fully energy, indoor air quality (IAQ) and hygrothermal combined model should be verified. If verification results are confirmed, then the results simulated by the fully combined model should be validated based on the ASHRAE Standard criteria and compared with the results simulated by the single models.

STEP 9: The final output of this step will be used for the precise prediction of the whole building performance case study.

2.2 Description of the whole building systems

To develop a combined model with performance predictability for the whole building, it is necessary to define the information and conditions of different parts of the whole building system for this model. The whole building systems as shown in Figure 2.2 include the following categories:

- Climate condition system:

Information required for different climatic situations for each type of building case is defined as a climate condition system. This information includes environmental factors such as geographic location, temperature, relative humidity, contaminant concentration and other climatic measures that determine the surrounding environmental condition and its information is used in the equations of heat flow, moisture flow and contaminant flow.

- Solar radiation system:

The information about the direct and diffuse solar radiation that incident the building envelope exterior surface is defined in this system and is included in the heat flow balance equations of other systems of the whole building.

- Envelope system:

This system is another part of the whole building system in which heat flow, moisture flow and contaminant flow balances between the two parts of the interior and exterior surface are performed quantitatively.

- Zone system:

In this system, the balances of heat flow, moisture flow and contaminant flow between the zone with other parts of the whole building system are performed quantitatively.

- HVAC system:

In this system, heat flow, moisture flow and contaminant flow balances inside HVAC air handlers are performed quantitatively.

- Airflow system:

This system acts as a carrier of heat, moisture and contaminant through air infiltration, exfiltration and inter-zonal which is quantified in heat flow, moisture flow and contaminant flow.

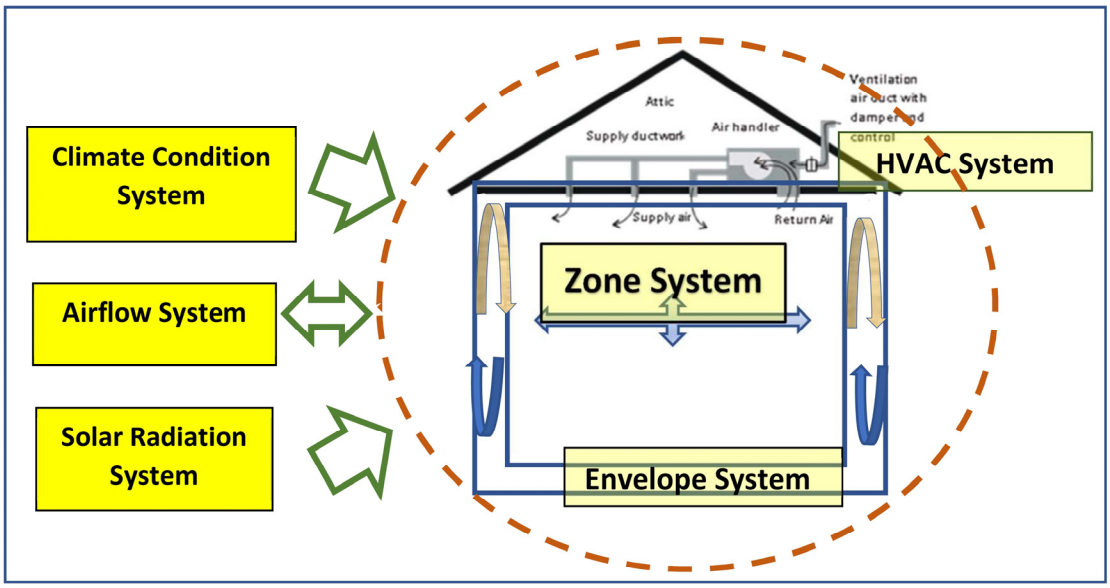

Figure 2.2 Components of the whole building systems

2.3 Whole building performance analysis approach by the combined model

Given that, the task of developing a combined model is to simulate the whole building performance measures for all three areas of energy efficiency, indoor air quality and moisture performance, so to implement these simulations, a combination mechanism has been designed. Figure 2.3 shows the mechanism for applying the whole building system combined model.

The combined model implementation mechanism includes the following points:

- Since the whole building systems include the climate condition, solar radiation, envelope, HVAC, airflow, and zone systems, the input data required by all these systems are entered into the combined model.

- The combined model in three areas of energy, indoor air quality and moisture, simulates the performance of the whole building simultaneously.

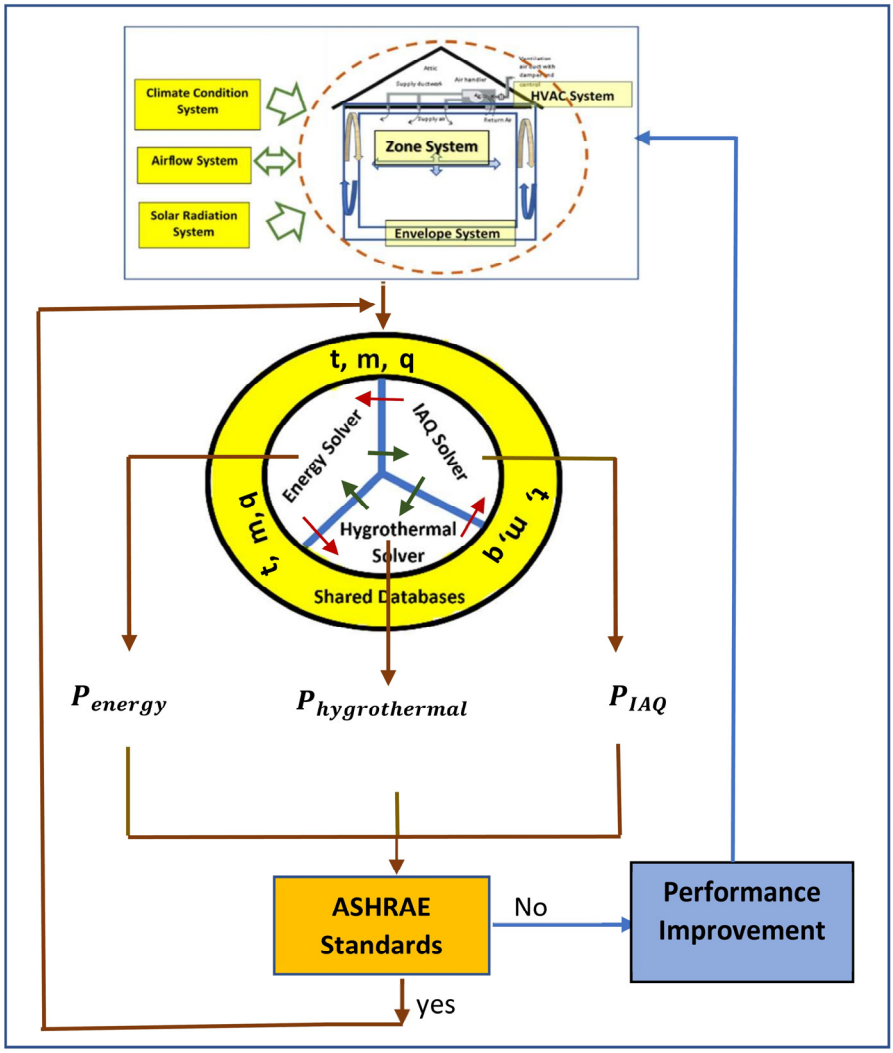

Figure 2.3 Whole building performance analysis approach (P_{energy}= energy performance, $P_{hygrothermal}$ = moisture performance, P_{IAQ} = indoor air quality performance, indoor air Temperature, m= indoor airflow and q=indoor heating/cooling flow)

- Simulation of whole building performances is performed by exchanging and changing control variables of "t" as indoor air temperatures, "m" as indoor airflows and "q" as indoor heating/cooling flows between energy, indoor air quality and hygrothermal solvers.

- For the combined model to simulate the results of whole building performance, the governing equations of heat flow balance, moisture flow balance and contaminant flow balance should be solved for all envelope, HVAC, airflow, and zone systems.

- The values of whole building performance measures are simulated in the fields of energy, indoor air quality and moisture terms, then simulated results are compared with the acceptable levels of ASHRAE Standards of 90.1, 62.1, 160 and 55 and these comparisons are calculated as percentage differences values.

- If the percentage difference values are negative or zero, simulated whole building performance is acceptable in the relevant fields and ASHRAE Standards criteria are satisfied, and then this procedure has been stopped at this stage. Otherwise, the performance should be improved with solutions and the proposed procedure should be performed again until ASHRAE Standards are satisfied.

With the help of the described mechanism, the whole building performance can be designed to simulate the measures of energy efficiency, indoor air quality and moisture performance in acceptable condition compared to the ASHRAE Standards.

2.4 Structure of whole building performance governing equations

The combined model computational method is based on solving the equations of heat flow, contaminant flow and moisture flow balances between the zone system with the envelope system, airflow system and HVAC system. Therefore, the simultaneous calculations between the governing equations in the zone system with the envelope system, airflow system and HVAC system are the basis of the method presented in the combined model for the whole building.

The governing equations of the envelope system as shown in Figure 2.4 include heat flow balance ($\dot{E}_{enve}$), moisture balance ($\dot{W}_{enve}$) and contaminate balance ($\dot{M}_{enve}$). These equations are solved simultaneously by the combined model for the envelope system.

The governing equations of the HVAC system as shown in Figure 2.5 include the balances of HVAC air heat flow $(\dot{E}_{HVAC})$, HVAC air moisture flow $(\dot{W}_{HVAC})$ and HVAC air contaminant flow ($\dot{M}_{HVAC}$). These equations are solved simultaneously by the combined model for the HVAC system.

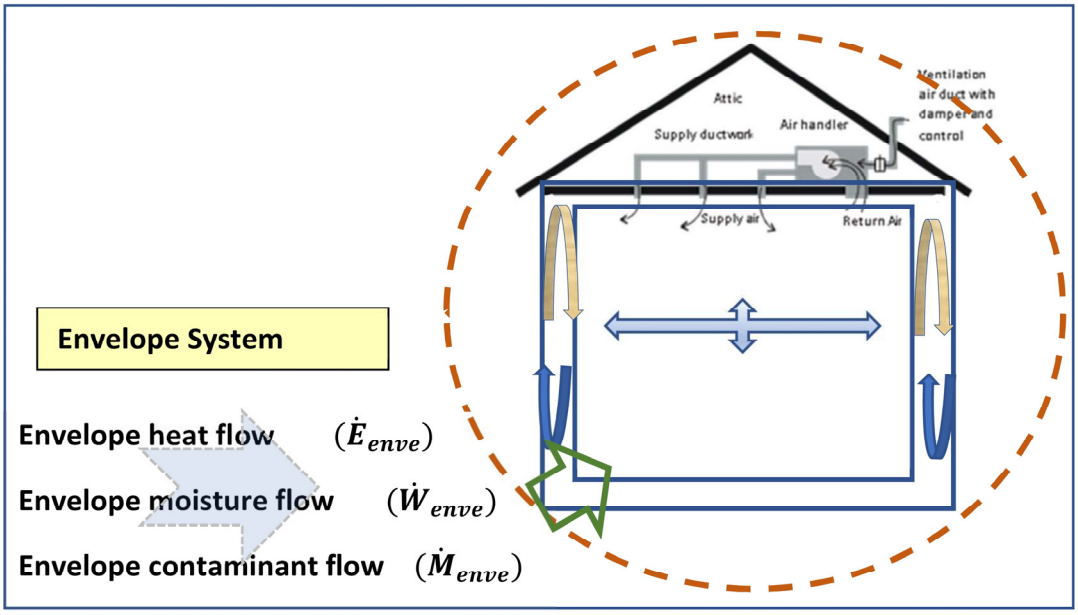

Figure 2.4 The governing equations balances for the envelope system

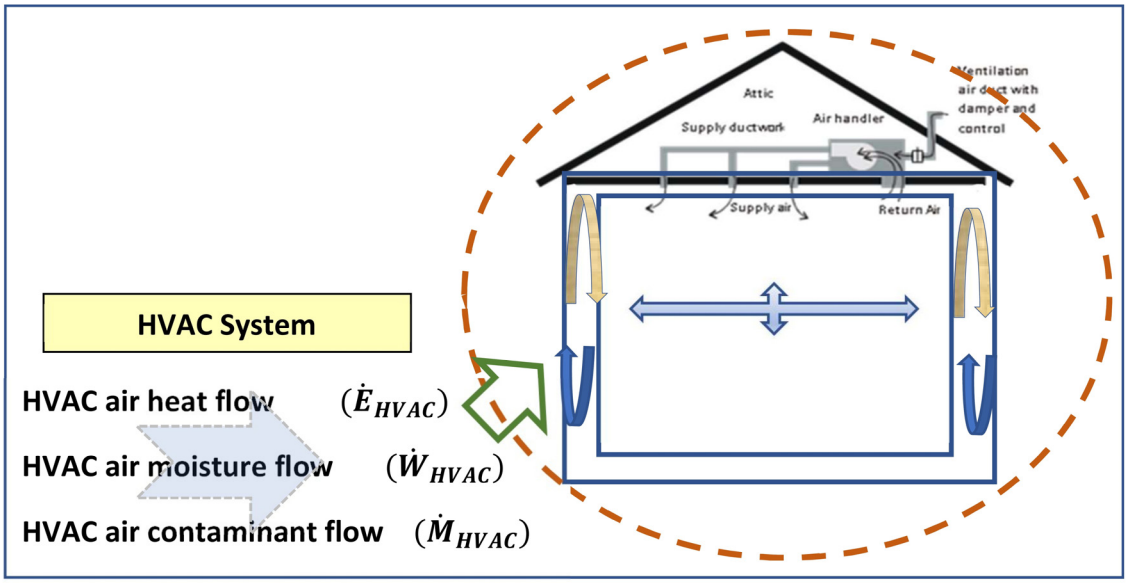

Figure 2.5 The governing equations balances for the HVAC system

The governing equations of the airflow system as shown in Figure 2.6 due to infiltration, exfiltration, and inter-zonal include the balances of air heat flow $(\dot{E}_{air})$, air moisture flow $(\dot{W}_{air})$ and air contaminant flow $(\dot{M}_{air})$. These equations are solved simultaneously by the combined model for the airflow system.

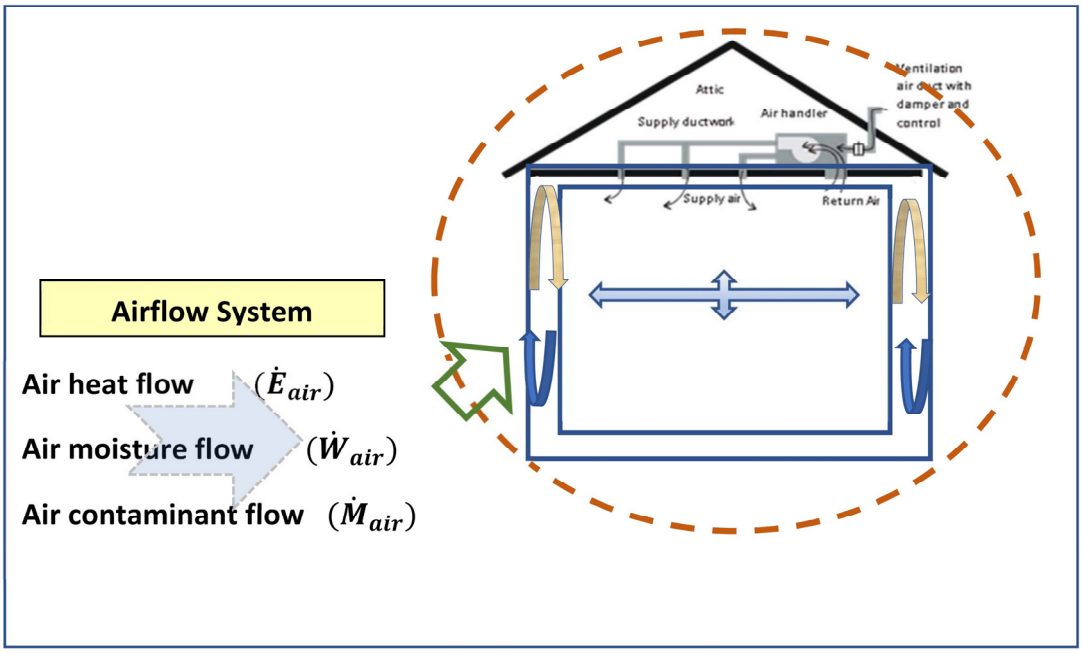

Figure 2.6 The governing equations balances for the airflow system

The total governing equations have been calculated for the heat flow ($\dot{E}_{total}$), moisture flow ($\dot{W}_{total}$) and contaminant flow ($\dot{M}_{total}$) between the zone system and other whole building systems such as the building envelope, HVAC and airflow systems according to the presented conditions in Figure 2.7. In this case, the combined model will be able to simulate the results of whole building performance based on energy efficiency, indoor air quality and moisture performance criteria.

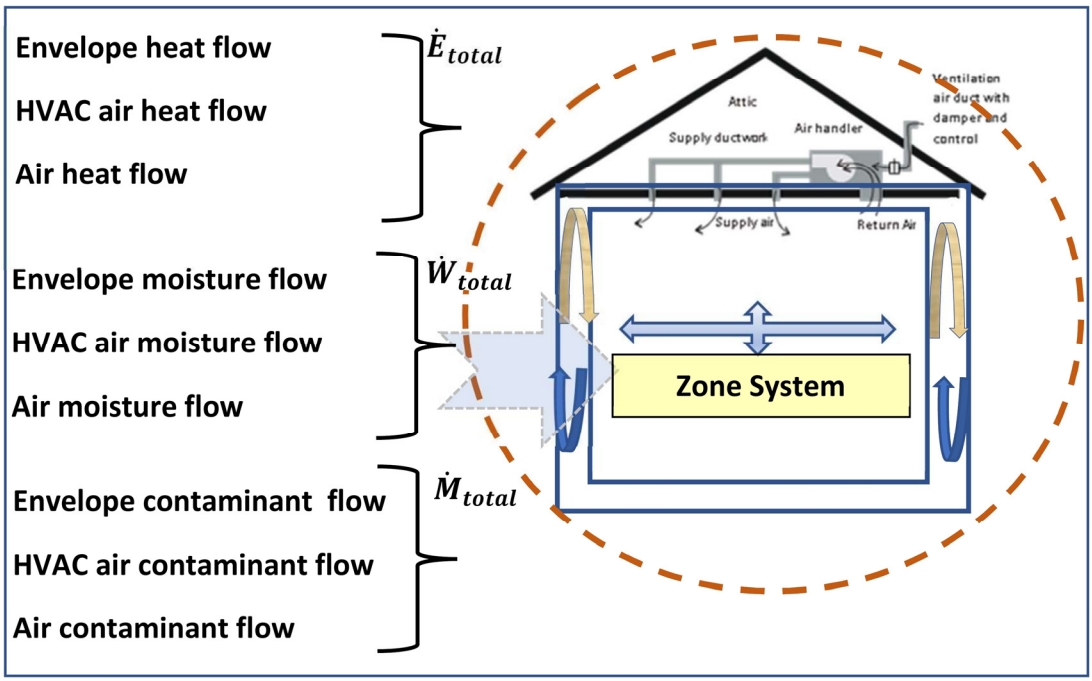

Figure 2.7 The governing equations balances for the zone system

2.5 Organization of papers extracted from doctoral research

In this research, a new model has been developed based on a combination of sub-models of EnergyPlus, CONTAM and WUFI using the co-simulation method. Since the combined model has been developed according to the flowchart of Figure 2.1 in 9 steps. The combination of EnergyPlus, CONTAM and WUFI has been evaluated in three phases using the co-simulation method. Three papers have been organized based on these three phases of co-simulation feasibility assessment.

2.6 A brief discussion of the first published paper subject to the development of EnergyPlus and CONTAM coupled model

The purpose of publishing first paper was to present the assumptions, methodology, results, discussion, and conclusions of the first phase for developing a coupled model. The development of a coupled model is evaluated only in the possibility of combining two models

of EnergyPlus as energy sub-model and CONTAM as indoor air quality sub-model, using the co-simulation method. In the introduction, a literature review has been investigated and focused on high-performance building design research using EnergyPlus tools for energy analysis and CONTAM for indoor air quality analysis. In the Methodology, the possibility of combining EnergyPlus and CONTAM has been investigated using the co-simulation method. The main factor in the co-simulation method between EnergyPlus and CONTAM models occurs due to the exchange of control variables between these models. This method, developed by Dols, Emmerich, & Polidoro (2016), uses the standard functional mock-up interface (FMI) to link EnergyPlus and CONTAM. FMI is a tool-independent standard that enables data exchange between the EnergyPlus and CONTAM models through a functional mock-up unit (FMU). For this purpose, the CONTAM model must be implemented in the standard functional mock-up interface (FMI). Therefore, the CONTAM model must be exported into a functional mock-up unit (FMU). In the last step of the Methodology section, a three-story house is described as a case study. To compare the capabilities of the coupled model with the single models of EnergyPlus and CONTAM, Montreal is used for this study as a cold and humid climate, Vancouver as moderate and humid and Miami as hot and humid climate conditions. To evaluate the accuracy of the coupled model developed based on the co-simulation method between EnergyPlus and CONTAM in comparison with the single models of EnergyPlus and CONTAM, three scenarios are defined for the case of a three-story house. The results of comparing the simulated energy and indoor air quality measures of these scenarios with the base case are presented in the results section. These scenarios include 1- airtight, 2-exhaust fan and 3- airtight with exhaust fan and filter upgraded. In the Results section minimum, average, and maximum values of air change rates, indoor PM_5 concentrations, indoor CO_2 concentrations, and indoor VOCs concentration as indoor air quality measures and electrical-gas energy consumptions as energy measures by cases of baseline with scenarios 1 to 3 have been evaluated.

2.7 A brief discussion of the second published paper subject to the development of CONTAM and WUFI coupled model

The second phase of the development of a coupled model with the subject to the feasibility study of CONTAM with WUFI has been performed using the co-simulation method. This paper is presented in sections of 1- Introduction, 2- Methodology, 3- Results, 4- Discussion and 5- Conclusion. In the Introduction section, literature of similar research on building performance modeling in indoor air quality, moisture and thermal comfort areas has been reviewed The Methodology section has been performed in four steps. In step 1, the mechanism for combining CONTAM with WUFI in the development of a coupled model is described. The mechanism for combining CONTAM with WUFI in step 1, is performed based on the exchange of the main airflow control variable and the sub-variable of geometry between CONTAM and WUFI. In step 2, the governing equations of single and coupled models are investigated. The details of heat flow balance and moisture flow balance related to the WUFI sub-model and contaminant flow balance related to the CONTAM sub-model are described. In addition, the total airflow rate exchange procedure has been completely analyzed as the basis for the possibility of combining the coupled solutions of all three balance equations of heat, moisture and contaminant. In step 3, the case of a three-story house is defined by the coupled model in comparison with single models of CONTAM and WUFI to simulate indoor air quality and energy efficiency measures. In step 4, the accuracy of the coupled model is verified using a paired sample t-test method in two parts. These two parts include: (1) paired samples 'differences and (2) paired samples' correlations. To consider the advantages of the coupled model capability compared to the CONTAM and WUFI single models, the simulated measures in the fields of indoor air quality, moisture and thermal comfort have been compared with each other. To perform an analytical comparison, the ASHRAE Standard was used to compare the results simulated by each of the coupled and single models. In the Results section, four scenarios of airtight fan-off, airtight fan-on, leaky fan-off, and leaky fan-on for the case of a three-story house have been assumed. The percentage differences are calculated for indoor air quality, moisture and thermal comfort measures simulated by the coupled and single models,

and then compared with each other in three different climatic conditions of Montreal, Vancouver and Miami. Finally, the details of the reasons for differences in the results of the optimal scenarios simulated by the coupled models with the CONTAM and WUFI single models are analyzed.

2.8 A brief discussion of the third published paper subject to the development of EnergyPlus, CONTAM and WUFI combined model

The third paper is presented for research conducted in the third phase and is the final phase. The results of the possibility of combining EnergyPlus with CONTAM in the first phase and also the possibility of combining CONTAM with WUFI in the second phase has been evaluated. In this phase, based on the results of the previous two phases, the fully combined model has been developed. The presentation of the third phase for fully combined development in this paper includes 1- Introduction, 2- Methodology, 3- Results, 4- Discussion and 5- Conclusion. In the Introduction section, a literature review related to research on combined models has been performed. The results of past research showed that energy efficiency, indoor air quality and moisture performance measures can not be used separately to analyze building performance and need to be used in a combined method. The necessity to develop a combined model with the ability to calculate all three measures of energy efficiency, indoor air quality and moisture performance in this study is concluded as the main goal. The methodology is presented in four parts of subsections. In the first part, the combining EnergyPlus, CONTAM and WUFI mechanism using the co-simulation method is presented. In the second part, the governing equations with details of common control variables are presented. In the third part, the case study is defined along with floor plans, input data assumptions and other information. The method and details of verifying the accuracy of the combined model is analyzed in the fourth part. The combination mechanism of EnergyPlus, CONTAM and WUFI has been obtained based on the experience gained from the results of the first and second phases of this research. By using the paired sample t-test method, the accuracy of the combined model is verified. Four scenarios of 1- airtight fan-off, 2- airtight fan-on, 3- leaky fan-off and leaky fan-on have been defined. The results of the simulated measures of the combined model are

compared with the simulated results of the single models using the percentage difference method with an acceptable level of ASHRAE Standards 90.1, 62.1 and 160. Finally, the reasons for the differences between the simulated results of the optimal scenarios between the combined and single models are analyzed and the fully combined model has been recommended as a benchmark for the whole building performance analysis.

CHAPITRE 3

ASSESSING THE ENERGY AND INDOOR AIR QUALITY PERFORMANCE FOR A THREE-STORY BUILDING USING AN INTEGRATED MODEL, PART ONE: THE NEED FOR INTEGRATION

Seyedmohammadreza Heibati [a], Wahid Maref [a,] and Hamed H. Saber [b]

[a] Department of Construction Engineering, École de Technologie Supérieure (ÉTS), University of Québec, Montréal, QC H3C 1K3, Canada; Seyedmohammadreza.Heibati.1@ens.etsmtl.ca
[b] Prince Saud bin Thuniyan Research Center, Mechanical Engineering Department, Jubail University College, Al Jubail 35716, Saudi Arabia; SABERH@ucj.edu.sa

Paper published in Energies, MDPI, 14 December 2019

3.1 Abstract

In building applications, there is a dynamic interaction/coupling between the energy performance and the indoor air quality (IAQ) performance. Previously, the performance of energy consumption (EC) and IAQ has been evaluated independently. In this study, an energy performance model (EnergyPlus) and IAQ performance model (CONTAM: contaminant transport analysis) were simultaneously coupled as a new integrated simulation model in which the control variables were exchanged between the two models. As a result, the exchanges of temperature and airflow variables are corrected. The verification of the new model is based on the comparison of the simulation and analytical results of temperature and airflow variables. Thereafter, three scenarios of airtightness of the envelope only, exhaust fan ventilation only and both of airtightness envelope and exhaust fan with upgraded filters for an Air Handling System are defined for a 3-story house. In the first step, the IAQ and EC improvement parameter's part for scenarios 1 and 2 are simulated independently by the EnergyPlus model and CONTAM model. In the next step, these parameters are simulated in scenario 3 using the integrated simulation model. These simulations are performed for different weather conditions of Montreal, Vancouver and Miami. The positive and negative impacts of each scenario in different cities are compared and analyzed separately based on the single of EnergyPlus and

CONTAM capabilities with the integrated simulation model. The results of the integrated simulation model showed that the exchange of control variables between both EnergyPlus and CONTAM produced accurate results for the performance of both energy and IAQ. Finally, the necessity of using the present integrated simulation model is discussed.

Keywords: integrated simulation models; EnergyPlus; CONTAM; energy consumption; indoor air quality; heat; air and moisture transport

3.2 Introduction

A high-performance building is one of the most important goals in building research. More recently, the focus on energy-efficient buildings and their energy needs can be met annually with high-efficiency and high-energy sources locally (Federal, 2008). However, the effect of energy consumption (EC) in buildings on the indoor air quality (IAQ) is usually neglected (Kusiak, 1988). Nowadays, the accuracy of IAQ and airflow modeling in buildings has been reduced due to the limitation of being unable to consider the impact of some energy performance technologies simultaneously (Ng, Musser, Persily, & Emmerich, 2013).

The idea of coupling methodologies for energy and IAQ was first carried out by Adams et al. (Adams, Sgamboti, Sherber, & Thompson, 1993) using a coupled thermal–airflow model, in which the energy performance was improved by 20% and the contaminant level was reduced. Combined methods of modeling energy and airflow have been used in some energy simulation tools. These models are capable of simultaneously simulating energy and multi-zone airflow, but the limitation regarding accurate airflow calculations is the main problem (Gowri, Winiarski, & Jarnagin, 2009; Ng, Quiles, Dols, & Emmerich, 2018) proposed a method for estimating the infiltration in commercial buildings using EnergyPlus, which considers the effects of wind but not temperature, thus ignoring the stack effect and key building features, such as vertical shafts, in infiltration models. To the best of our knowledge, most building performance models in previous research studies have focused on energy consumption or indoor air quality aspects, and coupling methods have limitations in these models (Bai, Wang,

Zhu, & Zhang, 2003; Cai, Wu, Zhong, & Ren, 2009; Iwaro & Mwasha, 2010; Jin, Wu, Li, & Gao, 2009; Li & Yao, 2009).

In designing sustainable, human-friendly buildings, a number of multidisciplinary issues, such as ecology, energy consumption performance, thermal comfort, and indoor air quality interact with each other (Zhang, Bai, Chang, & Ding, 2011). Therefore, those issues should be grouped and addressed simultaneously using optimization techniques in two stages: (1) during the conceptual design of the building, and (2) during the post-occupancy stage (Fan & Ito, 2014). Energy consumption in existing buildings can be significantly reduced through appropriate retrofitting techniques (Ardente, Beccali, Cellura, & Mistretta, 2011; Chidiac, Catania, Morofsky, & Foo, 2011; Golić, Kosorić, & Furundžić, 2011; Hestnes & Kofoed, 2002; Xing, Hewitt, & Griffiths, 2011), and energy models should be used for optimizing the passive and active systems of the buildings (Heibati, Maref, & Saber, 2021c; Heibati & Atabi, 2013; Heibati, Atabi, Khalajiassadi, & Emamzadeh, 2013). As provided in many previous studies (e.g., see References (Kolokotsa, Tsiavos, Stavrakakis, Kalaitzakis, & Antonidakis, 2001; Neto & Fiorelli, 2008; Thörn, 1998)), there is a growing demand for the better performance of heating and ventilation systems as indoor environments affect occupants' well-being and productivity. Furthermore, the inefficient operation of HVAC (heating, ventilation, and air conditioning) systems may also cause some energy waste (Angel, 2012; Brambley et al., 2005).

Specific consideration was given to the energy simulation with the EnergyPlus model that uses a multi-zone thermal balance to calculate the energy loads based on the temperature and airflow generated by the HVAC (Crawley et al., 2001). Costanzo and Donn (Costanzo & Donn, 2017) used a coupled method for three EnergyPlus, UrbaWind, and Daysim simulation tools for thermal, CFD (computational fluid dynamics), and daylighting analysis, respectively. Using an integrated approach, it was possible to calculate the impact of the most relevant parameters on thermal and visual comfort with a high accuracy (Costanzo & Donn, 2017).

EnergyPlus calculates the amount of energy load needed for the HVAC systems. This energy load was calculated by Crawley et al. (Crawley et al., 2001) is based on the air temperature

zone generated by the HVAC systems and airflow rates. The EnergyPlus has a limited airflow network solver (AFN) that can calculate pressure-dependent interzone airflows for a limited airflow distribution (Energy, 2021). Because of the EnergyPlus' limitation in calculating interzone airflows using AFN tools, Shirzadi, Mirzaei, & Naghashzadegan (2018) used the coupling between an AFN cross-ventilation model and a CFD dataset output for an orifice-based model to increase the accuracy of the airflow rate prediction.

Complementary to EnergyPlus is a CONTAM (contaminant transport analysis) model that calculates the airflows in the whole multi-zone buildings (Feustel & Dieris, 1992). The CONTAM model calculates the airflow based on the contaminating concentrations generated in the whole multi-zone buildings. This model was developed by the National Institute of Standards and Technology (NIST) for the Standardization's Building and Fire Research Laboratory (BFRL) (Dols & Polidoro, 2015) . Currently, CONTAM assumes the airflow temperature to be the set point of the thermostat (Dols & Underhill, 2018). As none of these two models can calculate the effect of the interactions between temperature and air pressure fields, coupling between them was examined in Dols and Underhill (Dols & Underhill, 2018). Also, Chen, Gu, & Zhang, (2015) used EnergyPlus and CHAMPS (combined heat, air, moisture, and pollutant simulation)-Multi-zone to simulate IAQ.

In a typical parametric evaluation of building performance, one uses some assumptions to calculate the effect of the changes in other variables (Clark et al., 2019; Dols & Underhill, 2018). For example, when calculating energy consumption with EnergyPlus, one assumes the interzonal airflow rates. On the other hand, when calculating ventilation rates and the movements of pollutants for evaluating the IAQ, one assumes the temperature of air in different spaces.

The main objective of this research study called "Part 1" was to address the limitations of the single energy and IAQ models in the previous studies. As such, an integrated model called an "Integrated Simulation Model" was developed in this study. Due to the match between the CONTAM model and the EnergyPlus model for exchanging data capabilities of the airflows

and temperatures, they were used to develop the present integrated simulation model. In this model, a co-simulation method for exchanging the control variables of temperatures and airflow rates between EnergyPlus and CONTAM was used to simultaneously perform energy balance and mass balance calculations. Another study called “Part 2” that is currently being conducted is mainly focusing on developing an integrated model to couple the energy-end IAQ performance with the heat, air, and moisture (HAM) transport in building envelopes, subjected to different climatic conditions. The results of the Part 2 study will be published at a later date.

To highlight the limitations of using single models (i.e. the calculations of both the IAQ performance and the energy performance are not coupled) compared to the coupled model, the simulation results were compared to each other for energy and IAQ measures for a whole three-story house when it is subjected to the climatic conditions of Montreal and Miami. Finally, in this study, the results of the present integrated simulation model are provided to show the differences between its results in comparison with the CONTOM and EnergyPlus single models.

3.3 Methodology

In this study, the reason why EnergyPlus and CONTAM were adopted is that the Contam3DExporter tool input files can be used to convert these files to usable files for both models. This tool was used to exchange the control variables between the two models simultaneously. Furthermore, Contam3DExporter tool can replicate the input files that are needed for the EnergyPlus and ContamX based on the exchange of the actual temperature and the airflow rates of the control variables that are exchanged between ContamX and EnergyPlus with one-hour time steps over a period of 24 h. Thereafter, these variables were repeated for the next day.

In the first step, we started with the method of coupling between CONTAM ("CONTAM 3.2," 2021) and EnergyPlus (2021). In the second step, we compared the results obtained by using the EnergyPlus and CONTAM programs separately and those obtained by using the co-

simulation. As will be shown later, the analysis of different variables, such as air change rates, indoor particle concentrations, and electrical and gas energy consumptions in northern and southern climates suggested that it was important to incorporate changes enabling us to proceed with the integrated real time modeling.

3.3.1 Coupling procedure between EnergyPlus and CONTAM

The performed coupling procedure was based on the integrated calculation of the energy and mass balance equations. EnergyPlus computes the energy balance for the zones of the whole building using (Nouidui, Wetter, & Zuo, 2014).

$$\dot{E}_Z = \sum_{i=1}^{n_{zone}} \dot{m}_i C_p (T_{zi} - T_z) + \dot{m}_{inf} C_p (T_{out} - T_z) + \sum_{j=1}^{n_{surf}} h_{sj} A_{sj} (T_{sj} - T_z) + \dot{E}_{in} + \dot{E}_{havc}, \quad (3.1)$$

where the parameters $\dot{E}_z$, $\dot{E}_{in}$, and $\dot{E}_{hvac}$ are the heat rates for energy balance, internal thermal load, and thermal load of the HVAC systems, respectively. The parameters $T_z, T_{zi}, T_{out},$ and T_{sj} are, respectively, the temperatures of the zone, inter-zones, and outside and interior surfaces of the building. Also, the parameters $\dot{m}_i$, $\dot{m}_{inf}$, C_p, h_{sj}, and A_{sj} are the inter-zone mass airflow rates, infiltration airflow rate, specific heat of air, convective heat coefficients, and areas of the jth interface, respectively.

The inter-zone mass and infiltration airflow rates in Equation (3.1) are chosen by the software user. The HVAC-induced airflow rates in Equation (3.1) are also calculated based on the thermal comfort of set-point temperature for the whole building based on the energy balance. The mass balance in CONTAM model is performed using (see Equation (3.2)) (Nouidui, Wetter, & Zuo, 2014):

$$\sum_{i=1}^{n_{zone}} \dot{m}_i + \dot{m}_{inf} + \dot{m}_{hvac} = 0 \quad (3.2)$$

were,

$$\dot{m}_i = f(\Delta p_i^n, \rho_i), \tag{3.3}$$

$$\rho_i = f(T_z, T_{zi}) \tag{3.4}$$

The inter-zone airflow rates provided by Equation (3.3) are a function of the air pressure difference between the inter-zones (Δp_i^n) and the air density (ρ_i). The latter is a function of the zone temperatures (Equation (3.4)).

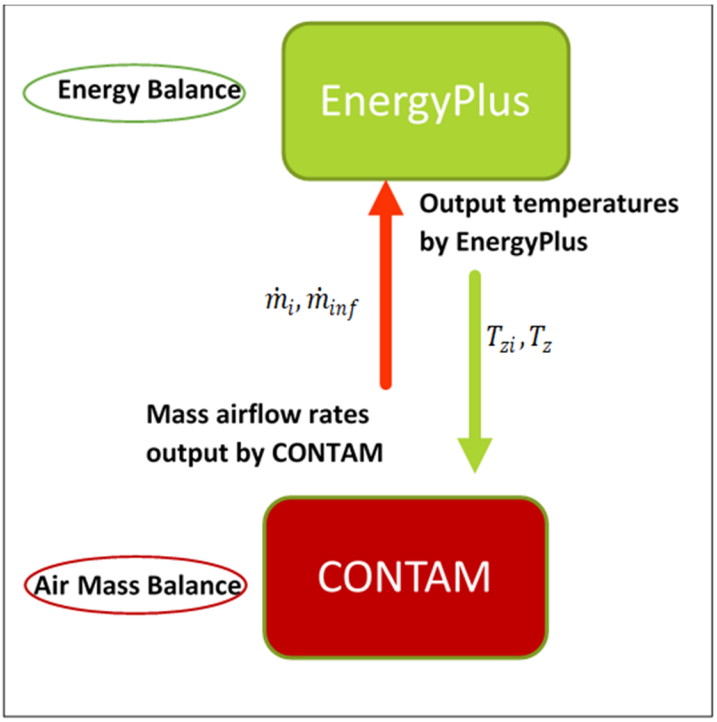

Figure 3.1 Coupling approach for EnergyPlus and CONTAM

As EnergyPlus performs the energy balance using the airflow rates calculated using CONTAM, and as the calculated zone and inter-zone temperatures via energy balance in EnergyPlus are used in the CONTAM, one can design an integrated model. As such, by co-simulating the mass and energy balances, it is possible to simultaneously simulate energy consumption, thermal comfort, and indoor air quality. According to Figure 3.1, EnergyPlus can use the output results of the system airflow rates calculated by the CONTAM mass balance procedures to perform energy balance calculations. For calculating the inter zones airflow rates, calculated zone and inter-zone temperatures by energy balance of EenrgyPlus are used

in CONTAM as well. Considering that the CONTAM system's airflow rates can be calculated using IAQ criteria, it is possible to improve thermal comfort and indoor air quality simultaneously by co-simulating the mass and energy balances.

3.3.2 Co-simulation method between EnergyPlus and CONTAM

The procedures of the co-simulation approach between EnergyPlus and CONTAM are shown in Figure 3.2 As shown in this figure, the PRJ file (project file) was designed using the format of CONTAM and the IDF file (input data file) was designed using the format of EnergyPlus. The process initially started with ContamW, which created plan information for each floor of the building as a PRJ file. The information in the PRJ file was entered into ContamX directly, which was the CONTAM simulation engine. On the other hand, the file from the Contam3DExporter tool was converted to an IDF file format. Thus, the initial data could be imported into EnergyPlus. The task of the 3DExporter tool was to convert the PRJ file into two types of VEF file (variable exchange file) and XML file (extensible markup language file) formats. The information in the VEF file and XML file were exchanged during the co-simulation process between ContamX and EnergyPlus according to Figure 3.2. Finally, the IDF file could be viewed and edited via SketchUp software (NREL, 2019). This file included geometry, infiltration airflow, inter-zone or mixing airflow, and HVAC system airflow.

During co-simulation, the data transferred from EnergyPlus to CONTAM included the zone temperature, ventilation system airflow, outdoor air fraction, exhaust fan airflow, air temperature, wind speed, biometric pressure, and wind direction information. In addition, the data transferred from ContamX to EnergyPlus included information on the infiltration airflow zone, inter-zone airflow, and the control value of airflow in user-defined contaminant level.

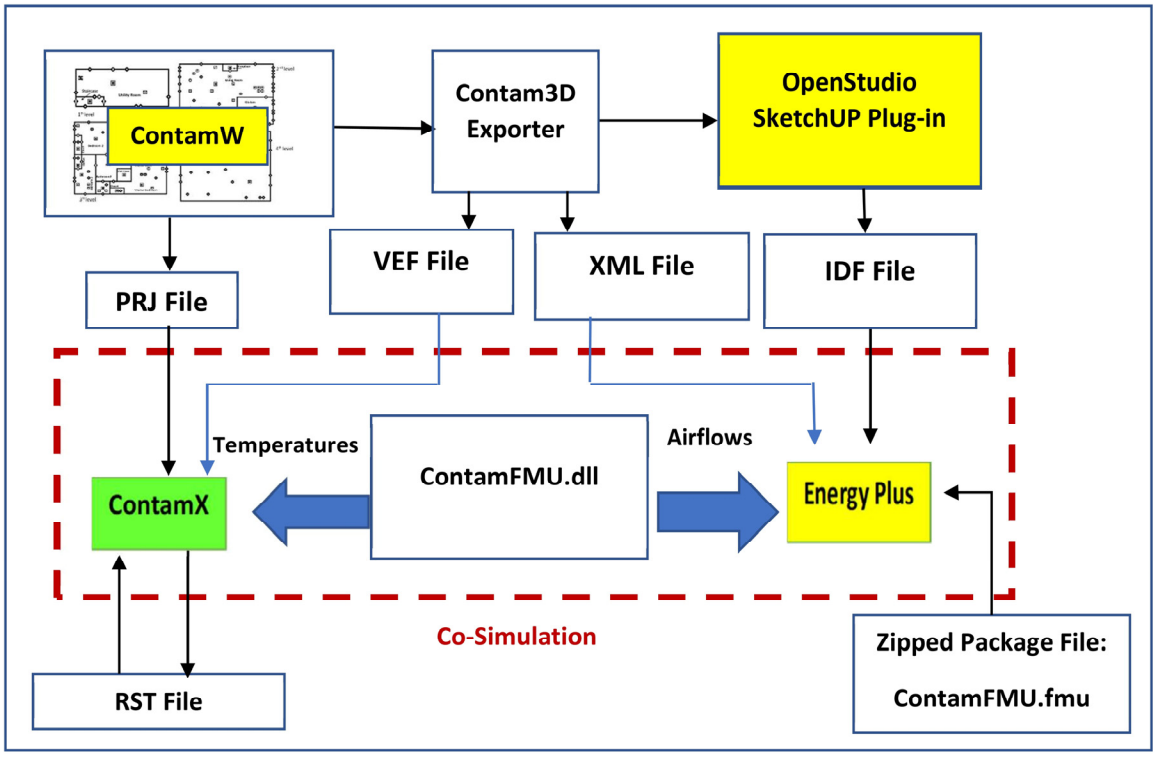

Figure 3.2 Co-simulation mechanism for EnergyPlus and CONTAM adapted from Dols et al. (2015), DLL: dynamic link library, FMU: functional mock-up unit, IDF: input data files, PRJ: project file, RST: restart file, VEF: variable exchange files, XML: extensible markup language files

Finally, the control variables of the zipped package file, called the Contam FMU (functional mock-up unit), were exchanged and distributed between ContamX and EnergyPlus. ContamX simulated a file with the RST (restart) file format to synchronize the time of data exchange between the two models within 24 h.

3.3.3 Governing equations

The calculations for the heat balance in different zones of the building were performed by EnergyPlus Figure 3.3 in three parts. First, the equations of heat transfer from all interfaces (walls, doors, windows) are described as (Equation (3.5)) (U.S. Department of Energy, 2021):

$$E_{conv} = \sum_{j=1}^{N} A_j h_j \left(T_{surf,j} - T_{zone}\right) \tag{3.5}$$

where N, A_j, h_j, $T_{surf,j}$, and T_{zone} are the number of surfaces in the room, the area of the *j*th interface, the convection coefficient of the *j*th interface, the temperature of the *j*th interface, the temperature of the *j*th interface, and the zone temperature, respectively.

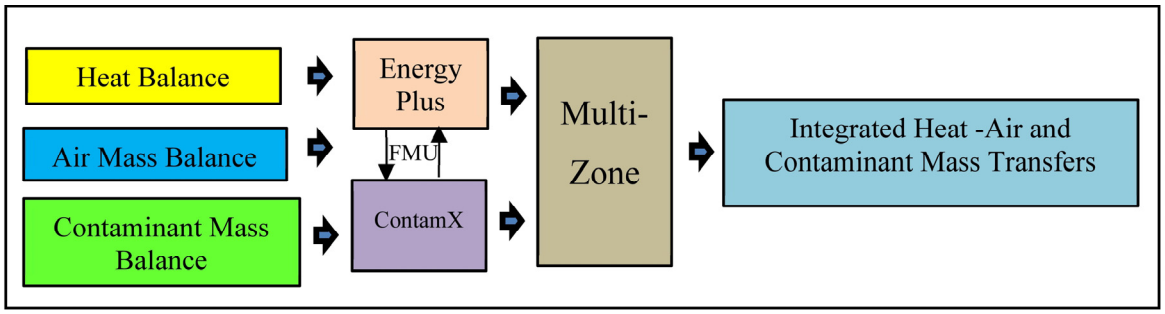

Figure 3.3 Integrated calculation method for heat, air mass, and contaminant mass balances based on governing equations of the model development

Next, the airflow heat transfer via infiltration–exfiltration and inter-zonal airflow is calculated using Equation (3.6) (Energy, 2021):

$$E_{flow,i} = \sum \dot{M}_{j\to i}^{air} \cdot C_p^{air}\left(T_{zone,i} - T_{ref}\right) - \sum \dot{M}_{i\to j}^{air} \cdot C_p^{air}\left(T_{zone} - T_{ref}\right) \tag{3.6}$$

where, $\dot{M}_{j\to i}^{air}$, C_p^{air}, $\dot{M}_{i\to j}^{air}$, $T_{zone,i}$, T_{ref}, and T_{zone} are the mass flow rate of air from *j* to *i*, specific heat coefficient of air, the mass flow rate of air from *i* to *j*, the temperature of the i_{th} zone, the temperature of the reference zone, and temperature of the zone, respectively. Finally, the thermal load of the HVAC system is determined as follows (U.S. Department of Energy, 2021):

$$E_{hvac} = E_{sup} - E_{ret} \tag{3.7}$$

$$E_{sup} = \dot{Q}_{sup} \cdot \rho_{sup} \cdot C_p^{air} \cdot \left(T_{sup,i} - T_{ref}\right) \tag{3.8}$$

$$E_{ret} = \dot{Q}_{ret} \cdot \rho_{ret} \cdot C_p^{air} \cdot \left(T_{zone,i} - T_{ref}\right) \tag{3.9}$$

where, E_{sup} and E_{ret} represent the HVAC supply duct heat flow and the HVAC return duct heat flow, respectively (Equation (3.7)). In Equations (3.8) and (3.9), $\dot{Q}_{sup}$, $\dot{Q}_{ret}$, ρ_{sup}, ρ_{ret}, C_p^{air}, $T_{sup,i}$, and $T_{zone,i}$ are the supply air duct volumetric flow rate, return air duct volumetric flow rate, supply air duct density, return air duct density, air specific heat at constant pressure, i_{th} supply air duct temperature, and the i_{th} zone air temperature, respectively.

The CONTAM model was used to calculate inter-zone airflow rates, infiltration airflow rates, and HVAC system airflow rates simultaneously for the whole building. The balance of the air mass rate between each node from zone *i* to zone *j* in CONTAM is performed using the driving forces as follows Equation (3.10) (Dols & Polidoro, 2015):

$$\dot{M}_{i\to j}^{air} = V_{zone,i}\frac{\partial \rho_i^{air}}{\partial t} = \sum_j^N \left(s_{i\to j}K_g\left|p_i - p_j\right|^{n_{i\to j}}\right) + \dot{M}_{sup}^{air} - \dot{M}_{ret}^{air} = 0 \tag{3.10}$$

where $V_{zone,i}$, ρ_i^{air}, $s_{i\to j}$, K_g, p_i, p_j, $n_{i\to j}$, $\dot{M}_{sup}^{air}$, and $\dot{M}_{ret}^{air}$ are the volume of zone *i*, density of airflow at zone *i*, flow direct sign (1 if $p_i < p_j$ and −1 if $p_i \geq p_j$), airflow coefficients, pressure field of zone *i*, pressure field of zone *j*, flow exponent from zone *i* to zone *j*, mass supply airflow rates, and mass return airflow rates, respectively. The mass balance provides the contaminant concentration transfer as follows (Dols & Polidoro, 2015):

$$\frac{dm_i^\alpha}{dt} = \sum_j F_{j\to i}\left(1-\eta_j^\alpha\right)C_j^\alpha + G_i^\alpha + m_i\sum_\beta K^{\alpha,\beta}C_i^\beta - \sum_j F_{i\to j}C_i^\alpha - R_i^\alpha C_i^\alpha \tag{3.11}$$

$$R_i^\alpha = \sum_\alpha R^\alpha C_i^\alpha \tag{3.12}$$

$$C_i^\alpha = \frac{m_i^\alpha}{m_i} \tag{3.13}$$

$$m_i = \sum_\alpha m_i^\alpha \tag{3.14}$$

The rate of mass gain of contaminant α in control volume *i* is calculated by Equation (3.11). Thus, $F_{j\to i}$, $F_{i\to j}$, C_i^α, C_i^β, C_j^α, G_i^α, m_i, η_j^α, $K^{\alpha,\beta}$, and R_i^α are inward flow rate of air from zone j to zone i, outward flow rate of air from zone i to zone j, concentration of contaminant α in

zone i, concentration of contaminant β in zone i, concentration of contaminant α in zone j, generation rate of contaminant α in zone i, mass of air in zone i, filter efficiency for contaminant α in the path from zone j to zone i, kinetic first order chemical reaction coefficient in zone i between contaminant α and β, and removal coefficient of contaminant α in zone i, respectively. In Equation (3.12), R^{α} is the gas constant of contaminants α and in Equation (3.13), the concentration of contaminants α in control volume i (C_i^{α}) is calculated using the ratio of the mass of the individual contaminants α (m_i^{α}) to the mass of air in control volume i (m_i). In Equation (3.14), the mass of air in control volume i (m_i) is calculated using the sum of the masses of the individual contaminants α in the control volume i (m_i^{α}).

The integrated simulation model can dynamically perform simultaneous heat, air mass, and contaminant mass balances. To solve the governing equations simultaneously, dynamic data is exchanged as control variables by the FMU between EnergyPlus and ContamX. The exchanged parameters from EnergyPlus to ContamX include zone outdoor temperature, outdoor environment data, ventilation system airflow rates for zone supply and return airflow rates, outdoor airflow fractions of outdoor airflow controllers, exhaust fan airflow rates, and energy recovery fan airflow rates (Dols & Polidoro, 2015). Furthermore, the exchanged parameters from ContamX to EnergyPlus include zone infiltration airflow rates, inter-zone airflow rates, and ventilation airflow based on the contaminant level (Dols & Polidoro, 2015). Finally, by exchanging the data of dynamic control variables, the integrated simulation model can calculate heat, air mass, and contaminant mass transfers, simultaneously, for the whole building.

3.3.4 Description of the case study

In this research study, the simulations of energy consumption (EC) and indoor air quality (IAQ) for a three-story house were performed when it was subjected to two different climatic conditions, namely those in Montreal and Miami. Table 3.1 lists the information on geometries, thermal properties, age of construction, and occupancy for the three-story house in the baseline case.

The basement, as a level 1 with a surface area of 24 m^2 and a volume of 72 m^3, had a hot-water heating system, gas furnace, and dryer. At level 2, with an area of 35 m^2 and a volume of 105 m^3, there was a living room with a fireplace, one bathroom, and one closet. Level 3 had a total area of 37 m^2 and a volume of 111 m^3, with two bedrooms and one master bedroom having its own bathroom and closet. The fourth level had an attic with a surface of 13 m^2 and a volume of 50 m^3. Table 3.2 provides the details of the climate characteristics for Montreal, Miami and Vancouver that were used to simulate a three-story house for different scenarios.

Table 3.1 Characterization of the parameters for a three-story house baseline case (reference case)

	Parameter	**Range/Type**
Geometry	Orientation	0°–180°
	Floor-to-Floor Height	3.6 m
	Floor-to-Ceiling Height	2.7 m
	Window-to-Wall Ratio: S, E, N, W	40%
Envelope	Roof Surfaces	Wood standard (construction), roof, build-up (exterior finish)
	Above Grade Walls	Wood frame, 2 × 6, in on centers (construction); wood/plywood (exterior finish); ¾ in fiberboard sheathing R-2 (exterior insulation)
	Ground Floor	Earth contact (exposure); six-inch concrete (construction); vinyl tile (interior finish)
	Top Floor Ceiling (Below Attic)	Drywall finish (interior finish); metal stud, 24-inch on centers (framing); R-19 batt (batt insulation)
	Ceilings	Plaster finish (interior finish)
	Floors	Vinyl tile (interior finish); six-inch concrete (construction)
Exterior Windows	Double PPG	Starphire/air/clear 6 mm (glass type); aluminum (frame type)
Occupants	A Family of Five People	An adult male, adult female, and three children of ages 5, 11, and 14 years
Age of Construction	22 Years	Renovated 5 years ago

The input data used in the EnergyPlus and CONTAM models included the dimensions, material properties, type of insulation, details of the weather data, type of flow paths, mechanical systems, details on contaminants and filter type, etc. The energy balance was always performed using EnergyPlus. Since the airflow rate can be calculated using CONTAM, this parameter had a very important role in transporting the energy generated by energy sources in HVAC systems. The energy transported by the airflow was transmitted between the inter-zones and the outdoor environment.

Table 3.2 Annual standard climate data adapted from ClimaTemps.com (2019)

Climate Characteristics			
Parameters	**Montreal**	**Vancouver**	**Miami**
Altitude (m)	27	4	5
Latitude	45°30′N	49°11'N	25°45′N
Longitude	73°25′W	123°10'W	80°23′W
Average Annual Max Temperature (°C)	11	14	28
Average Annual Temperature (°C)	6	10	24
Average Min Temperature (°C)	1	6	21
Average Annual Precipitation (mm)	1017	1167	1420
Annual Number of Wet Days	166	164	132
Average Annual Sunlight (hours/day)	5 h 05′	5 h 01’	8 h 03′
Average Annual Daylight (hours/day)	12 h 00′	12 h 00’	12 h 00′
Annual Percentage of Sunny daylight hours (Cloudy)	42 (58)	42 (58)	67 (33)
Annual Sun altitude at solar noon on the 21st day	44.8°	41.1	64.5°

ContamW is used to create the CONTAM project. All floor plans of each level for the case study of the 3-story house depicted in ContamW are shown in Figure 3.4. The CONTAM project included the geometry, weather data, transient contaminant data, airflow path elements, windows, air-handling systems (AHSs) and filters, duct elements, input controls, sinks and sources of contaminants and species, and other relevant data. Finally, the CONTAM project was created by ContamW in a PRJ file format. In the next step, by running CONTAM3DExport, the PRJ file was converted to an IDF file for EnergyPlus. The IDF file included building geometry, surface materials and constructions, air loops, exhaust fans, and partial external interface objects. The desired HVAC component was added to the IDF file in the IDF Editor to generate or remove energy, heating/cooling coils, internal gains, and

thermostats. Also, the IDF file was used to modify the rectangular elements using the Open Studio SketchUp Plug-in tool (NREL, 2019).

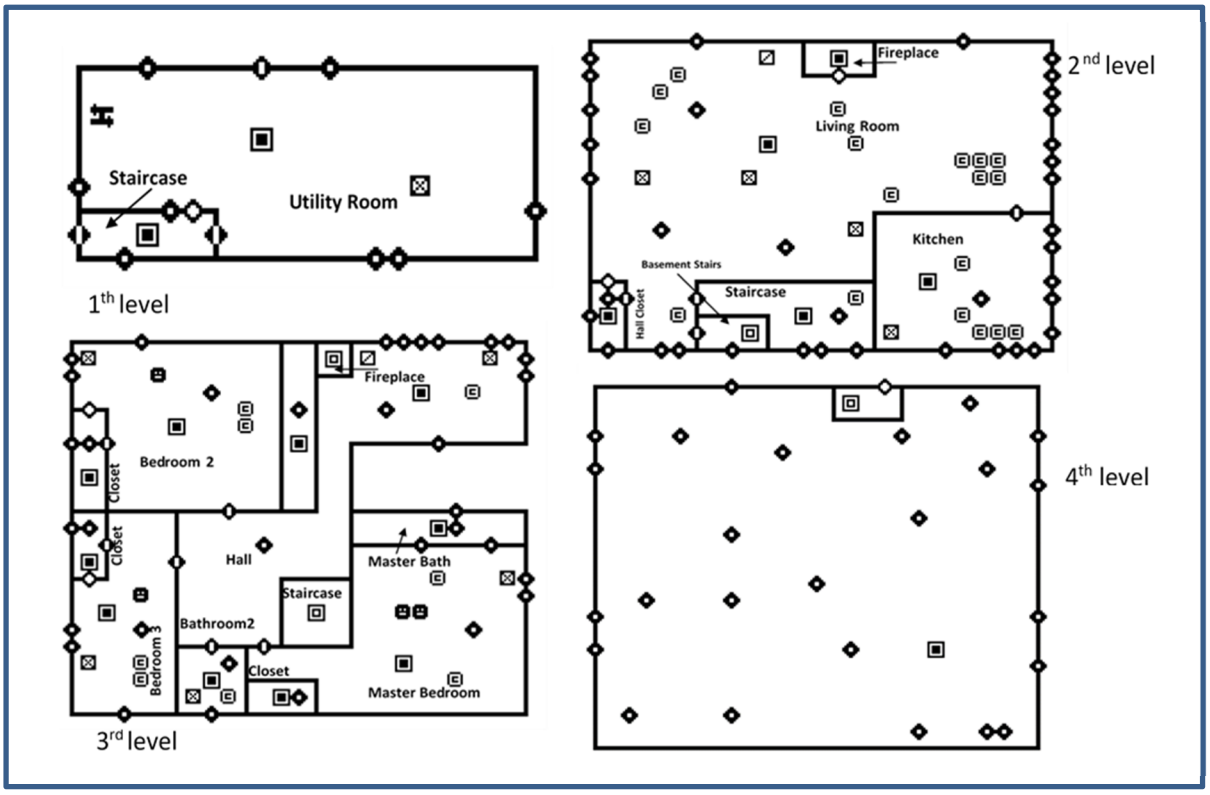

Figure 3.4 Floor plan of three-story house in ContamW

The IDF file, along with the ContamFMU.fmu file, was used in the same directory of EnergyPlus. The ContamFMU.fmu file is a zip file and was unzipped during the integrated simulation. This zip file included modelDescription.xml (extensible markup language file), contam.prj (project file), contam.vef (variable exchange file), ContamFMU.dll (dynamic link library), and contamx3.exe. These files contained parameters and algorithms created by EnergyPlus and were used to exchange the control variables between EnergyPlus and ContamX during the co-simulation process. In the time step setting for the co-simulation, the start and end dates of the contam.prj file in the ContamFMU.fmu file must be set together with the EnergyPlus IDF file. Before starting the co-simulation, the contam.prj and contamx3.exe files of ContamFMU.fmu files were copied to the next directory of EnergyPlus. ContamW then opened the contam.prj file and the co-simulation was set by exchanging control variables

between EnergyPlus and ContamX for a single day. At the end of the first day, the CONTAM restart file was generated as a project file used by ContamX during the warm-up period in the co-simulation. At the end of the co-simulation, ContamW could display the output results (Dols & Polidoro, 2015).

To show the differences in the results obtained by the single models (EnergyPlus and CONTAM) and those obtained by the present integrated simulation model, a three-story house was simulated when this house was subjected to several climatic conditions in North America. However, this paper presents the results of only three cities: (a) one cold and humid (Montreal), (b) cool and humid (Vancouver), and (c) a hot and humid city (Miami). The weather data for the year 2018 was used in this study. Figure 3.5 shows the monthly average temperature and relative humidity for Montreal, Vancouver and Miami. The city of Montreal has a humid climate with no dry season. The winters are cold, snowy, icy, and windy, with daily average temperatures from −9 °C to −11 °C (ClimaTemps.com, 2019). Summers are warm and humid with a daily average temperature between 26 °C and 28 °C (ClimaTemps.com, 2019). Spring and fall are pleasantly mild but there is a possibility of large changes in temperature in these seasons.

Vancouver is a temperate climate and has the warmest winter compared to other Canadian cities, with rain starting in mid-November and continuing through March (ClimaTemps.com, 2019). Vancouver is Canada's rainiest city. This city has a mild winter, with a daily average temperature of about 4 °C to 6 °C and average relative humidity of 86.3% and a summer daily average temperature of 14 °C to 19 °C and relative humidity of 79% (ClimaTemps.com, 2019).

The city of Miami has a tropical monsoon climate. The summer is hot and humid, and the winter is short and warm. In summer, the daily average temperature is between 29 °C to 35 °C and the average relative humidity is 71%. As shown in Figure 3.5, it also has a winter with a daily average temperature between 20 °C to 24 °C and a relative humidity of 79% (ClimaTemps.com, 2019).

In Figure 3.5, the monthly mean values of temperatures and relative humidity for Montreal, Vancouver and Miami have been compared for the year 2018. In these comparisons, it can be concluded that Miami is one of the warmest cities compared to the other two cities, with low fluctuations occurring at temperatures of 20 °C and 28 °C and relative humidity varying between 64% and 83% during the year. Vancouver also has a temperate climate, with temperatures oscillating between 4 °C in February and 19 °C in July for a year. Montreal has relatively cold winters and warm, humid summers, and therefore temperature fluctuates from -9 ° C in January to 24 ° C in July and relative humidity oscillation ranges from 59% to 81%. Due to the climate differences, in this study, the obtained results using the single models of EnergyPlus and CONTAM methods are compared with that obtained using the integrated simulation model for these cities.

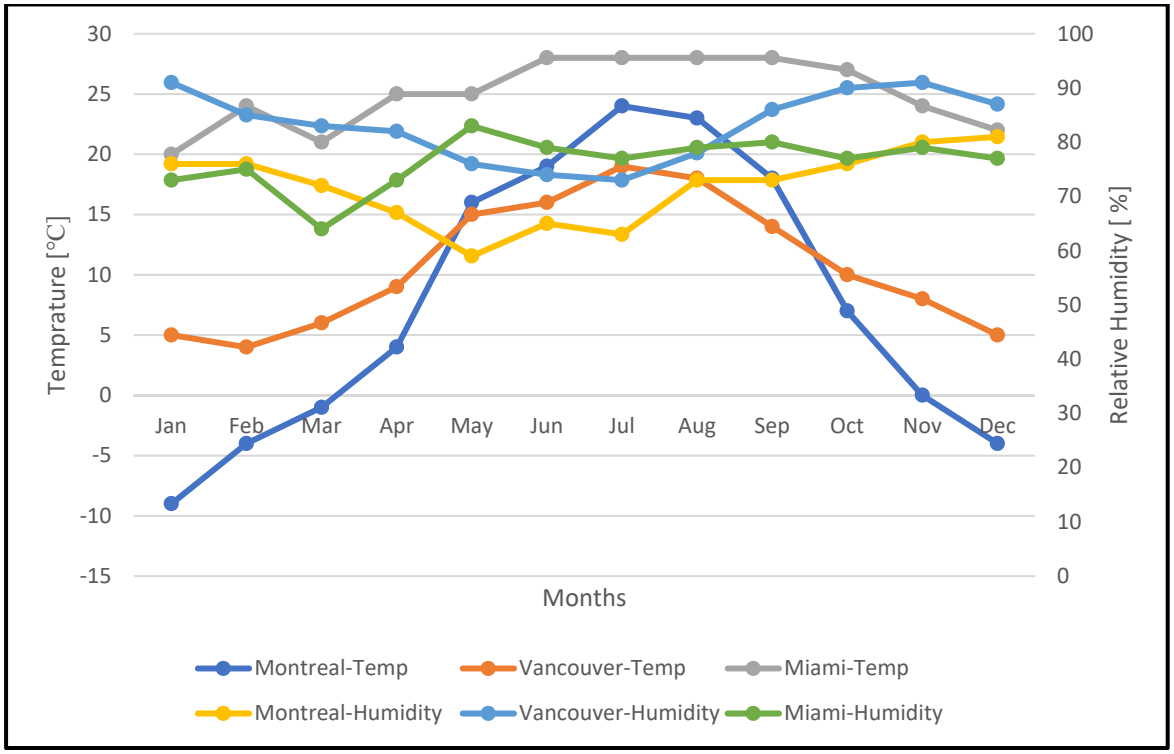

Figure 3.5 Monthly average air temperature and relative humidity for Montreal, Vancouver and Miami, data adapted from ClimaTemps.com (2019)

3.4 Results

For the scenarios listed in Table 3.3, this section provides the simulation results of (1) energy consumption (EC) and indoor air quality (IAQ) obtained by the single models for the baseline scenario as a reference, (2) EC and IAQ obtained by the single models for scenario 1, 2 and (3) EC and IAQ obtained by the present integrated simulation model for scenario 3.

Table 3.3 Status of the proposed scenarios compared to the baseline

Cases		Airtightening	Exhaust Fan	Filter Upgrading
1	Baseline	No	No	No
2	Scenario 1	Yes	No	No
3	Scenario 2	No	Yes	No
4	Scenario 3	Yes	Yes	Yes

The simulated variables in all scenarios listed in Table 3.3 include: (a) air exchange rates, (b) indoor particle concentrations, (c) indoor CO_2 concentrations, (d) indoor VOCs concentrations, and (e) the electrical and gas energy consumptions. In scenarios 1, 2 the single models of EnergyPlus and CONTAM were used independently to simulate these variables. The variables of scenario 3, however, were simulated by the present integrated simulation model. To better evaluate the models' accuracy, the variables of scenario 3 were also simulated by the single models. In this case, we can easily show the differences between the results obtained by the single models and those obtained by the present integrated simulation model.

3.4.1 The baseline case

In the baseline, the air change rates and concentrations of indoor contaminants for CO_2 and particles were simulated under the different climatic conditions of Montreal and Miami. The

three-story house for a population of five persons was defined as having an air-handling system of 0.40 m^3/s and a MERV (minimum efficiency reporting value) 4 filter for the baseline. PM_5 particles in the range of 5.0 µm to 10 µm were considered in this research study. Concentration rate values were considered for indoor particle sources based on the measurements by Elbayoumi et al. (2014). Given that one of the sources of indoor CO_2 generation is the occupants, its concentration values were assumed to be 24.4 mg/s for sleeping status and 40 mg/s for awake status according to the ASHRAE (American society of heating, refrigerating and air-conditioning engineers) standard (ASHRAE, 2017). Another source of CO_2 is the outdoor air with a concentration of 348.57 ppm (630 mg/m^3) (Persily, 1998).

Sources of indoor VOCs generations are selected and used for each room of the house based on the measurements made by Myatt (2015). The value of outdoor VOCs concentration is used based on the measurements conducted by Persily (1998).

For Montreal, the outdoor particle concentrations used were based on the measurements by Smargiassi, Baldwin, Pilger, Dugandzic, & Brauer (2005). Also, the outdoor particle concentrations used for Vancouver and Miami were based on the measurements by Travers, Higbee, & Hyland (2007) and Cao, Yang, Lu, & Zhang (2011), respectively.

3.4.2 Results of scenarios 1 through 3

For scenario 1, only the airtightness of the building enclosure was improved by 45% of the baseline scenario. In scenario 2, to reduce indoor particles, CO2 and VOCs concentrations, the type of ventilation is improved from infiltration only to exhaust fan. For this purpose, the exhaust fan with 50 L/s airflow rate is used. Scenario 3, however, included a combination of enclosure air tightening, ventilation upgrading to exhaust fans, and filter upgrading to MERV (minimum efficiency reporting value) 12.

For Montreal, Vancouver, and Miami, the simulation results were obtained using CONTAM, EnergyPlus, and the present integrated simulation models for scenarios 1, 2 and 3. The

minimum, average, and maximum values of air change rates, indoor particle concentrations PM_5, indoor CO_2 concentrations, indoor VOCs concentrations, and electrical and gas energy consumptions are shown in Figures 3.6–3.11.

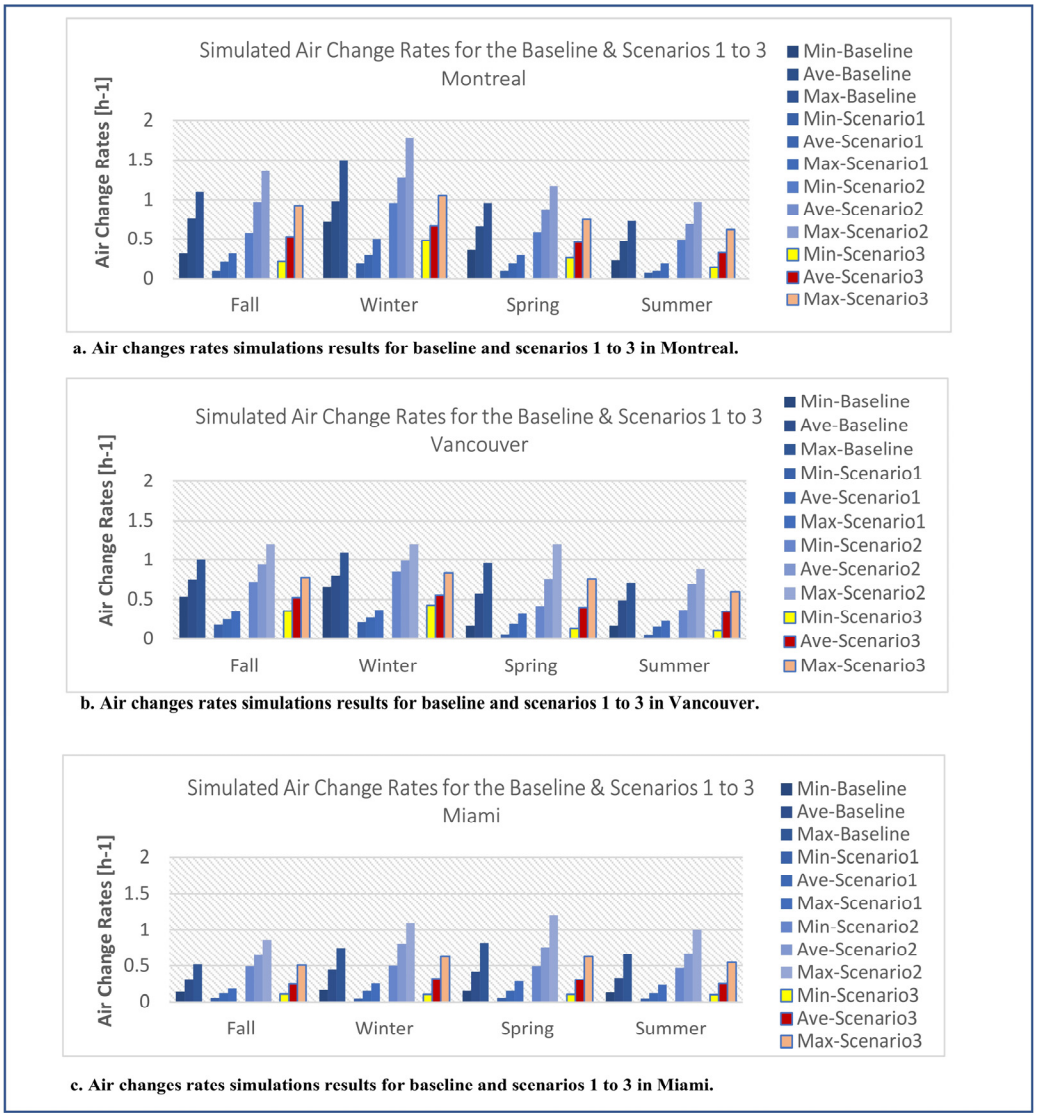

Figure 3.6 Simulation results for air change rates in the baseline, scenarios 1 to 3 for (a) Montreal adapted from Heibati et al. (2019a, p 5), (b) Vancouver, and (c) Miam

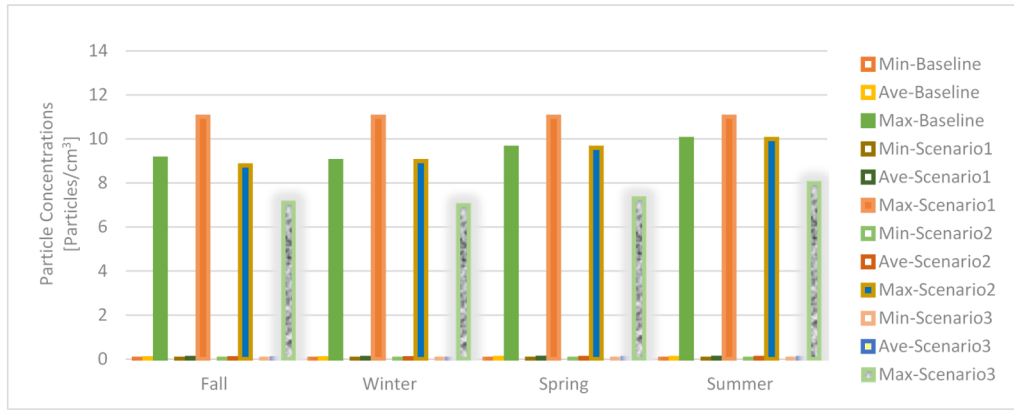

a. Indoor particles concentrations (P5) simulations results for baseline and scenarios 1 to 3 in Montreal.

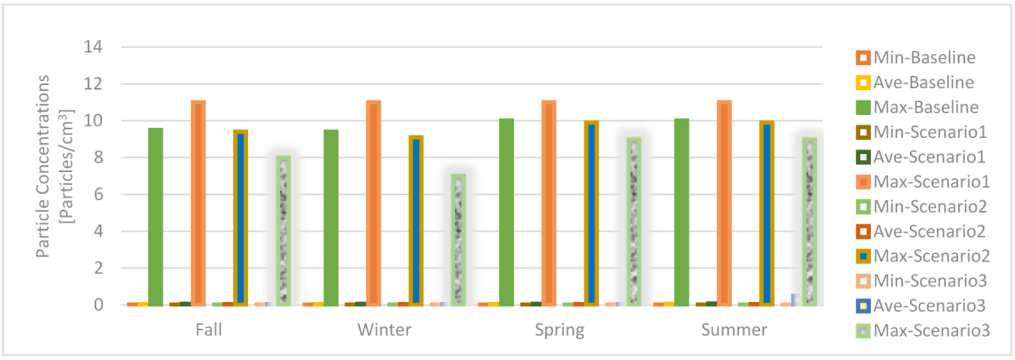

b. Indoor particles concentrations (P5) simulations results for baseline and scenarios 1 to 3 in Vancouver.

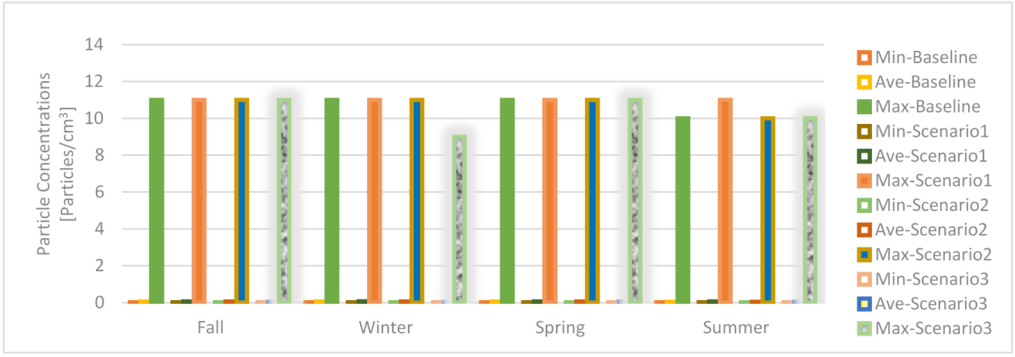

c. Indoor particles concentrations (P5) simulations results for baseline and scenarios 1 to 3 in Miami.

Figure3.7 Simulation results for indoor particle concentrations (PM_5) in the baseline and scenarios 1 to 3 for (a) Montreal adapted from Heibati et al. (2019a, p 5), (b) Vancouver, and (c) Miami

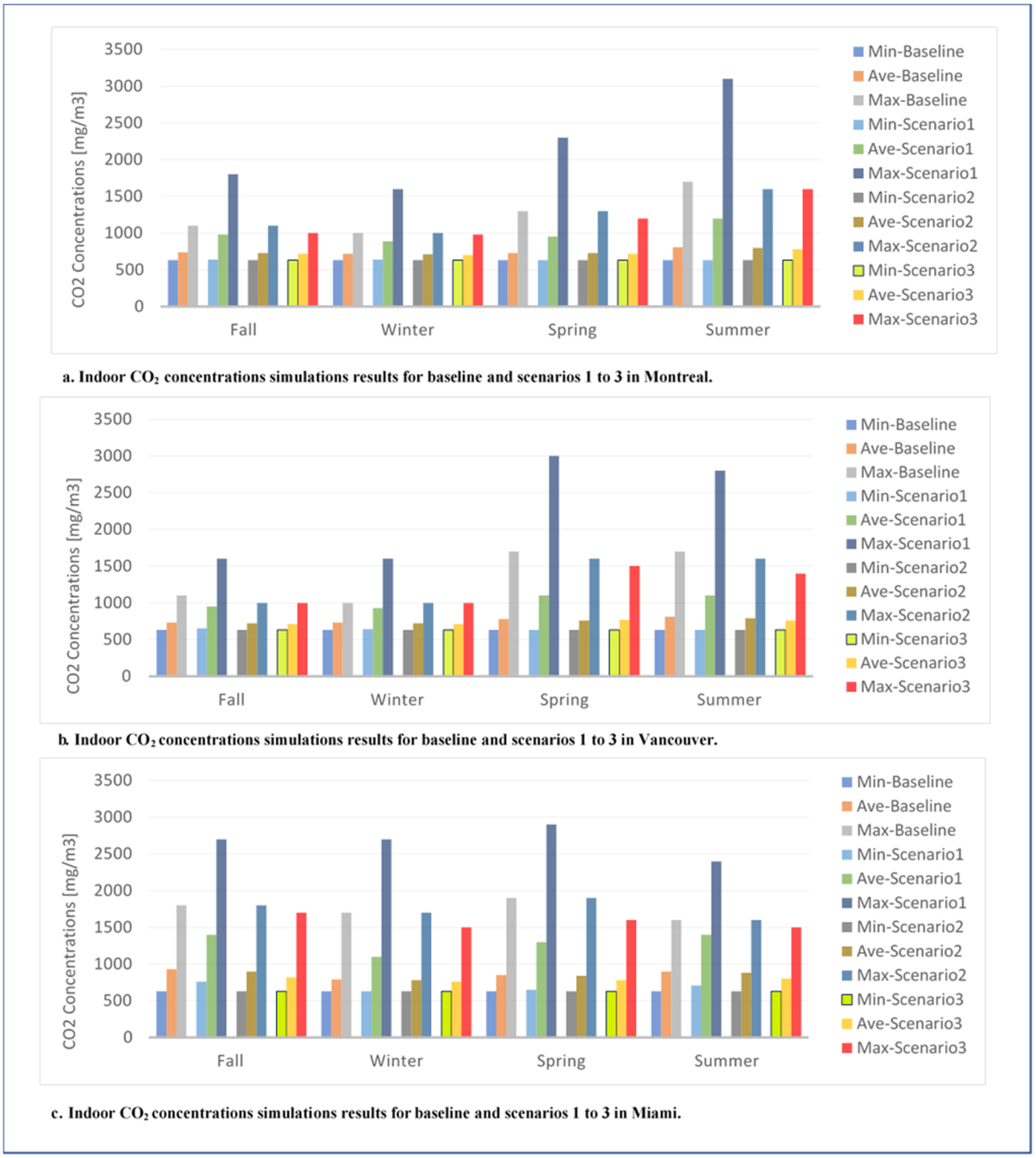

a. Indoor CO_2 concentrations simulations results for baseline and scenarios 1 to 3 in Montreal.

b. Indoor CO_2 concentrations simulations results for baseline and scenarios 1 to 3 in Vancouver.

c. Indoor CO_2 concentrations simulations results for baseline and scenarios 1 to 3 in Miami.

Figure 3.8 Simulations results for the indoor CO_2 concentrations in the baseline and scenarios 1 to 3 for (a) Montreal, (b) Vancouver, and (c) Miami

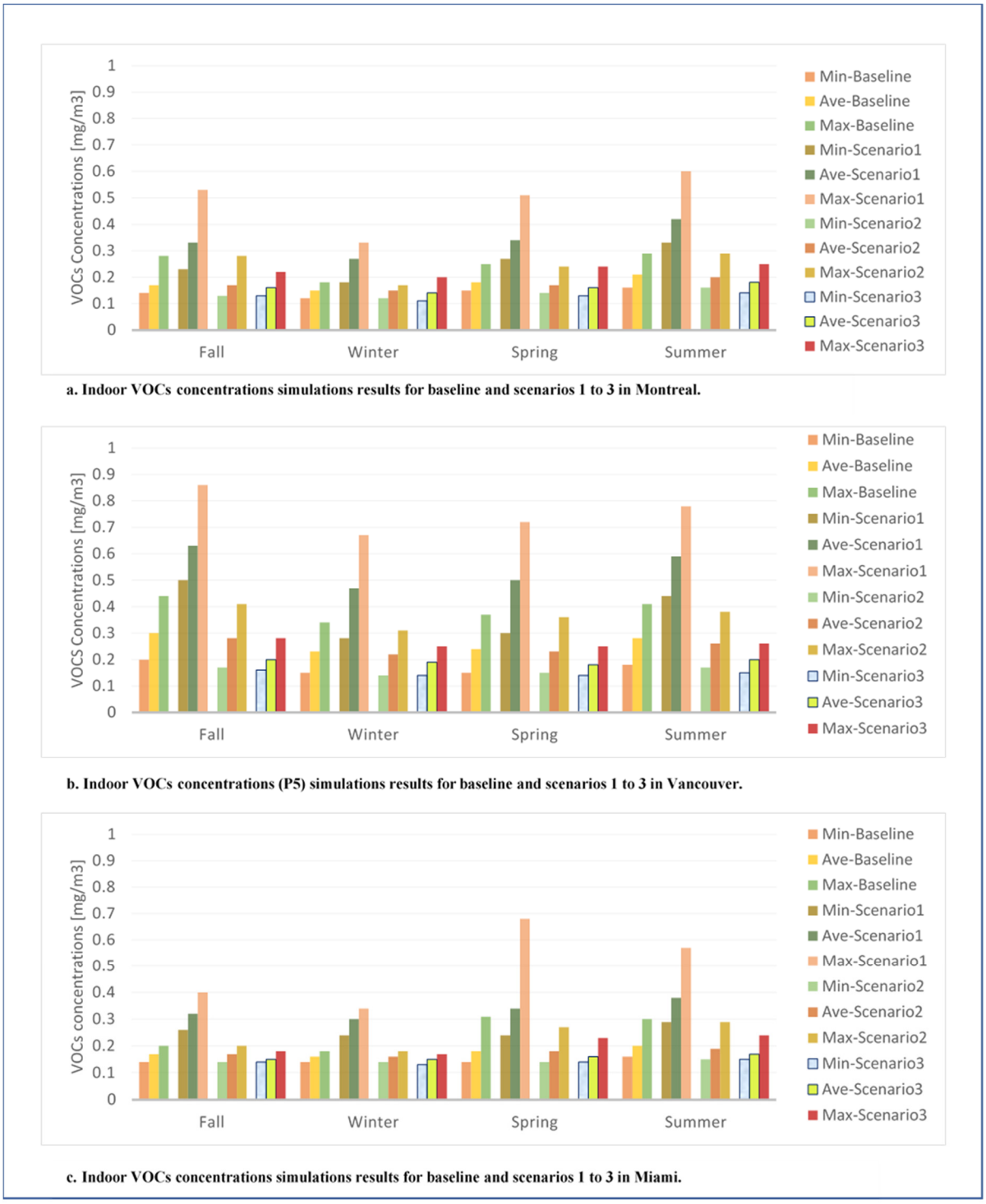

Figure 3.9 Simulations results for indoor VOCs concentrations in the baseline and scenarios 1 to 3 for (a) Montreal, (b) Vancouver, and (c) Miami

a. Electric energy consumptions simulations result for baseline and scenarios 1 to 3 in Montreal.

b. Electric energy consumptions simulations result for baseline and scenarios 1 to 3 in Vancouver.

c. Electric energy consumptions simulations result for baseline and scenarios 1 to 3 in Miami.

Figure 3.10 Simulation results for electrical energy consumptions in the baseline and scenarios 1 to 3 for (a) Montreal, (b) Vancouver, and (c) Miami

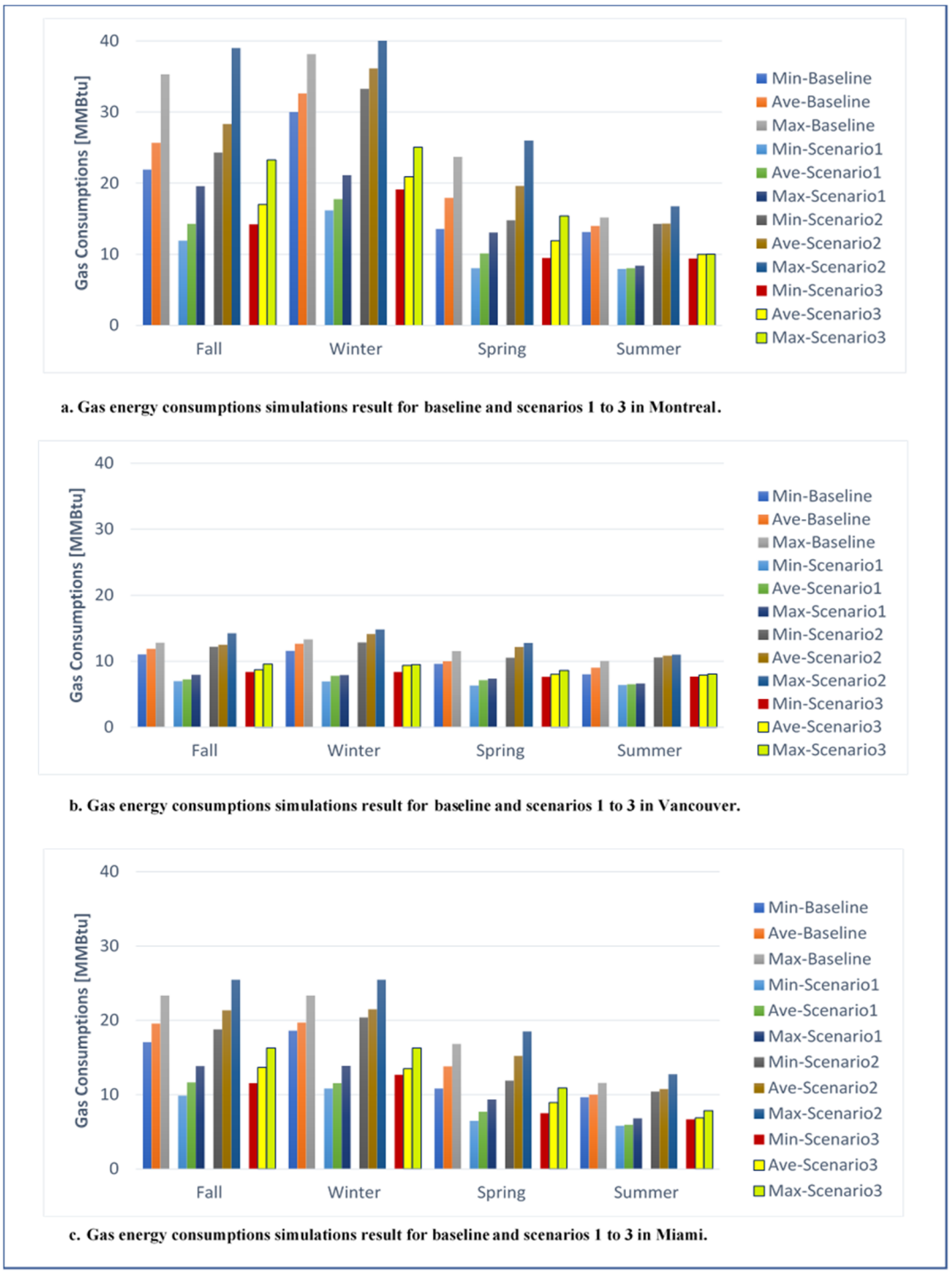

Figure 3.11 Simulations results for gas energy consumptions in the baseline and scenarios 1 to 3 for (a) Montreal adapted from Heibati et al. (2019a, p 5), (b) Vancouver, and (c) Miami

For different climatic conditions, Table 3.4 compares the percentage of the average decrease (↓) or average increase (↑) in the annual values of each scenario in relation to the baseline measures for the air change rates, indoor particle concentrations PM_5, indoor CO_2 concentrations, indoor VOCs concentrations, and gas and electrical energy consumptions.

Table 3.4 Comparisons of energy consumption (EC) and indoor air quality (IAQ) measures for the baseline and scenarios 1 to 3 based on the percentage of average changes

	Percentage Ratio of Average Decrease (↓) or Increase (↑) Annual Values of Each Scenario per Baseline Measures (%)																	
Measures	**Air change Rates**			**Indoor PM_5 Concentrations**			**Indoor CO_2 Concentrations**			**Indoor VOCs Concentrations**			**Electric Energy Consumptions**			**Gas Energy Consumptions**		
Cities	Montreal	Vancouver	Miami	Montreal	Vancouver	Miami	Montréal	Vancouver	Miami	Montréal	Vancouver	Miami	Montréal	Vancouver	Miami	Montréal	Vancouver	Miami
Scenario 1	70 %↓	66.6%↓	65 %↓	16.7%↑	13.1%↑	2.4%↑	44.6%↑	41.2%↑	43.6%↑	90.4%↑	91.2%↑	104 %↑	14.2%↓	11.1%↓	28.4%↓	44.3%↓	41.5%↓	35.2%↓
Scenario 2	33.2%↑	29.4%↑	85.9%↑	0.8%↓	1.5%↓	0 %	1.2%↓	3.3%↓	0.5%↓	2.6%↓	3 %↓	6.4 %↓	17.5%↑	13%↑	11.7%↑	11%↑	9.3%↑	12.9%↑
Scenario 3	26 %↓	26.5%↓	20.9%↓	21.8%↓	14 %↓	4.7%↓	3.7%↓	6.4%↓	7.8%↓	9.7%↓	11.8%↓	27.1%↓	2.6%↓	7.7%↓	15.2%↓	34 %↓	31.7%↓	22.5%↓

Figures 3.6–3.11 show the simulation results (air change rates, indoor particle concentrations PM_5, indoor CO_2 concentrations, indoor VOCs concentrations) obtained by CONTAM and the results obtained by EnergyPlus (gas and electrical energy consumptions). These results were obtained for three different climates (Montreal, Vancouver and Miami).

3.5 Discussion

Given the improved energy consumption due to the envelope airtightness in scenario 1, this condition negatively affected both the indoor air quality (IAQ) and air exchange rates. The air change rate values in scenario 1 are shown in Figure3.6 a, b and c for each of the three different cities of Montreal, Vancouver and Miami, respectively. Based on ASHRAE 62.2 (ASHRAE, 2016b), the air change rates should not be below the rate of 0.35 h^{-1}. In Montreal, the average air change rates in the fall, winter, summer, and spring were calculated to be 0.21 h^{-1}, 0.33 h^{-1}, 0.2 h^{-1}, and 0.33 h^{-1}, respectively, which were below the ASHRAE standard value. In Vancouver (Figure 3.6 b), the air change rates in scenario 1 are below the ASHRAE 62.2

Standard, for spring and summer only calculated at 0.18 $h^{-1}$and 0.14 h^{-1}, respectively. Additionally, in Miami (see Figure 3.6 c), the average air change rates in scenario 1 were also below the ASHRAE 62.2 Standard for fall, winter, spring, and summer (0.11 h^{-1}, 0.15 h^{-1}, 0.16 h^{-1}, and 0.13 h^{-1}, respectively).

The obtained values for the concentrations of indoor contaminants in scenario 1 are shown in Figures 3.7 to 3.9 for all three cities of Montreal, Vancouver and Miami. In scenario 1, the average concentration of indoor particles (PM_5) in the three cities was the same value of 3.68 particles/cm^3 (Figures 3.7a, b and c). Furthermore, the average indoor CO_2 concentrations for the cities of Montreal, Vancouver and Miami were calculated as 1280 mg/m3, 1302.5 mg/m3 and 1554.17 mg/m3, respectively (Figures 3.8a, b and c). Therefore, it can be concluded that scenario 1 in Miami is the worst in terms of indoor CO_2 concentration compared to the other two cities. The average indoor VOCs concentrations of scenario 1 for Montreal, Vancouver and Miami were 0.36 mg/m3, 0.36 mg/m3 and 0.56 mg/m3, respectively (Figures 3.9a, b and c). In scenario 1, Miami is the worst condition in terms of indoor VOCs concentrations compared to the other cities. Also, in scenario 1, the indoor VOCs concentrations are similar for Montreal and Vancouver.

Regarding the energy performance, the envelope airtightness in scenario 1 resulted in reducing the energy consumption (EC) where the highest annual average decrease ratio of the air change rates with the baseline scenario for the city of Montreal was 70%. This decrease in this ratio resulted in air change rates of less than 0.35 h^{-1}, which is not recommended by the ASHRAE 62.2 Standard (ASHRAE, 2016).

For the different scenarios, the results of the changes in the concentration of indoor contaminants are compared in Figures 3.7 through 3.9. Using an exhaust fan with 50 L/s airflow rate in scenario 2 leads to increase electrical and gas consumptions. The impacts of scenario 2 on increasing electricity and gas consumptions for Montreal, Vancouver and Miami, are shown in Figures 3.10 through 3.11. The average electrical energy consumptions for scenario 2 in Montreal, Vancouver and Miami were calculated as 1.62 MWh, 1.09 MWh, and

3.05 MWh, respectively (Figures 3.10a, b and c). Scenario 2 in the hot climate condition of Miami has resulted in the highest consumption of electricity compared to the other cities (Figure 3.10c). On the other hand, the average gas energy consumption for the cities of Montreal, Vancouver and Miami were also calculated as 25.75 MMBtu, 17.7 MMBtu and 12.37 MMBtu, respectively (Figures 3.11a, b and c). Scenario 2 would have the highest gas consumption in the city of Montreal, which is the coldest city compared with the other cities (Figure 3.11a).

To reduce the indoor contaminant, by installing an exhaust fan with 50 L/s airflows in scenario 2, the annual average decrease ratio of indoor particle concentrations (PM_5) to the baseline scenario for Montreal, and Vancouver is 0.8% and 1.5%, respectively, and for Miami is unchanged. The annual average decrease ratio of CO_2 concentrations to the baseline scenario for the cities of Montreal, Vancouver and Miami were calculated at 1.2%, 3.3% and 0.5%, respectively. Also, the annual average decrease ratio of VOCs concentrations to baseline scenario for the three cities of Montreal, Vancouver and Miami were calculated as 2.6%, 3% and 6.4%, respectively. Comparing these results, it can be concluded that the installation of an exhaust fan only in scenario 2 had very little effect on the reduction of indoor contaminants, and even in Miami for indoor particle concentrations, no changes have been made compared to the baseline scenario. The most calculated impact of IAQ improvement for scenario 2 is related to the annual average decrease ratio of VOCs concentration in Miami.

To improve EC in scenario 3, the exterior envelope was more airtight, i.e. 42% higher than the baseline. In addition, to improve the IAQ in scenario 3, an exhaust fan with a capacity of 26 L/s was changed to continuous ventilation. A highly efficient particle air filter (MERV 12) was used to further reduce the indoor particle concentration. The improvements in the EC and IAQ obtained with the present integrated simulation model in scenario 3 are provided in Table 3.4.

In scenario 3, the results for the case of envelope airtightness, and exhaust fan installations were obtained using the integrated simulation model where the filter was upgraded from a MERV 4 to a MERV 12 AHS. Therefore, the possibility of a simultaneously controlled

improvement of EC and IAQ could be investigated. Scenario 3 could therefore have the greatest impact on both the reduction of electric and gas consumption and the reduction of indoor contaminant concentrations. Comparing the energy parameters, it can be concluded that scenario 3 has the highest annual average decrease ratio of electric and gas energy consumption compared to the baseline scenario for Miami and Montreal cities of 15.2% and 34%, respectively. This improvement in Miami is due to the improvement of the controlled envelope airtightness and exhaust fan ventilation status in scenario 3, which has the greatest effect for hot cities such as Miami in reducing the consumption of electric energy to space cooling of the whole building in the hot days compared to other scenarios and baseline scenario. On the other hand, the same improvement in scenario 3 in Montreal has the greatest impact on reducing gas energy consumption due to less need for gas fuel to space heating the whole building on very cold days. In terms of decreasing indoor contaminant concentrations, the integrated simulation model calculates the greatest impact of scenario 3 on an annual average decrease ratio of indoor particulate (PM_5) concentrations, indoor CO_2 concentrations, and indoor VOCs concentrations to the baseline scenario with values of 21.8% for Montreal, 7.8% and 27.1% for Miami, respectively.

According to Table 3.4, the difference in electricity consumption in scenario 1 with baseline obtained by EnergyPlus for Montreal, Vancouver and Miami were calculated as -14.2%, -11.1% and -28.4%, respectively, and for scenario 2, were obtained 17.5%, 13% and 11.7%, respectively. This difference in electricity consumption between scenario 3 and the baseline was obtained from the integrated simulation model for Montreal, Vancouver and Miami as -2.6%, -7.7% and -15.2%, respectively. To illustrate the differences in energy results as a result of using EnergyPlus only versus the integrated simulation model (see Figure 3.12), a comparison of the percentage of this difference with the baseline scenario for gas energy consumption is shown as a measure of energy results. According to Figure 3.12, the difference in gas energy consumption results obtained by EnergyPlus with baseline in scenario 1 for Montreal, Vancouver and Miami were calculated as -44.3%, -41.5% and -35.2%, respectively, and for scenario 2, were obtained as 11%, 9.3% and 12.9%, respectively. If the integrated simulation model is used to calculate the difference in gas energy between scenario 3 and

baseline, this difference would be like -34%, -31.7% and -22.5% for the cities of Montreal, Vancouver and Miami, respectively. (See Table 3.4).

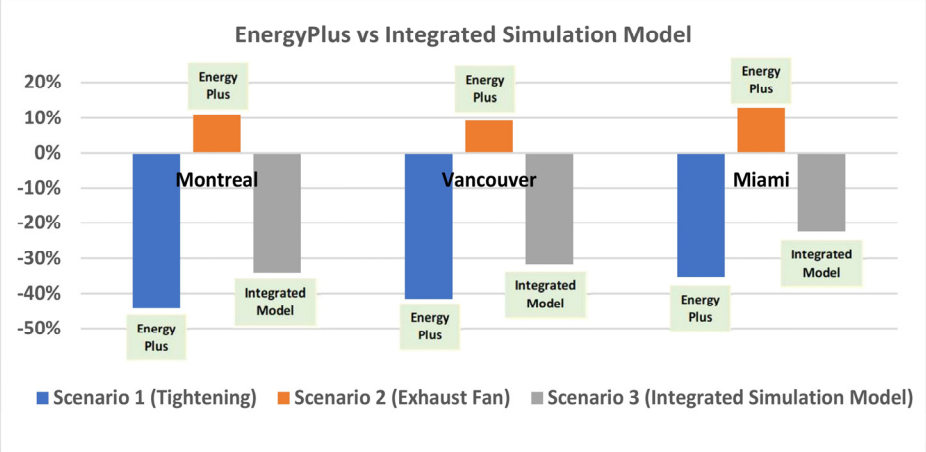

Figure 3.12 Comparison of energy percentage difference with the baseline as a result of using EnergyPlus only vs the integrated simulation model for gas energy consumption

As shown in Figure 3.13, the difference between IAQ results as a result of using CONTAM only versus the integrated simulation model with a baseline for indoor particle concentrations (PM_5) is presented as the measure of the IAQ. According to Figure 3.13, the difference in indoor particle concentrations (PM_5) was obtained by CONTAM in scenario 1 with the baseline for Montreal, Vancouver and Miami were calculated as 16.7%, 13.1% and 2.4%, respectively, and also these differences for scenario 2 with a baseline were obtained in Montreal and Vancouver as -0.8 % and -1.5%, respectively, and no difference in Miami. Whereas the difference in indoor particle concentrations (PM_5) results using the integrated simulation model with a baseline for Montreal, Vancouver and Miami were calculated as -21.8%, -14% and -4.7%, respectively.

According to Table 3.4, the difference of other contaminant results such as Indoor CO_2 concentrations obtained by CONTAM for scenario 1 with baseline in Montreal, Vancouver and Miami were calculated as 44.6%, 41.2 and 43.6%, respectively, and also for VOCs concentrations were obtained as 90.4%, 91.2 and 104%, respectively. For scenario 2, the

difference in Indoor CO_2 concentrations results obtained by CONTAM with a baseline for Montreal, Vancouver and Miami were achieved as -1.2%, -3.3 and -0.5%, respectively, as well as for Indoor VOCs concentrations were calculated as -2.6%, -3% and -6.4%, respectively. Also, Table 3.4 shows that the difference between the results of Indoor CO_2 concentrations obtained by integrated simulation models for scenario 3 with a baseline in the Montreal, Vancouver and Miami were calculated as -3.7%, -6.4% and -7.8% and -9.7%, respectively, and for Indoor VOCs concentrations, were attained as -9.7%, -11.8% and -27.1%, respectively.

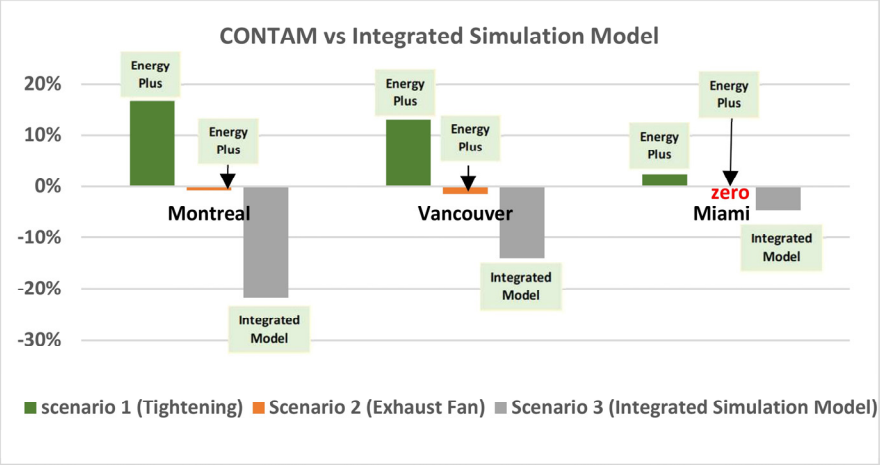

Figure 3.13 Comparison of percentage difference of IAQ results with the baseline as a result of using CONTAM only vs integrated simulation model for indoor particle concentrations (PM5)

The differences in air change rates obtained by the CONTAM only versus the integrated simulation model with the baseline are shown in Figure 3.14. As shown in this figure and Table 3.4, the differences in air change rates obtained by CONTAM for scenario 1 in Montreal, Vancouver and Miami were calculated as -70%, -66.6% and -65%, respectively, and for scenario 2, the same cities were calculated as 33.2%, 29.4% and 85.9%, respectively. However, the difference between the results of the air change rates obtained by integrated simulation models for scenario 3 in Montreal, Vancouver and Miami have been calculated as -26%, -26.5% and -20.9%, respectively.

Note that the EC and IAQ results of scenarios 1 and 2 were only obtained with the single CONTAM model, EnergyPlus model, and the result of scenario 3 was obtained by the present integrated simulation model. (Figures 3.12 to 3.14; Table 3.4)

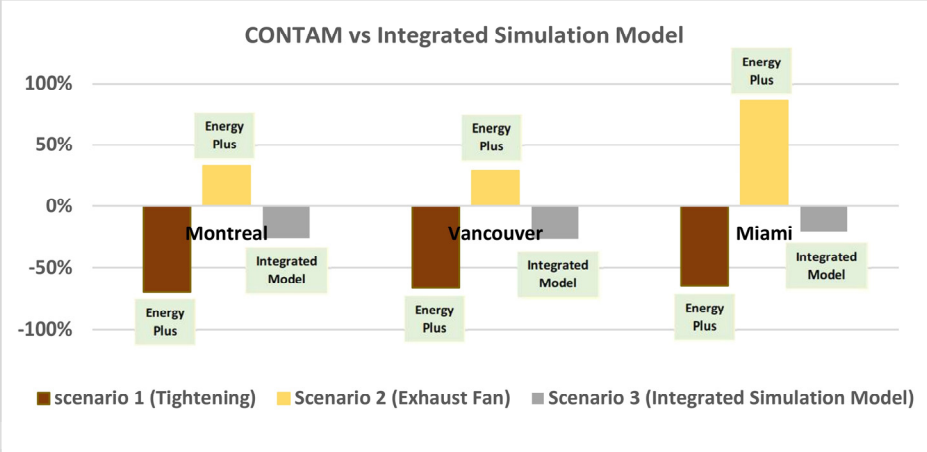

Figure 3.14 Comparison of IAQ results percentage difference with baseline as a result of using CONTAM only versus the integrated simulation model for air change rates

The ultimate goal of this study was to examine the differences in the results obtained by the integrated simulation model and single models. To this end, scenario 3 was chosen as a reference and Table 3.5 shows the average annual total energy consumption and air change rates.

At this step of the research, to better highlight, the difference in the accuracy of the studied models, the two cold and humid climates of Montreal and the other warm and humid Miami have been analyzed only.

As shown in this table, the average annual total energy consumptions for scenario 3, simulated using EnergyPlus, were 25.536 GJ and 19.283 GJ, and the corresponding values obtained by the integrated simulation model were 21.184 GJ and 17.296 GJ for Montreal and Miami, respectively. Also, Figure 3.15 shows that the differences between the average annual total

energy consumptions simulated by EnergyPlus versus the integrated simulation model were 4.352 GJ and 1.987 GJ, respectively, for Montreal and Miami.

Table 3.5 Simulated average annual results of the total energy consumptions and the air change rates using single models of EnergyPlus and CONTAM versus integrated simulation model for scenario 3

Scenario 3 Results	**Montreal**		**Miami**	
Average Annual Total Energy Consumptions (GJ)	EnergyPlus	Integrated Simulation Model	EnergyPlus	Integrated Simulation Model
	25.536	21.184	19.283	17.296
Average Annual Air Change Rates (h^{-1})	CONTAM	Integrated Simulation Model	CONTAM	Integrated Simulation Model
	0.597	0.538	0.445	0.318

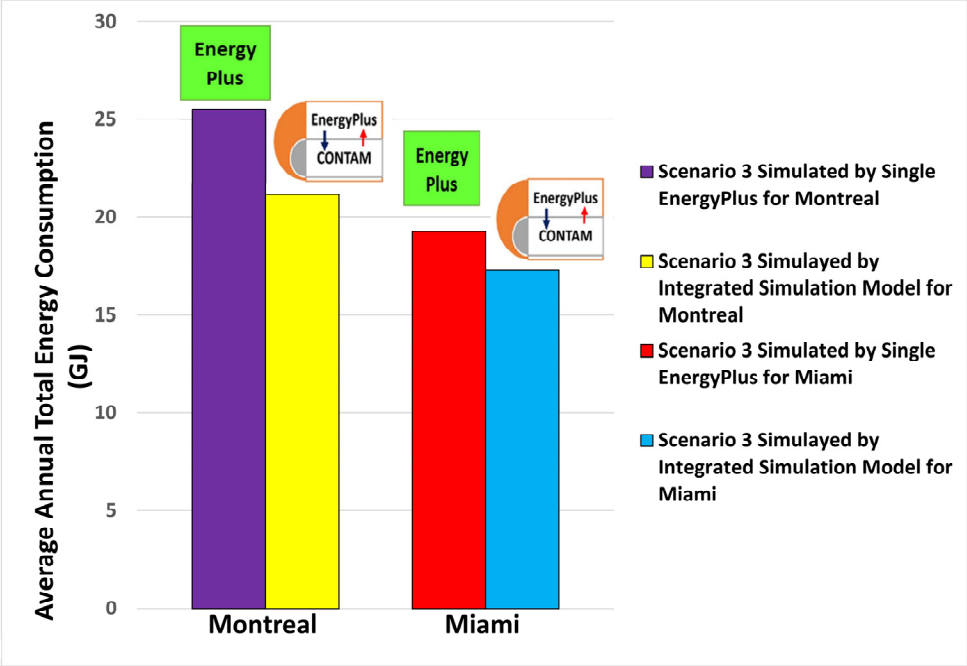

Figure 3.15 Comparison between the average annual total energy consumptions simulated by EnergyPlus and the integrated simulation model for scenario 3 in Montreal and Miami

The simulation results of the average annual air change rates by CONTAM for scenario 3 were 0.597 h^{-1} and 0.538 h^{-1} for Montreal and Miami, respectively (see Table 3.5). These simulated IAQ measures for scenario 3 using the integrated simulation model were 0.445 h^{-1} and 0.318 h^{-1} for Montreal and Miami, respectively. Additionally, the differences between the average annual air change rates simulated using the CONTAM versus that simulated using the present integrated simulation model were 0.059 h^{-1} and 0.127 h^{-1} for Montreal and Miami, respectively (Figure 3.16).

The differences in the energy consumption and the air change rates shown in Table 3.5 and Figures 3.15 and 3.16 were significant. The energy consumption difference was higher in the cold climate in Montreal because a well-insulated house consumes less energy in a warm climate. In Miami, this difference was about 10 percent.

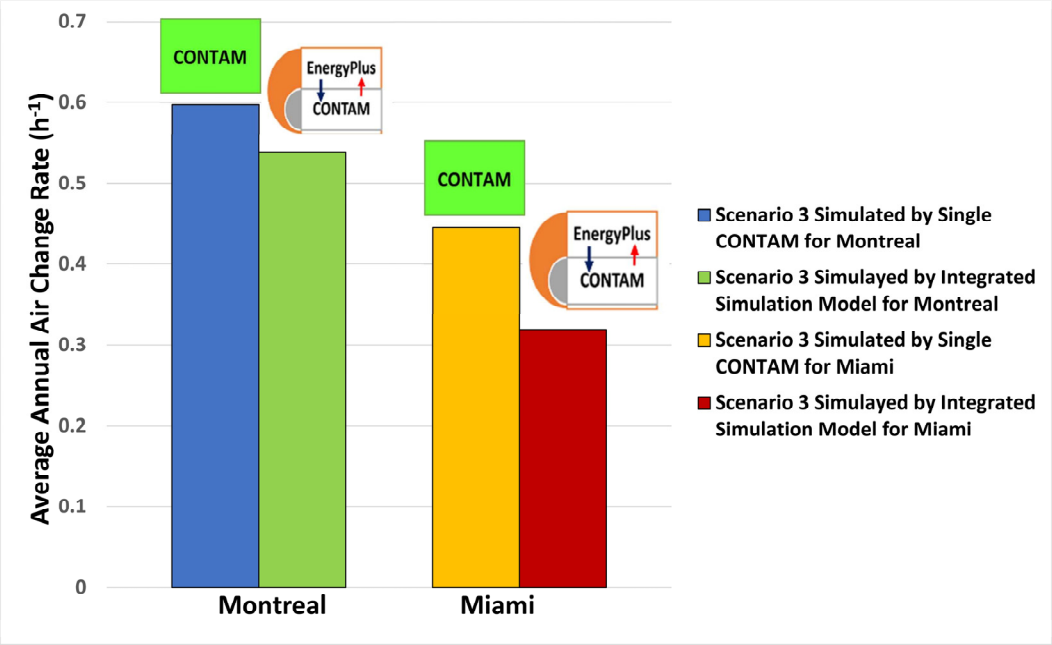

Figure 3.16 Comparison between the average annual air change rates simulated by CONTAM and the integrated simulation model for scenario 3 in Montreal and Miami

3.6 Conclusions

In this research study, an integrated simulation model was developed using a co-simulation method that can be used to simultaneously predict the energy consumption (EC) and indoor air quality (IAQ) performance of buildings subjected to different climatic conditions. The CONTAM model and the EnergyPlus model were integrated to develop this model. Because of the interactive/coupling of EC and IAQ, the predicted results with the present integrated simulation model were more realistic than those obtained with the single models. The present integrated simulation model addressed the computational limitations of the EnergyPlus and CONTAM single models by dynamically exchanging the simulated real-time temperatures and the simulated airflow rates. To show the differences in the results for the EC and IAQ performance obtained using the present integrated simulation model and those obtained using a single model, three scenarios were conducted for a three-story house when this house was subjected to the different climatic conditions of three cities in North America (Montreal, Vancouver and Miami).

The accuracy of the integrated simulation model is confirmed by the Dols et al. verification method (Dols, Emmerich, & Polidoro, 2016). To show the differences in results of the energy and IAQ performance obtained by the integrated simulation model versus the results of using single models, firstly, according to Figure 3.12 and Table 3.4, these differences in energy results obtained by the EnergyPlus only versus the integrated simulation model were compared. Secondly, concerning Figures 3.13, 3.14 and Table 3.4, the differences in the IAQ results as a result of using CONTAM only versus the integrated simulation model were compared.

The results of the single models and the integrated simulation model for the energy performance were compared in Figure 3.15 and Table 3.5. Additionally, the results of the single models and the integrated simulation model for the IAQ performance were compared in Figure 3.16 and Table 3.5. These comparisons showed that due to the opportunity to exchange the correct temperature and airflow rate variables simultaneously in the present integrated

simulation model, the difference between the EC-IAQ results with the baseline indicates the improvement in assessing the performance of the buildings. Finally, considering the energy consumption and indoor air quality results obtained from the single models (EnergyPlus and CONTAM) and comparing them with those obtained from the present integrated simulation model for Montreal and Miami, it was found that the results of scenario 3 found using co-simulation were better than other scenarios for improving EC and IAQ together.

This research study, called “Part 1,” generated some energy savings caused by the specific construction measures but we do not dwell on their interpretation as the objective of the paper was to demonstrate the need for changing the paradigm of thinking. By moving from the individual (i.e. uncoupled) models to an integrated system, we are basically reducing the gap between models and practice. It is important to point out that the limitation of this research study was that the moisture transport in the building envelope was not accounted for. The next step in our research, which is in progress, is to conduct another study, called “Part 2,” which introduces liquid and vapor forms of water movements in building envelopes. In Part 2, a heat, air, and moisture (HAM) transport model is currently being coupled with the present integrated simulation model to simultaneously assess: (a) the energy performance, (b) indoor air quality performance, and (c) the risk of condensation and mold growth inside the building envelope. The obtained results for the building envelope of different cladding systems, subjected to different climatic conditions in North America, will be published at a later date.

Author Contributions: Conceptualization, S.H., W.M. and H.H.S.; methodology, S.H., W.M. and H.H.S.; software, S.H.; validation, S.H., W.M. and H.H.S.; formal analysis, S.H.; investigation, S.H.; resources, S.H.; data curation, S.H.; writing—original draft preparation, S.H.; writing—review and editing, S.H., W.M. and H.H.S.; visualization, S.H.; supervision, W.M. and H.H.S.; project administration, W.M. and H.H.S.

CHAPITRE 4

ASSESSING THE ENERGY, INDOOR AIR QUALITY, AND MOISTURE PERFORMANCE FOR A THREE-STORY BUILDING USING AN INTEGRATED MODEL, PART TWO: INTEGRATING THE INDOOR AIR QUALITY, MOISTURE, AND THERMAL COMFORT

Seyedmohammadreza Heibati [a], Wahid Maref [a,] and Hamed H. Saber [b]

[a] Department of Construction Engineering, École de Technologie Supérieure (ÉTS), University of Québec, Montreal, QC H3C 1K3, Canada; Seyedmohammadreza.Heibati.1@ens.etsmtl.ca
[b] Prince Saud bin Thuniyan Research Center, Mechanical Engineering Department, Jubail University College, Al Jubail 35716, Saudi Arabia; SABERH@ucj.edu.sa

Paper published in Energies, MDPI, 5 August 2021

4.1 Abstract

In this paper, an integrated model that coupled CONTAM and WUFI was developed to assess the indoor air quality (IAQ), moisture, and thermal comfort performance. The coupling method of CONTAM and WUFI is described based on the exchange of airflow rate control variables as infiltration, natural and mechanical ventilation parameters between heat and moisture flow balance equations in WUFI and contaminant flow balances equations in CONTAM. To evaluate the predictions of the integrated model compared to single models of CONTAM and WUFI, four scenarios were used. These scenarios are airtight fan-off, airtight fan-on, leaky fan-off, and leaky fan-on, and were defined for a three-story house subjected to three different climate conditions of Montreal, Vancouver, and Miami. The measures of the simulated indoor CO_2, $PM_{2.5}$, and VOCs obtained by CONTAM; the simulated indoor relative humidity (RH), predicted percentage of dissatisfied (PPD), and predicted mean vote (PMV) obtained by WUFI; and those obtained by the integrated model are compared separately for all scenarios in Montreal, Vancouver, and Miami. Finally, the optimal scenarios are selected. The simulated results of the optimal scenarios with the integrated model method (−28.88% to 46.39%) are different from those obtained with the single models. This is due to the inability of the single models to correct the airflow variables.

Keywords: integrated model; CONTAM; WUFI; indoor air quality performance, moisture performance, thermal comfort performance

4.2 Introduction

A building can be defined as a system that balances the energy, air, and moisture flows with its surroundings. Indoor air quality, moisture and thermal comfort are important parameters for buildings that can be controlled based on energy, air, and moisture flows characteristics. Currently, there are many tools that can be used for determining energy, indoor air quality and moisture building performances. Residents' satisfaction with the thermal condition of the indoor environment increases the performance of the buildings (Zhang, de Dear, & Hancock, 2019)**.** Energy models are accurate tools for optimizing active and passive building systems (Heibati & Atabi, 2013; Heibati et al., 2013; Rabani, Bayera Madessa, & Nord, 2021).

Thermal comfort measures have been developed since the 1960s to calculate building performance and the predicted mean vote (PMV) has been used as one of the numerical measures of thermal comfort (Fanger, 1970). ASHRAE Standard 55 (ASHRAE, 2017a) is one of the most important international thermal comfort standards. Many tools have been developed by the researchers to calculate thermal comfort as an indicator of building performance. Some of these tools, such as FTCR (Functions for Thermal Comfort Research) (Schweiker, 2016) and pythermalcomfort (Tartarini & Schiavon, 2020) are open source tools that require prior coding skills.

Another tool called the centre for the built environment (CBE) was developed by Schiavon, Hoyt, & Piccioli (2014) which can visually calculate the thermal comfort measures according to the ASHRAE 55 Standard without the need for having to write code. Chen, (2009) used indoor air quality calculation tools to calculate building indoor air quality performance. It has been concluded that CFD models were the most popular and can be coupled with other ventilation models to increase their accuracy in calculating the indoor air quality performance

of the building. In another study, Wang & Chen, (2008) concluded that with the help of coupling CONTAM with CFD models, the errors created by some assumptions can be solved and they validated their results with experimental data.

Some researchers have used coupling method between energy models with indoor air quality models to increase the accuracy of performance calculation for double skin facade system in natural ventilation (Wang & Wong, 2008). Gao, Zhang, & Niu (2007) developed a high-precision model by combining thermal comfort and indoor air quality (IAQ) models.

Chang, Wi, Kang, & Kim (2020) used WUFI (Wäme und Feuchte instationär) Pro 5.3 (Künzel, 1995) to perform a moisture risk assessment based on hygrothermal properties analysis for ply-lam cross-laminated timber (CLT) house envelope. The WUFI program can calculate the thermal and moisture properties of a building material as hygrothermal performance by calculating heat and moisture flow balances ("Details:Physics-Wufiwiki," 2020). The performance calculation of thermal and moisture properties of building materials using WUFI tools was performed in 2003 by Canada Mortgage and Housing Corporation for more than 45 building simulation programs (Ibrahim, Sayegh, Bianco, & Wurtz, 2019). In most studies, WUFI tools were used to minimize moisture problems in preventing mold growth risk at indoor envelope surfaces in order to calculate moisture performance (Mundt-Petersen & Harderup, 2015). The problem with moisture performance simulation tools for building materials is that these tools can only estimate hygric behavior and do not predict pollutant behavior, for example, for building materials with a moisture buffering capacity (Le, Zhang, Liu, Samri, & Langlet, 2020). Relative humidity (RH) is the main parameter needed for evaluating thermal comfort and moisture performance. One of the passive methods to keep moisture in the acceptable level in order to improve thermal comfort is to use building materials with moisture buffering capacity (Zu, Qin, Rode, & Libralato, 2020). Some researchers have concluded that building materials such as gypsum board, ceiling tiles, furniture, and carpet with adsorption / desorption capability of indoor VOCs, can affect the indoor air quality (Hunter-Sellars, Tee, Parkin, & Williams, 2020). Hemp concrete is one of the materials with high moisture buffering capacity that with hygric and pollutant behavior can increase the performance of the building

in terms of moisture and IAQ as well as thermal comfort (Promis, Dutra, Douzane, Le, & Langlet, 2019). Researchers have concluded that this dual behavior of porous media materials is due to the similarity between the properties of moisture transfer and indoor contaminants such as VOCs (Rode, Grunewald, Liu, Qin, & Zhang, 2020).

Le et al. (2020) developed a coupled moisture, air, and pollutant transport model. In that model, the similarity between adsorption/desorption effects for moisture and VOCs was presented by materials with the potential of buffering capacity, which relative humidity and temperature can affect both.

According to the literature review's results, it can be concluded that because of temperature, airflow and relative humidity (RH) on each of the measures of thermal comfort, indoor air quality and moisture performance, all three measures need to be integrated to allow simultaneous correction for the common variables. The study of the results of the single research of the CONTAM (Dols et al., 2016; Moschetti & Carlucci, 2017; Sowa & Mijakowski, 2020) and WUFI (Chang, Kang, Wi, Jeong, & Kim, 2017; Fedorik, Alitalo, Savolainen, Räinä, & Illikainen, 2021; Moujalled et al., 2018) models concluded the need to develop an integrated model for a more accurate calculation of building indoor air quality, moisture and thermal comfort performances.

In this research project, an integrated model is developed in which the first part related to coupling the energy and indoor air quality was presented in a previous paper (Heibati, Maref, & Saber, 2019). This paper presents the second part of the research project related to the development of the integrated model to couple the indoor air quality, moisture, and thermal comfort performances. Also, the results obtained with single models (i.e. CONTAM ("CONTAM 3.2," 2016) and WUFI ("WUFI® Plus," 2021)) are compared with those obtained with the present integrated model.

The accuracy of this integrated model was verified using paired sample t-tests. This method was performed by Heibati et al. (2013) for integrated energy models. But single model

predictions are made separately for indoor air quality performance or moisture performances and airflow with its dependent variables are defined as input data by the user (Mckeen & Liao, 2021; "WUFI® Plus," 2021). In the integrated model, however, airflows are exchanged and modified as control variables between CONTAM and WUFI sub models. The reason for this advantage of airflows is due to the integrated calculation of heat, moisture and contaminant equation balances. Finally, the interactions between the indoor air quality, moisture and thermal comfort performances are balanced and the accuracy of the predictions of this new model is increased.

4.3 Methodology

An integrated model is developed to simultaneously assess the building performance related to: (1) indoor air quality and (2) moisture with thermal comfort. For this purpose, two single models of CONTAM (ContamW and ContamX, version: 3.2.0.2) and WUFI (WUFI Plus, version: 3.2.0.1) are used. In the first phase, the capability of each of the CONTAM and WUFI models for a case study is evaluated. In the second phase, with the help of the coupling method, an integrated model is developed to calculate simultaneously the performance of indoor air quality, moisture, and thermal comfort.

For this purpose, the approach used in this study consists of three sections. The first section describes the coupling method of CONTAM and WUFI. In the second one, the governing equations of the single models as well as the coupling equation are described. In the third section, a case study is conducted to compare the building performance obtained with the single models and the integrated model at three different climates of Montreal, Vancouver and Miami.

4.3.1 Coupling method of CONTAM and WUFI

The coupling mechanism of the two CONTAM and WUFI models is conducted by exchanging control variables and converting the output and input data formats of each model. When one or more output variables can act as readable input for another model and vice versa and because

of this exchange, the variable(s) is/are updated. This process is called a co-simulation mechanism, which is presented in Figure 4.1. The main variable in this research is airflow rate and the sub-variable is geometry data, which are exchanged between both CONTAM and WUFI models according to 4.1.

CONTAM mainly consists of two separate programs. These two programs are: 1- ContamW and 2- ContamX. ContamW provides a graphical interface for the user to view the results simulated by ContamX. ContamX can simulate files in PRJ file (project file) format. After entering graphical and numerical data by the user through ContamW, this data is stored in the format of PRJ files. It is then provided as an input file to ContamX for processing and simulation, and finally these results can be viewed graphically through ContamW.

In the airflow rate exchange between CONTAM and WUFI, the output of the air change rate simulated by ContamX ("CONTAM 3.2," 2016), in ACH (air change rate) file format is first converted to TXT (text) file format by Microsoft Excel. This simulated output contains daily and average annual data for airflow through the paths and ducts. After changing the format, this output is provided to WUFI as input information. In WUFI, this data is used in the natural and mechanical ventilations. The airflow rate outputs simulated by WUFI, which include updated hourly ventilation data, are then converted to an XLSX (Excel Workbook) file via the Excel exporter menu, and then the natural and mechanical ventilation parts are separated. In ContamW ("CONTAM 3.2," 2016), the airflow element models selected for the infiltration and mechanical ventilation, are the leakage area of the power law model and the constant mass flow fan model, respectively (Dols & Polidoro, 2015). WUFI output data related to the mechanical ventilation part is then used as the design flow rate of the fan model according to Figure 4.1. The natural ventilation-infiltration air-volume flow rate ($\dot{Q}$) as output part is converted to ELA (effective leakage area) by Excel convertor airflow to ELA, based on the converter factor, and then used as input data leakage area model of ContamW. Convert factor tool is executed according to Equations (4.1) through (3) (Chan, Price, Sohn, & Gadgil, 2003a; Sherman & Dickerhoff, 1998) .

$$ACH = \frac{(3600 \times \dot{Q})}{V} \tag{4.1}$$

$$NL = ACH \tag{4.2}$$

$$NL = 1000 \cdot \frac{ELA}{A_f} \cdot (\frac{H}{2.5})^{0.3} \tag{4.3}$$

where ACH, $\dot{Q}$, V, NL, ELA, A_f, and H correspond to the air change rate (h^{-1}), natural ventilation–infiltration air–volume flow rate (m^3/s), building net volume (m^3), normalized leakage, effective leakage area, floor area (m^2), and building height (m), respectively.

It is assumed in WUFI that the natural ventilation–infiltration air–volume flow rate is a function of the internal and external temperatures' difference. The reason for this relationship is presented according to Equations (4.4)–(4.6). The natural ventilation–infiltration air–volume flow rate is calculated based on the amount of heat flow from natural ventilation–infiltration according to Equations (4.4) and (4.5). Conversely, heat flow from natural ventilation–infiltration is a function of the internal and external temperatures' difference based on Equations (4.4) and (4.5) (U.S. Department of Energy, 2021).

$$\dot{m}_{nat-infiltration} = \dot{Q} \cdot \rho \tag{4.4}$$

$$\dot{q}_{nat-infiltration} = \dot{m}_{nat-infiltration} \cdot (h_i - h_e) \tag{4.5}$$

$$h_i - h_e = (1006 + x_e \cdot 1840) \cdot (\theta_i - \theta_e) \tag{4.6}$$

In Equations (4.4–4.6), $\dot{m}_{nat-infiltration}$, ρ, $\dot{q}_{nat-infiltration}$, h_i, h_e, x_e , θ_i, and θ_e correspond to the airflow of natural ventilation–infiltration (kg/s), air density of internal air (kg/m^3), heat flow from natural ventilation–infiltration (W), specific enthalpy internal air (J/kg), specific enthalpy external air (J/kg), moisture content of external air (kg/kg), internal air temperature (°C), and external air temperature of (°C), respectively.

In this coupling method, it is assumed that in the ContamW sub model section, the infiltration model is based on the following empirical (power law model (ASHRAE, 2017b)) relationship

between the natural ventilation-infiltration air-volume flow rate and the pressure difference across a crack or opening in the building envelope (see Equation (4.7)). ContamW is able to calculate natural ventilation-infiltration air-volume flow using the power law model in Equation (4.7) and using component leakage area formulation through Equations (4.8) and (4.9) (ASHRAE, 2017b) which has been used to characterize openings for infiltration calculations. Equation (4.8) presents the relationship between ELA and a series of pressurization tests where the airflow rate is measured at a series of reference condition pressure. On the other hand, ELA relates to natural ventilation-infiltration air-volume flow rate based on power law model through the Equations (4.7) to (4.9).

$$\dot{Q} = C \cdot (\Delta P_r)^n \tag{4.7}$$

$$ELA = \dot{Q}_r \cdot \frac{\sqrt{\frac{\rho}{2 \cdot \Delta P_r}}}{C_d} \tag{4.8}$$

$$C = ELA \cdot C_d \cdot \sqrt{2} \cdot (\Delta P_r)^{\frac{1}{2}-n} \tag{4.9}$$

In Equations (4.7)–(4.9), C, ΔP_r, n, $\dot{Q}_r$, and C_d correspond to the flow coefficient ($m^3/(s \cdot Pa^n)$), reference pressure difference (Pa), flow exponent, predicted airflow rate at ΔP_r (m^3/s) (from curve fit to pressurization test data), and discharge coefficients. There are two sets of reference conditions for the discharge coefficient: $C_d = 1$ and $\Delta P_r = 4$ (Pa) or $C_d = 0.6$ and $\Delta P_r = 10$ (Pa) (ASHRAE, 2017b). Additionally the effective leakage area is used in ContamW at a pressure difference (ΔP_r) of 4 Pa, flow exponent (n) of 0.65 and discharge coefficient (C_d) of 1 (Chan et al., 2003a). According to Figure 4.1, both WUFI and CONTAM models use simulated airflow rate simulation data instead of assumed input variable of airflow rate. Consequently, the co-simulation for this main control variable is completed.

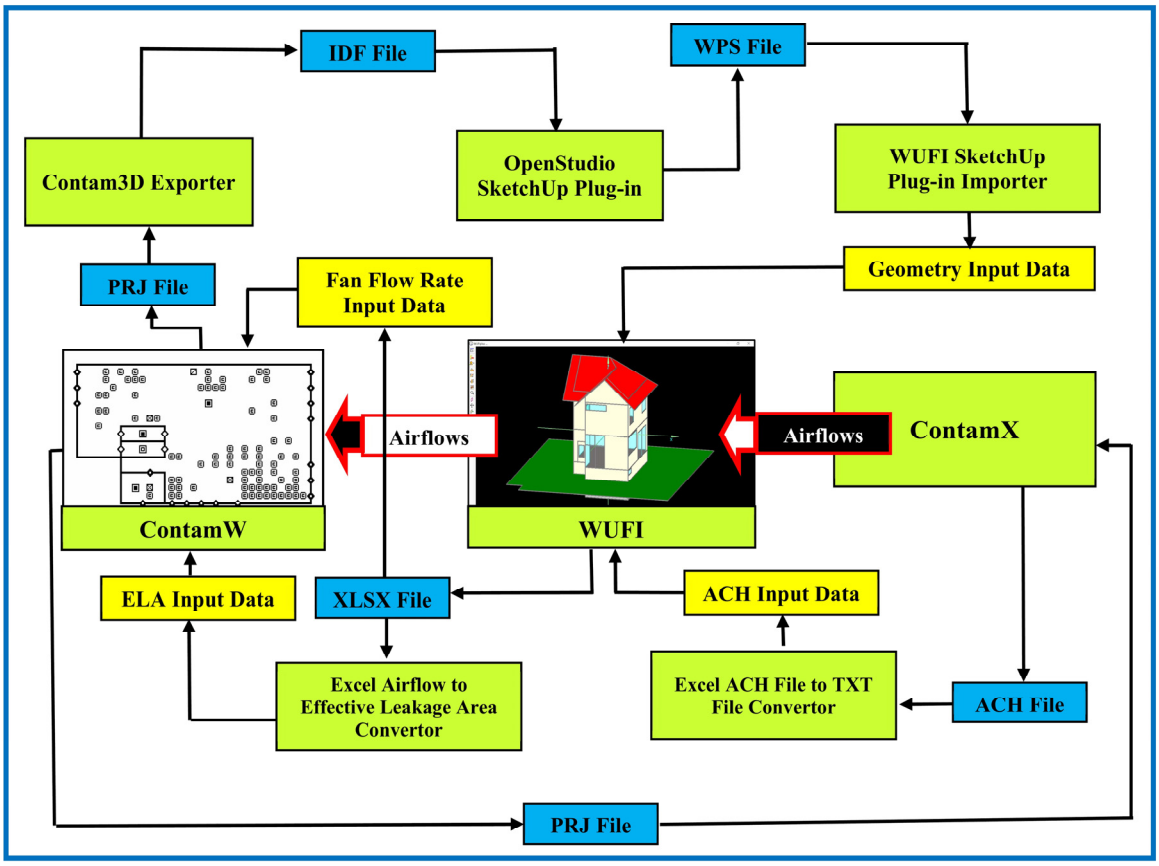

Figure 4.1 Co-simulation mechanism for CONTAM and WUFI, ACH: air change rate, PRJ: project file, XLSX: Excel Microsoft Office open XML format spreadsheet file (XML: extensible markup language), ELA: effective leakage area, CONTAM: contaminant transport analysis, IDF: input data file, WPS: WUFI plugin in SketchUp file

In the next step, the geometry data simulated by ContamW is converted from PRJ files (project file) to IDF files (input data files) with the help of Contam3D Exporter. The IDF file can be read by the importer of OpenStudio SketchUp Plug-in and the details of this geometry can be controlled and modified. It is then read as a WPS file (WUFI Plugin in SketchUp file) by WUFI SketchUp Plug-in importers as an input geometry file to WUFI. In this procedure, the simulated geometry data is controlled and modified as a sub-variable by CONTAM in Sketchup and then used as input data in WUFI. Finally, the exchange of both airflow rate and geometry control variables as shown in Figure 4.1 between CONTAM and WUFI complete the co-simulation process in this part of the study.

The governing equations of the integrated model, which include the coupling of the flow rates of heat, moisture and contaminant, are provided by Equations (4.10) through (4.12) (Antretter et al., 2018; Dols & Polidoro, 2015). Equations (4.10) and (4.11) are providing the heat and moisture balance equations by WUFI, respectively. Equation (4.12) represents the contaminant flow balance equation by CONTAM in this combination.

$$\frac{dQ_{heat,i}}{dt} = \sum_j \dot{q}^{opaque}_{component,j} + \sum_j \dot{q}^{transparent}_{component,j} + \dot{q}_{solar} + \dot{q}_{internal} + \dot{q}_{nat-infiltration} + \dot{q}_{mech-ventilation} \tag{4.10}$$

$$\frac{dW_{moist,i}}{dt} = \sum_j \dot{w}_{component,j} + \dot{w}_{indoor} + \dot{w}_{nat-infiltration} + \dot{w}_{mech-ventilation} \tag{4.11}$$

$$\frac{dm^{\alpha}_{cont,i}}{dt} = \sum_j \dot{m}_{air-inward_{(j,i)}} \cdot \left(1 - \eta^{\alpha}_{j,i}\right) \cdot C^{\alpha}_j + G^{\alpha}_i + m_{air_i} \sum_{\beta} K_i{}^{\alpha,\beta} \cdot C^{\beta}_i - \sum_j \dot{m}_{air-outward_{(i,j)}} \cdot C^{\alpha}_i - R^{\alpha}_i \cdot C^{\alpha}_i \tag{4.12}$$

In Equation (4.10), $\frac{dQ_{heat,i}}{dt}$, $\dot{q}^{opaque}_{component,j}$, $\dot{q}^{transparent}_{component,j}$, $\dot{q}_{solar}$, $\dot{q}_{internal}$, $\dot{q}_{nat-infiltration}$, and $\dot{q}_{mech-ventilation}$ correspond to the heat flow rate in zone *i* (room) (W), heat transfer flow over opaque component *j* (W), heat transfer flow over transparent component *j* (W), short-wave solar radiation leading directly to heating the internal air or interior furnishing and components surface (W), convective heat sources in the room (W), heat flow from the natural ventilation–infiltration (W), and convective heat flow from the building mechanical ventilation systems (W), respectively (Antretter et al., 2018).

In addition, in Equation (4.11), $\frac{dw_{moist,i}}{dt}$, $\dot{w}_{component,j}$, $\dot{w}_{internal}$, $\dot{w}_{nat-infiltration}$, and $\dot{w}_{mech-ventilation}$ correspond to the moisture flow rate in zone *i* (kg/s), moisture flow between inner wall surface *j* and the room air (kg/s), moisture source in the room (kg/s), moisture flow due to the natural ventilation–infiltration (kg/s), and moisture flow due to the building of mechanical ventilation systems (kg/s), respectively (Antretter et al., 2018).

In Equation (4.12), $\frac{dm_{cont,i}^{\alpha}}{dt}$, $\dot{m}_{air-inward_{(j,i)}}$, $\dot{m}_{air-outward_{(i,j)}}$, C_i^{α}, C_i^{β}, C_j^{α}, G_i^{α}, m_{air_i}, $\eta_{j,i}^{\alpha}$, $K_i^{\alpha,\beta}$, and R_i^{α} correspond to the contaminant of α flow rate in zone *i* (kg/s), inward flow rate of air from zone *j* to zone *i* (kg/s), outward flow rate of air from zone *i* to zone *j* (kg/s), concentration of contaminant α in zone i (kg/kg), concentration of contaminant β in zone *i* (kg/kg), concentration of contaminant α in zone *j* (kg/kg), generation rate of contaminant α in zone *i* (kg/s), mass of air in zone *i* (kg), filter efficiency for contaminant α in the path from zone *j* to zone *i*, kinetic first order chemical reaction coefficients in zone *i* between contaminant α and β (s^{-1}), and removal coefficient of contaminant α in zone *i* (kg/s), respectively (Dols & Polidoro, 2015).

The variables dependent on the heat flow rate in zone *i* ($\frac{dQ_{heat,i}}{dt}$) are calculated based on Equations (4.13) through (4.21) (Antretter et al., 2018). A transmission heat flow over opaque component j ($\dot{q}_{component,j}^{opaque}$) is calculated based on Equation (4.13). In this equation, A_C, R_{si}, θ_i, and θ_{si} correspond to the surface of the opaque component (m^2), heat transfer resistance interior ($m^2 \cdot K/W$), internal room air temperature (°C), and interior surface temperature (°C), respectively.

$$\dot{q}_{component,j}^{opaque} = A_C \cdot \frac{1}{R_{si}} \cdot (\theta_i - \theta_{si}) \quad (4.13)$$

In addition, a transmission heat flow over transparent component *i* ($\dot{q}_{component,j}^{transparent}$) is calculated based on Equation (4.14).

$$\dot{q}_{component,j}^{transparent} = [(\theta_e - \theta_i) - E \cdot (I_{l,e} - \sigma \cdot T^4) \cdot R_e + I_{l,i} \cdot R_i] \cdot U_W \cdot A_W \quad (4.14)$$

In Equation (4.14), θ_e, E, $I_{l,e}$, $I_{l,i}$, σ, T, R_e, R_i, U_w, and A_w correspond to the external temperature (°C), emissivity (average of glazing and frame), long-wave radiation balance of the exterior surface (W/m^2), long-wave radiation balance of interior surfaces (W/m^2), Stefan

Boltzmann constant $5.67 \cdot 10^{-8}$ (W/m^2·K^4), temperature of the exterior surface (K), heat transfer resistance, exterior (m^2·K⁄W), heat transfer resistance, interior (m^2·K/W), heat transfer coefficient of the entire window (W⁄m^2·K), and total surface area (window frames + glazing) (m^2), respectively. In Equation (4.15), short-wave solar radiation ($\dot{q}_{solar}$) (W) is calculated by the summation of $\dot{q}_{solar,i}$ and $\dot{q}_{solar,c}$, which are solar gain for the internal air or interior furnishing (W), and solar- gain for the components surface (W), respectively.

$$\dot{q}_{solar} = \dot{q}_{solar,i} + \dot{q}_{solar,c} \tag{4.15}$$

$$\dot{q}_{solar,i} = f_{sa} \cdot \dot{q}_{solar,G} \tag{4.16}$$

$$\dot{q}_{solar,c} = (1 - f_{sa}) \cdot \dot{q}_{solar,G} \tag{4.17}$$

$$\dot{q}_{solar,G} = \sum_{w} [(I_{s,dir} \cdot f_{sh,dir} \cdot SHGC_{dir} + I_{s,diff} \cdot f_{sh,diff} \cdot SHGC_{diff}) \cdot A_w \cdot f_f \tag{4.18}$$

Both $\dot{q}_{solar,i}$ and $\dot{q}_{solar,c}$ are calculated based on Equations (4.16) and (4.17), and the overall heat gain of the solar radiation through all transparent components ($\dot{q}_{solar,G}$) is calculated by Equation (4.18). In Equations (4.16) and (4.17), f_{sa} is the assigned radiation coefficient air as proportional heat gain due to entering radiation directly into the room air. In Equation (4.18), $I_{s,dir}$, $I_{s,diff}$, $f_{sh,dir}$, $f_{sh,diff}$, f_f, $SHGC_{dir}$, $SHGC_{diff}$, and A_w correspond to the direct solar radiation on the component surface (W⁄m^2), diffuse solar radiation (W⁄m^2), shading coefficient direct radiation, shading coefficient diffuse radiation, frame coefficient (percentage of transparent area), direct solar heat gain coefficient (depending on the angle), solar heat gain coefficient of the diffuse radiation, and window area (m^2), respectively. Convective heat sources in the room ($\dot{q}_{Internal}$) are calculated according to Equation (4.19) by the summation of all individual convective heat sources.

$$\dot{q}_{Internal} = \sum_{k} \dot{q}_{Individual,k} \tag{4.19}$$

In Equation (4.19), $\dot{q}_{Individual,k}$ is the heat production from the k^{th} heat individual source in the zone (W) and heat flow from natural ventilation–infiltration ($\dot{q}_{nat-ventilation}$) is obtained from Equation (4.20).

$$\dot{q}_{nat-infiltration} = \dot{m}_{nat-infiltration} \cdot (h_i - h_e) \quad (4.20)$$

In Equation (4.20), $\dot{m}_{nat-infiltration}$, h_i, and h_e correspond to the airflow of natural ventilation–infiltration (kg/s), specific enthalpy internal air (J/kg), specific enthalpy external air (J/kg), respectively. The convective heat flow from the building mechanical ventilation systems ($\dot{q}_{mech-ventilation}$) is calculated by Equation (4.21).

$$\dot{q}_{mech-ventilation} = \dot{m}_{supply} \cdot (h_i - h_e) \cdot (1 - \eta_{HR}) \quad (4.21)$$

In Equation (4.21), $\dot{m}_{supply}$ and η_{HR} correspond to the airflow of the supply mechanical ventilation (kg/s) and heat recovery rates, respectively.

Other parameters related to moisture flow rate in zone i $\frac{dW_{moist,i}}{dt}$ are defined in Equations (4.22) through (25). Moisture flow between inner wall surface j and the room air ($\dot{w}_{component,j}$) is calculated based on Equation (4.22).

$$\dot{w}_{component,j} = A_C \cdot \beta \cdot (P_p - P_{p,c}) \quad (4.22)$$

In Equation (4.22), β, P_p, and $P_{p,c}$ correspond to the water vapor transfer coefficient (kg/m^3·s·Pa), partial water vapor pressure in the zone (Pa), and partial water vapor pressure on component surface (Pa), respectively. The moisture source in the room ($\dot{w}_{internal}$) is calculated based on Equation (4.23).

$$\dot{w}_{internal} = \sum_k \dot{w}_{individual,k} \tag{4.23}$$

In Equation (4.23) $\dot{w}_{individual,k}$ is the moisture production from the individual moisture source in the zone (kg/s) and the moisture flow due to the natural ventilation–infiltration ($\dot{w}_{nat-infiltration}$) is defined according to Equation (4.24).

$$\dot{w}_{nat-Infiltration} = \dot{m}_{nat-Infiltration} \cdot (x_e - x_i) \tag{4.24}$$

In Equation (4.24), x_e and x_i correspond to the moisture content external air (kg/kg) and moisture content internal air (kg/kg), respectively. The calculation of moisture flow due to the building mechanical ventilation systems ($\dot{w}_{mech-ventilation}$) is shown in Equation (4.25).

$$\dot{w}_{mech-ventilation} = \dot{m}_{supply} \cdot (x_e - x_i) \cdot (1 - \eta_{MR}) \tag{4.25}$$

In Equation (4.25), η_{MR} is the moisture recovery rate and other variables are defined similarly to Equations (4.24) and (4.21).

The balance of contaminants α flow rate in zone *i* ($\frac{dm^{\alpha}_{cont,i}}{dt}$) consists of two main parts (Dols, 2001). The first part is related to the equations of removing contamination α from zone *i*, which includes:

1. the outward contaminant α flow rate from zone *i* with the rate of $\sum_j \dot{m}_{air-outward_{(i,j)}} \cdot C_i^{\alpha}$;
2. the contaminant α removal in the zone *i* with the rate of $R_i^{\alpha} \cdot C_i^{\alpha}$; and
3. the first-order chemical reactions with contaminant β at the rate of $m_{air_i} \sum_{\beta} {K_i}^{\alpha,\beta} \cdot C_i^{\beta}$.

The second part contains the equations of adding contamination α to zone *i*. This section includes: (1) inward contaminate α flow rate to zone *i* with the rate of $\sum_j \dot{m}_{air-inward_{(j,i)}} \cdot (1-\eta_i^{\alpha}) \cdot C_j^{\alpha}$ and (2) generation of contaminants α in zone *i* with the rate of G_i^{α} (Dols, 2001).

The integrated model in this study is based on the coupling of CONTAM and WUFI. The coupling method between the governing equations of CONTAM and WIFI is shown in Figure 4.2. In Equations (4.10) through (4.12), all three heat, moisture, and contaminant flow rates can be connected by airflow rates. By exchanging airflow rates as a common control variable, the coupling mechanism between the governing equations of CONTAM and WUFI have been achieved for the developing of an integrated model. According to Figure 4.2 in WUFI, the control variables include infiltration as well as natural and mechanical ventilation in the process of heat and moisture flow rate balances. In CONTAM, the control variable includes inward and outward airflow rates related to the contaminant balance.

In the integrated model, the airflow rate control variables for CONTAM and WUFI are exchanged with each other using Equations (4.26) and (4.27), and according to Figure 4.2, resulting in heat, moisture, and contaminant balance equations being coupled with a common airflow rate.

$$\dot{m}_{air-total} = \dot{m}_{nat-infiltration} + \dot{m}_{supply} \tag{4.26}$$

$$\dot{m}_{air-inward_{total}} = \dot{m}_{air-outward_{total}} = \dot{m}_{air-total} \tag{4.27}$$

In Equations (4.26) and (4.27), by the summation of airflow rates of infiltration–natural ventilation ($\dot{m}_{nat-infiltration}$) and supply mechanical ventilation ($\dot{m}_{supply}$), simulated by WUFI, the new airflow rate of $\dot{m}_{air-total}$ is obtained. When this $\dot{m}_{air-total}$ is equal to the total of the inward and outward airflow rates of $\dot{m}_{air-inward_{total}}$ and $\dot{m}_{air-outward_{total}}$, they can be used as new airflow rates in CONTAM. This procedure can be reversed, in which case WUFI can use the output results of the CONTAM airflow rates. As a result of this two-way exchange,

according to Figure 4.2, an integrated model with airflow rates influenced by both WUFI and CONTAM models have been developed.

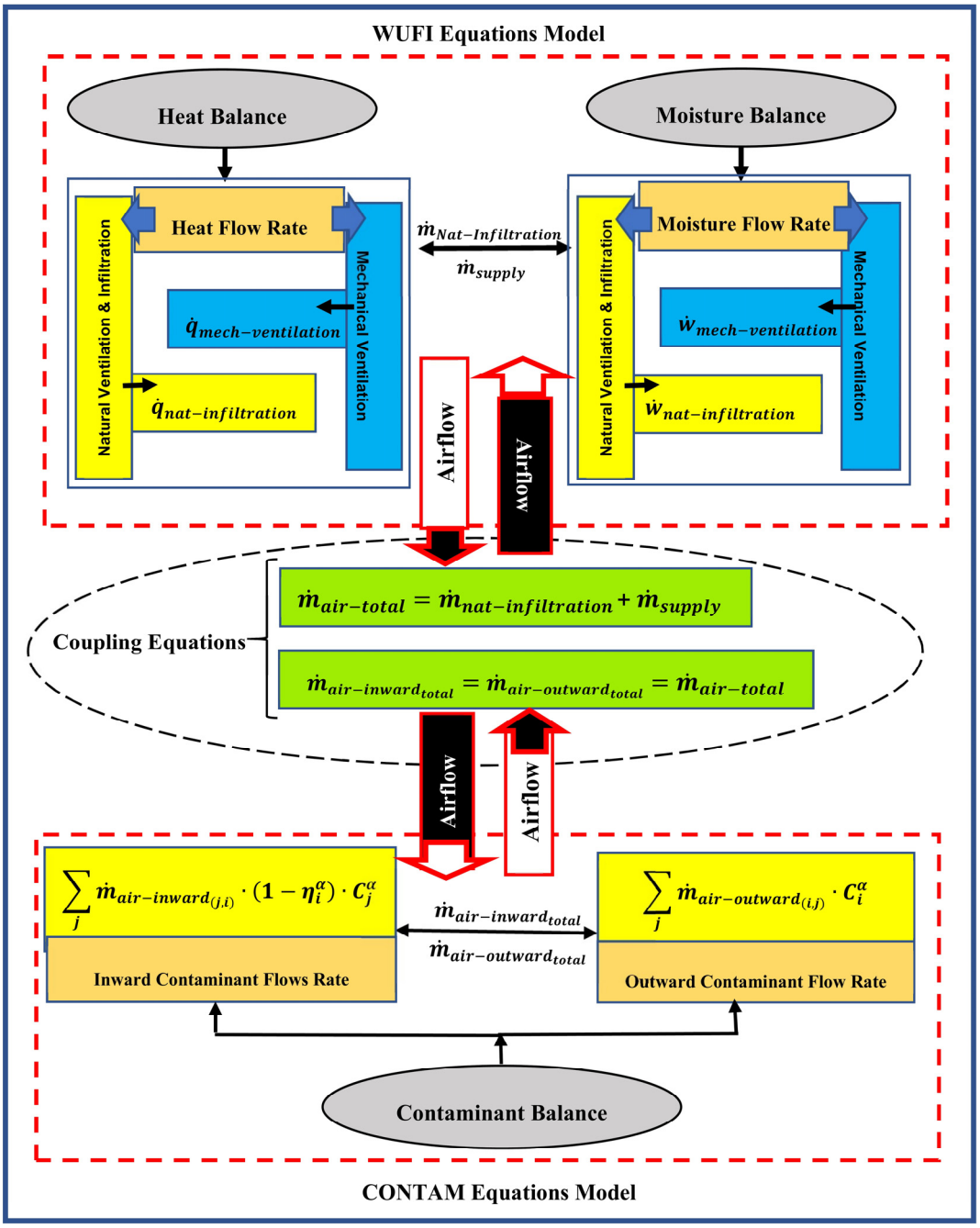

Figure 4.2 Coupling equations approach between CONTAM and WUFI

4.3.2 Description of the case study

In this study, a three-story house was used as a case study. This house has three levels: basement, main floor, and bedroom floor. The main assumptions include those that are described below. The basement includes zones, a utility room (area: 3.24 m^2, volume: 9.72 m^3), an exercise room (area: 18.65 m^2, volume: 55.95 m^3), parking (area: 12.97 m^2, volume: 38.91 m^3), and a staircase (area: 0.81 m^2, volume: 2.43 m^3) with the first level total area of 35.67 m^2 and volume of 107.01 m^3. The main floor includes zones of the living room with a kitchen (area: 34.88 m^2, volume: 104.64 m^3), a washroom (area: 1.62 m^2, volume: 4.86 m^3), and a staircase (area: 1.62 m^2, volume: 4.86 m^3) with the second level total area of 38.12 m^2 and volume of 114.36 m^3. The bedroom floor includes three bedrooms (area: 18.10 m^2, volume: 54.30 m^3), two bathrooms (area: 3.78 m^2, volume: 11.34 m^3), a hall (area: 12.43 m^2, volume: 37.29 m^3), and a staircase (area: 1.62 m^2, volume: 4.86 m^3) with the third level total area of 35.93 m^2 and volume of 107.79 m^3. The floor-to-floor height is assumed to be 3 m for all levels.

It is important to emphasize that the ultimate goal of this study is to simultaneously assess the indoor air quality, moisture, and thermal comfort performances with the present integrated model and then to compare the obtained results using this model with those obtained using the single models (i.e. CONTAM and WUFI). To arrive at this goal, the case study of a three-story house as described above was selected in which the first level has a total area of 35.67 m^2 and a volume of 107.01 m^3, second level a total area of 38.12 m^2 and volume of 114.36 m^3, and third level a total area of 35.93 m^2 and volume of 107.79 m^3. This three-story house is commonly built in many locations in North America. However, the present integrated model can also be used to assess the indoor air quality, moisture, and thermal comfort performances of other types of one, two, and three-story houses. Most recently, the EnergyPlus model was successfully coupled with the present integrated model developed in this study so as to simultaneously assess the energy, indoor air quality, moisture, and thermal comfort performances for the same three-story house considered in this study, subjected to the climatic conditions of Montreal, Vancouver, and Miami (Heibati et al., 2021a).

The number of occupants of this house is five persons with two adults and three children of ages 4, 10, and 13 years.

The contaminants considered in this case study are indoor CO_2, indoor $PM_{2.5}$, and indoor VOCs. The only source for indoor CO_2 is assumed to be the respiration of the occupants. The source of indoor $PM_{2.5}$ is in the kitchen through cooking and in the living room through kitty litter. Indoor VOCs are available through the dining table, sofa, desk chair, bedside table, and cabinets. VOCs are assumed to include benzene, toluene, ethylbenzene, xylene, and styrene.

Air handling system is simple and recirculating type. The total volumetric airflow is 0.35 m^3/s. In this AHS, a typical furnace filter of MERV (minimum efficiency reporting value) with the rating of 4 in a single pass is used. The maximum space heating capacities of 5.2 kW, 5.2 kW and 7 kW and also maximum space cooling capacities of 18.16 kW, 15.10 kW and 10.59 kW for Montreal, Vancouver and Miami, respectively, have been used (ASHRAE, 2019b; Michael Bluejay, 2022). An exhaust fan with a capacity of 24 L/s is considered in on or off positions. In addition, the minimum and maximum zone temperatures of 20 °C and 26 °C, and the minimum and maximum relative humidity (RH) of 30% and 70%, respectively, are assumed as the design conditions.

The component assembly RSI (R-value system international) required for the case study based on ASHRAE Standard 90.1(ASHRAE, 2019b) has been defined for the three climate zones of 6-A, 5-A, and 1-A for Montreal, Vancouver, and Miami, respectively. The RSI value for the ground floor of 13.221 $m^2 \cdot K/W$, 10.671 $m^2 \cdot K/W$, and 5.241 $m^2 \cdot K/W$; below grade walls of 5.445 $m^2 \cdot K/W$, 3.695 $m^2 \cdot K/W$, and 0.695 $m^2 \cdot K/W$; above grade walls of 7.070 $m^2 \cdot K/W$, 7.070 $m^2 \cdot K/W$, and 4.445 $m^2 \cdot K/W$; intermediate floor–ceiling of 6.801 $m^2 \cdot K/W$, 6.801 $m^2 \cdot K/W$, and 0.651 $m^2 \cdot K/W$; roof of 10.488 $m^2 \cdot K/W$, 10.488 $m^2 \cdot K/W$, and 4.678 $m^2 \cdot K/W$; reflected double-glazed windows of 0.366 $m^2 \cdot K/W$, 0.366 $m^2 \cdot K/W$, and 0.277 $m^2 \cdot K/W$; external door of 0.350 $m^2 \cdot K/W$, 0.350 $m^2 \cdot K/W$, and 0.350 $m^2 \cdot K/W$; and interior walls of 1.2 $m^2 \cdot K/W$, 1.2 $m^2 \cdot K/W$, and 1.2 $m^2 \cdot K/W$ in Montreal, Vancouver, and Miami, respectively, have been assumed.

The thermal bridge for the wall to floor with a linear thermal transmittance of 0.03 W/m·K and for the wall to roof with a linear thermal transmittance of 0.04 W/m·K have been assumed as 25 (m) + 25 (m) = 50 (m) length.

The lists of all assumptions (see Table 4.1) are presented separately for CONTAM and WUFI models. This data is also used for the integrated model that couples CONTAM and WUFI. According to Table 4.1, the assumptions input data required for the COTAM model include parameters related to the status of the envelope leakage area, flow rate of the exhaust fan, number of envelope paths, number of zones, types of contaminants, outdoor contaminants' concentration, number of indoor contaminant source elements, generation rates of contaminants, and air-handling system. In addition, the assumptions input parameters required for WUFI according to Table 4.1 include geometry, thermal resistance of components (RSI), internal load, design conditions temperature, infiltration and ventilation rates, and HVAC load and capacities. The assumptions input parameters for weather data files for CONTAM and WUFI are presented in Table 4.2. CONTAM uses weather data sources of EnergyPlus (EnergyPlus, 2020). For CONTAM, the EPW (EnergyPlus weather data file) file must be converted to a WTH (weather file) using the CONTAM Weather File Creator ("CONTAM Utilities - CONTAM Weather File Creator," 2014). Finally, WUFI uses the weather data files from its database.

The integrated model capability has been evaluated in comparison with the single models of CONTAM and WUFI for three different climatic zones. Three different climates of cold-humid, moderate-humid, and warm-humid, respectively, for Montreal, Vancouver, and Miami have been selected. Table 4.2 compares the input data for geometry, temperature, wet days, sunlight, daylight, and solar position for all three different climatic zones of Montreal, Vancouver, and Miami. These parameters are defined in the form of a weather data file and as others required parameters presented in Table 4.2 for these different climate zones, provided to single models of CONTAM and WUFI as well as the integrated model. Finally, the output of the modeling in the single models and the integrated model are presented as results.

Simulated outputs by single models of CONTAM and WUFI as well as the integrated model have been assumed as concentrations of the indoor CO_2, indoor $PM_{2.5}$, and indoor VOCs, as well as the relative humidity (RH), predicted percentage of dissatisfied (PPD), and predicted mean vote (PMV). Output-simulated indoor CO_2, indoor $PM_{2.5}$, and indoor VOCs are assumed as daily values, while relative humidity (RH), predicted percentage of dissatisfied (PPD), and predicted mean vote (PMV) are assumed to be hourly values.

Table 4.1 The list of all assumptions input data parameters for the single and coupled models of CONTAM and WUFI

Program	Parameter	Values
	Weather Data	Montreal, Vancouver, and Miami: CONTAM (WTH files); WUFI (database)
CONTAM	Envelope Effective Leakage Area (m^2 @4 Pa, Exponent: 0.65, Discharge Coefficient: 1) (Chan et al., 2003a)	Airtight = 0.04 Leaky = 0.3
	Exhaust Fan (L/s)	Fan On = 24, Fan Off = 0
	Number of Envelope Paths	42
	Number of Zones	15
	Contaminants, 3	CO_2, $PM_{2.5}$, and VOCs
	Outdoor Contaminant Concentration (mg/m^3) (Canada, 2018; Division of Air Resource Management; Emmerich, Howard-Reed, & Gupte, 2005; Haghighat, Donnini, & D'Addario, 1992)	**CO_2:** 665.8 (Montreal), 665.8 (Vancouver), and 630 (Miami). **$PM_{2.5}$:** 0.027 (Montreal), 0.027 (Vancouver), and 0.035 (Miami). **VOCs:** 0.132 (Montreal), 0.322 (Vancouver), and 0.100 (Miami)
	Number of Indoor Contaminant Source Elements	21
	Indoor CO_2 Source Generation Rate (mg/s) (Emmerich et al., 2005)	**Awake:** [11 (adult male), 9.8 (adult female), 8.6 (child 13 years old), 6.8 (child 10 years old), and 3.8 (child 4 years old)]. **Sleeping:** [6.6 (adult male), 6.2 (adult females), 5.2 (child 13 years old), 4.1 (child 10 years old), and 2.3 (child 4 years old)]
	Indoor $PM_{2.5}$ Source Generation Rate (mg/h) (Howard-Reed, Wallace, & Emmerich, 2003; Wallace, Emmerich, & Howard-Reed, 2004)	**Kitchen cooking:** [65.45 (breakfast), 40.90 (lunch), and 8.18 (dinner)]. **Living room:** [5.5 (kitty litter)]
	Indoor VOCs Source Generation Rate (mg/h·unit) (Ho, Kim, Ryeul Sohn, Hee Oh, & Ahn, 2011)	10 (dining table), 3 (sofa), 2 (desk chair), 1 (bedside table), and 0.5 (cabinet)
	Filtration-Minimum Efficiency Reporting Value (MERV) rating	4
	Occupants	5 (an adult male, adult female, and three children of ages 4, 10, and 13 years old)

	Air Handling System (Pekdogan et al.) Airflow Rate (m^3/s)	0.35 (supply), 0.35 (return)
WUFI	Geometry	Total floor area 109.72 (m^2), net volume 329.16 (m^3), floor-to-ceiling height 2.7 (m), orientation 0°–180°,and window-to-wall ratio: S, E, N, 40%
	Component Assembly RSI (m^2.K/W) (ASHRAE, 2019b)	**Montreal:** 13.221 (ground floor), 5.445 (below grade walls), 7.070 (above grade walls), 6.801 (intermediate floor–ceiling), 10.488 (roof), 0.366 (reflected double-glazed windows), 0.350 (external door), and 1.2 (interior wall) **Vancouver:** 10.671 (ground floor), 3.695 (below grade walls), 7.070 (above grade walls), 6.801 (intermediate floor–ceiling), 10.488 (roof), 0.366 (reflected double-glazed windows), 0.350 (external door), and 1.2 (interior wall) **Miami:** 5.241 (ground floor), 0.695 (below grade walls), 4.445 (above grade walls), 0.651 (intermediate floor–ceiling), 4.678 (roof), 0.277 (reflective aluminum frame-fixed windows), 0.350 (external door), and 1.2 (interior wall)
	Internal Load Category	Family household (5 persons)
	Design Temperature (°C)	20
	Infiltration and Ventilation Rate (h^{-1}) (Chan et al., 2003a)	**Airtight**: 0.4 (fan off) and 0.7 (fan on); **Leaky**: 3.2 (fan off) and 3.5 (fan on)
	HVAC Load Capacity (ASHRAE, 2019b; Bluejay, 2022)	**Montreal**: 18.16 (heating load) and 5.2 (cooling load); **Vancouver**: 15.10 (heating load) and 5.2 (cooling load); and **Miami**: 10.59 (heating load) and 7 (cooling load)
	HVAC Airflow Capacity (m^3/s) (Craig, Richard, & Gniffin)	0.4 (Montreal), 0.365 (Vancouver), and 0.377 (Miami)
	Building Envelope Conditions (outside to inside)	**Ground floor**: XPS surface skin (heat conductivity: 0.03 W/mK; bulk density: 40 kg/m^3; porosity: 0.95; specific heat capacity: 1500 J/kg.K; water vapor diffusion resistance factor: 450; and typical built-in moisture: 0 kg/m^3); XPS Core (heat conductivity: 0.03 W/mK; bulk density: 40 kg/m^3; porosity: 0.95; specific heat capacity: 1500 J/kg.K; water vapor diffusion resistance factor: 100; and typical built-in moisture: 0 kg/m^3); XPS surface skin, concrete (w/c: water-cement-ratio of 0.5; heat conductivity: 1.7 W/mK; bulk density: 2308 kg/m^3; porosity: 0.15; specific heat capacity: 850 J/kg.K; water vapor diffusion resistance factor: 179; and typical built-in moisture: 100 kg/m^3); PVC roof membrane (heat conductivity: 0.16 W/mK; bulk density: 1000 kg/m^3; porosity: 2E-4; specific heat capacity: 1500 J/kg.K; water vapor diffusion resistance factor: 15000; and typical built-in moisture: 0 kg/m^3); EPS (except for Miami) (heat conductivity: 0.04 W/mK; bulk density: 30 kg/m^3 porosity: 0.95; specific heat capacity: 1500 J/kg.K; water vapor diffusion resistance factor: 50; and typical built-in moisture: 0 kg/m^3); and gypsum fibreboard (heat conductivity: 0.32 W/mK; bulk density: 1153 kg/m^3; porosity: 0.52; specific heat capacity: 1200 J/kg.K; water vapor diffusion resistance factor: 16; and typical built-in moisture: 35 kg/m^3). **Below grade wall:** mineral plaster (stucco, A-value: 0.1 $kg/m^2h^{0.5}$; heat conductivity: 0.8 W/mK; bulk density: 1900 kg/m^3; porosity: 0.24; specific heat capacity: 850 J/kg.K; water vapor diffusion resistance factor: 25; typical built-in moisture: 210 kg/m^3; reference water content: 45 kg/m^3; free water saturation: 210 kg/m^3; and water absorption coefficient: 0.0017 $kg/m^2s^{0.5}$); oriented strand board (heat conductivity: 0.13 W/mK; bulk density: 630 kg/m^3; porosity: 0.6; specific heat capacity: 1400 J/kg.K; water vapor diffusion resistance factor: 650; and typical built-in moisture: 95 kg/m^3); wood-fibre board (heat conductivity: 0.05 W/mK; bulk density: 300 kg/m^3; porosity: 0.8; specific heat capacity: 1400 J/kg.K; water vapor diffusion resistance factor: 12.5; and typical built-in moisture: 45 kg/m^3); EPS (except for Miami); polyethylene membrane (poly; 0.07 perm; heat conductivity: 2.3 W/mK; bulk density: 130 kg/m^3; porosity: 0.001; specific heat capacity: 2300 J/kg.K; water vapor diffusion resistance factor: 50000; and typical built-in moisture: 0 kg/m^3); chipboard (heat conductivity: 0.11 W/mK; bulk density: 600 kg/m^3; porosity: 0.5; specific heat capacity: 1400 J/kg.K; water vapor diffusion resistance factor: 70; and typical built-in moisture: 90 kg/m^3); and gypsum board (heat conductivity: 0.2 W/mK; bulk density: 850 kg/m^3; porosity: 0.65; specific heat capacity: 850 J/kg.K; water vapor diffusion resistance factor: 8.3; and typical built-in moisture: 6.3 kg/m^3). **Above grade wall**: mineral plaster (stucco, A-value: 0.1 $kg/m^2h^{0.5}$); oriented strand board; wood-fibre board; EPS; polyethylene membrane; chipboard; and gypsum board. **Intermediate floor–ceiling:** oak-radial (heat conductivity: 0.13 W/mK; bulk density: 685 kg/m^3;

		porosity: 0.72; specific heat capacity: 1400 J/kg.K; water vapor diffusion resistance factor: 140; and typical built-in moisture: 115 kg/m^3); air layer 40 mm (heat conductivity: 0.23 W/mK; bulk density: 1.3 kg/m^3; porosity: 0.999; specific heat capacity: 1000 J/kg.K; water vapor diffusion resistance factor: 0.38; and typical built-in moisture: 0 kg/m^3); EPS (except for Miami); softwood (heat conductivity: 0.09 W/mK; bulk density: 400 kg/m^3; porosity: 0.73; specific heat capacity: 1400 J/kg.K; water vapor diffusion resistance factor: 200; and typical built-in moisture: 60 kg/m^3); and gypsum board. **Roof:** 60 min building paper (heat conductivity: 12 W/mK; bulk density: 280 kg/m^3; porosity: 0.001; specific heat capacity: 1500 J/kg.K; water vapor diffusion resistance factor: 144; and typical built-in moisture: 0 kg/m^3); mineral insulation board (heat conductivity: 0.043 W/mK; bulk density: 115 kg/m^3; porosity: 0.95; specific heat capacity: 850 J/kg.K; water vapor diffusion resistance factor: 3.4; and typical built-in moisture: 4.5 kg/m^3); softwood; vapor retarder (1 perm) (heat conductivity: 2.3 W/mK; bulk density: 130 kg/m^3; porosity: 0.001; specific heat capacity: 2300 J/kg.K; water vapor diffusion resistance factor: 3300; and typical built-in moisture: 0 kg/m^3); air layer 40 mm; wood-fibre insulation board (heat conductivity: 0.042 W/mK; bulk density: 155 kg/m^3; porosity: 0.981; specific heat capacity: 1400 J/kg.K; water vapor diffusion resistance factor: 3; and typical built-in moisture: 19 kg/m^3); polyethylene membrane (poly; 0.07 perm); and softwoods.

Table 4.2 List of annual weather data values' assumptions, data adapted from Montreal, Quebec Climate & Temperature (2021); Miami, Florida Climate & Temperature (2021) and Vancouver, British Columbia Climate & Temperature (2021)

Climate Characteristics			
Parameters	**Montreal**	**Vancouver**	**Miami**
Altitude (m)	27	4	5
Latitude	45°30′ N	49°11′ N	25°45′ N
Longitude	73°25′ W	123°10′ W	80°23′ W
Average Annual Max. Temperature (°C)	11	14	28
Average Annual Temperature (°C)	6	10	24
Average Min. Temperature (°C)	1	6	21
Average Annual Precipitation (mm)	1017	1167	1420
Annual Number of Wet Days	166	164	132
Average Annual Sunlight (hours/day)	5 h 05′	5 h 01′	8 h 03′
Average Annual Daylight (hours/day)	12 h 00′	12 h 00′	12 h 00′
Annual Percentage of Sunny Daylight Hours (cloudy)	42 (58)	42 (58)	67 (33)
Annual Sun Altitude at Solar Noon on the 21st day	44.8°	41.1°	64.5°

4.3.3 Verification of the developed integrated model

For the verification of the present integrated model, the statistical method of paired sample t-test with the help of SPSS tools ("IBM SPSS Statistics," 2021) was used. In this method, the differences between actual and simulated data are compared based on statistical criteria. In

addition, the values of indoor CO_2 concentration and relative humidity (RH) were selected as indoor air quality and moisture data, respectively. The simulated and actual values of these data for the three-story house case of the leaky fan-on in Vancouver are shown in the Tables 4.3 and 4.4.

Table 4.3 shows the daily indoor CO_2 concentration data for the case of the leaky fan-on in Vancouver for the 15th day of each month for 2020. The simulated data is calculated by the integrated model and the actual data is measured by the CO_2 meter monitor.

Table 4.3 Daily indoor CO_2 concentration data for the 15th day of each month in 2020 for the case of the leaky fan-on in Vancouver

Data ((kg/kg) × 10^{-4})	**Month**											
	1	**2**	**3**	**4**	**5**	**6**	**7**	**8**	**9**	**10**	**11**	**12**
Simulated	8.24	8.79	8.82	8.29	8.84	8.85	8.35	8.87	8.87	8.33	8.83	8.78
Actual	8.44	8.72	8.74	8.48	8.75	8.75	8.50	8.75	8.73	8.45	8.68	8.61

Table 4.4 shows the hourly relative humidity (RH) data for the case of the leaky fan-on in Vancouver for the 15th day of each month for 2020. In this table, the values of the simulated data are calculated by the integrated model and the actual values are measured by the humidity meter monitor.

Table 4.4 Hourly relative humidity (RH) data for the 15th day of each month in 2020 for the case of the leaky fan-on in Vancouver

Data $\frac{(\%)}{hour}$	**Month**											
	1	**2**	**3**	**4**	**5**	**6**	**7**	**8**	**9**	**10**	**11**	**12**
Simulated	21.02	32.11	44.45	26.88	45.70	46.56	60.63	59.06	56.17	30.39	35.31	19.53
Actual	22.39	31.04	43.51	27.92	44.65	47.55	60.79	60.01	55.61	29.77	33.38	18.68

A paired sample *t*-test is performed as a statistical verification method in two steps: (1) paired samples' differences and (2) paired samples' correlations. Each simulated and actual data are compared with each other during these two steps using the paired sample *t*-test method and when the results of these comparisons are positive, the accuracy of the integrated model is confirmed and verified as per the references (Heibati et al., 2021c; Heibati & Atabi, 2013; Zhu,

2006). The results of the paired samples' differences and paired samples' correlation analysis for the simulated and actual data for the case of the leaky fan-on in Vancouver are shown in Tables 4.5 and 4.6, respectively.

Table 4.5 reveals that the standard deviation difference between the simulated and actual data for indoor CO_2 concentration and relative humidity (RH) are 0.14212 and 1.07103, respectively (being > half mean difference), with the significance level of 0.608 and 0.513, respectively (being > 0.05). As such, there are no significant differences between the simulated and actual data for indoor CO_2 concentration and relative humidity (RH).

Table 4.5 reveals that the standard deviation difference between the simulated and actual data for indoor CO_2 concentration and relative humidity (RH) are 0.14212 and 1.07103, respectively (being > half mean difference), with the significance level of 0.608 and 0.513, respectively (being > 0.05). As such, there are no significant differences between the simulated and actual data for indoor CO_2 concentration and relative humidity (RH).

Table 4.5 Paired samples' differences t-test results between the simulated and actual data for indoor CO_2 concentration and indoor relative humidity (RH) in 2020 for the case of the leaky fan-on in Vancouver

	Simulated Versus Actual Data	Paired differences							
		Mean	Standard Deviation	Standard Error Mean	95% Confidence Interval of the Difference		*t*-Statistic	df	Significance (two-tailed)
					Lower	Upper			
1	Indoor CO_2 concentration ((kg/kg) $\times 10^{-4}$)	0.02167	0.14212	0.04103	−0.06863	0.11196	0.528	11	0.608
2	Indoor relative humidity $\frac{(\%)}{hour}$	0.20917	1.07103	0.30918	−0.47133	0.88966	0.677	11	0.513

Table 4.6 shows that the correlation coefficients for the simulated and actual data of indoor CO_2 concentration and indoor relative humidity (RH) are 0.965 and 0.997, respectively (being

> 0.5), with the significance level of <0.05. Thus, the simulated and actual data are significantly correlated and in good agreements.

Table 4.6 Paired samples correlations t-test results between simulated and actual data for indoor CO_2 concentration and indoor relative humidity (RH) in 2020 for case of leaky fan-on in Vancouver

Simulated Versus Actual Data		Measurers		
		N	**Correlation**	**Level of Significance**
1	Indoor CO_2 concentration ((kg/kg) $\times 10^{-4}$)	12	0.965	0.000
2	Indoor relative humidity $\frac{(\%)}{hour}$	12	0.997	0.000

According to the coordination of the simulated and actual data using the paired sample *t*-test method, the accuracy of the integrated model developed in this study is validated.

4.4 Results

For each single model of CONTAM and WUFI compared to the integrated model, four scenarios are defined according to Table 4.7. These scenarios include: (1) airtight fan-off, (2) airtight fan-on, (3) leaky fan-off, and (4) leaky fan-on. The parameter values of each of the four scenarios for the case of three-story house are defined in Table 4.1.

Table 4.7 Proposed scenarios for single and integrated models

Status		Airtight	Leaky	Fan Off	Fan On
1	Scenario 1	Yes	No	Yes	No
2	Scenario 2	Yes	No	No	Yes
3	Scenario 3	No	Yes	Yes	No
4	Scenario 4	No	Yes	No	Yes

The purpose of presenting these scenarios is to assess the feasibility of the integrated model in simulating the performance of indoor air quality, moisture, and thermal comfort areas in comparison with single models in different climatic conditions.

4.4.1 Results of single model of CONTAM

The CONTAM's results for calculating indoor air quality performance are divided into three parts: (1) results related to indoor CO_2 percentage difference, (2) results related to indoor $PM_{2.5}$ percentage difference, and (3) results related to indoor VOCs percentage difference according to Figures 4.3–4.5. Each of these results is also simulated daily for the three different climatic regions of Montreal, Vancouver, and Miami for a period of one year (Figures 4.3–4.5). In each of Figures 4.3–4.5, the results of four scenarios listed in Table 4.7 are simulated using CONTAM. To assess the indoor air quality performance for these scenarios, the percentage difference method was used to compare indoor contaminants' concentration with the acceptable level of ASHRAE Standard 62.1 (ASHRAE, 2019a). The results of this percentage difference of indoor CO_2, $PM_{2.5}$, and VOCs with ASHRAE Standard 62.1 are shown in Figures 4.3–4.5, respectively.

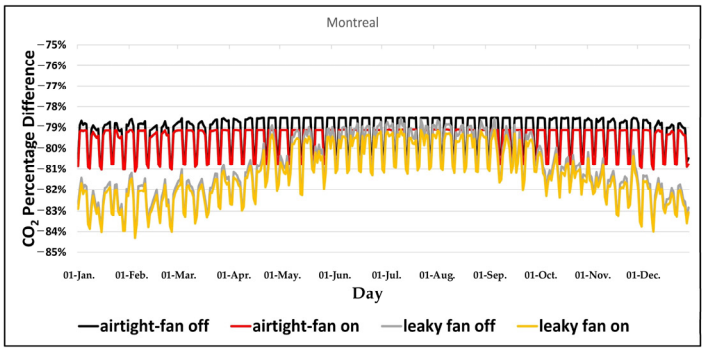

a. indoor CO_2 percentage difference in Montreal.

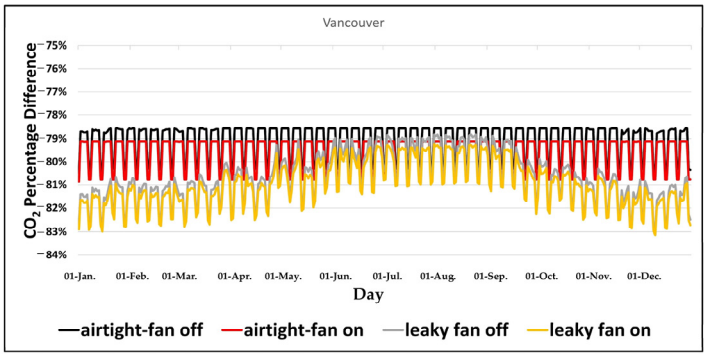

b. indoor CO_2 percentage difference in Vancouver.

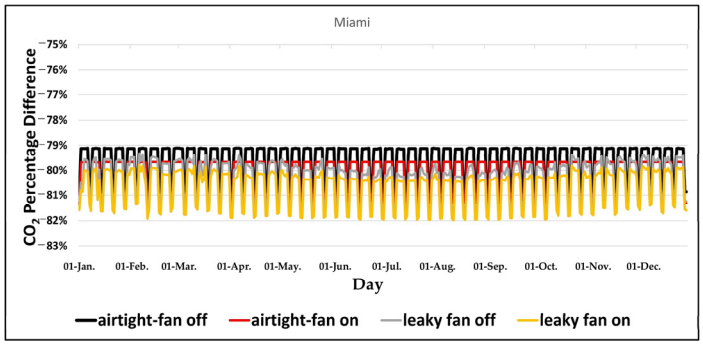

c. indoor CO_2 percentage difference in Miami.

Figure 4.3 Percentage differences comparison of daily indoor CO_2 concentrations with acceptable level of ASHRAE Standard 62.1 simulated by CONTAM for four scenarios in (a) Montreal, (b) Vancouver, and (c) Miami

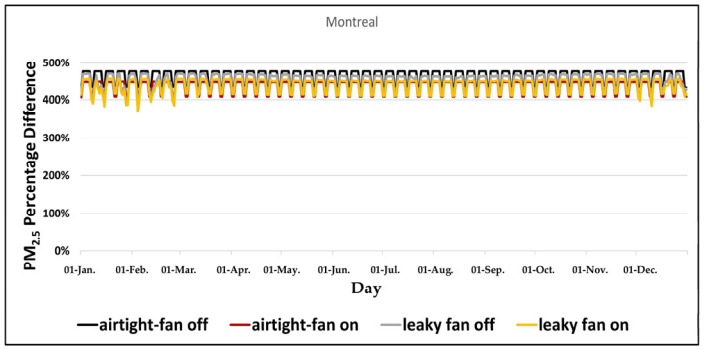

a. indoor $PM_{2.5}$ percentage difference in Montreal.

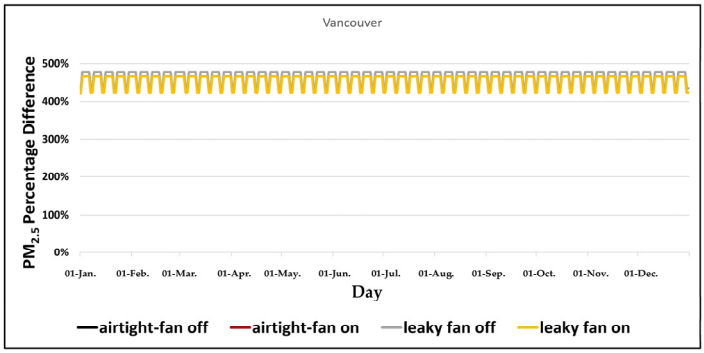

b. indoor $PM_{2.5}$ percentage difference in Vancouver.

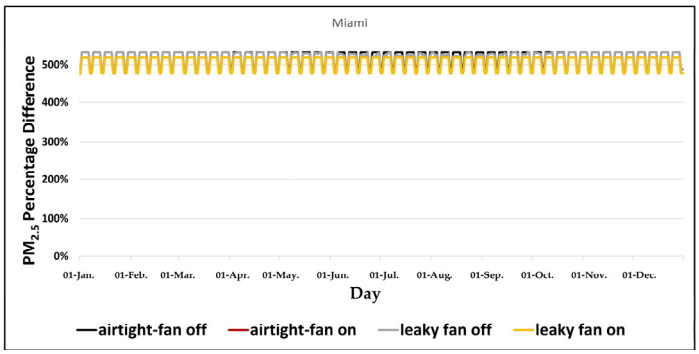

c. indoor $PM_{2.5}$ percentage difference in Miami.

Figure 4.4 Percentage differences comparison of daily indoor $PM_{2.5}$ concentrations with acceptable level of ASHRAE Standard 62.1 simulated by CONTAM for four scenarios in (a) Montreal, (b) Vancouver, and (c) Miami

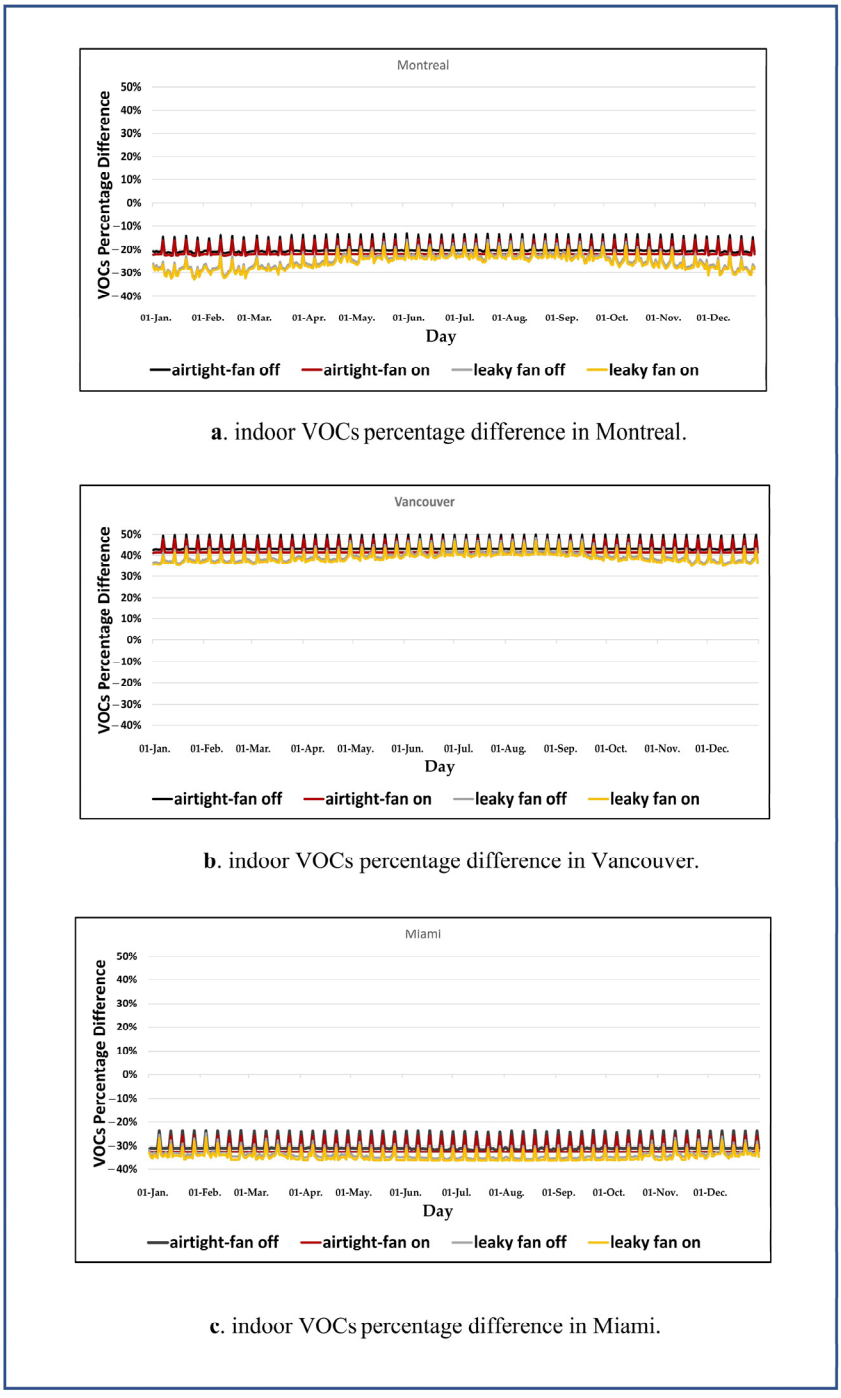

a. indoor VOCs percentage difference in Montreal.

b. indoor VOCs percentage difference in Vancouver.

c. indoor VOCs percentage difference in Miami.

Figure 4.5 Percentage differences comparison of daily indoor VOCs concentrations with acceptable level of ASHRAE Standard 62.1 simulated by CONTAM for four scenarios in (a) Montreal, (b) Vancouver, and (c) Miami

4.4.2 Result of single model of WUFI

Given that WUFI can calculate heat and moisture balances simultaneously, the WUFI simulation results consist of two main parts: (1) results related to the relative humidity (RH) percentage difference on the acceptable level of ASHRAE Standard 160 for evaluating the moisture performance, and (2) results related to the predicted percentage of dissatisfied (PPD) and predicted mean vote (PMV) measures for the thermal comfort performance assessment. These results are presented separately for different climatic conditions of Montreal, Vancouver, and Miami, and for a one-year period daily in Figures 4.6–4.8. The results of indoor relative humidity (RH), the predicted percentage of dissatisfied (PPD), and predicted mean vote (PMV) simulated by WUFI for each scenario (see Table 4.7) are provided in Figures 4.6–4.8. In order to assess the performance, the simulation results of indoor relative humidity (RH), predicted mean vote (PMV), and the percentage difference of these measures with the acceptable level of ASHRAE Standard 160 (ASHRAE, 2016a) for moisture (see Figure 4.6), and ASHRAE Standard 55 (ASHRAE, 2017a) for thermal comfort (see Figures 4.7 and 4.8), are used. Figures 4.7 also shows the predicted percentage of dissatisfied (PPD) simulation results by WUFI as an independent measure for evaluating thermal comfort performance for all scenarios in Montreal, Vancouver, and Miami.

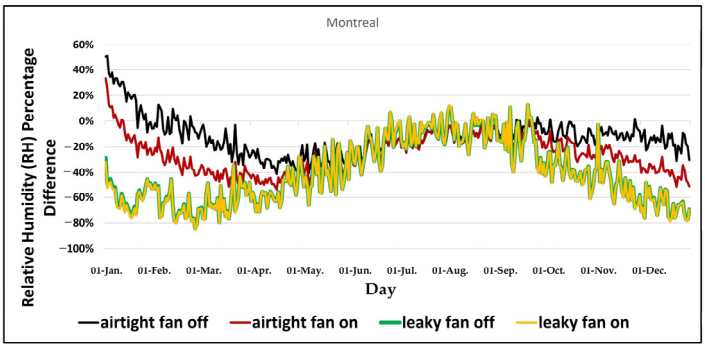

a. indoor relative humidity (RH) percentage difference in Montreal.

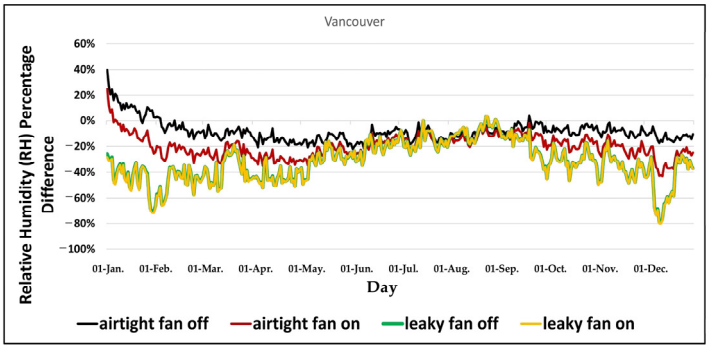

b. indoor relative humidity (RH) percentage difference in Vancouver.

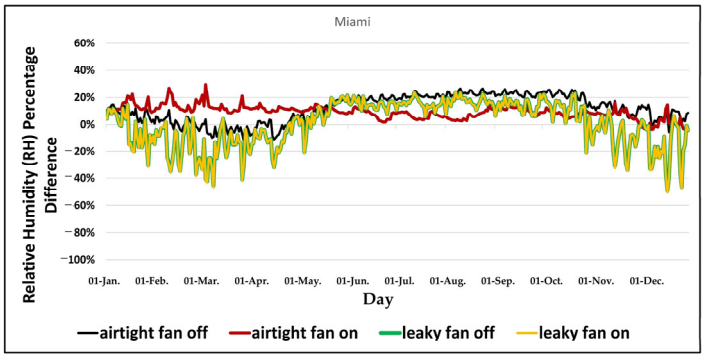

c. indoor relative humidity (RH) percentage difference in Miami.

Figure 4.6 Percentage differences comparison of hourly indoor relative humidity with acceptable level of ASHRAE Standard 160 simulated by WUFI for four scenarios in (a) Montreal, (b) Vancouver, and (c) Miami

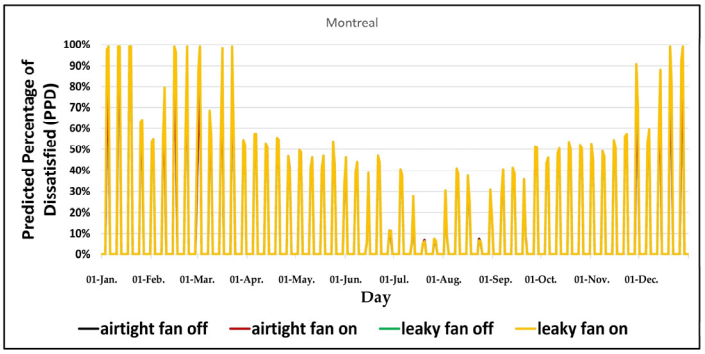

a.predicted percentage of dissatisfied (PPD) in Montreal.

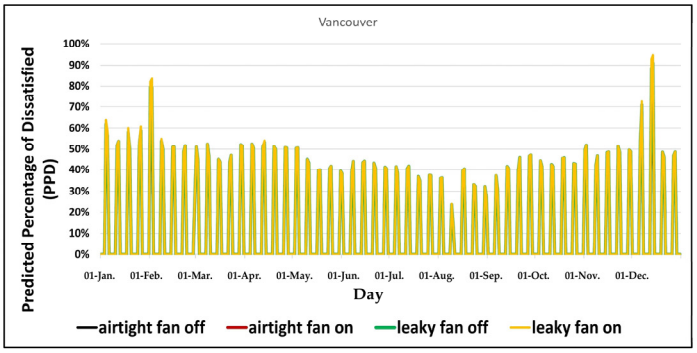

b.predicted percentage of dissatisfied (PPD) in Vancouver.

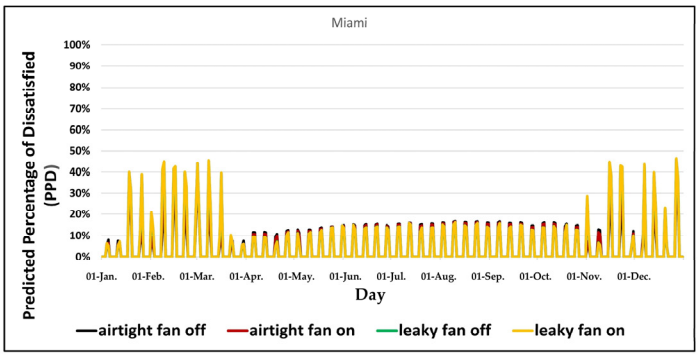

c.predicted percentage of dissatisfied (PPD) in Miami.

Figure 4.7 Comparison of predicted percentage of dissatisfied (PPD) based on acceptable level of ASHRAE Standard 55 simulated by WUFI for four scenarios in (a) Montreal, (b) Vancouver, and (c) Miami

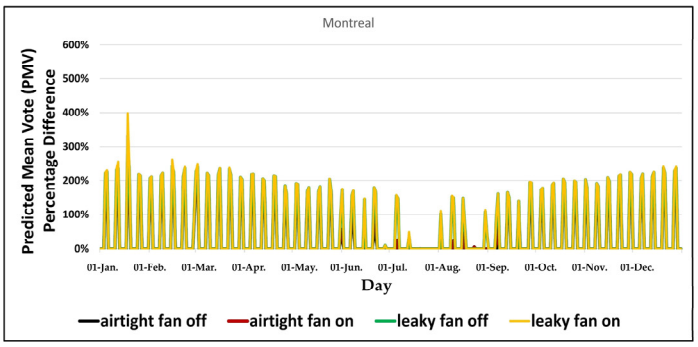

a. predicted mean vote (PMV) percentage difference in Montreal.

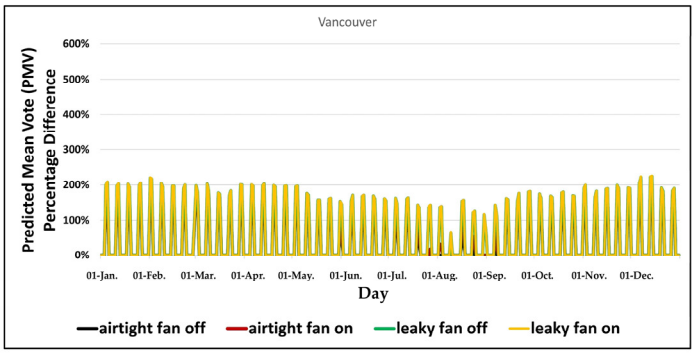

b. predicted mean vote (PMV) percentage difference in Vancouver.

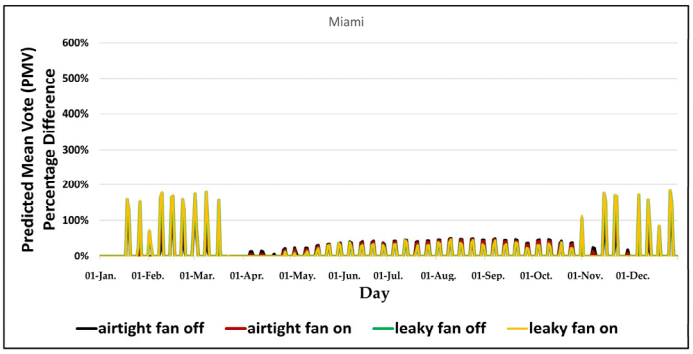

c. predicted mean vote (PMV) percentage difference in Miami.

Figure 4.8 Percentage differences comparison of hourly predicted mean vote (PMV) with acceptable level of ASHRAE Standard 55 simulated by WUFI for four scenarios in (a) Montreal, (b) Vancouver, and (c) Miami

4.4.3 Results of integrated model

The integrated model developed through the coupling mechanism of CONTAM and WUFI provides the simulation results of indoor air quality, moisture, and thermal comfort performances. Therefore, the simulation results of the integrated model include: (1) indoor CO_2 percentage difference, (2) indoor $PM_{2.5}$ percentage difference, (3) indoor VOCs percentage difference, (4) indoor relative humidity (RH) percentage difference, (5) predicted percentage of dissatisfied (PPD), and (6) predicted mean vote (PMV). These results are shown in Figures 4.9–4.14 similarly to the results of the single models for the three different climate cities of Montreal, Vancouver, and Miami on a daily basis for one year. Along with the results obtained by the integrated model, all three ASHRAE standards of 62.1, 160, and 55 (ASHRAE, 2016a, 2017a, 2019a) have been used in order to calculate the percentage difference between the simulated parameters with the acceptable level of ASHRAE standards. Therefore, the results of the simulated performances for all four scenarios are comparable to each other as well as to the other results (Figures 4.9–4.14).

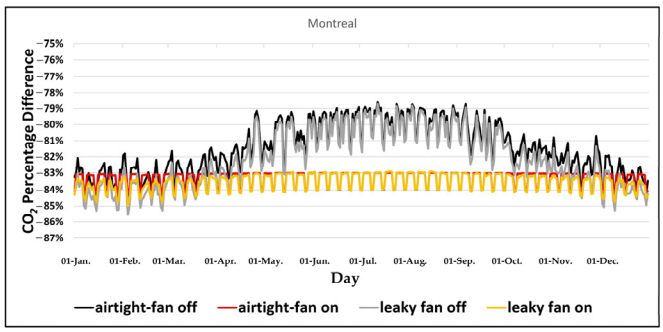

a. indoor CO_2 percentage difference in Montreal.

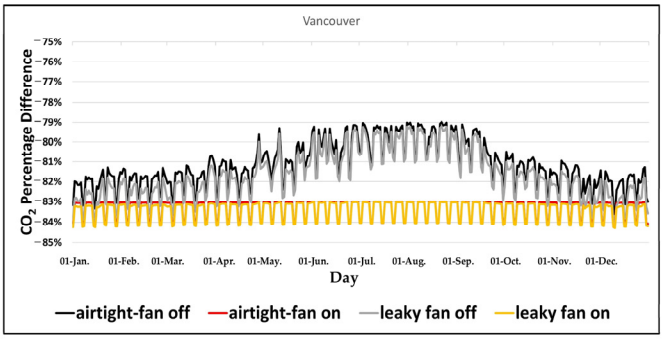

b. indoor CO_2 percentage difference in Vancouver.

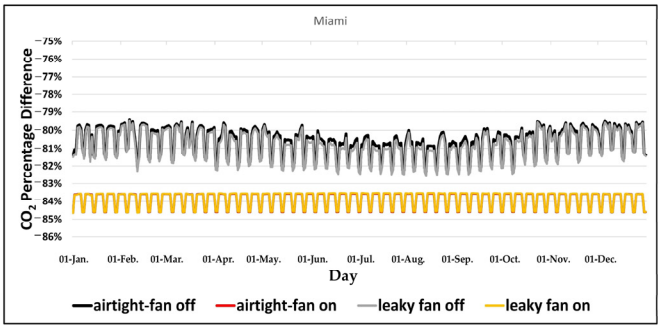

c. indoor CO_2 percentage difference in Miami.

Figure 4.9 Percentage differences comparison of daily indoor CO_2 concentrations with acceptable level of ASHRAE Standard 62.1 simulated by the integrated model for four scenarios in (a) Montreal, (b) Vancouver, and (c) Miami

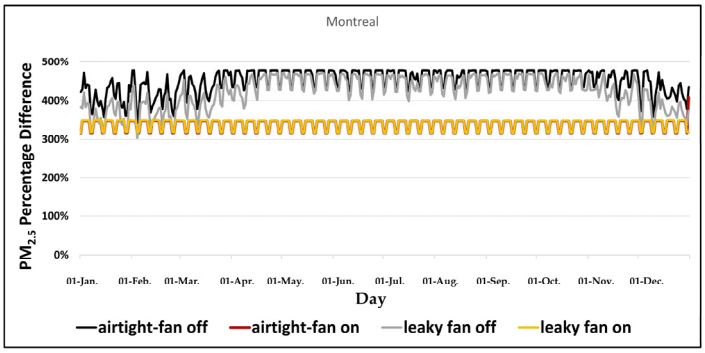

a. indoor $PM_{2.5}$ percentage difference in Montreal.

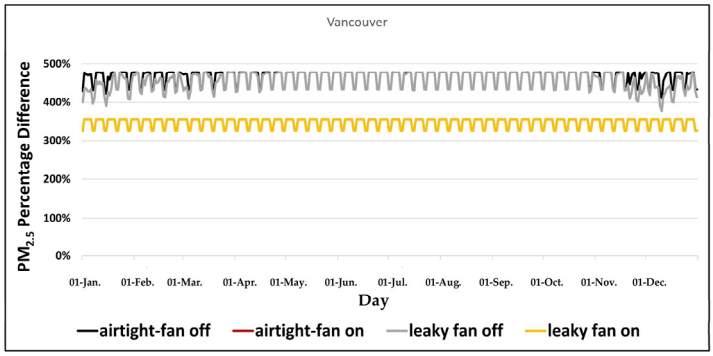

b. indoor $PM_{2.5}$ percentage difference in Vancouver.

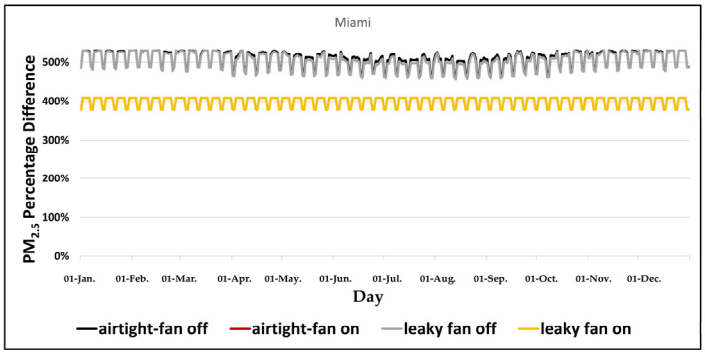

c. indoor $PM_{2.5}$ percentage difference in Miami.

Figure 4.10 Percentage differences comparison of daily indoor $PM_{2.5}$ concentrations with acceptable level of ASHRAE Standard 62.1 simulated by the integrated model for four scenarios in (a) Montreal, (b) Vancouver, and (c) Miami

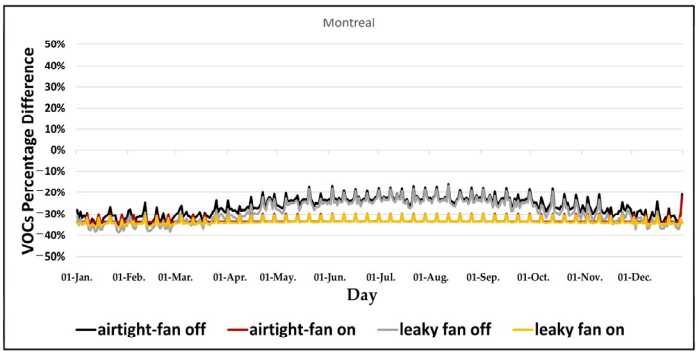

a. indoor VOCs percentage difference in Montreal.

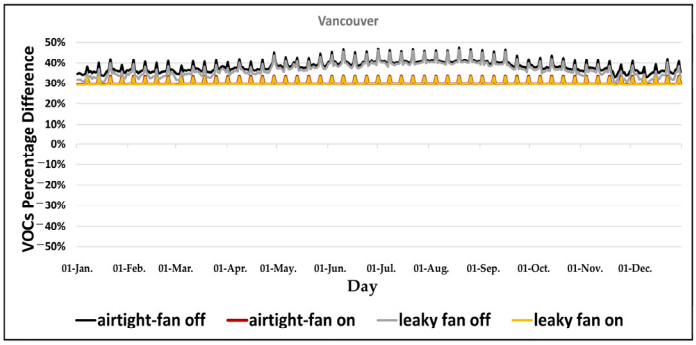

b. indoor VOCs percentage difference in Vancouver.

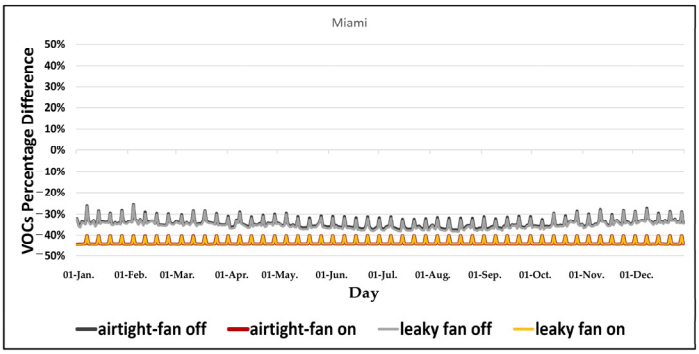

c. indoor VOCs percentage difference in Miami.

Figure 4.11 Percentage differences comparison of daily indoor VOCs concentrations with acceptable level of ASHRAE Standard 62.1 simulated by the integrated model for four scenarios in (a) Montreal, (b) Vancouver, and (c) Miami

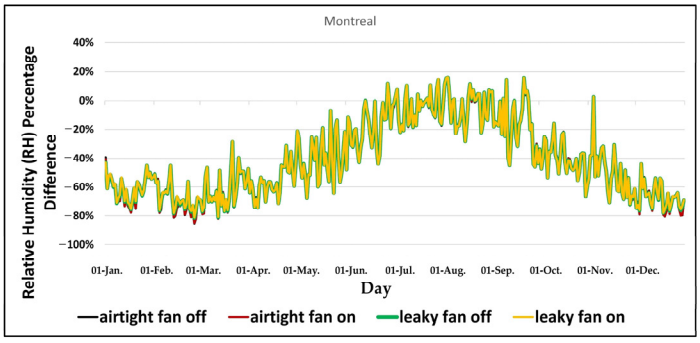

a. indoor relative humidity (RH) percentage difference in Montreal.

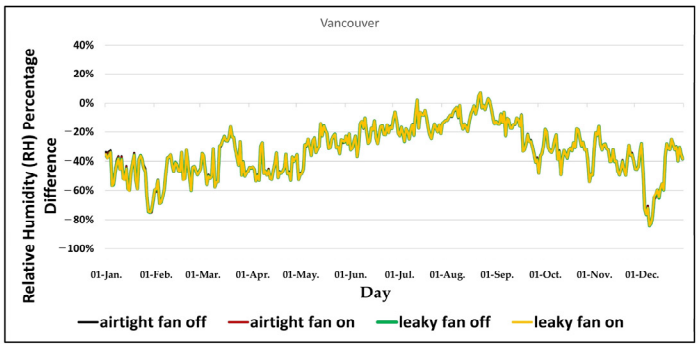

b. indoor relative humidity (RH) percentage difference in Vancouver.

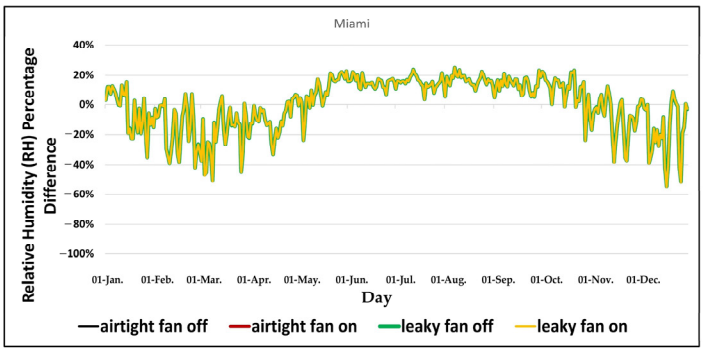

c. indoor relative humidity (RH) percentage difference in Miami.

Figure 4.12 Percentage differences comparison of hourly indoor relative humidity with acceptable level of ASHRAE Standard 160 simulated by the integrated model for four scenarios in (a) Montreal, (b) Vancouver, and (c) Miami

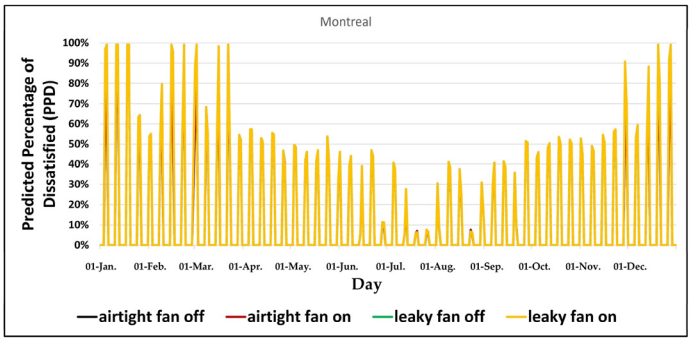

a.predicted percentage of dissatisfied (PPD) in Montreal.

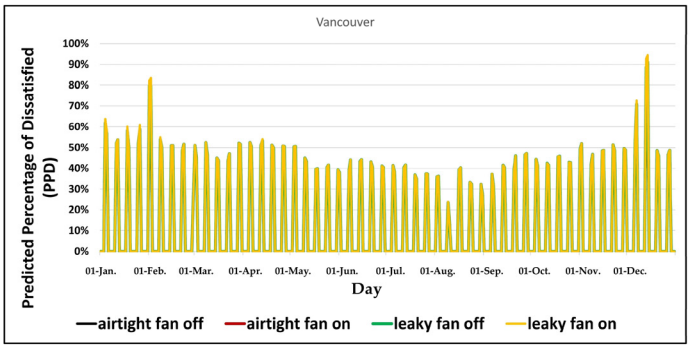

b.predicted percentage of dissatisfied (PPD) in Vancouver.

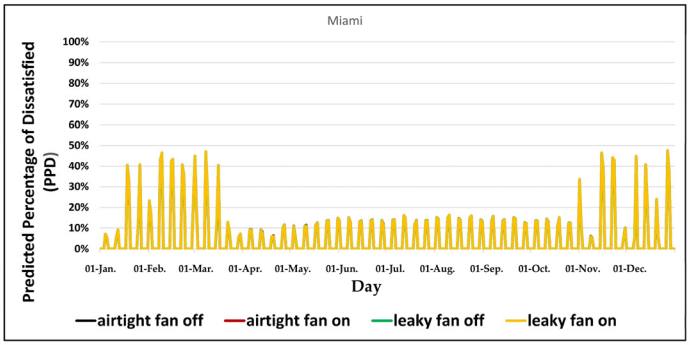

c.predicted percentage of dissatisfied (PPD) in Miami.

Figure 4.13 Comparison of predicted percentage of dissatisfied (PPD) based on acceptable level of ASHRAE Standard 55 simulated by the integrated model for four scenarios in (a) Montreal, (b) Vancouver, and (c) Miami

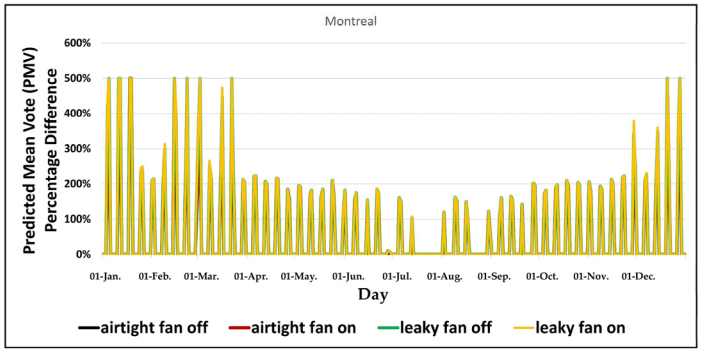

a. predicted mean vote (PMV) percentage difference in Montreal.

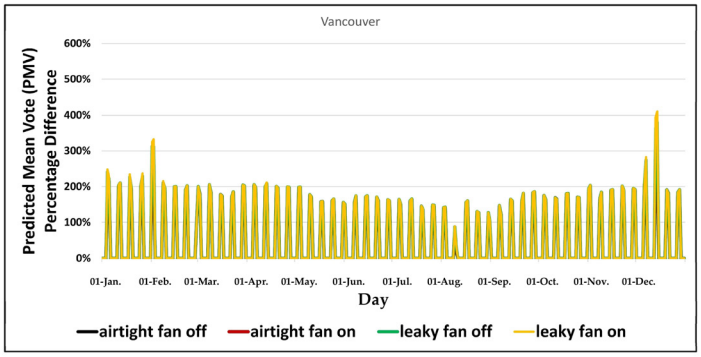

b. predicted mean vote (PMV) percentage difference in Vancouver.

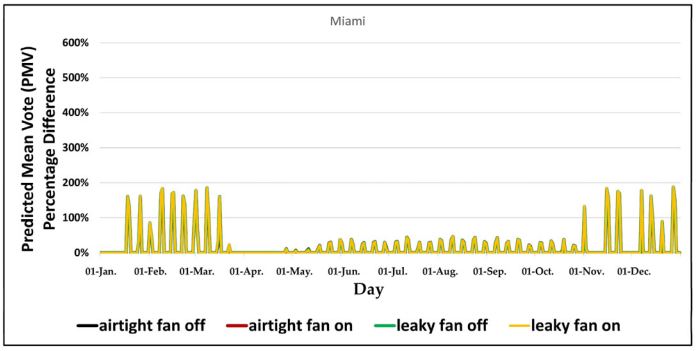

c. predicted mean vote (PMV) percentage difference in Miami.

Figure 4.14 Percentage differences comparison of hourly predicted mean vote (PMV) with acceptable level of ASHRAE Standard 55 simulated by the integrated model for four scenarios in (a) Montreal, (b) Vancouver, and (c) Miami

4.5 Discussion

The advantage of developing an integrated model compared to single CONTAM and WUFI models is that this model can simulate the performances' measures of both single models seamlessly. For the four scenarios of different values of leakage area and ventilation rate in the different climatic conditions (Table 4.7), the performance results simulated by all three CONTAM, WUFI, and integrated models are discussed.

With CONTAM, the method of calculating the percentage differences of indoor CO_2, $PM_{2.5}$, and VOCs with ASHRAE Standard 62.1 was used to evaluate indoor air quality performance. The obtained results for the Montreal, Vancouver, and Miami climates are shown in Figure 4.3a, b, c, respectively. As shown in these figures for the simulated indoor CO_2 concentration results, the minimum values on the scenarios' curves have the highest negative percentage difference with the level of ASHRAE Standard 62.1 (indoor $CO_2 < 6300$ mg/m^3) (ASHRAE, 2019a) and have the highest performances. For scenarios 1, 2, 3, and 4, this percentage difference in Montreal resulted in values of −80.85, −81.13, −84.13, and −84.30%, respectively; in Vancouver, in values of −80.49, −80.87, −82.93, and −83.15%, respectively; and in Miami, in values of −80.96, −81.41, −81.82, and −81.98%, respectively.

According to Figure 4.4a, b, c in CONTAM's indoor $PM_{2.5}$ concentration simulation, the minimum values on the scenarios' curves have the lowest percentage difference with the level of ASHRAE Standard 62.1 (indoor $PM_{2.5} < 15$ μg/m^3) (ASHRAE, 2019a) level and have the highest performances. For scenarios 1, 2, 3 and 4, this percentage difference in Montreal, resulted in values of 432.26%, 406.69%, 378.39% and 369.03%, respectively, in Vancouver, resulted in values of 432.26%, 420.65%, 432.18% and 420.65%, respectively, in Miami, resulted in values of 485.81%, 474.27%, 479.11% and 474.27%, respectively.

In the simulation of indoor VOCs concentration by CONTAM according to 4.5a, b, c minimum values on the scenarios curves have the highest performances based on percentage difference with ASHRAE Standard 62.1 (indoor VOCs < 300 μg/m^3) (ASHRAE, 2019a) . For scenarios

1, 2, 3, and 4, this percentage difference in Montreal resulted in values of −21.65, −22.77, −32.13, and −32.89%, respectively; in Vancouver, in values of 42.45, 41.12, 35.94, and 34.98%, respectively; and in Miami, in values of −32.13, −32.89, −35.90, and −36.47%, respectively.

In terms of WUFI, the minimum values of the scenarios' curves of the indoor relative humidity (RH) in Figure 4.6a, b, c show the highest negative percentage difference with the level of ASHRAE Standard 160 (indoor RH < 80%) (ASHRAE, 2016a) and have the highest performances. For scenarios 1, 2, 3, and 4, this percentage difference in Montreal resulted in values of −41.29, −53.60, −84.18, and −85.16%, respectively; in Vancouver, in values of −22.10, −43.06, −79.10, and −80.13%, respectively; and in Miami, in values of −11.83, −3.57, −49.26, and −50.53%, respectively.

WUFI can also simulate the predicted percentage of dissatisfied (PPD) and predicted mean vote (PMV) measures related to thermal comfort. The criterion for measuring the performance of thermal comfort is the acceptable level of ASHRAE Standard 55 (ASHRAE, 2017a) for the predicted percentage of dissatisfied (PPD) and predicted mean vote (PMV). The PPD value should be less than 10%. The PMV value should be less than 0.5 and greater than −0.5.

In Figures 4.7a, b, c for the predicted percentage of dissatisfied (PPD), the minimum values for scenarios' curves have the highest performances in the acceptable level of ASHRAE Standard 55 (PPD < 10%) (ASHRAE, 2017a). The PPD value for all scenarios in Montreal, Vancouver, and Miami are zero percent.

For the predicted mean vote (PMV) presented in Figure 4.8a, b, c, the minimum values for scenarios' curves have the highest performances in the acceptable level of ASHRAE Standard 55 (−0.5 < PMV < +0.5) (ASHRAE, 2017a). The percentage difference values with ASHRAE Standard 55 for all scenarios in Montreal, Vancouver and Miami are zero percent.

The results of the integrated model are presented in two groups to calculate the performance of indoor air quality, moisture, and thermal comfort. In the first group, the results of indoor CO_2, $PM_{2.5}$, and VOCs concentrations are presented in Figures 4.9–4.11. In the second group, the results of indoor relative humidity (RH), predicted percentage of dissatisfied (PPD), and predicted mean vote (PMV) are shown in Figures 4.12–4.14.

For simulated indoor CO_2 concentration results, Figure 4.9a, b, c show that the minimum values on the scenarios' curves have the highest performances based on the percentage difference with ASHRAE Standard 62.1 (ASHRAE, 2019a). For scenarios 1, 2, 3, and 4, this percentage difference in Montreal resulted in values of −84.88, −84.18, −85.55, and −84.98%, respectively; in Vancouver, in values of −83.61, −84.11, −84.25, and −84.29%, respectively; and in Miami, in values of −82.31, −84.64, −82.53, and −84.65%, respectively. Whereas for the simulated indoor $PM_{2.5}$ concentration, minimum values on the scenarios' curves have the highest performances based on the percentage difference with ASHRAE Standard 62.1 (ASHRAE, 2019a). For scenarios 1, 2, 3, and 4, this percentage difference in Montreal resulted in values of 342.98, 316.53, 303.31, and 317.42%, respectively; in Vancouver, in values of 411.21, 324.11, 377.02, and 324.11%, respectively; and in Miami, in values of −463.31, 377.74, 455.97, and 377.74%, respectively (see Figure 4.10a–c).

For the simulation of indoor VOCs concentration, Figures 4.11, a, b, c show that the minimum values on the scenarios' curves have the highest performances based on the percentage difference with ASHRAE Standard 62.1 (ASHRAE, 2019a). For scenarios 1, 2, 3, and 4, this percentage difference in Montreal resulted in values of −35.62, −33.94, −38.63, and −36.22%, respectively; in Vancouver, in values of 33.05, 29.56, 30.16, and 29.12%, respectively; and in Miami, in values of −37.63, −44.38, −38.39, and −44.42%, respectively.

For the simulated indoor relative humidity (RH) by the integrated model, Figures 4.12a, b, c show that minimum values on the scenarios' curves have the highest performances based on the percentage difference with ASHRAE Standard 160 (ASHRAE, 2016a). For scenarios 1, 2, 3, and 4, this percentage difference in Montreal resulted in values of −85.35, −84.96, −81.64,

and −81.25%, respectively; in Vancouver, in values of −82.52, −83.04, −84.31, and −84.23%, respectively; and in Miami, in values of −53.05, −53.81, −54.56, and −54.94%, respectively. Whereas for the predicted percentage of dissatisfied (PPD), the minimum values for scenarios' curves have the highest performances in the acceptable level of ASHRAE Standard 55 (ASHRAE, 2017a). The PPD value for all scenarios in Montreal, Vancouver, and Miami are zero percent (see Figure 4.13a–c). For the simulated predicted mean vote (PMV) by the integrated model, the minimum values for scenarios' curves have the highest performances in the acceptable level of ASHRAE Standard 55 (ASHRAE, 2017a). The percentage difference values with ASHRAE Standard 55 for all scenarios in Montreal, Vancouver, and Miami are zero percent (see Figure 4.14a, b, c).

Table 4.8 Comparison of average percentage differences of indoor air quality measures with acceptable level of ASHRAE Standard 62.1, simulated by CONTAM and integrated model

	Indoor CO_2						**Indoor $PM_{2.5}$**						**Indoor VOCs**					
Cities	**Montreal**		**Vancouver**		**Miami**		**Montreal**		**Vancouver**		**Miami**		**Montréal**		**Vancouver**		**Miami**	
Models	CONTAM Model	Integrated Model	CONTAM Model	Integrated Model	CONTAM Model	Integrated Model	CONTAM Model	Integrated Model	CONTAM Model	Integrated Model	CONTAM Model	Integrated Model	CONTAM Model	Integrated Model	CONTAM Model	Integrated Model	CONTAM Model	Integrated Model
S1	−79.17%	−81.51%	−79.08%	−81.17%	−79.63%	−80.63%	465.31%	450.39%	465.31%	464.63%	518.94%	509.56%	−19.65%	−26.40%	43.92%	38.55%	−30.17%	−34.55%
S2	−79.62%	−83.34%	−79.59%	−83.33%	−80.14%	−83.86%	438.50%	339.15%	452.59%	346.59%	506.19%	400.13%	−21.10%	−33.11%	42.34%	30.26%	−31.67%	−43.70%
S3	−80.95%	−82.13%	−80.66%	−81.64%	−80.29%	−80.80%	452.92%	423.43%	465.23%	457.48%	516.77%	505.07%	−24.51%	−28.69%	39.99%	36.92%	−33.67%	−35.05%
S4	−81.25%	−83.53%	−80.96%	−83.41%	−80.65%	−83.85%	440.76%	339.77%	452.59%	346.59%	506.19%	400.13%	−25.58%	−33.65%	38.89%	30.06%	−34.78%	−43.67%

In summary, the comparison of the scenarios' results for the single models of CONTAM and WUFI as well as for the present integrated model are presented in Figures 4.3–4.14. In addition, the obtained results by the single models are compared with those obtained by the integrated model for the simulated indoor air quality, moisture, and thermal comfort performances in Tables 4.8 and 4.9.

As shown in Table 4.8, for simulated indoor CO_2 concentration, in Montreal, scenarios 1, 2, 3, and 4 resulted in average values of −79.17, −79.62, −80.95, and −81.25% by CONTAM, and −81.51, −83.34, −82.13, and −83.53% by the integrated model, respectively; in Vancouver, scenarios 1, 2, 3, and 4 resulted in average values of −79.08, −79.59, −80.66, and −80.96% by CONTAM, and −81.17, −83.33, −81.64, and −83.41% by the integrated model, respectively; and in Miami, scenarios 1, 2, 3, and 4 resulted in average values of –79.63, −80.14, −80.29, and −80.65% by CONTAM, and −80.63, −83.86, −80.80, and −83.85% by the integrated model, respectively.

As shown in Table 4.8 for the indoor $PM_{2.5}$ concentration, in Montreal, scenarios 1, 2, 3, and 4 resulted in average values of 465.31, 438.50, 452.92, and 440.76% by CONTAM, and 450.39, 339.15, 423.43, and 339.77% by the integrated model, respectively; in Vancouver, scenarios 1, 2, 3, and 4 resulted in average values of 465.31, 452.59, 465.23, and 452.59% by CONTAM, and 464.63, 346.59, 457.48, and 346.59% by the integrated model, respectively; and in Miami, scenarios 1, 2, 3, and 4 resulted in average values of 518.94, 506.19, 516.77, and 506.19% by CONTAM, and 509.56, 400.13, −505.07, and 400.13% by the integrated model, respectively.

For indoor VOCs concentration (see Table 4.8), in Montreal, scenarios 1, 2, 3, and 4 resulted in average values of −19.65, −21.10, −24.51, and −25.58% by CONTAM, and −26.40, −33.11, −28.69, and −33.65% by the integrated model, respectively; in Vancouver, scenarios 1, 2, 3, and 4 resulted in average values of 43.92, 42.34, 39.99, and 38.89% by CONTAM, and 38.55, 30.26, 36.92, and 30.06% by the integrated model, respectively; and in Miami, scenarios 1, 2, 3, and 4 resulted in average values of −30.17, −31.67, −33.67, and −34.78% by CONTAM, and −34.55, −43.70, −35.05, and −43.67% by the integrated model, respectively.

In Table 4.9, the simulated indoor relative humidity (RH), predicted percentage of dissatisfied (PPD), and predicted mean vote (PMV) are compared between the scenarios as average values obtained with WUFI and the integrated model. For simulated indoor relative humidity (RH), in Montreal, scenarios 1, 2, 3, and 4 resulted in average values of −12.19, −25.62, −40.30, and

−40.59% by WUFI, and −41.06, −41.04, −40.62, and −40.50% by the integrated model, respectively; in Vancouver, scenarios 1, 2, 3, and 4 resulted in average values of −8.36, −19.58, −31.44, and −31.71% by WUFI, and −32.23, −32.34, −32.539, and −32.543% by the integrated model, respectively; and in Miami, scenarios 1, 2, 3, and 4 resulted in average values of 12.01, 9.21, 0.99, and 0.90% by WUFI, and 0.73, 0.69, 0.65, and 0.64% by the integrated model, respectively.

For the simulated predicted percentage of dissatisfied (PPD), Table 4.9 shows that in Montreal, scenarios 1, 2, 3, and 4 resulted in average values of 9.75, 10.68, 12.57, and 12.72% by WUFI, and 13.54, 13.72, 14.73, and 14.85% by the integrated model, respectively; in Vancouver, scenarios 1, 2, 3, and 4 resulted in average values of 9.90, 10.86, 12.59, and 12.65% by WUFI, and 12.81, 12.87, 13.26, and 13.34% by the integrated model, respectively; and in Miami, scenarios 1, 2, 3, and 4 resulted in average values of 4.21, 4.55, 5.15, and 5.17% by WUFI, and 5.22, 5.24, 5.25, and 5.26% by the integrated model, respectively.

Table 4.9 Comparison of average percentage differences of moisture performance and thermal comfort measures with acceptable level of ASHRAE Standards 160 and 55, respectively, simulated by CONTAM and the integrated model

	Indoor Relative Humidity (RH)						**Predicted Percentage of Dissatisfied (PPD)**						**Predicted Mean Vote (PMV)**					
Cities	**Montreal**		**Vancouver**		**Miami**		**Montreal**		**Vancouver**		**Miami**		**Montréal**		**Vancouver**		**Miami**	
Models	WUFI Model	Integrated Model	WUFI Model	Integrated Model	WUFI Model	Integrated Model	WUFI Model	Integrated Model	WUFI Model	Integrated Model	WUFI Model	Integrated Model	WUFI Model	Integrated Model	WUFI Model	Integrated Model	WUFI Model	Integrated Model
S1	−12.19%	−41.06%	−8.36%	−32.23%	12.01%	0.73%	9.75%	13.54%	9.90%	12.81%	4.21%	5.22%	36.19%	52.98%	38.07%	50.41%	10.65%	14.93%
S2	−25.62%	−41.04%	−19.58%	−32.34%	9.21%	0.69%	10.68%	13.72%	10.86%	12.87%	4.55%	5.24%	39.87%	54.07%	42.09%	50.67%	12.28%	14.98%
S3	−40.30%	−40.62%	−31.44%	−32.539%	0.99%	0.65%	12.57%	14.73%	12.59%	13.26%	5.15%	5.25%	48.34%	60.75%	49.55%	52.32%	14.64%	15.04%
S4	−40.59%	−40.50%	−31.71%	−32.543%	0.90%	0.64%	12.72%	14.85%	12.65%	13.34%	5.17%	5.26%	49.00%	61.50%	49.76%	52.73%	14.72%	15.07%

Table 4.9 shows that for the simulated predicted mean vote (PMV) in Montreal, scenarios 1, 2, 3, and 4 resulted in average values of 36.19, 39.87, 48.34, and 49.00% by WUFI, and 52.98, 54.07, 60.75, and 61.50% by the integrated model, respectively; in Vancouver, scenarios 1, 2, 3, and 4 resulted in average values of 38.07, 42.09, 49.55, and 49.76% by WUFI, and 50.41, 50.67, 52.32, and 52.73% by the integrated model, respectively; and in Miami, scenarios 1, 2, 3, and 4 resulted in average values of 10.65, 12.28, 14.64, and 14.72% by WUFI, and 14.93, 14.98, 15.04, and 15.07% by the integrated model, respectively.

By using both single models and the present integrated model to assess the performance of the three-story house described earlier when it is subjected to the climatic conditions of Montreal, Vancouver, and Miami, the main outcomes of this study include the following:

1. Scenario 4 resulted in the optimal scenario for the indoor CO_2 performance in both the CONTAM model and the integrated model methods in Montreal and Vancouver. The integrated model calculates the indoor CO_2 performance for Scenario 4 in Montreal and Vancouver by differences of 2.80% and 3.02%, respectively, more than the CONTAM model. The reason for this difference is because in the CONTAM model method, the effective leakage area of 0.3 m^2 and exhaust fan airflow of 24 L/s are defined by the users as airflows input data**.** In contrast, the airflows in the integrated model method are corrected by the co-simulation mechanism for CONTAM–WUFI.

2. To calculate indoor CO_2 performance in Miami, the results of Scenario 4, the optimal scenario using the integrated model method, are 3.98% different from the results of Scenario 2, the optimal scenario using the CONTAM model method. The reason for this difference is that the calculation of indoor CO_2 performance in Scenario 2 is defined by the user based on the effective leakage area of 0.04 m^2 and exhaust fan airflow of 24 L/s. The integrated model method in Scenario 4 calculates indoor CO_2 performance based on the corrected airflows using the co-simulation mechanism of CONTAM-WUFI.

3. In calculating the indoor $PM_{2.5}$ performance, the results of Scenario 2, the optimal scenario by the integrated model method, are −22.65% different from the CONTAM model method.

The reason for this difference is that in the CONTAM model method, effective leakage area of 0.04 m^2 and exhaust fan airflow of 24 L/s are defined as input airflows data by the user. Thus, in the integrated model method, with the help of the co-simulation mechanism of CONTAM–WUFI, the airflow values have been corrected.

4. Scenarios 2 and 4 are predicted for both Vancouver and Miami in the optimal level of indoor $PM_{2.5}$ performance. The indoor $PM_{2.5}$ performance values calculated for these scenarios by the integrated model method are −23.4% and −20.95% different from the CONTAM model method for Vancouver and Miami, respectively**.** The reason for this difference is that in the CONTAM model method, the effective leakage areas of 0.04 m^2 and 0.3 m^2 and exhaust fan airflow rate of 24 L/s for scenarios 2 and 4, respectively, are defined as input data airflows by the user. In contrast, the corrected airflows variables have been used by the integrated model method based on the co-simulation mechanism for CONTAM–WUFI.

5. The values of the indoor VOCs performance for Scenario 4, the optimal scenario by the integrated model method, are 31.54% and −22.70% different from the CONTAM model method for Montreal and Vancouver, respectively. The reason for this difference is that in the CONTAM model method, the effective leakage area of 0.3 m^2 and exhaust fan airflow of 24 L/s are defined as airflows input data by the user. In the integrated model, the airflow variables are corrected by the co-simulation mechanism of CONTAM–WUFI.

6. To calculate the indoor VOCs performance in Miami, the results of Scenario 2, the optimal scenario through the integrated model method, are 25.86% different from Scenario 4, the optimal scenario through the CONTAM model method. The reason for this difference is that the effective leakage area of 0.3 (m^2) and exhaust fan airflow of 24 L/s for Scenario 4 are defined by the user as the input airflows data in the CONTAM model method. As in the integrated model method in Scenario 2, the corrected airflows data is used by the co-simulation mechanism of CONTAM–WUFI.

7. In Montreal, for the calculation of the indoor relative humidity (RH) performance, the results of Scenario 3, the optimal scenario through the integrated model method, are 7.39% different from the results of Scenario 4, the optimal scenario based on the WUFI model method. Therefore, the reason for this difference is that in the WUFI model method, infiltration of 3.2 h^{-1} and mechanical ventilation of 0.3 h^{-1} for Scenario 4 are defined as airflows input data by the user. In addition, in the integrated model method for Scenario 3, corrected airflows are used by the co-simulation mechanism of CONTAM–WUFI.

8. The results of Scenario 4, the optimal scenario in calculating indoor relative humidity (RH) performance through the integrated model method, are 2.55% and −28.8% different from the WUFI model method results for Vancouver and Miami, respectively. The reason for this difference is that the infiltration of 3.2 h^{-1} and mechanical ventilation of 0.3 h^{-1} are defined by the user as the input airflows data in the WUFI model method. In the integrated model method, the airflow's data is corrected by the co-simulation mechanism of CONTAM–WUFI.

9. In calculating the indoor percentage of dissatisfied (PPD) performance, the results of Scenario 1, the optimal scenario through the integrated model method, resulted in a 39.58, 29.39, and 23.99% difference in Montreal, Vancouver, and Miami, respectively, from the WUFI model method. The reason for this difference is that the infiltration of 0.4 h^{-1} is defined as the input airflow data by the user in the WUFI model method. In contrast, in the integrated model method, air flow data corrected by the co-simulation mechanism of CONTAM–WUFI are used.

10. In calculating the indoor predicted mean vote (PMV) performance, Scenario 1, the optimal scenario through the integrated model method, resulted in a 52.98, 32.41, and 40.18% difference in Montreal, Vancouver, and Miami, respectively, from the WUFI model method. The reason for this difference is that the infiltration of 0.4 h^{-1} is defined as airflow input data by the user in the WUFI model method. However, the airflow data is corrected

through the co-simulation mechanism of CONTAM–WUFI in the integrated model method.

4.6 Conclusions

In this research study, an integrated model was developed to predict the performances of indoor air quality, moisture, and thermal comfort. In this model, the three balances of heat, moisture, and contaminate flows are simultaneously coupled. The exchange of the airflow rate parameter between CONTAM and WUFI, using a coupling method for developing the integrated model, made it possible to control and modify this parameter and the simulation results based on ASHRAE Standard 62.1, 160, and 55 levels. With the integrated model, a modified airflow rate can be designed for buildings with the high performances of indoor air quality, moisture, and thermal comfort conditions according to ASHRAE Standard criteria.

To evaluate the integrated model in comparison with single models of CONTAM and WUFI, simulated indoor CO_2, $PM_{2.5}$, and VOCs concentrations, as well as indoor air quality measures, indoor relative humidity (RH) as moisture measures, percentage of dissatisfied (PPD), and predicted mean vote (PMV) as thermal comfort measures were provided in this study. The results of indoor CO_2, $PM_{2.5}$, and VOCs simulated by CONTAM were compared with the integrated model, and the results of indoor relative humidity (RH), percentage of dissatisfied (PPD), and predicted mean vote (PMV) by WUFI were compared with the integrated model, as well.

As per the differences between the results of the single models and the present integrated model, it can be deduced that when the integrated model method replaces the single models' methods, the airflow data corrected by the CONTAM–WUFI co-simulation mechanism will replace with the airflow input data assumed by the user. Therefore, as these airflow data in the integrated model are corrected based on the capabilities of the coupled CONTAM–WUFI sub-models, it can accurately predict the results of the calculated indoor air quality, thermal

comfort, and moisture performance for optimum scenarios for buildings subjected to various climatic conditions.

Considering that the accuracy of the integrated model was verified by the paired sample *t*-test method, it can be concluded that the results of the integrated model can be used as a benchmark in predicting the performances of indoor air quality, moisture, and thermal comfort compared to other single models. Therefore, any differences between the results obtained with the present integrated model and those obtained with the single models (i.e. CONTAM and WUFI) suggest that the integrated model method can be a reliable alternative to the single model method for accurately assessing the indoor air quality, moisture, and thermal comfort performances for one-story, two-story, and three-story buildings when they are subjected to various climatic conditions. Last but not least, the EnergyPlus model was recently coupled with the present integrated model to simultaneously assess the overall performance (i.e. energy, indoor air quality, and moisture with thermal comfort performances) of the same three-story house considered in this study when it was subjected to the climatic conditions of Montreal, Vancouver, and Miami (Heibati et al., 2021a).

Author Contributions: Conceptualization, S.H., W.M. and H.H.S.; methodology, S.H., W.M. and H.H.S.; software, S.H.; validation, S.H., W.M. and H.H.S.; formal analysis, S.H.; investigation, S.H.; resources, S.H.; data curation, S.H.; writing—original draft preparation, S.H.; writing—review and editing, S.H., W.M. and H.H.S.; visualization, S.H.; supervision, W.M. and H.H.S.; project administration, W.M. and H.H.S.

CHAPITRE 5

ASSESSING THE ENERGY, INDOOR AIR QUALITY, AND MOISTURE PERFORMANCE FOR A THREE-STORY BUILDING USING AN INTEGRATED MODEL, PART THREE: DEVELOPMENT OF INTEGRATED MODEL AND APPLICATIONS

Seyedmohammadreza Heibati [a], Wahid Maref [a,] and Hamed H. Saber [b]

[a] Department of Construction Engineering, École de Technologie Supérieure (ÉTS), University of Québec, Montreal, QC H3C 1K3, Canada; Seyedmohammadreza.Heibati.1@ens.etsmtl.ca
[b] Prince Saud bin Thuniyan Research Center, Mechanical Engineering Department, Jubail University College, Al Jubail 35716, Saudi Arabia; SABERH@ucj.edu.sa

Paper published in Energies, MDPI, 8 September 2021

5.1 Abstract

The overall building performance depends mainly on the energy performance, indoor air quality, and moisture performance. In order to accurately calculate the building performance, the development of a model with the ability to integrate all three performances is required. In this research, a combination of three models namely EnergyPlus for energy, CONTAM for indoor air quality, and WUFI for moisture transport are used to develop an integrated model. The mechanism of this combination is based on the exchange of temperatures, airflows, and heating-cooling flows control variables between all three sub-models. By using the paired sample *t*-test, an integrated model is verified, and its accuracy is validated. The accuracy of the integrated model is verified by the paired sample *t*-test. To analyze the accuracy of the integrated model in comparison with single models, four scenarios of airtight fan-off, airtight fan-on, leaky fan-off, and leaky fan-on are defined for a three-story-house subjected to three different climate cities of Montreal, Vancouver, and Miami. Percentage differences of simulated measures with the ASHRAE Standard are considered as the performance criteria. The simulated results by single and integrated models are compared and analyzed. Finally, the scenarios with the high performances are evaluated in terms of energy efficiency, indoor air

quality, and moisture for Montreal, Vancouver, and Miami. Overall, it can be concluded that an integrated model should be developed.

Keywords: integrated model; EnergyPlus; CONTAM; WUFI; energy performance; indoor air quality; moisture performance

5.2 Introduction

There are three aspects to be used for increasing the performance of the buildings. These aspects include energy consumption, indoor air quality, and moisture control (Trofimova, Cheshmehzangi, Deng, & Hancock, 2021). Conducting numerical modeling is one of the most important tools in calculating building performance. Silva & Ghisi (2014) analyzed all the physical parameters and user behaviors that affect building performance in the energy sector using the EnergyPlus. To calculate the efficiency of a built school campus in London, Jain et al. (2020) considered the interrelationships between energy and indoor air environment, and they concluded that building performance depends on two important parameters, energy, and indoor air quality (IAQ) perspective (Jain et al., 2020). Underhill, Dols, Lee, Fabian, & Levy (2020) evaluated a coupled model of energy and indoor air quality using the co-simulation method, and the conclusion of this integrated model has high accuracy in calculating both energy and indoor air quality parameters (Underhill et al., 2020). Energy, thermal comfort, and indoor air quality performance for underground buildings were evaluated by Yu, Kang, & Zhai (2020). Berger, Guernouti, Woloszyn, & Buhe (2015) developed a performance building model based on a combination of heat and moisture transfer, and they concluded that excessive levels of moisture can lead to damage due to frost, heat, and mechanical effects on building materials, as well as mold growth or the effect on indoor air quality thermal comfort. EnergyPlus is a whole building energy simulation tool that can calculate energy performance in a building (EnergyPlus, 2021). This model is one of the acceptable tools for the community around the world for calculating building energy performance (Stadler, Firestone, Curtil, & Marnay, 2006). Fumo, Mago, & Luck (2010) used EnergyPlus to estimate the energy performance of a building by simulation of predetermined coefficients as the benchmark

energy model. It is important to point out that CONTAM is a multizone building airflow and contaminant transport simulation tool that can calculate indoor air quality performance in a building ("CONTAM 3.2," 2021). Wang, Dols, & Chen (2010) used CONTAM as a multizone airflow network computer program for building ventilation and indoor air quality analysis. They used the CFD features with CONTAM to calculate indoor air quality for a residential house (Wang et al., 2010). Dols et al. (2016) developed a coupled model of CONTAM with EnergyPlus using the co-simulation method. They verified the accuracy of the simulated results compared to the analytical results and attributed the high accuracy of this integrated model due to the interdependencies between airflow and heat flow as CONTAM and EnergyPlus outputs, respectively. Lv et al. (2020) used WUFI to calculate the moisture performance for the inner wall surface of the office building based on the analysis of relative humidity (RH) and heat flow parameters in reducing indoor mold growth risk. WUFI is a whole building envelope simulation tool that calculates moisture performance for a building as a holistic model ("WUFI® Plus," 2021). WUFI was developed by Künzel (1995) as a tool that calculates the risk of mold growth by coupling heat and moisture transport in building components. The capacity and parameters of HVAC systems in WUFI are assumed to be ideal, and this can reduce the accuracy of assessing the moisture performance for building envelope components (i.e., walls and roofs) (Pazold et al., 2012). Due to the interrelationship between building envelope and HVAC systems variables, Pazold et al. (2012) used Modelica as a tool for real-time HVAC system capacity calculation, and coupled it with WUFI, and developed a model with high computational accuracy. This confirms the necessity to calculate moisture performance and energy performance together to increase computational accuracy. Some materials with moisture buffering capacity have a dual effect on both adsorption/desorption for moisture and some contaminants such as VOCs. This type of buffering material can adsorb or desorb moisture and VOCs from ambient air can maintain its value in the appropriate levels of moisture and indoor air quality performances (Hunter-Sellars et al., 2020). Many recent studies have been performed to exploit the combination of EnergyPlus and CONTAM models that the results of this coupling are more accurately compared to single models (Underhill et al., 2020). WUFI models with CONTAM have been used to increase the accuracy of assessing performances of indoor air quality and moisture (Heibati et al., 2021b). To the best of our

knowledge, in the previous studies, several researchers have studied a maximum of two performances combination.

Most studies further include energy with indoor air quality (Chen et al., 2015; Persily & Emmerich, 2012), moisture with indoor air quality analyzes (Meklin et al., 2003), and also energy with moisture (Tariku, 2008) in a integrated way. Some energy efficiency, indoor air quality, and moisture effect strategies have negative interactions with each other (Feijó-Muñoz et al., 2018). This is because similar research has not been presented to provide a integrated model of all three energy, indoor air quality, and moisture, in order to evaluate the necessity of combining all three performances in an integrated way, previous research on the interaction of each of these measures have been presented. Researchers who have studied on negative interaction between moisture effect and energy efficiency have concluded that the moisture effect can lead to an increase in annual building energy consumption (Barbosa & Mendes, 2008). In other cases, changes in moisture content and adsorption/desorption (i.e. sorption curve) ability in envelope materials can lead to not only increased/decreased thermal conductivity (Moon, Ryu, & Kim, 2014) but also the risk of condensation and mold growth (see (Saber, Lacasse, & Moore, 2017; Saber & Maref, 2019; Saber, Maref, & Hajiah, 2019) for more details). Neglecting the moisture transport in assessing the overall building performance may lead to inaccurate energy demand predictions (Mendes, Winkelmann, Lamberts, & Philippi, 2003). There are negative interactions between energy efficiency and moisture effect, which increase the potential for mold growth risk in-built environments with increasing thermal insulation (Saber et al., 2017; Saber & Maref, 2019; Saber et al., 2019). Reducing ventilation rates to improve energy consumption in the building can lead to increasing concentrations of contaminants in indoor air, which indicates a negative interaction between energy and indoor air quality parameters (Persily & Emmerich, 2012). Additionally, increasing cooling equipment efficiency can increase indoor humidity levels if the latent loads are not sufficiently designed for system control (Moon, 2005). The study can be one of the reasons for the negative interaction of energy efficiency with indoor air quality. Some strategies have shown that the energy efficiency, indoor air quality and moisture effect, have positive interactions with each other (Persily & Emmerich, 2012). For example, using

residential heat recovery ventilation has led to improving indoor air quality and energy saving which can show positive interaction (Roseme, 1980). Airside economizer operation acts as a system that shows positive interaction by increasing energy saving, indoor air quality and moisture control (Doty, 2009). Moon et al. analyzed the effect of moisture transportation on energy efficiency and indoor air quality and concluded that discarding moisture transportation could reduce the accuracy of calculating overall building performance for other energy and indoor air quality measures (Moon et al., 2014). In order to investigate the positive and negative effects of each energy efficiency, indoor air quality and moisture effect on each other, they must be evaluated in an integrated manner. Given that there are correlations between energy performance, indoor air quality performance, and moisture performance for the whole building, which can be concluded that the creation of an integrated model leads to an increase in the accuracy of overall building performance. This integrated model does not have the limitations of single models in calculating only one performance measure of the building because it is able to predict simultaneously all three measures of energy, indoor air quality, and moisture effect. By using this integrated model, it is possible to control and balance the positive and negative interactions for all three measures of energy efficiency, indoor air quality, and moisture effects. The interrelationship between energy, indoor air quality and moisture models to calculate building performance can be developed by the exchange control variables such as temperatures and airflow (Dols et al., 2016).

The ultimate aim of this research is to develop an integrated model by coupling the EnergyPlus, CONTAM, and WUFI sub-models. This coupling includes exchanging airflows, temperatures, and other dependent variables between the three sub-models so as to increase the computational accuracy. The novelty of the integrated model in relation with the single models is its ability to simultaneously predict energy, indoor air quality, and moisture performances for different types of the building whereas the single models predict independently only one of these performances (energy performance, indoor air quality performance and moisture performance). In single models, temperature and airflow variables with dependent variables are defined by the user as input data ("CONTAM 3.2," 2021; EnergyPlus, 2021; "WUFI® Plus," 2021). In the integrated model, the exchange of control variables within EnergyPlus,

CONTAM, and WUFI sub-models lead to the correction of these variables. This results in increasing the accuracy of the integrated model prediction.

5.3 Methodology

In this research, an integrated model has been developed based on a combination of three models that includes EnergyPlus, CONTAM, and WUFI. This integrated model has been developed in three phases. In the first phase, the coupling of EnergyPlus with CONTAM is provided in our previous publication (Heibati et al., 2019). In the second phase, the possibility of combining WUFI with the CONTAM model has been evaluated (Heibati et al., 2021b). In the third phase, an integrated model of energy, indoor air quality and moisture have been developed based on a combination of all three models of EnergyPlus, CONTAM, and WUFI.

In this paper, a combination method of EnergyPlus, CONTAM, and WUFI as the third phase is conducted. In addition, the equations for the integrated model are presented. The common parameters that can be exchanged between the governing equations are also identified and analyzed. Model verification analysis is performed to measure the integrated model's accurateness. Finally, the difference between the actual data with simulated results for a three-story house as a case study was performed using the method of paired sample *t*-test. Additionally, the simulated results extracted by the integrated model are compared and analyzed to those obtained by EnergyPlus, CONTAM, and WUFI single models, in three different climates of Montreal, Vancouver, and Miami.

5.3.1 Combination method of EnergyPlus, CONTAM and WUFI

An integrated model has been developed based on interconnections to combine the three sub-models of EnergyPlus, CONTAM, and WUFI. In this integrated model, the sub-model of EnergyPlus simulates energy measures. These measures mainly include hourly gas and electric energy consumptions in various parts of the building. The sub-model of CONTAM is responsible for simulating indoor air quality measures. These measures include air change rate

and indoor contaminant concentration such as CO_2, CO, VOCs, NOX, particles, and other indoor air pollutants. Lastly, the WUFI sub-model also simulates moisture and thermal comfort measures. These measures for moisture performance include relative humidity (RH) and the thermal comfort that includes predicted mean vote (PMV), predicted percentage of dissatisfied (PPD) and other related parameters.

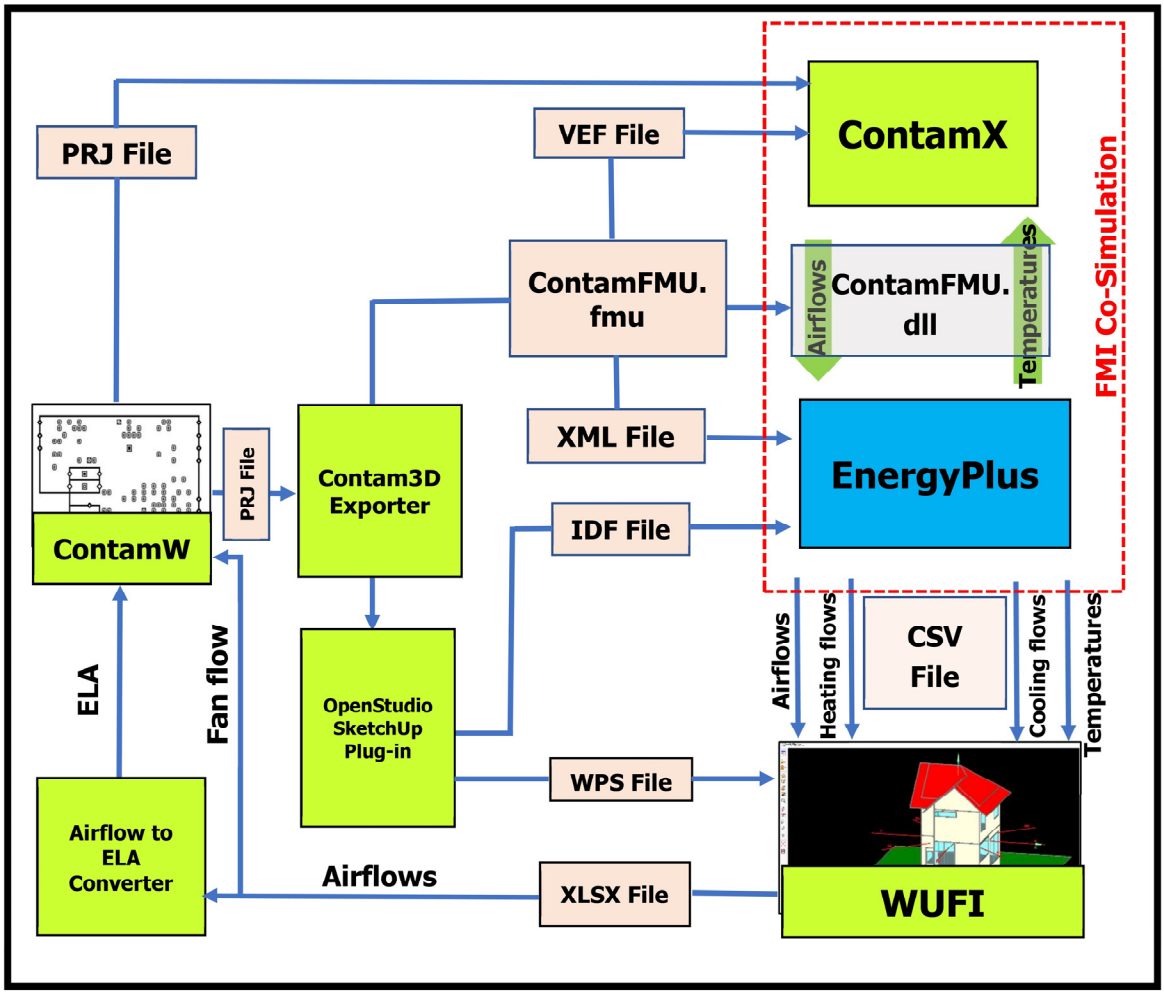

Figure 5.1 Combination mechanism for EnergyPlus, CONTAM, and WUFI, DLL: dynamic link library, VEF: variable exchange file, FMI: functional mock-up interface, FMU: functional mock-up unit, XML: extensible markup language, WPS: WUFI Passive-SketchUp, IDF: input data file, CONTAM: contaminant transport analysis model, ELA: effective leakage area, XLSX: Excel Microsoft Office Open XML format spreadsheet file, PRJ: project and CSV: comma-separated values

As shown in Figure 5.1, the interconnection and consequently integrations between each of the sub-models of EnergyPlus, CONTAM, and WUFI have been applied subject to the exchange of common control variables. The most important of these common control variables are indoor air temperatures and different types of airflows in the form of infiltration, natural, and mechanical ventilation. The three sub-models have been integrated into three phases according to Figure 5.1. In this interrelationship, common control variables are exchanged in a conversion loop between the three sub-models.

In the first phase, the coupling mechanism between EnergyPlus and CONTAM is performed based on the co-simulation method. This method was developed by Dols et al. (Dols et al., 2016). The co-simulation method based on the standard functional mock-up interface provides the link between EnergyPlus and CONTAM (Nouidui et al., 2014). The functional mock-up interface (FMI) standard is a tool-independent standard that supports exchange data and co-simulation of dynamic models (MODELICA, 2017). The CONTAM model consists of two separate programs: (1) ContamW and (2) ContamX ("CONTAM 3.2," 2021). The ContamW runs as a graphic user interface and can be used to define the case of the building and also to view the simulated results. The ContamX, however, simulates and calculates indoor air quality measures. The input data related to the description of the building case study is saved as a project (PRJ) file in ContamW and can also be read in ContamW and ContamX. For co-simulation, the CONTAM model must first be implemented in the FMI standard. This model is implemented by exporting the CONTAM model into a functional mockup unit (FMU). The created FMU is called ContamFMU.fmu, which is a compressed zip file and can then be imported into EnergyPlus for co-simulation. The program that exports the CONTAM model to ContamFMU.fmu is called the CONTAM3DExporter tool which was developed by the National Institute of Standards and Technology (NIST) ("Contam3DExport," 2020).

The CONTAM3DExporter tool converts the PRJ file created by ContamW into two files as shown in Figure 5.1. These two files are (1) input data file (IDF file) and (2) ContamFMU.fmu. The IDF file contains information about geometry, airflow infiltration, inter-zone airflow, and HVAC system airflows. Finally, this IDF file is provided to EnergyPlus. ContamFMU.fmu

includes packages of compressed zipped files for controlling and exchanging common variables between EnergyPlus and CONTAM. The components of this package include XML file, VEF file, ContamFMU.dll (XML: extensible markup language, VEF: variable exchange file and dll: dynamic link library), and other files required in co-simulation. The XML file is exchanged with EnergyPlus and provides data on zone infiltration, inter-zone airflows, and control values of airflow ventilation. The VEF file is exchanged with ContamX and provides data on zone temperature, ventilation system airflows, outdoor airflow fractions, exhaust fan airflow, outdoor environment data, and output variables. Additionally, the ContamFMU.dll acts as a control file in exchanging temperature and airflow control variables along with other required information between EnergyPlus and ContamX. The temperatures and airflow control variables are exchanged between EnergyPlus and ContamX as shown in Figure 5.1 using ContamFMU.dll. This exchange leads to the integration of these two sub-models and the creation of coupled EnergyPlus–CONTAM (Heibati et al., 2019).

In the second phase, the simulated variables resulted from the co-simulation in the previous phase are used as WUFI input data. Thus, the interconnection is made between the coupled EnergyPlus-CONTAM with WUFI. This mechanism is based on the replacement of simulated variables of coupled EnergyPlus-CONTAM with input data of WUFI. In this replacement control variables, airflows, temperature, heating, and cooling flows are exchanged as CSV files (CSV: comma-separated values) as shown in Figure 5.1. The simulated paths and duct airflows in coupled EnergyPlus-CONTAM are replaced separately with input data of natural, mechanical, and interzone airflows in WUFI. The simulated heating and cooling temperatures in coupled EnergyPlus-CONTAM are replaced with input data of maximum and minimum temperatures in WUFI. Finally, the simulated space heating and cooling energy consumptions per hour in coupled EnergyPlus-CONTAM are also replaced by input data of heating and cooling space capacities in WUFI.

Integration of the developed model is completed by performing the third phase. This phase consists of two parts. In the first part, the airflows control variables simulated in WUFI as shown in Figure 5.1 are used as input data for flow rates of exhaust fan and leakage area. The

simulated control variables related to the natural and mechanical ventilation in WUFI in the form of an XLSX file, as shown in Figure 5.1, are replaced by the input data of ELA (effective leakage area) and fan flow rate in ContamW, respectively. The simulated natural ventilation of WUFI is replaced with ELA input data in ContamW by using an Excel converter (airflow to effective leakage area converter tool).

The airflow to ELA converter operates on the basis of Equations (5.1)–(5.3) (Chan, Price, Sohn, & Gadgil, 2003b; Heibati et al., 2021b; Sherman & Dickerhoff, 1998).

$$ACH = \frac{\dot{m}}{V_{net}} \tag{5.1}$$

$$NL \approx ACH \tag{5.2}$$

$$NL = 1000 \cdot \frac{ELA}{A_f} \cdot \left(\frac{H}{2.5}\right)^{0.3} \tag{5.3}$$

where ACH for air change per hour (h^{-1}), $\dot{m}$ for volumetric airflow rate (m^3/h), V_{net} for building net volume (m^3), NL for normalized leakage, ELA for effective leakage area, A_f for a floor area (m^2) and H for building height (m) are considered (for more details regarding airflow element models and effective leakage area calculation conditions values in ContamW, see (S. Heibati et al., 2021b).

In the next step, the geometry data simulated by ContamW is converted from the PRJ file to an IDF file with the help of CONTAM3DExporter. The IDF file can be viewed and edited by the importer of the OpenStudio SketchUp Plug-in extension and the details of this geometry can also be controlled and modified ("OpenStudio," 2021). The geometry modified file can be exported from SketchUp into WUFI by the WUFI SketchUp's Plug-in as an extension in SketchUp. The format of this imported file is WPS (WUFI Passive-SketchUp) for geometry files. In this procedure, the simulated modified geometry data is used as input geometry data in WUFI.

The exchange of both airflows and geometry control variables as shown in Figure 5.1 between WUFI and CONTAM completes the interconnection process in the final step. Exchange of common control variables airflows, temperatures, heating and cooling flows, geometry data, and other involved variables, leads to integration between sub-models of EnergyPlus, CONTAM, and WUFI dynamically resulting in simulating the energy, indoor air quality, and moisture for whole-building performance.

5.3.2 Governing equations

The equations for the integrated model are the combination of the energy, moisture, and contaminant flow balances according to Equations (5.4)–(5.6), respectively.

$$\frac{dE_{heat,i}}{dt} = \sum_k \dot{E}^{opaque}_{component,k} + \sum_k \dot{E}^{transparent}_{component,k} + \dot{E}_{solar} + \dot{E}_{internal} + \dot{E}_{nat-infiltration} + \dot{E}_{mech-ventilation} \quad (5.4)$$

$$\frac{dw_{moist,i}}{dt} = \sum_k \dot{w}_{component,k} + \dot{w}_{indoor} + \dot{w}_{nat-infiltration} + \dot{w}_{mech-ventilation} \quad (5.5)$$

$$\frac{dm^{\alpha}_{cont,i}}{dt} = \sum_j \dot{m}_{air-inward_{(j,i)}} \cdot \left(1 - \eta^{\alpha}_{j,i}\right) \cdot C^{\alpha}_j + G^{\alpha}_i + m_{air_i} \cdot \sum_{\beta} K_i{}^{\alpha,\beta} \cdot C^{\beta}_i - \sum_j \dot{m}_{air-outward_{(i,j)}} \cdot C^{\alpha}_i - R^{\alpha}_i \cdot C^{\alpha}_i \quad (5.6)$$

In Equations (5.4)–(5.6), $\frac{dE_{heat,i}}{dt}$ as heat flow rate in the zone *i* (room) (W), $\frac{dw_{moist,i}}{dt}$ as moisture flow rate of the zone *i* (kg/s) and $\frac{dm^{\alpha}_{cont,i}}{dt}$ as a contaminant of α flow rate in the zone i (kg/s) have been calculated (Antretter et al., 2018; Dols & Polidoro, 2015; U.S. Department of Energy, 2021).

In the integrated model, all three equations related to the balances of energy, moisture, and contaminant flows are connected to each other by exchanging two types of common control

variables. These two common control variables are airflows and temperatures. The airflows are created by air exchange as a result of infiltration, natural and mechanical ventilation between the interior and the exterior air of the building. Air exchange is associated with changes in the air temperatures of zones.

The airflows of natural ventilation and infiltration ($\dot{m}_{nat-infiltration}$), and supply mechanical ventilation ($\dot{m}_{supply}$) are connected to each other via the equations of energy and moisture flow balances, according to Equations (5.7)–(5.15). The total airflow according to Equation (5.16) is equal to the sum of $\dot{m}_{nat-infiltration}$ and $\dot{m}_{supply}$. According to Equation (5.17), this total airflow can replace the airflows of $\dot{m}_{air-outward_{(i,j)}}$ and $\dot{m}_{air-inward_{(j,i)}}$ in the contaminant flow balance. Thus, the airflows control variables are exchanged between all three equations of energy, moisture, and contaminant flows balances. Equations (5.7)–(5.9) relate to the calculation of energy flows due to natural ventilation, infiltration, and mechanical ventilation as part of the energy balance equation.

$$\dot{E}_{nat-infiltration} = \dot{m}_{nat-infiltration} \cdot (h_i - h_o) \tag{5.7}$$

$$h_i - h_o = (1006 + x_o \cdot 1840) \cdot (T_i - T_o) \tag{5.8}$$

Convective heat flow from building mechanical ventilation systems ($\dot{E}_{mech-ventilation}$) is calculated by Equation (5.9).

$$\dot{E}_{mech-ventilation} = \dot{m}_{supply} \cdot (h_i - h_o) \cdot (1 - \eta_{HR}) \tag{5.9}$$

In Equations (5.10)–(5.15), the moisture flows due to natural ventilation, infiltration, and mechanical ventilation as part of the moisture balance equation have been calculated.

$$\dot{w}_{nat-Infiltration} = \dot{m}_{nat-Infiltration} \cdot (x_o - x_i) \tag{5.10}$$

$$x_o = 0.622 \cdot \frac{P_{p_o}}{P_b - P_{p_o}} \tag{5.11}$$

$$x_i = 0.622 \cdot \frac{P_{p_i}}{P_b - P_{p_i}} \tag{5.12}$$

$$P_{p_o} = \varphi \cdot P_{s_o}(T_o) \tag{5.13}$$

$$P_{p_i} = \varphi \cdot P_{s_i}(T_i) \tag{5.14}$$

In Equations (5.14)–(5.18), x_i, P_{p_o}, P_{p_i}, P_b, φ, P_{s_o} and P_{s_i} are moisture content of inner air (kg/kg), water vapor partial pressure of outer air (Pa), water vapor partial pressure of inner air (Pa), barometric pressure (Pa), relative humidity, saturated vapor pressure depending on outer air temperature (Pa), and saturated vapor pressure depending on inner air temperature (Pa), respectively.

$$\dot{w}_{mech-ventilation} = \dot{m}_{supply} \cdot (x_o - x_i) \cdot (1 - \eta_{MR}) \tag{5.15}$$

In Equation (5.16), the total airflow of ith zone ($\dot{m}_{(air-total)_i}$), is resulted by airflow rates of natural ventilation and infiltration ($\dot{m}_{nat-infiltration}$) plus supply mechanical ventilation ($\dot{m}_{supply}$).

$$\dot{m}_{(air-total)_i} = \dot{m}_{nat-infiltration} + \dot{m}_{supply} \tag{5.16}$$

$$\dot{m}_{air-inward_{total}} = \dot{m}_{air-outward_{total}} = \dot{m}_{(air-total)_i} \tag{5.17}$$

According to Equation (5.17), this total airflow of ith zone replaces the total of outward and inward airflows ($\dot{m}_{air-outward_{total}}, \dot{m}_{air-inward_{total}}$) used in the contaminant balance equation. In Equation (5.18), the total airflow of ith zone ($\dot{m}_{(air-total)_i}$) depends on the density variable of the room air of ith zone (ρ_i). According to Equation (5.19), this density depends on the densities for dry air ($\rho_{a,i}$) and water Vapor ($\rho_{w,i}$) of ith zone. The densities of dry air ($\rho_{a,i}$) and water Vapor ($\rho_{w,i}$) of ith zone depend on the absolute inner air temperature of ith zone (θ_i) in Equations (5.20) and (5.21), respectively, and finally the absolute inner air temperature of ith zone (θ_i) depends on the inner air temperature (T_i) of ith zone in Equation (5.22).

Based on this, it can be concluded that the total airflow of the ith zone depends on the inner air temperature of the ith zone. Therefore, the mechanism of exchange of the inner air temperature of the ith zone between all three equations of energy, moisture, and contaminant balances can prove the interdependency of total airflow to inner air temperature based on Equations (5.18)–(5.22). Due to the dependence of total airflow on inner air temperature, it can be concluded that temperatures are exchanged simultaneously with the exchange of airflows control variables.

$$\dot{m}_{(air-total)_i} = \dot{V}_{(air-total)_i} \cdot \rho_i \tag{5.18}$$

$$\rho_i = \rho_{a,i} + \rho_{w,i} \tag{5.19}$$

$$\rho_{a,i} = \frac{P_b - P_{p_i}}{R_a \cdot \theta_i} \tag{5.20}$$

$$\rho_{w,i} = \frac{P_b - P_{p_i}}{R_w \cdot \theta_i} \tag{5.21}$$

$$\theta_i = 273.15 + T_i \tag{5.22}$$

In Equations (5.18)–(5.22), $\dot{m}_{(air-total)_i}$, $\dot{V}_{(air-total)_i}$, ρ_i, $\rho_{a,i}$, $\rho_{w,i}$, R_a, R_w and θ_i are total airflow of ith zone (kg/s), total volumetric airflow of ith zone (m^3/s), density for the room air of ith zone (kg/m^3), density for dry air of ith zone (kg/m^3), density for water Vapor of ith zone (kg/m^3), gas constant of dry air (=287.05 J/kgK), gas constant water vapor (=461.495 J/kgK), and absolute inner air temperature of ith zone (K).

The dependence of energy flow on temperatures can be proved based on Equations (5.7)–(5.9). In these equations, the relationships between specific enthalpy of the inner air (h_i) and specific enthalpy of the outer air (h_o) with the outer air temperature (T_o) and the inner air temperature (T_i) of ith zone, respectively, are presented. The dependence of moisture flow on temperatures can be proved based on Equations (5.10)–(5.15). In these equations, the relationships between moisture content of outer air (x_o) and moisture content inner air (x_i) with outer air temperature (T_o) and inner air temperature (T_i) of ith zone, respectively, are presented. The exchange of total airflow and inner air temperatures between the equations of energy, moisture, and

contaminant flows balances as common variables lead to the combination potentials of energy, moisture, and indoor air quality models.

5.3.3 The case study description

The case study is a three-story house. This case has three levels: basement, main floor, and bedroom floor. The basement includes a utility room, exercise room, parking, and staircase with an area of 35.67 m^2 and a volume of 107.01 m^3. The main level includes the living room, kitchen, washroom, and staircases with an area of 38.12 m^2 and a volume of 114.36 m^3. The bedroom level includes three bedrooms, two bathrooms, a hall, and staircases with an area of 35.93 m^2 and a volume of 107.79 m^3. The floor plans and a 3D view of the three-story house are shown in Figures 5.2 and 5.3, respectively. Figure 5.2, created by WUFI, shows the position of all three levels of the basement, main and bedrooms, as well as the configuration of each of the components of exterior walls, roof, windows, and other openings in a 3D view in order to introduce the style of this type of residential three-story house. Figure 5.3, designed by CONTAM, shows the floor plans of the three-story-house case study to locate the levels of the basement (utility room, exercise room, parking, and staircases), main (living room, kitchen, washrooms, and staircases) and bedrooms (three bedrooms, two bathrooms, halls, and staircases), with configurations of zones, AHS (air-handling systems), source and sinks of contaminants, walls, and airflow paths.

A total floor area of 109.72 m^2, net volume of 329.16 m^3, floor-to-ceiling height of 2.7 m, orientation of 0–180°and the window to the wall ratio of S, E, N, 40% have been assumed as geometry for the case study. The envelope effective leakage area (ELA) of this case study is considered at a pressure of 4 Pa, exponent of 0.65, discharge coefficient of 1 for the airtight and leaky cases of 0.04 m^2 and 0.3 m^2 (Chan et al., 2003b), respectively. The exhaust fan with the flow rates of 24 L/s is operated in an on or off position. The number of zones and envelope airflow paths are 15 and 42, respectively. Envelope airflow paths represent doors, windows, cracks, and exhausts. A simple recirculating air handling system with a total volumetric airflow of 0.35 m^3/s is used in this house. The maximum space heating and cooling loads for this case

study are 18.16 kW and 5.2 kW for Montreal, respectively, 15.10 kW and 5.2 kW for Vancouver, respectively, 10.59 kW and 7 kW for Miami, respectively (ASHRAE, 2019b; Michael Bluejay, 2022). Moreover, the maximum airflow required to provide space heating/cooling loads in Montreal, Vancouver, and Miami are 0.4 m^3/s, 0.365 m^3/s, and 0.377 m^3/s (Craig et al.). A design condition zone temperature of 20 °C has been defined.

The occupants of the case study include an adult male, an adult female, and also three children of ages 4, 10, and 13 years. The indoor sources of CO_2 in this study are the respiration of the occupants. Indoor CO_2 generation rates of 11 mg/s and 9.8 mg/s in awake and 6.6 mg/s and 6.2 mg/s in sleeping, have been considered for the adult male and female, respectively (Emmerich et al., 2005). Indoor CO_2 generation rates of 3.8 mg/s, 6.8 mg/s, and 8.6 mg/s in awake and 2.3 mg/s, 4.1 mg/s, and 5.2 mg/s in sleeping, have been considered for the children of ages 4, 10, and 13 years, respectively (Emmerich et al., 2005). The air filter with a MERV (minimum efficiency reporting value) rating of 4 with the supply of AHS ventilation has been used.

Heat transfer coefficient (U-value) or thermal resistance (RSI: R-value system international) for assemblies used in case study's components of the ground floor, below-grade walls, above-grade walls, intermediate floor ceilings, roof, external doors, and interior walls are determined based on the climate zones categorized in ASHRAE Standard 90.1. The cities of Montreal, Vancouver and Miami are categorized into ASHRAE climate zones of 6-A, 5-A, and 1-A, respectively. Climate zones of 6-A, 5-A, and 1-A are defined as cold-humid, moderate-humid, and warm-humid in ASHRAE Standard 90.1. Based on this, the maximum acceptable U-value or minimum acceptable RSI in ASHRAE Standard 90.1 is considered as the assemblies' U-value or RSI input data criteria. Window types of the case study have also been selected based on ASHRAE criteria from the WUFI database. In this database, reflected double-glazed windows with a U-value of 2.730 $W/m^2 \cdot K$ and frame factor of 0.7 for Montreal and Vancouver as well as the window type of reflective aluminum frame-fixed with U-value of 3.610 $W/m^2 \cdot K$ and frame factor of 0.7 for Miami are assumed.

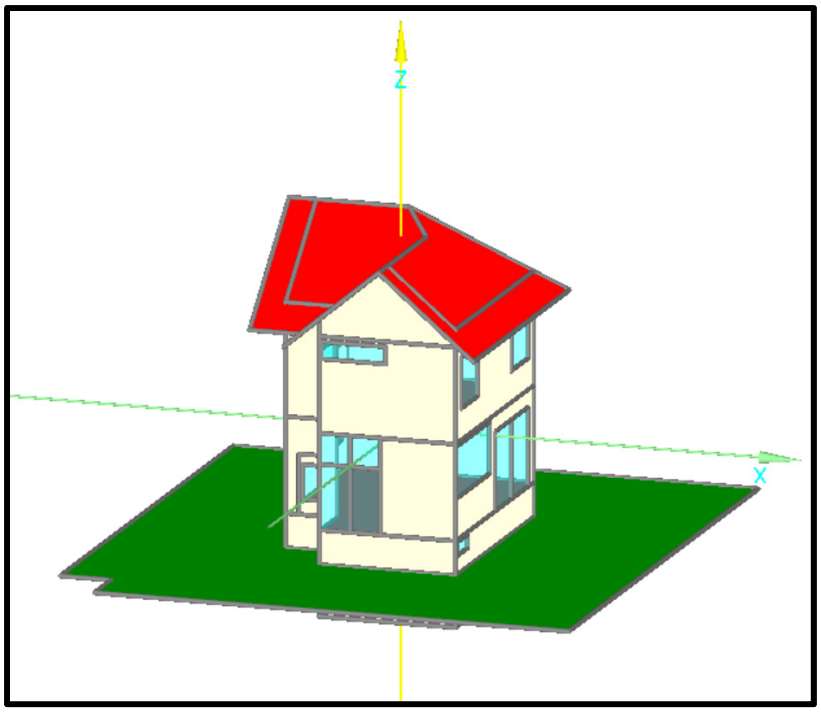

Figure 5.2 A 3D view of the three-story house showing the three levels and configuration of existing components of exterior walls, roof, windows, and other openings created by WUFI

In Montreal, for the ground floor with RSI of 13.221 m^2 K/W, for below-grade walls with 5.445 RSI of m^2 K/W, for above-grade walls with RSI of 7.070 m^2 K/W, for intermediate floor ceilings with RSI of 6.801 m^2 K/W, for the roof with RSI of 10.488 m^2 K/W, for reflected double-glazed windows with RSI of 0.366 m^2 K/W, for external doors with RSI of 0.350 m^2 K/W and for interior walls with RSI of 1.2 m^2 K/W have been assumed (ASHRAE, 2019b). In Vancouver, for the ground floor with RSI of 10.671 m^2 K/W, for below-grade walls with RSI of 3.695 m^2 K/W, for above-grade walls with RSI of 7.070 m^2 K/W, for intermediate floor ceilings with RSI of 6.801 m^2 K/W, for the roof with RSI of 10.488 m^2 K/W, for reflected double-glazed windows with RSI of 0.366 m^2 K/W, for external doors with RSI of 0.350 m^2 K/Wand for interior walls with RSI of 1.2 m^2 K/W have been considered (ASHRAE, 2019b). In Miami, for the ground floor with RSI of 5.241 m^2 K/W, for below-grade walls with RSI of 0.695 m^2 K/W, for above-grade walls with RSI of 4.445 m^2 K/W, for intermediate floor

ceilings with RSI of 0.651 m^2 K/W, for the roof with RSI of 4.678 m^2 K/W, for reflective aluminum frame-fixed windows with RSI of 0.277 m^2 K/W, for external doors with RSI of 0.350 m^2 K/W and for interior walls with RSI of 1.2 m^2 K/W have been chosen (ASHRAE, 2019b).

The materials of XPS (extruded polystyrene) surface skin, XPS Core, XPS surface skin, concrete w/c (water-cement-ratio) of 0.5, PVC roof membrane, EPS (expanded polystyrene, except for Miami), and gypsum fibreboard have been used from outside to inside for the ground floor. The materials of mineral plaster, oriented strand board, wood fibreboard, EPS (except for Miami), polyethylene membrane, chipboard, and gypsum board have been assumed from outside to inside for below-grade walls. The materials of mineral plaster, oriented strand board, wood fibreboard, EPS, polyethylene membrane, chipboard, and gypsum board have been selected from outside to inside for above-grade walls. The materials of oak radial, air layer, EPS (except for Miami), softwood, and gypsum board have been considered from outside to inside for intermediate floor ceilings. The materials of 60 min building paper, mineral insulation board, softwood, Vapor retarder, air layer, wood-fibre insulation board, polyethylene membrane, and softwood have been assumed from outside to inside for the roof. The wall-to-roof and wall-to-floor thermal bridges are 0.03 W/m·K, 0.04 W/m·K, respectively.

The data assumptions of infiltration, ventilation, envelopes, geometry, occupants, and thermal bridges have been applied as input data for EnergyPlus. The input data of the envelope leakage area, number of envelope paths, flow rate of the exhaust fan number of zones, indoor contaminant source elements, concentrations of outdoor contaminants, contaminant types, contaminants generation rates, and air-handling system capacities are considered for the CONTAM model. The input parameters of geometry, internal load categories, component assembly U-value, design conditions temperature, HVAC load and capacities, infiltration, and ventilation rates are used for the WUFI model.

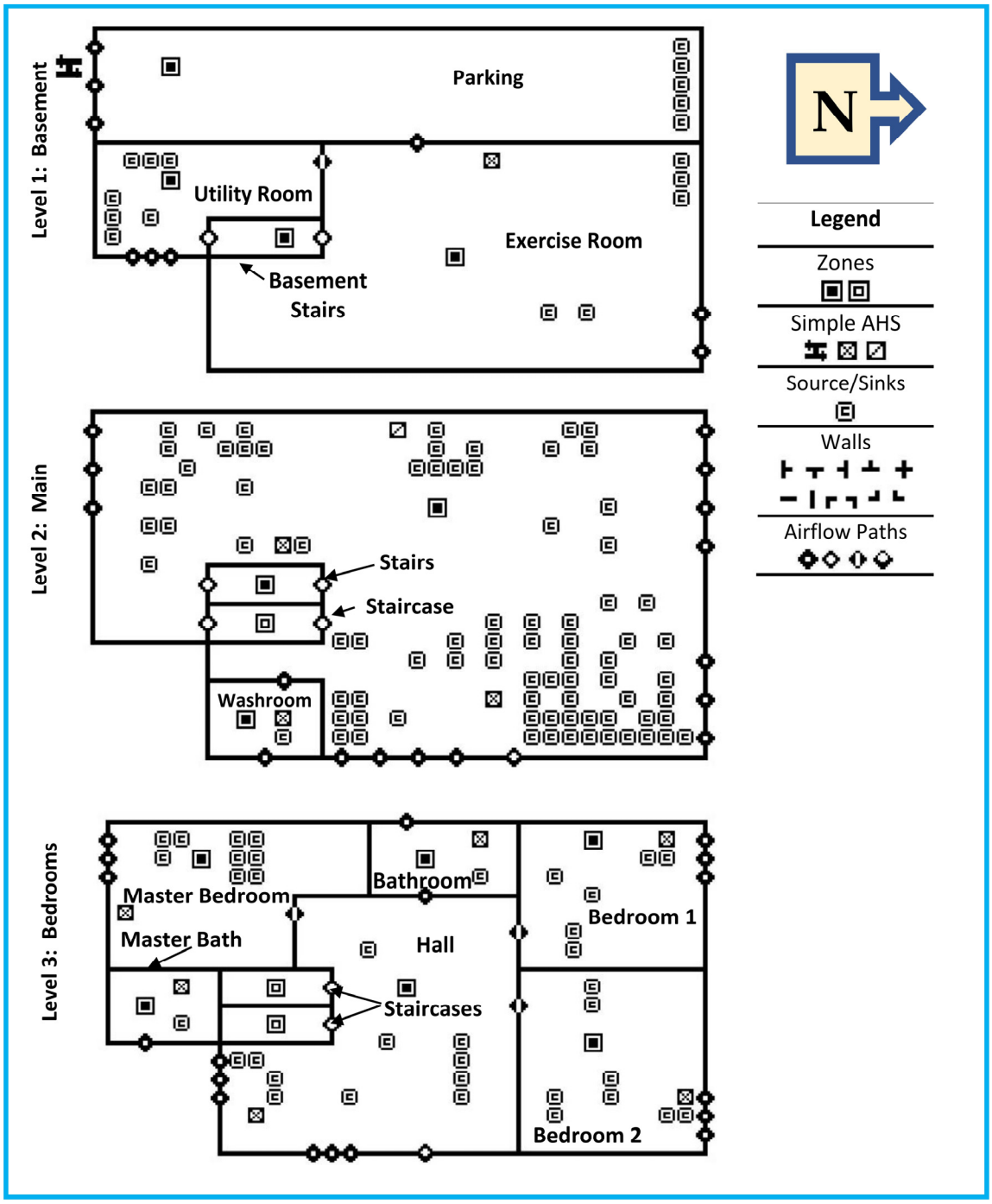

Figure 5.3 Floor plans of basement level (utility room, exercise room, parking, and staircases), main level (living room, kitchen, washroom, and staircases), and bedrooms level (three bedrooms, two bathrooms, hall, and staircases), with locations of zones, AHS (air-handling system), source and sinks of contaminants, walls, and airflow paths for three-story house created by CONTAM

The input data and formats for EnergyPlus is EPW (EnergyPlus weather file) (EnergyPlus, 2020). CONTAM can use the weather data files by using CONTAM Weather File Creator to convert the EPW file to a WTH (weather) ("CONTAM Utilities - CONTAM Weather File Creator," 2014). In WUFI, the weather data files have been selected from the weather database. Finally, all input data for EnegyPlus, CONTAM, and WUFI models are used as input data for the integrated model for comparison and analyzing the simulated results (for more details see (Heibati et al., 2021b)).

5.3.4 Developed integrated model verification

The present integrated model has been verified based on paired sample *t*-test method by using the SPSS tool ("IBM SPSS Statistics," 2021) as the statistical method. This method was previously used for the verification of energy models (Heibati et al., 2021c; Heibati & Atabi, 2013; Heibati et al., 2013). The reasons for choosing the paired sample *t*-test method to verify the accuracy of the present integrated model are: (a) it is simple and valid as a statistical method for analyzing the differences between actual and simulated data, and (b) this method is quite accurate where the differences between the actual and simulated data are tested in two steps based on statistically reliable criteria. These two steps include (1) paired samples difference and (2) paired samples correlation.

Briefly, in paired samples difference method, the difference between the actual and simulated data samples was tested. When the standard deviation differences between the actual and simulated data are greater than half of the mean difference and also the significance level is greater than 0.05, then it is concluded that there is no significant difference between the actual and simulated data. When this step is confirmed, the second step for paired sample correlation is then performed for further testing.

In the paired samples correlation method, the correlations between the actual and simulated samples are tested. When the correlation coefficient between the actual and simulated data is greater than 0.5 and the significance level is less than 0.05, then there is no significant

difference between the actual and simulated data. When the second stage of the test is also confirmed, it can be concluded that the actual and simulated data are very similar based on statistical criteria.

In this research, the values of daily space heating energy consumption, daily indoor CO_2 concentration, and hourly relative humidity (RH) are selected as energy, indoor air quality, and moisture data, respectively.

The actual and simulated values of these data for the three-story house case of leaky fan-on in Montreal are shown in Tables 5.1–5.3. Table 5.1 presents daily space heating energy consumption data for the 15th day of each month of the year 2020 for the case of leaky fan-on in Montreal. The simulated data is calculated using the integrated model and the actual data is measured by the plug-in energy monitor.

Table 5.1 Daily space heating energy consumption data for the 15th day of the months in 2020 for cases of leaky fan-on in Montreal

Data (kWh)	Month											
	Jan.	**Feb.**	**Mar.**	**Apr.**	**May.**	**Jun.**	**Jul.**	**Aug.**	**Sep.**	**Oct.**	**Nov.**	**Dec.**
Actual	14.48	23.24	45.84	47.92	43.90	9.88	1.08	0.00	17.24	43.40	46.60	45.84
Simulated	14.82	23.30	45.49	47.70	43.06	9.56	1.44	0.00	17.59	43.55	46.44	45.67

Table 5.2 Daily indoor CO_2 concentration data for the 15th day of the months in 2020 for cases of leaky fan-on in Montreal

Data ((kg/kg) × 10^{-4})	Month											
	Jan.	**Feb.**	**Mar.**	**Apr.**	**May.**	**Jun.**	**Jul.**	**Aug.**	**Sep.**	**Oct.**	**Nov.**	**Dec.**
Actual	8.32	8.60	8.69	8.47	8.76	8.77	8.50	8.77	8.72	8.42	8.63	8.56
Simulated	8.01	8.55	8.72	8.27	8.85	8.89	8.36	8.91	8.84	8.27	8.74	8.68

Table 5.2 shows the daily indoor CO_2 concentration data for the case of leaky fan-on in Montreal for the 15th day of each month for 2020. The simulated data is calculated by the integrated model and the actual data is measured by the CO_2 meter monitor.

The hourly relative humidity (RH) data for the case of leaky fan-on in Montreal for the 15th day of each month for 2020. In this table, the values of the simulated data are calculated by the integrated model and the actual values are measured by the humidity meter monitor.

Table 5.3 Hourly relative humidity (RH) data for the 15th day of the months in 2020 for cases of leaky fan-on in Montreal

Data $\frac{(\%)}{hour}$	Month											
	Jan.	**Feb.**	**Mar.**	**Apr.**	**May.**	**Jun.**	**Jul.**	**Aug.**	**Sep.**	**Oct.**	**Nov.**	**Dec.**
Actual	58.71	66.88	63.02	57.12	53.57	68.86	64.62	61.37	74.23	68.74	70.10	68.29
Simulated	52.50	68.98	61.09	49.14	40.78	70.12	61.33	55.08	81.33	70.51	72.50	68.95

The results of paired samples differences and paired sample correlation analysis for actual and simulated data for the case of leaky fan-on in Montreal are shown in Tables 5.4 and 5.5, respectively.

Table 5.4 reveals that the standard deviation difference between actual and simulated data for daily space heating energy consumption, daily indoor CO_2 concentration, and hourly relative humidity (RH) are 0.35341, 0.15474, and 5.56633, respectively (being > half mean difference) with the significance level of 0.527, 0.827 and 0.254, respectively (being > 0.05). As such, there are no significant differences between actual and simulated data for space heating energy consumption, indoor CO_2 concentration, and relative humidity (RH).

Table 5.5 shows that the correlation coefficients for actual and simulated data of space heating energy consumption, indoor CO_2 concentration and indoor relative humidity (RH) are 1.000, 0.973, and 0.995, respectively (being > 0.5) with a significance level of <0.05. Thus, the actual and simulated data are in good agreement.

Table 5.4 Paired sample difference t-test results between actual and simulated data for daily space heating energy consumption, daily indoor CO_2 concentration, and hourly indoor relative humidity (RH) in 2020 for cases of leaky fan-on in Montreal

Actual versus Simulated Data		Paired Differences							
		Mean	**Standard. Deviation**	**Standard. Error Mean**	**95% Confidence Interval of the Difference**		***t*-value**	**df**	**Significance (Two-Tailed)**
					Lower	**Upper**			
1	Daily space heating energy consumption (kWh)	0.06667	0.35341	0.10202	−0.15788	0.29121	0.653	11	0.527
2	Daily indoor CO_2 concentration ((kg/kg) × 10^{-4})	0.01000	0.15474	0.04467	−0.08832	0.10832	0.224	11	0.827
3	Hourly Indoor relative humidity $\frac{(\%)}{hour}$	1.93333	5.56633	1.60686	−1.60334	5.47001	1,203	11	0.254

Table 5.5 Paired sample correlation t-test results between actual and simulated data for daily space heating energy consumption, daily indoor CO_2 concentration, and hourly indoor relative humidity (RH) in 2020 for cases of leaky fan-on in Montreal

Actual versus Simulated Data		Measurers		
		N	**Correlation**	**Level of Significance**
1	Space heating energy consumption (kWh)	12	1.000	0.000
2	Indoor CO_2 concentration ((kg/kg) × 10^{-4})	12	0.973	0.000
3	Indoor relative humidity $\frac{(\%)}{hour}$	12	0.995	0.000

According to the results of using the paired sample *t*-test method for evaluating the differences between actual and simulated data, the integrated model showed a high accuracy.

5.4 Results

The effect of the accuracy of the results simulated by the integrated model compared to the single models is presented in this section. Four scenarios are defined for a case of a three-story house.

For a case of a three-story house subjected to three different climatic zones of Montreal, Vancouver, and Miami, the scenarios that were chosen to analyze the accuracy of the integrated model compared to single models are based on 4 common features: (1) reducing energy consumption with reducing indoor air quality, (2) reducing energy consumption with increasing indoor air quality, (3) investigate the moisture performance due to reducing indoor air quality, and (4) investigate the moisture performance due to increasing indoor air quality. These four scenarios are called in this study as: (1) airtight fan-off, (2) airtight fan-on, (3) leaky fan-off, and (4) leaky fan-on. Additionally, by choosing these four scenarios, the accuracy of the integrated model in determining the optimal scenarios in each of energy performance, indoor air quality, and moisture performance can be evaluated more simply and realistically compared to single models.

The measures of space heating/cooling energy consumptions, indoor CO_2 concentration, and relative humidity (RH) for all four scenarios are simulated in the first phase by single models of EnergyPlus, CONTAM, and WUFI, respectively. In the second phase, all measures of space heating/cooling energy consumptions, indoor CO_2 concentration, and relative humidity (RH) are simulated by the integrated model.

The single models with the integrated model scenarios are compared by using the percentage differences of the simulated results with the acceptable level of ASHRAE Standard in different climates of Montreal, Vancouver, and Miami for each scenario.

5.4.1 Results of EnergyPlus single model

In this research, the simulated hourly space heating/cooling energy consumptions obtained with EnergyPlus are considered as energy performance measures for different scenarios of a three-story house. The energy performance measure is presented in these results by calculation of the percentage difference between the simulated hourly space heating/cooling energy consumptions and the acceptable ASHRAE Standard 90.1 levels (ASHRAE, 2019b). The obtained results for all four scenarios of airtight fan-off, airtight fan-on, leaky fan-off, and leaky fan-on are shown in Figure 5.4a–c. These results are compared for three different climatic conditions of Montreal, Vancouver, and Miami**.**

5.4.2 Results of CONTAM single model

The results of simulated daily indoor CO_2 concentration are obtained by CONTAM as indoor air quality performance for different three-story house case scenarios. The indoor air quality measure is presented in the results based on the calculation of the percentage difference between the simulated daily indoor CO_2 concentrations and the ASHRAE Standard 62.1 levels (ASHRAE, 2019a). The results for each of the four scenarios of airtight fan-off, airtight fan-on, leaky fan-off, and leaky fan-on are shown in Figure 5.5a–c for three different climatic conditions of Montreal, Vancouver, and Miami.

5.4.3 Result of WUFI single model

The simulated hourly indoor relative humidity (RH) obtained by WUFI is considered as moisture performance for the three-story house case with different scenarios. This measure is presented as a result based on the calculation of the percentage difference between the simulated hourly indoor relative humidity (RH) levels and the ASHRAE Standard 160 level (ASHRAE, 2016a). These results are shown for each of the scenarios (airtight fan-off, airtight fan-on, leaky fan-off, and leaky fan-on) in Figure 5.6a–c for three different climatic conditions of Montreal, Vancouver, and Miami.

5.4.4 Results of the integrated model

With the present integrated model, all three performances of energy, indoor air quality, and moisture are calculated simultaneously. The results of the integrated model are calculated based on the percentage differences between the levels of the simulated hourly space heating/cooling energy consumptions, simulated daily indoor CO_2 concentrations, and simulated hourly relative humidity (RH), with ASHRAE Standards 90.1, 62.1, and 160 levels, respectively these results are shown for each of the four scenarios of (1) airtight fan-off , (2) airtight fan-on, (3) leaky fan-off and (4) leaky fan-on in Figures 5.7–5.9a–c for three climates of Montreal, Vancouver, and Miami.

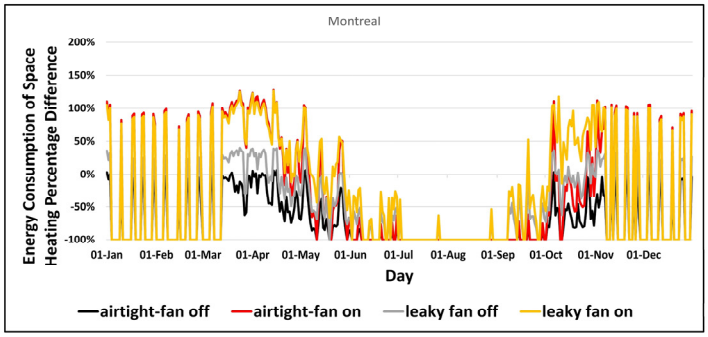

a. energy consumption of space heating percentage difference in Montreal.

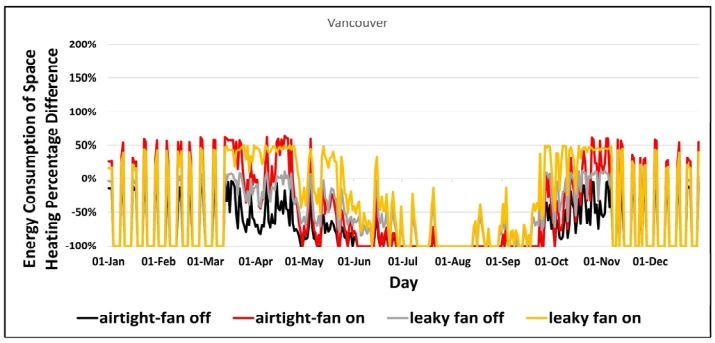

b. energy consumption of space heating percentage difference in Vancouver.

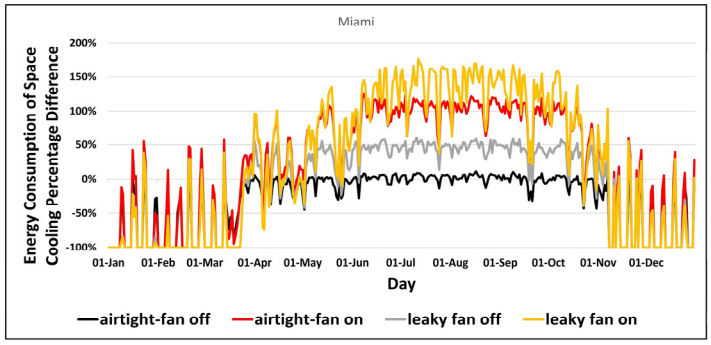

c. energy consumption of space cooling percentage difference in Miami.

Figure 5.4 Percentage differences comparison of hourly space heating/cooling energy consumptions with acceptable level of ASHRAE Standard 90.1 simulated by EnergyPlus model for four scenarios in (a) Montreal, (b) Vancouver, and (c) Miami

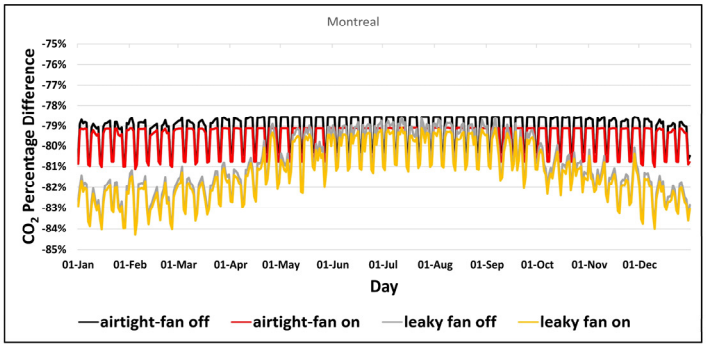

a. indoor CO_2 percentage difference in Montreal.

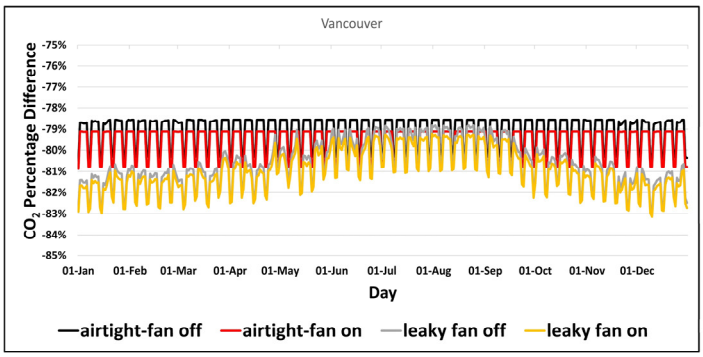

b. indoor CO_2 percentage difference in Vancouver.

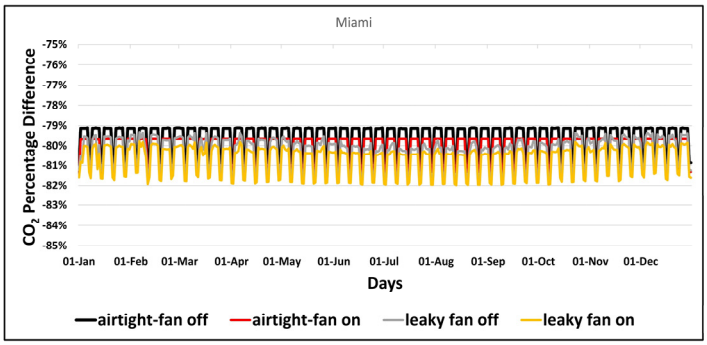

c. indoor CO_2 percentage difference in Miami.

Figure 5.5 Percentage differences comparison of daily indoor CO_2 concentrations with acceptable level of ASHRAE Standard 62.1 simulated by CONTAM for four scenarios in (a) Montreal, (b) Vancouver, and (c) Miami Taken from Heibati et al. (2021b, p 16)

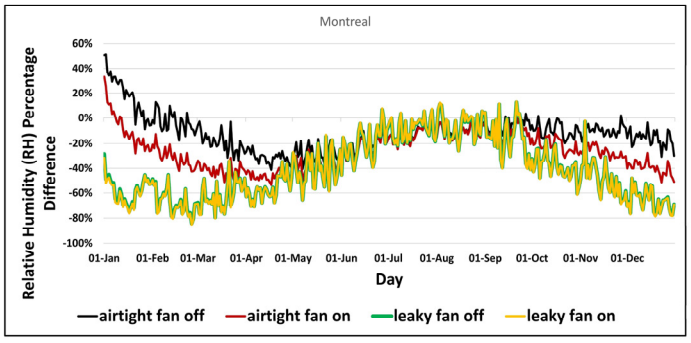

a. indoor relative humidity (RH) percentage difference in Montreal.

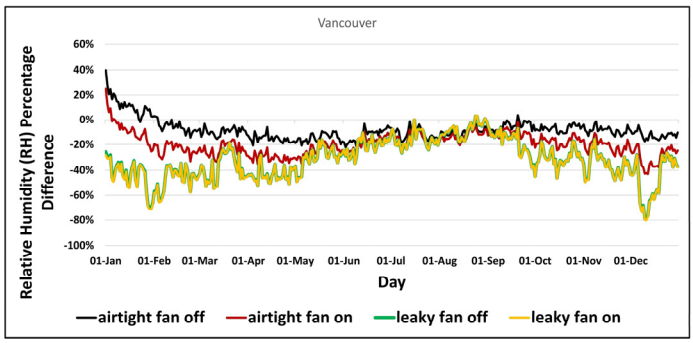

b. indoor relative humidity (RH) percentage difference in Vancouver.

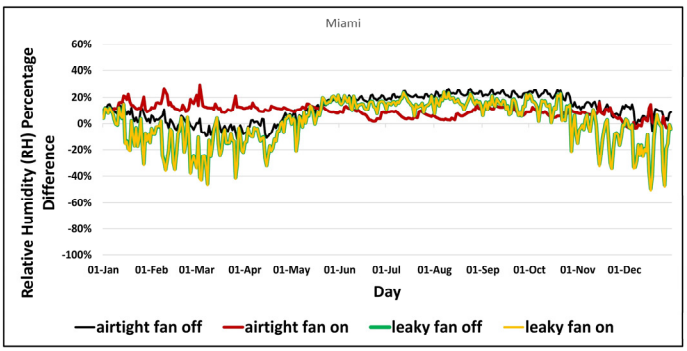

c. indoor relative humidity (RH) percentage difference in Miami.

Figure 5.6 Percentage differences comparison of hourly indoor relative humidity concentrations with acceptable level of ASHRAE Standard 160 simulated by WUFI for four scenarios in (a) Montreal, (b) Vancouver, and (c) Miami Taken from Heibati et al. (2021b, p 19)

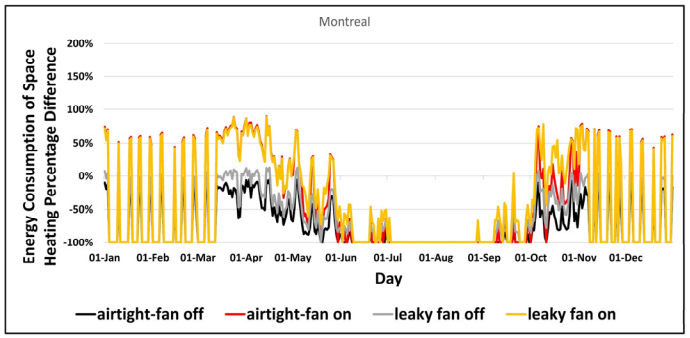

a. consumption of space heating percentage difference in Montreal.

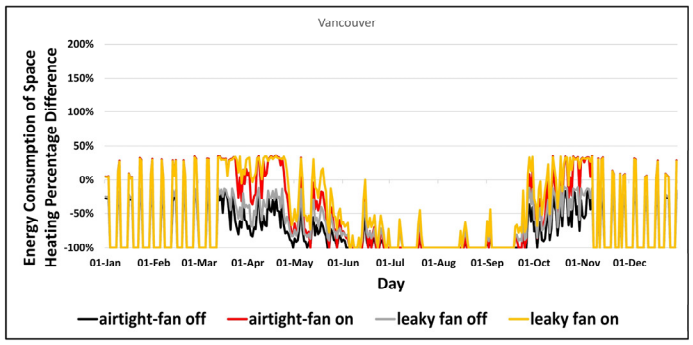

b. consumption of space heating percentage difference in Vancouver.

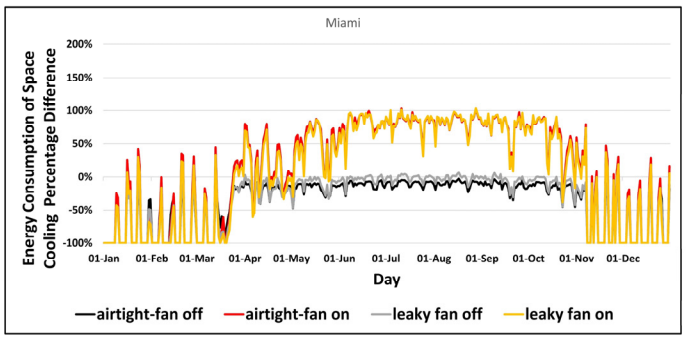

c. consumption of space cooling percentage difference in Miami.

Figure 5.7 Percentage differences comparison of hourly space heating/cooling energy consumptions with acceptable level of ASHRAE Standard 90.1 simulated by the fully integrated model for four scenarios in (a) Montreal, (b) Vancouver, and (c) Miami

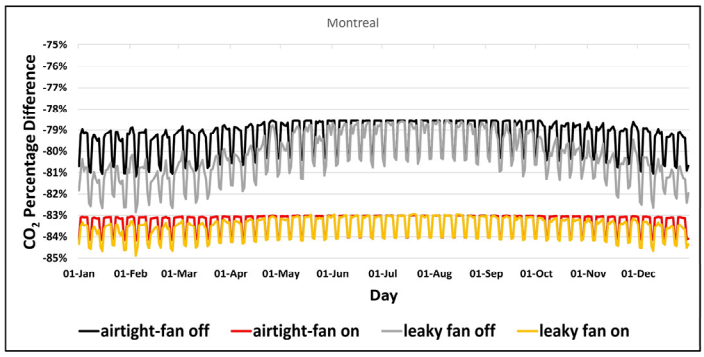

a. indoor CO_2 percentage difference in Montreal.

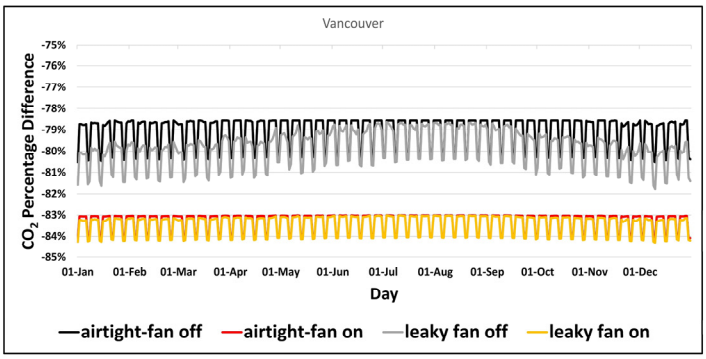

b. indoor CO_2 percentage difference in Vancouver.

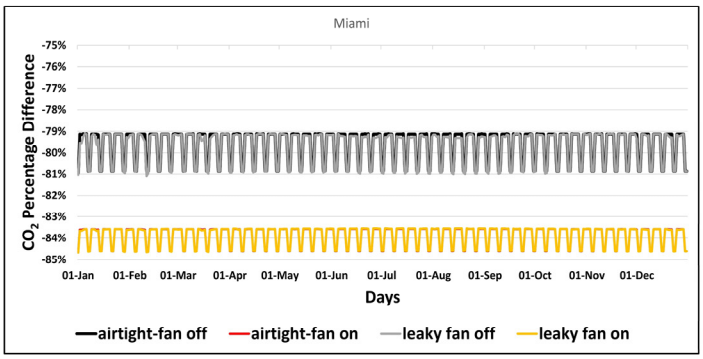

c. indoor CO_2 percentage difference in Miami.

Figure 5.8 Percentage differences comparison of daily indoor CO_2 concentrations with acceptable level of ASHRAE Standard 62.1 simulated by the fully integrated model for four scenarios in (a) Montreal, (b) Vancouver, and (c) Miami

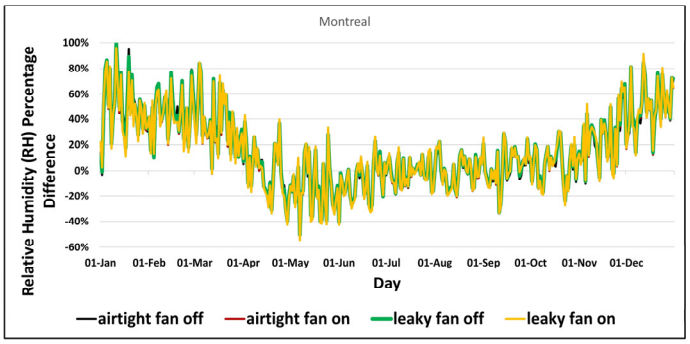

a. indoor relative humidity (RH) percentage difference in Montreal.

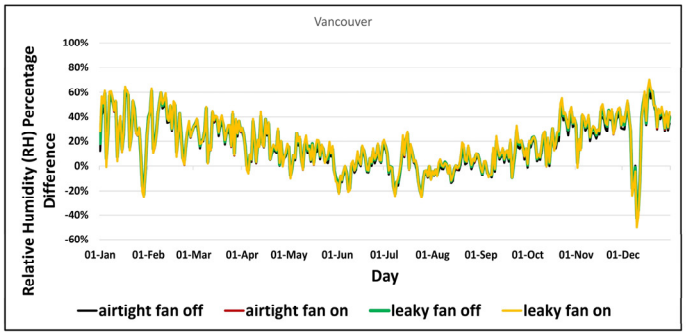

b. indoor relative humidity (RH) percentage difference in Vancouver.

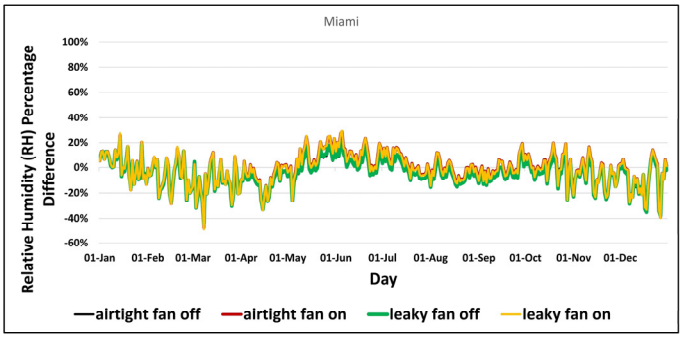

c. indoor relative humidity (RH) percentage difference in Miami.

Figure 5.9 Percentage differences comparison of hourly indoor relative humidity concentrations with acceptable level of ASHRAE Standard 160 simulated by the fully integrated model for four scenarios in (a) Montreal, (b) Vancouver, and (c) Miami

5.5 Discussion

In this research study, an integrated model was developed to predict with high accuracy for building applications, the energy, indoor air quality, and moisture performances, dynamically. The mechanism that was used to develop the integrated model is based on the exchange of airflows and temperatures control variables between EnergyPlus, CONTAM and WUFI sub-models. This model was developed in three phases. In the first phase, EnergyPlus, and CONTAM were coupled using a co-simulation method based on exchanging airflows and temperatures. The details and assessment of this method were presented in a previous study (Heibati et al., 2019). In the second phase, the CONTAM has been integrated with WUFI. The mechanism of this combination is based on the exchange of simulated air flows, temperatures, heating, and cooling flow variables between CONTAM with WUFI input data (Heibati et al., 2021b). In the final phase, which is the subject of this paper, the exchange of simulated WUFI airflows with the input data of CONTAM completes the EnergyPlus, CONTAM, and WUFI sub-models exchange control variables. The exchange of control variables between sub-models increases the integrated model accuracy. The integrated model's accuracy was verified by using paired sample *t*-test method. Moreover, the predictions of the integrated model were compared with single models. These comparisons are applied to four different scenarios in a three-story house. The simulated results included measures of performance of energy, indoor air quality, and moisture.

In this study, the ASHRAE Standards 90.1, 62.1, and 160 were used as the standard criteria for calculating the performances of energy, indoor air quality, and moisture, respectively. Using the percentage difference method, the results of simulated hourly energy consumptions of space heating/cooling, daily indoor CO_2 concentrations, and hourly indoor relative humidity (RH) with acceptable levels of ASHRAE Standards 90.1, 62.1, and 160 are compared and their differences are calculated. This percentage difference for the results of all 4 scenarios is calculated by single models and integrated models. For different scenarios considered in this study, the simulation results of every single model and integrated model for Montreal, Vancouver, and Miami are presented separately in Figures 5.4–5.9 and Tables 5.6–5.8.

Table 5.6 Energy performance analysis results by comparison of average percentage differences of hourly space heating/cooling energy consumptions with acceptable level of ASHRAE Standard 90.1, simulated by EnergyPlus and the fully integrated model

Energy Performance Analysis						
Cities	**Montreal**		**Vancouver**		**Miami**	
Models	**EnergyPlus Model**	**Integrated Model**	**EnergyPlus Model**	**Integrated Model**	**EnergyPlus Model**	**Integrated Model**
S1	−73.06%	−75.09%	−75.76%	−77.58%	−29.60%	−37.38%
S2	−40.97%	−46.85%	−54.17%	−56.35%	23.21%	12.09%
S3	−53.65%	−65.20%	−56.14%	−69.86%	−10.06%	−34.19%
S4	−26.01%	−40.12%	−35.14%	−48.65%	27.71%	8.25%

Table 5.7 IAQ performance analysis results by comparison of average percentage differences of daily indoor CO_2 concentrations with acceptable level of ASHRAE Standard 62.1, simulated by CONTAM and the fully integrated model

IAQ Performance Analysis						
Cities	**Montreal**		**Vancouver**		**Miami**	
Models	**CONTAM Model**	**Integrated Model**	**CONTAM Model**	**Integrated Model**	**CONTAM Model**	**Integrated Model**
S1	−79.17%	−79.32%	−79.08%	−79.09%	−79.63%	−79.63%
S2	−79.62%	−83.35%	−79.59%	−83.33%	−80.14%	−83.87%
S3	−80.95%	−80.26%	−80.66%	−79.85%	−80.29%	−79.68%
S4	−81.25%	−83.53%	−80.96%	−83.42%	−80.65%	−83.87%

Table 5.8 Moisture performance analysis results by comparison of average percentage differences of hourly relative humidity with acceptable level of ASHRAE Standard 160, simulated by WUFI and the fully integrated model

Moisture Performance Analysis						
Cities	**Montreal**		**Vancouver**		**Miami**	
Models	**WUFI Model**	**Integrated Model**	**WUFI Model**	**Integrated Model**	**WUFI Model**	**Integrated Model**
S1	−12.19%	14.92%	−8.36%	15.93%	12.01%	−4.64%
S2	−25.62%	14.17%	−19.58%	17.93%	9.21%	−0.99%
S3	−40.30%	15.99%	−31.44%	18.25%	0.99%	−4.15%
S4	−40.59%	15.15%	−31.71%	18.87%	0.90%	−1.25%

It is important to point out that the scenarios in which the simulated result values are less than the ASHRAE Standard level have a negative percentage difference. Moreover, the scenarios in which simulated results values are higher than the ASHRAE Standard level have a positive percentage difference. The results of the simulated results with the single models are compared with the present integrated model for performances of energy, indoor air quality, and moisture.

In Figure 5.4a–c, hourly energy consumptions (kWh) of space heating/cooling simulated by EnergyPlus, are compared with the acceptable power value (kW) of ASHRAE Standard 90.1, for scenarios 1, 2, 3, and 4, in Montreal, Vancouver, and Miami. The level that is acceptable by the ASHRAE Standard 90.1 is less than 1.72 kW for the building with a floor area of 109.72 m^2 (ASHRAE, 2019b). Additionally, the simulated hourly space heating/cooling energy consumptions are compared with the acceptable level of ASHRAE Standard 90.1 (<1.72 kW), using the percentage difference method. The percentage difference is calculated by Equation (5.23) to compare the hourly space heating/cooling energy consumption results simulated by EnergyPlus with the level that is satisfactory by the ASHRAE Standard 90.1.

$$\text{Percentage difference of energy consumption (\%)} = \frac{\text{power of hourly energy consumption } \left(\frac{\text{kWh}}{\text{h}}\right) - \text{ASHRAE Standard 90.1 level of 1.72 kW}}{\text{ASHRAE Standard 90.1 level of 1.72 kW}} \times 100 \quad (5.23)$$

The usefulness of this method is, however, to present a dimensionless criterion as a percentage in order to compare the results of hourly space heating/cooling energy consumptions simulated by EnergyPlus for each of the scenarios with the level that is satisfactory by the ASHRAE Standard 90.1. These percentage differences are presented in four curves for each of the scenarios 1 to 4 for the entire days of 2020.

When the level of simulated hourly space heating/cooling energy consumption is more or less than the level that is satisfactory by the ASHRAE Standard 90.1, the resulted percentage difference values are positive or negative for different points of each of the four scenarios curves, respectively.

As shown in Figure 5.4a–c, in scenarios curves, the minimum values have the highest negative percentage difference compared to ASHRAE Standard 90.1 level (<1.72 kW) (ASHRAE, 2019b). Therefore, these values have the highest performances. This percentage difference value is −100% in Montreal, Vancouver, Miami for scenarios 1 to 4. The percentage difference value of −100% means that since the maximum acceptable space heating/cooling energy consumption of ASHRAE Standard 90.1 per hour is 1.72 kW, then the value of hourly space heating/cooling energy consumption simulated by the EnergyPlus is zero kWh. When the value of zero kWh is calculated by Equation (5.23), the value of −100% has resulted.

Figure 5.5a–c shows comparisons between daily indoor CO_2 concentrations (kg/kg) simulated by CONTAM and the level that is acceptable by the ASHRAE Standard 62.1, for scenarios 1 to 4, in Montreal, Vancouver, and Miami. The level that is acceptable by the ASHRAE Standard 62.1 for indoor CO_2 concentration is less than 52.32×10^{-4} kg/kg (ASHRAE, 2019a).

Equation (5.24) provides the percentage difference calculation relation for scenarios 1 to 4. Equation (5.24) is used in order to compare the results of daily indoor CO_2 concentrations simulated by CONTAM with an acceptable level of ASHRAE Standard 62.1.

$$\text{Percentage difference of indoor } CO_2 \text{ concentration (\%)} = \frac{\text{indoor } CO_2 \text{ Concentration } \left(\frac{\text{kg}}{\text{kg}}\right) - \text{ASHRAE Standard 62.1 levels of } 52.32 \times 10^{-4}\ \frac{\text{kg}}{\text{kg}}}{\text{ASHRAE Standard 62.1 levels of } 52.32 \times 10^{-4}\ \frac{\text{kg}}{\text{kg}}} \times 100 \tag{5.24}$$

This method provides a dimensionless measure as a percentage to compare the results of daily indoor CO_2 concentrations, simulated by CONTAM for each of the scenarios with the acceptable level of ASHRAE Standard 62.1. These comparisons were performed in four curves of scenarios 1 to 4 for the days of 2020. If the level of simulated daily indoor CO_2 concentrations is more or less than the level that is acceptable by the ASHRAE Standard 62.1 criteria, then the values of percentage difference are positive or negative for different points of scenarios curves, respectively.

In scenarios curves, as shown in Figure 5.5a–c, the minimum values have the highest negative percentage difference compared to ASHRAE Standard 62.1 (indoor CO_2 <52.32×10^{-4} kg/kg) (ASHRAE, 2019a). So, these values have the highest performances. The percentage differences in the city of Montreal are calculated as the results values of −80.85% for scenario 1, −81.13% for scenario 2, −84.13% for scenario 3, and −84.30% for scenario 4. The percentage differences in the city of Vancouver are considered as the results values of −80.49% for scenario 1, −80.87% for scenario 2, −82.93% for scenario 3, and −83.15% for scenario 4. The percentage differences in Miami are calculated as the results values of −80.96% for scenario 1, −81.41% for scenario 2, −81.82% for scenario 3, and −81.98% for scenario 4.

Note that the percentage differences of all scenarios in CONTAM are less than −80%. These percentage differences values of less than −80% mean that since the maximum acceptable indoor CO_2 concentration according to ASHRAE Standard 62.1 is 52.32×10^{-4} kg/kg, so the

daily indoor CO_2 concentrations simulated by CONATM are less than 51.90×10^{-4} kg/kg for all scenarios. As indicated above, the values of less than −80% are calculated by Equation (5.24) for all scenarios.

With WUFI according to Figure 5.6a–c, the simulated hourly indoor relative humidity (RH) is compared with the level that is satisfactory by the ASHRAE Standard 160, for scenarios 1 to 4, in Montreal, Vancouver, and Miami. The level that is acceptable by the ASHRAE Standard 160 for indoor relative humidity (RH) is less than 80% (ASHRAE, 2016a).

Finally, for the four scenarios considered in this study, the percentage difference is calculated by Equation (5.25) to compare the hourly indoor relative humidity (RH) results simulated by WUFI with the level that is acceptable by the ASHRAE Standard 160.

$$\text{Percentage difference of indoor relative humidity (\%)} = \frac{\text{indoor relative humidity (\%)} - \text{ASHRAE Standard 160 level of 80\%}}{\text{ASHRAE Standard 160 level of 80\%}} \times 100 \tag{5.25}$$

The usefulness of this method is to create a dimensionless criterion as a percentage to compare the results of hourly indoor relative humidity (RH), simulated by WUFI for each of the scenarios with the level that is acceptable by the ASHRAE Standard 160. This percentage difference method has resulted in the four curves for four scenarios 1 to 4 for the days of 2020. When the level of simulated hourly indoor relative humidity (RH) is more or less than the level that is acceptable by the ASHRAE Standard 160, the values of percentage difference calculation are positive or negative for different points of scenarios curves, respectively.

According to Figure 5.6a–c, in scenarios curves, the minimum values have the highest negative percentage difference compared to ASHRAE Standard 160 level (indoor RH <80%) (ASHRAE, 2016a). Therefore, it is concluded that these values have the highest performances. The percentage differences in Montreal are considered as the result values of −41.29% for scenario 1, −53.60% for scenario2, −84.18% for scenario 3, and −85.16% for scenario 4. The

percentage differences in Vancouver are calculated as the results values of −22.10% for scenario 1, −43.06%, for scenario 2, −79.10% for scenario 3, and −80.13% for scenario 4. The percentage differences in Miami are calculated as the results values of −11.83% for scenario 1, −3.57% for scenario 2, −49.26% for scenario 3, and −50.53% for scenario 4. Thus, the percentage differences of all scenarios are between −3.57% through −85.16%, which means that, since the maximum acceptable moisture content to minimize mold growth according to ASHRAE Standard 160 is 80%, so the hourly indoor relative humidity (RH), simulated by WUFI for all scenarios are between 79.97% through 79.31%. The percentage difference values between −3.57% through −85.16% for all scenarios in WUFI are calculated by Equation (5.25).

With the integrated model, the simulated hourly energy consumptions (kWh) of space heating/cooling, daily indoor CO_2 concentrations (kg/kg), and hourly indoor relative humidity (RH) (%) are compared with the levels that are acceptable by the ASHRAE Standards 90.1, 62.1 and 160, respectively, in cities of Montreal, Vancouver, and Miami for scenarios 1 to 4. Furthermore, the percentage difference method was used for comparing the simulated hourly energy consumptions of space heating/cooling, daily indoor CO_2 concentrations, and hourly indoor relative humidity (RH) with the levels that are acceptable by the ASHRAE Standards 90.1, 62.1, and 160, respectively.

For hourly energy consumptions (kWh) of space heating/cooling simulated by the integrated model, Figure 5.7a–c shows that in scenarios curves, the minimum values have the percentage difference compared to ASHRAE Standard 90.1. These values have the highest performances.

The percentage difference is calculated by Equation (5.23) to compare the hourly space heating/cooling energy consumption results simulated by the integrated model with the acceptable level of ASHRAE Standard 90.1. This percentage difference in Montreal, Vancouver, and Miami has resulted in a value of −100%. This means that since the maximum acceptable space heating/cooling energy consumption of ASHRAE Standard 90.1 per hour is 1.72 kW, so the value of hourly space heating/cooling energy consumption simulated by the

integrated model is zero kWh. The value of −100% has resulted when the value of zero kWh is calculated by Equation (5.23).

For the simulated daily indoor CO_2 concentrations by the integrated model, Figure 5.8a–c, shows that in scenarios curves, the minimum values have the highest negative percentage difference compared to ASHRAE Standard 62.1. The values of these percentage differences have the highest performances. Equation (5.24) is used for the calculation of the percentage difference for comparing results of daily indoor CO_2 concentrations simulated by the integrated model with the level that is acceptable by the ASHRAE Standard 62.1. These percentage differences in Montreal are calculated as values of −81.18% for scenario 1, −84.17% for scenario 2, −82.86% for scenario 3, and −84.89% for scenario 4. The percentage differences in Vancouver are considered as the results values of −80.52% for scenario 1, −84.11% for scenario 2, −81.78% for scenario 3, and −84.30% for scenario 4. In Miami, this percentage difference is calculated as values of −80.96% for scenario 1, −84.65% for scenario 2, −81.10% for scenario 3, and −84.67% for scenario 4. The obtained percentage differences for all scenarios using the integrated model are less than −80%, which means that since the maximum acceptable indoor CO_2 concentration according to ASHRAE Standard 62.1 is 52.32×10^{-4} kg/kg, so the daily indoor CO_2 concentrations simulated by the integrated model are less than 51.90×10^{-4} kg/kg for all scenarios.

Additionally, for the simulated indoor relative humidity (RH) by the integrated model, Figure 5.9a–c shows that in scenarios curves, the minimum values have the highest negative percentage difference compared to ASHRAE Standard 160 and also have the highest performances.

The percentage difference in the integrated model is calculated by Equation (5.25) to compare the hourly indoor relative humidity (RH) results simulated by the integrated model with the level that is acceptable by the ASHRAE Standard 160. These percentage differences in Montreal are estimated as the results values of −46.35% for scenario 1, −52.44% for scenario 2, −50.37% for scenario 3, and −54.39% for scenario 4. These percentage differences in

Vancouver are calculated as values of −36.92% for scenario 1, −47.67% for scenario 2, −43.55% for scenario 3, and −50.26% for scenario 4. The percentage differences in Miami are considered as result values of −42.63% for scenario 1, −47.88% for scenario 2, −44.75% for scenario 3, and −48.88% for scenario 4. The percentage difference of all scenarios in the integrated model is between −36.92% through −54.39%. These percentage difference values mean that, since the maximum acceptable moisture content to minimize mold growth according to ASHRAE Standard 160 is 80%, the hourly indoor relative humidity (RH), simulated by the integrated model for all scenarios, are between 79.70% through 79.56%.

Tables 5.6–5.8 show that the average performance of energy, indoor air quality, and moisture are compared for different scenarios between single and integrated models. The average performance calculation criterion is based on the average percentage difference of the simulated hourly space heating/cooling energy consumptions, daily indoor CO_2 concentration, and hourly indoor relative humidity (RH) with ASHRAE Standard 90.1, 62.1, and 160 levels.

As shown in Table 5.6 hourly energy consumptions of space heating/cooling, in Montreal, have been considered as the results average values of −73.06% for scenario 1, −40.97% for scenario 2, −53.65% for scenario 3, and −26.01% for scenario 4 by EnergyPlus and −75.09% for scenario 1, −46.85% for scenario 2, −65.20% for scenario 3, and −40.12% for scenario 4 by the integrated model, respectively.

The hourly energy consumptions of space heating/cooling in Vancouver (see Table 5.6), have been estimated as the results average values of −75.76% for scenario 1, −54.17% for scenario 2, −56.14% for scenario 3, and −35.14% for scenario 4 by EnergyPlus and −77.58% for scenario 1, −56.35% for scenario 2, −69.86% for scenario 3, and −48.65% for scenario 4 by the integrated model, respectively.

In Miami, according to Table 5.6, the hourly energy consumptions of space heating/cooling have been considered as the results average values of −29.60% for scenario 1, 23.21% for scenario 2, −10.06% for scenario 3, and 27.71% for scenario 4 by EnergyPlus and −37.38%

for scenario 1, 12.09% for scenario 2, −34.19% for scenario 3, and 8.25% for scenario 4 by the integrated model, respectively.

According to Table 5.7, the daily indoor CO_2 concentration in Montreal has been calculated as the results average values of −79.17% for scenario 1, −79.62% for scenario 2, −80.95% for scenario 3, and −81.25% for scenario 4 by CONTAM, and −79.32% for scenario 1, −83.35% for scenario 2, −80.26% for scenario 3, and −83.53% for scenario 4 by the integrated model, respectively.

In Vancouver, the daily indoor CO_2 concentration (see Table 5.7) has been calculated as the results average values of −79.08% for scenario 1, −79.59% for scenario 2, −80.66% for scenario 3, and −80.96% scenario 4 by CONTAM, and −79.09% for scenario 1, −83.33% for scenario 2, −79.85% for scenario 3, and −83.42% for scenario 4 by the integrated model, respectively.

The daily indoor CO_2 concentration (see Table 5.7) in Miami has been considered as results average values of −79.63% for scenario 1, −80.14% for scenario 2, −80.29% for scenario 3, and 80.65% scenario 4 by CONTAM, and −79.63% scenario 1, −83.87% for scenario 2, −79.68% for scenario 3, and −83.87% for scenario 4 by the integrated model, respectively.

As shown in Table 5.8, the hourly indoor relative humidity (RH) in Montreal has been calculated as the results average values of −12.19% for scenario 1, −25.62% for scenario 2, −40.30% for scenario 3, and −40.59% for scenario 4 by WUFI, and 14.92% for scenario 1, 14.17% for scenario 2, 15.99% for scenario 3, and 15.15% for scenario 4 by the integrated model, respectively.

The hourly indoor relative humidity (RH) in Vancouver according to Table 5.8 has been estimated as the results average values of −8.36% for scenario 1, −19.58% for scenario 2, −31.44% for scenario 3, and −31.71% for scenario 4 by WUFI, and 15.93% for scenario 1,

17.93% for scenario 2, 18.25% for scenario 3, and 18.87% for scenario 4 by the integrated model, respectively.

In Miami, the hourly indoor relative humidity (RH), according to Table 5.8, has been considered as results average values of 12.01% for scenario 1, 9.21% for scenario 2, 0.99% for scenario 3, and 0.90% for scenario 4 by WUFI, and −4.64% for scenario 1, −0.99% for scenario 2, −4.15% for scenario 3, and −1.25% for scenario 4 by the integrated model, respectively.

For the results of the hourly space heating/cooling energy consumptions, by EnergyPlus and the integrated model, scenario 1 has resulted in the highest energy performance for different climatic conditions. With CONTAM to simulate the daily indoor CO_2 concentration, scenario 4 has resulted in the highest indoor air quality performance values in Montreal, Vancouver, and Miami, and for the integrated model scenario 4 in Montreal and Vancouver and both scenarios 2 and 4 in Miami have the highest indoor air quality performance value. For the simulated hourly indoor relative humidity measures simulated by WUFI, scenario 4 has resulted in the highest moisture performance values in Montreal, Vancouver, and Miami, and this measure simulated by the integrated model, for scenario 2 in Montreal, and scenario 1 in Vancouver and Miami have the highest indoor air quality performance. Given that the results of some scenarios with the highest performance values for indoor air quality and moisture measures for the cities of Vancouver, and Miami are different between single models and the present integrated model, it can be concluded that using the integrated model instead of single models seems necessary.

Considering that the reason for using the percentage difference method was to estimate the difference between the results of single models and the present integrated model with an acceptable level of ASHRAE Standard of 90.1, 62.1, and 160 by dimensionless percentage criteria, so this method makes it easier to compare simulated results. Therefore, it was possible to conduct comparisons for the average percentage difference of simulated results between the integrated model with single models as provided in Tables 5.6–5.8.

The percentage difference method was used to compare the results of scenarios 1, 2, 3, and 4 in Montreal, Vancouver, and Miami to choose the optimal scenario. When the percentage difference between the value of the result simulated by the integrated model or single models with an acceptable level of ASHRAE Standard is negative, the scenario with the highest difference is considered as the optimum scenario. Additionally, when the percentage difference is positive, the scenario with the lowest difference is selected as the optimal scenario. These optimal scenarios are chosen based on ASHRAE Standard 90.1, 62.1, and 160 criteria in terms of energy, indoor air quality and moisture, respectively, for Montreal, Vancouver, and Miami.

As shown in Tables 5.6–5.8, the average percentage difference of simulated results of the integrated model is different from single models for optimal scenarios. On the other hand, the accuracy of the integrated model for energy, indoor air quality, and moisture result samples have been verified by the paired sample *t*-test method presented in Tables 5.4 and 5.5. The difference between the obtained results of a single method and the integrated method is due to the high accuracy of the present integrated model.

In summary, the reasons for the difference in the obtained results for the optimal scenarios simulated by single methods with the integrated method are:

1. Scenario 1 is predicted as the optimal scenario for hourly energy consumptions of space heating/cooling in both EnergyPlus model and the integrated model methods, in Montreal, Vancouver, and Miami. The values of hourly energy consumptions of space heating/cooling for scenario 1 as the optimal scenario, by the integrated model method, are 2.77%, 2.40%, and 26.28% different from the EnergyPlus model method for Montreal, Vancouver, and Miami, respectively. The reason for this difference is that in the EnergyPlus model method, infiltration of 0.4 h^{-1} and design air handling system airflow of 0.35 m^3/s are defined as airflows input data by the user. In the integrated model, the airflow variables are corrected by the combination mechanism for EnergyPlus, CONTAM, and WUFI.

2. Scenario 4 as an optimal scenario in terms of the daily indoor CO_2 concentration performance, through the integrated model method, 2.80% and 3.03% in Montreal and Vancouver are different from the CONTAM model method, respectively. The reason for this difference was because in the CONTAM model method, the effective leakage area of 0.3 m^2 and exhaust fan airflow of 24 L/s, as airflows input and junction temperature of 22.2 °C and default zone temperature of 20 °C as temperatures input data have been defined by the users. While the airflows and temperatures in the integrated model method have been corrected by the combination mechanism for EnergyPlus, CONTAM, and WUFI.

3. In Miami, scenarios 2 and 4 for the daily indoor CO_2 concentration performance have led to the optimal scenarios through the integrated model method and are 3.09% different from the results of scenario 4 as the optimal scenario based on the CONTAM model method. Therefore, the reason for this difference is the same as optimal scenarios situations for Montreal and Vancouver.

4. For the hourly indoor relative humidity (RH) performance in Montreal, scenario 2 is the optimal scenario through the integrated model method with −134.91% different from scenario 4 as the optimal scenario through the WUFI model method. The reason for this difference is that in the WUFI model method for scenario 4, infiltration of 3.2 h^{-1} and mechanical ventilation of 0.3 h^{-1} as airflows input data, minimal zone temperature of 20 °C and maximal zone temperature of 26 °C as temperatures input data and space heating capacity of 18.16 kW with cooling capacity of 5.2 kW as heating/cooling flows input data were defined by the users. However, in the integrated model method for scenario 2, the airflows, temperatures, and heating/cooling flows were corrected by the combination mechanism for EnergyPlus, CONTAM, and WUFI.

5. For the hourly indoor relative humidity performance, scenario 1 results in the optimal scenario through the integrated model method are −150.23% and −615.55% different from scenario 4 as an optimal scenario through the WUFI model method, in Vancouver and Miami, respectively. The reason for this difference is that in the WUFI model method for

scenario 1 as optimal scenario, infiltration of 0.4 h^{-1} as airflow input data, minimal zone temperature of 20 °C and maximal zone temperature of 26 °C as temperatures input data, space heating capacity of 15.10 kW with cooling capacity of 5.2 kW in Vancouver and space heating capacity of 10.59 kW with cooling capacity of 7 kW in Miami as heating/cooling flows input data were defined by the users. However, in the integrated model method for scenario 4 as an optimal scenario, the airflows, temperatures, and heating/cooling flows were corrected by the combination mechanism for EnergyPlus, CONTAM, and WUFI.

5.6 Conclusions

In this research study, an integrated model was developed to predict the performances of energy, indoor air quality, and moisture performances. To develop this integrated model, an interconnection between the three models of EnergyPlus, CONTAM, and WUFI was implemented. This interconnection was performed between energy, indoor air quality, and moisture models based on the energy, contaminant, and moisture balances. The energy, contaminant and moisture balance mechanisms were performed based on the simultaneous exchange of airflows and temperatures control variables between the sub-models of EnergyPlus, CONATM, and WUFI. These exchanges have led to the correction of airflows, temperatures, and heating/cooling flows control variables.

The method of the percentage differences between the hourly energy consumptions of space heating/cooling, daily indoor CO_2 concentrations, and hourly indoor relative humidity (RH) with acceptable levels of ASHRAE Standards 90.1, 62.1, and 160, was used for determining energy, indoor air quality, and moisture performances, respectively. The accuracy of the integrated model was verified based on paired sample *t*-test method. In order to analyze the accuracy of the integrated model, four scenarios for a three-story house were defined. Then, the obtained results with the integrated model for the hourly energy consumptions of space heating/cooling, daily indoor CO_2 concentrations, and hourly indoor relative humidity (RH) performance predictions of all four scenarios were compared with those obtained using the

single models. These comparisons were conducted for building subjected to the climatic conditions of Montreal, Vancouver, and Miami.

Considering that the accuracy of the integrated model was verified based on the paired sample *t*-test statistical method and analytical discussions described earlier by details, due to the difference between the optimal scenarios predicted by the single models and the integrated model, it can be concluded that this integrated model can be replaced by the single models. Other details that could be useful for potential replacement of the integrated model instead of the single models of EnergyPlus, CONTAM, and WUFI include the following:

- The integrated model can predict energy, indoor air quality, and moisture performances in an integrated procedure for each type of building, but the single models of EnergyPlus, CONTAM, and WUFI can calculate energy, indoor air quality, and moisture performance separately, respectively.

- The simulation results are predicted by the integrated model based on the combination mechanism for EnergyPlus, CONTAM, and WUFI sub-models. This mechanism is based on the simultaneous solution of all three energy, contaminant, and moisture balance equations. Whereas in the single models of EnergyPlus, CONTAM, and WUFI, the simulation results are calculated based on the energy, contaminant, and moisture balance equations, respectively, without any connections.

- In a single model of EnergyPlus, infiltration and design air handling system airflow values are defined as airflows input data by the user. In the integrated model, the airflow variables are corrected by the combination mechanism for EnergyPlus, CONTAM, and WUFI.

- In the single model of CONTAM the effective leakage area and exhaust fan airflow values, as airflows input and also junction temperature and default zone temperature values as temperatures input data, are defined by the users. While the airflows and temperatures in

the integrated model method are corrected by the combination mechanism for EnergyPlus, CONTAM, and WUFI.

- In a single model of WUFI infiltration and mechanical ventilation values as airflows input data, minimal and maximal zone temperature values as temperatures input data, and space heating/cooling capacity values as heating/cooling flows input data were defined by the users. However, in the integrated model, the airflows, temperatures, and heating/cooling flows were corrected by the combination mechanism for EnergyPlus, CONTAM, and WUFI.

In addition, the accuracy of the integrated model is due to the correction of control variables as a result of the simultaneous exchange between the EnergyPlus, CONTAM, and WUFI sub-models. Therefore, this integrated model can be used as a benchmark for assessing the energy, indoor air quality, and moisture performances of residential and mid-rise buildings, subjected to various climate conditions. Lastly, since in this research, an integrated model has been developed by combining EnergyPlus, CONTAM, and WUFI concerning co-simulation mechanism, this article contributes to creating an integrated modeling approach for predicting building performance using co-simulation method for integrating of single models to meet high accuracy in simulation results.

Author Contributions: Conceptualization, S.H., W.M. and H.H.S.; methodology, S.H., W.M. and H.H.S.; software, S.H.; validation, S.H., W.M. and H.H.S.; formal analysis, S.H.; investigation, S.H.; resources, S.H.; data curation, S.H.; writing—original draft preparation, S.H.; writing—review and editing, S.H., W.M. and H.H.S.; visualization, S.H.; supervision, W.M. and H.H.S.; project administration, W.M. and H.H.S. All authors have read and agreed to the published version of the manuscript.

5.7 Nomenclature

$\dot{E}^{opaque}_{component,k}$	Heat transfer flow over opaque component *k* (W)
$\dot{E}^{transparent}_{component,k}$	Heat transfer flow over transparent component *k* (W)
$\dot{E}_{internal}$	Convective heat sources in the room (W)
$\dot{E}_{mech-ventilatior}$	Convective heat flow from building mechanical ventilation systems (W)
$\dot{E}_{nat-infiltration}$	Heat flow from natural ventilation and infiltration (W)
$\dot{E}_{solar}$	Short-wave solar radiation leading directly to heating the inner air or interior furnishing (W)
$K_i^{\alpha,\beta}$	Kinetic first order chemical reaction coefficients in the zone i between contaminant α and β (s^{-1})
$\dot{V}_{(air-total)_i}$	Total volumetric airflow of i^{th} zone (m^3/s)
$\dot{m}_{(air-total)_i}$	Total airflow of i^{th} zone (kg/s)
$\dot{m}_{air-inward_{(j,i)}}$	Inward flow rate of air from zone j to zone i (kg/s)
$\dot{m}_{air-inward_{total}}$	Total of inward airflows (kg/s)
$\dot{m}_{air-outward_{(i,j)}}$	Outward flow rate of air from the zone i to zone j (kg/s)
$\dot{m}_{air-outward_{tota}}$	Total of outward airflows (kg/s)
$\dot{m}_{nat-infiltration}$	Airflow of natural ventilation and infiltration (kg/s)
$\dot{m}_{supply}$	Supply mechanical ventilation (kg/s)
$\dot{w}_{component,k}$	Moisture flow between inner component *k* and room air (kg/s)
$\dot{w}_{internal}$	Moisture flow of inner source into the room (kg/s),
$\dot{w}_{mech-ventilatior}$	Moisture flow due to building mechanical ventilation systems (kg/s),
$\dot{w}_{nat-infiltration}$	Moisture flow due to natural ventilation and infiltration (kg/s)
h_i	Specific enthalpy inner air (J/kg)
h_o	Specific enthalpy outer air (J/kg)
A_f	Floor area (m^2)
C_i^{α}	Concentration of contaminant α in zone i (kg/kg)

C_i^{β}	Concentration of contaminant β in zone i (kg/kg)
C_j^{α}	Concentration of contaminant α in zone j (kg/kg)
$E_{heat,i}$	Heating energy in zone *i* (room) (J)
G_i^{α}	Generation rate of contaminant α in zone i (kg/s)
P_{p_i}	Water vapor partial pressure of inner air (Pa)
P_{p_o}	Water vapor partial pressure of outer air (Pa)
P_{s_i}	Saturated vapor pressure depending on inner air temperature (Pa)
P_{s_o}	Saturated vapor pressure depending on outer air temperature (Pa)
P_b	Barometric pressure (Pa)
R_a	Gas constant of dry air (=287.05 J/kg.K)
R_i^{α}	Removal coefficient of contaminant α in zone i (kg/s)
R_w	Gas constant water vapor (=461.495 J/kgk)
T_i	Inner air temperature (°C)
T_o	Outer air temperature (°C)
V_{net}	Building net volume (m^3)
m_{air_i}	Mass of air in zone i (kg)
$\dot{m}$	Volumetric airflow rate (m^3/h)
$m_{cont,i}^{\alpha}$	Mass of contaminant of α in the zone i (kg)
$w_{moist,i}$	Moisture content of the zone i (kg)
x_i	Moisture content of inner air (kg/kg)
x_o	Moisture content of outer air (kg/kg)
η_{HR}	Heat recovery rate
η_{MR}	Moisture recovery rate
$\eta_{j,i}^{\alpha}$	Filter efficiency for contaminant α in the path from zone j to zone i
θ_i	Absolute inner air temperature of i^{th} zone (K).
$\rho_{a,i}$	Density for dry air of i^{th} zone (kg/m^3)
ρ_i	Density for the room air of i^{th} zone (kg/m^3)
$\rho_{w,i}$	Density for water Vapor of i^{th} zone (kg/m^3)

ACH	Air changes per hour (h^{-1})
AHS	Air handling system
CONTAM	Contaminant transport analysis model
CSV	Comma separated values
df	Degrees of freedom
DLL	Dynamic link library
ELA	Effective leakage area
EPS	Expanded polystyrene
EPW	EnergyPlus weather file
FMI	Functional mock-up interface
FMU	Functional mock-up unit
H	Building height (m)
HVAC	Heating, ventilation, and air conditioning
IAQ	Indoor air quality
IDF	Input data file
kg/kg	kg of contaminant/kg of dry air
MERV	Minimum efficiency reporting value
NL	Normalized leakage
PMV	Predicted mean vote
PPD	Predicted percentage of dissatisfied
PRJ	Project
RH	Relative humidity
RSI	R-value system international ($m^2 \cdot K/W$)
VEF	Variable exchange file
w/c	Water-cement-ratio
WPS	WUFI Passive-SketchUp
WTH	Weather
WUFI	Wäme und Feuchte instationär

XLSX	Excel Microsoft Office open XML format spreadsheet file
XML	Extensible markup language
XPS	Extruded polystyrene
t	Time (s)
φ	Relative humidity (%)

CHAPITRE 6

DISCUSSION OF THE RESULTS

6.1 Discussion of the research methodology

In this research, a fully combined model has been developed in three phases. An overview of the whole general methodology of this research is presented in Figure 6.1.

In the first phase of this research, EnergyPlus and CONTAM were selected as single models of energy efficiency and indoor air quality, respectively. Then, the feasibility of combining EnergyPlus with CONTAM was evaluated using the co-simulation method. The details of this method were fully presented in chapter 3. Combining EnergyPlus with CONTAM by co-simulation method was resulted in the development of a coupled model of EnergyPlus and CONTAM. The outputs resulted from simulated cases performed by the coupled model of EnergyPlus and CONTAM have been compared to those from simulated cases performed by the single models of EnergyPlus and CONTAM under the same climate conditions and the same assumptions. Therefore, the values of gas and electric energies obtained by EnergyPlus were compared with those by the coupled model of Energy and CONTAM. As well as the values of air change rates simulated by CONTAM were compared with air change rates simulated by the coupled model of Energy and CONTAM. The comparison of simulated results of single and coupled models was made for a three-story house with 3 levels with the same assumptions. These same assumptions include the same climates conditions for Montreal and Miami, exhaust fan with 50 L/s airflow rates, filter with a minimum efficiency reporting value (MERVE) of 12 and other same parameters presented in Tables 3.2 and 3.3. Comparing the results simulated by single and coupled models of EnergyPlus and CONTAM showed that the total energy consumption simulated by EnergyPlus is 4.352 GJ different from the coupled model in Montreal, and this difference was 1.987 GJ in Miami. In addition, the differences between the results of air change rates simulated by CONTAM versus the coupled model of EnergyPlus and CONTAM were 0.059 h^{-1} in Montreal and 0.127 h^{-1} in Miami. The most

important reason for the differences in values of total energy consumption and air change rates simulated by single versus coupled models was due to the exchange of airflows and temperature control variables between EnergyPlus and CONTAM during the co-simulation mechanism. Airflow variables include ventilation system airflow, outdoor air fraction, exhaust fan airflow and infiltration airflow. Temperatures variables include zone temperature and indoor air temperature. By exchanging airflows and temperatures control variables in the coupled models of EnergyPlus and CONTAM in the same boundary conditions (outdoor air temperature, wind speed, biometric pressure, and other weather data parameters) with single models of EnergyPlus and CONTAM, it can be concluded that the simulated results in the coupled model of EnergyPlus and CONTAM have been affected by the exchange of control variables of temperatures and airflows. To analyze the differences between the results simulated by the coupled model of EnergyPlus and CONTAM compared to single models, it is necessary to compare the results simulated by the fully integrated model of EnergyPlus, CONTAM and WUFI with the results of single models. For this purpose, the second phase of the development of the combination of CONTAM with WUFI has been evaluated.

In the second phase, according to Figure 6.1, the feasibility of CONTAM as an indoor air quality model with WUFI as a moisture performance model was investigated. The mechanism of combining CONTAM with WUFI was described in detail in Chapter 4. The results simulated by the coupled model of CONTAM and WUFI were compared with the single models of CONTAM and WUFI for the case of a three-story house in the same climate conditions and same assumptions according to Tables 4. 1 and 4.2. First, indoor CO_2, indoor $PM_{2.5}$ and VOCs concentrations simulated by the coupled model of CONTAM and WUFI were compared with indoor CO_2, indoor $PM_{2.5}$ and VOCs concentrations simulated by CONTAM with the same assumptions. In the next step, indoor relative humidity (RH), predicted percentage of dissatisfied (PPD) and predicted mean vote (PMV) simulated by the coupled model of CONTAM and WUFI was compared with relative humidity (RH), predicted percentage of dissatisfied (PPD), and predicted mean vote (PMV) simulated by WUFI with the same assumptions. This comparison has been made in three different weather conditions of Montreal, Vancouver and Miami.

The simulation results of coupled and single models were calculated as percentage differences with an acceptable level of ASHRAE Standard 62.1 for indoor CO_2, indoor $PM_{2.5}$ and indoor VOCs concentrations, ASHRAE Standard 160 for indoor relative humidity and ASHRAE Standard 55 for predicted mean vote (PMV). In addition, the criteria of percentage of dissatisfied (PPD) simulation results comparison are ASHRAE Standard 55.

In a three-story house as an effective leakage area of 0.04 m^2 and exhaust fan flow rate of 24 L/s in switch off mode for Montreal, the following conclusions can be drawn:

- The average percentage differences of indoor CO_2, indoor $PM_{2.5}$ and indoor VOCs concentrations with an acceptable level of ASHRAE Standard 62.1, simulated by the coupled model of CONTAM and WUFI are −2.34%, −14.92 % and −6.75% different from those simulated by the CONTAM, respectively.

- The average percentage differences of indoor relative humidity (RH) and predicted mean vote (PMV) with an acceptable level of ASHRAE Standard 160 and 55 simulated by the coupled model of CONTAM and WUFI are −28.87% and 16.79 % different from those simulated by WUFI, respectively.

- The average percentage of dissatisfied (PPD) simulated by the coupled model of CONTAM and WUFI is 3.79 % different from the average percentage of dissatisfied (PPD) simulated by WUFI based on ASHRAE Standard 55.

In a three-story house as an effective leakage area of 0.04 m^2 and exhaust fan flow rate of 24 L/s in switch off mode for Vancouver, the following analyzes are presented:

- The average percentage differences of indoor CO_2, indoor $PM_{2.5}$ and indoor VOCs concentrations with an acceptable level of ASHRAE Standard 62.1, simulated by the

coupled model of CONTAM and WUFI are −2.09%, −0.68% and −5.37% different from those simulated by the CONTAM, respectively.

- The average percentage differences of indoor relative humidity (RH) and predicted mean vote (PMV) with an acceptable level of ASHRAE Standard 160 and 55 simulated by the coupled model of CONTAM and WUFI are −23.87% and 12.34 % different from those simulated by WUFI, respectively.

- The average percentage of dissatisfied (PPD) simulated by the coupled model of CONTAM and WUFI is 2.91 % different from those simulated by WUFI based on ASHRAE Standard 55.

In the same assumptions of a three-story house an effective leakage area of 0.04 m^2 and exhaust fan flow rate of 24 L/s in switch off mode for Miami, the following analysis of the results are presented:

- The average percentage differences of indoor CO_2, indoor $PM_{2.5}$ and indoor VOCs concentrations with an acceptable level of ASHRAE Standard 62.1, simulated by the coupled model of CONTAM and WUFI are −1%, −9.38% and −4.38% different from those simulated by the CONTAM, respectively.

- The average percentage differences of indoor relative humidity (RH) and predicted mean vote (PMV) with an acceptable level of ASHRAE Standards 160 and 55 simulated by the coupled model of CONTAM and WUFI are −11.28% and 4.28% different from those simulated by WUFI, respectively.

- The average percentage of dissatisfied (PPD) simulated by the coupled model of CONTAM and WUFI is 1.01 % different from those simulated by WUFI based on ASHRAE Standard 55.

In the same assumptions of a three-story house with an effective leakage area of 0.04 m^2 and exhaust fan flow rate of 24 L/s in switch on mode for Montreal, the following analyzes can be reported as follow:

- The average percentage differences of indoor CO_2, indoor $PM_{2.5}$ and indoor VOCs concentrations with an acceptable level of ASHRAE Standard 62.1, simulated by the coupled model of CONTAM and WUFI are −3.74%, −99.35% and −12.01% different from those simulated by the CONTAM, respectively.

- The average percentage differences of indoor relative humidity (RH) and predicted mean vote (PMV) with an acceptable level of ASHRAE Standard 160 and 55 simulated by the coupled model of CONTAM and WUFI are −15.42% and 14.2 % different from those simulated by WUFI, respectively.

- The average percentage of dissatisfied (PPD) simulated by the coupled model of CONTAM and WUFI is 3.04 % different from those simulated by WUFI based on ASHRAE Standard 55.

In the same assumption of a three-story house with an effective leakage area of 0.04 m^2 and exhaust fan flow rate of 24 L/s in switch on mode for Vancouver, the following discussions can be considered:

- The average percentage differences of indoor CO_2, indoor $PM_{2.5}$ and indoor VOCs concentrations with an acceptable level of ASHRAE Standard 62.1, simulated by the coupled model of CONTAM and WUFI are −3.74%, −106% and −12.08% different from those simulated by the CONTAM, respectively.

- The average percentage differences of indoor relative humidity (RH) and predicted mean vote (PMV) with an acceptable level of ASHRAE Standards 160 and 55

simulated by the coupled model of CONTAM and WUFI are −12.76% and 8.58 % different from those simulated by WUFI, respectively.

- The average percentage of dissatisfied (PPD) simulated by the coupled model of CONTAM and WUFI is 2.01 % different from those simulated by WUFI based on ASHRAE Standard 55.

In the same assumption of a three-story house with an effective leakage area of 0.04 m^2 and exhaust fan flow rate of 24 L/s in switch on mode for Miami, the following discussions can be considered:

- The average percentage differences of indoor CO_2, indoor $PM_{2.5}$ and indoor VOCs concentrations with an acceptable level of ASHRAE Standard 62.1, simulated by the coupled model of CONTAM and WUFI are −3.72%, −106.06% and −12.03% different from those simulated by the CONTAM, respectively.

- The average percentage differences of indoor relative humidity (RH) and predicted mean vote (PMV) with an acceptable level of ASHRAE Standards 160 and 55 simulated by the coupled model of CONTAM and WUFI are −8.52% and 2.7 % different from those simulated by WUFI, respectively.

- The average percentage of dissatisfied (PPD) simulated by the coupled model of CONTAM and WUFI is 0.69 % different from those simulated by WUFI based on ASHRAE Standard 55.

In a three-story house with an effective leakage area of 0.3 m^2 and exhaust fan flow rate of 24 L/s in switch off mode for Montreal, the following conclusions can be drawn:

- The average percentage differences of indoor CO_2, indoor $PM_{2.5}$ and indoor VOCs concentrations with an acceptable level of ASHRAE Standard 62.1, simulated by the

coupled model of CONTAM and WUFI are −1.18%, −29.49% and −4.18% different from those simulated by the CONTAM, respectively.

- The average percentage differences of indoor relative humidity (RH) and predicted mean vote (PMV) with an acceptable level of ASHRAE Standards 160 and 55 simulated by the coupled model of CONTAM and WUFI are −0.32% and 12.41 % different from those simulated by WUFI, respectively.

- The average percentage of dissatisfied (PPD) simulated by the coupled model of CONTAM and WUFI is 2.16 % different from those simulated by WUFI based on ASHRAE Standard 55.

In a three-story house with an effective leakage area of 0.3 m^2 and exhaust fan flow rate of 24 L/s in switch off mode for Vancouver, the following analyzes are concluded:

- The average percentage differences of indoor CO_2, indoor $PM_{2.5}$ and indoor VOCs concentrations with an acceptable level of ASHRAE Standard 62.1, simulated by the coupled model of CONTAM and WUFI are −0.98%, −7.75% and −3.07% different from those simulated by the CONTAM, respectively.

- The average percentage differences of indoor relative humidity (RH) and predicted mean vote (PMV) with an acceptable level of ASHRAE Standards 160 and 55 simulated by the coupled model of CONTAM and WUFI are −1.09% and 2.77 % different from those simulated by WUFI, respectively.

- The average percentage of dissatisfied (PPD) simulated by the coupled model of CONTAM and WUFI is 0.67 % different from the one simulated by WUFI based on ASHRAE Standard 55.

In the same assumption of a three-story with an effective leakage area of 0.3 m^2 and exhaust fan flow rate of 24 L/s in switch off mode for Miami, the following are presented as an analysis of the results:

- The average percentage differences of indoor CO_2, indoor $PM_{2.5}$ and indoor VOCs concentrations with an acceptable level of ASHRAE Standard 62.1, simulated by the coupled model of CONTAM and WUFI are −0.51%, −11.7% and −1.38% different from those simulated by the CONTAM, respectively.

- The average percentage differences of indoor relative humidity (RH) and predicted mean vote (PMV) with an acceptable level of ASHRAE Standard 160 and 55 simulated by the coupled model of CONTAM and WUFI are −0.34% and 0.4% different from those simulated by WUFI, respectively.

- The average percentage of dissatisfied (PPD) simulated by the coupled model of CONTAM and WUFI is 0.1 % different from the one simulated by WUFI based on ASHRAE Standard 55.

In the same assumption of a three-story house with an effective leakage area of 0.3 m^2 and exhaust fan flow rate of 24 L/s in switch on mode for Montreal, the following analyzes can be mentioned:

- The average percentage differences of indoor CO_2, indoor $PM_{2.5}$ and indoor VOCs concentrations with an acceptable level of ASHRAE Standard 62.1, simulated by the coupled model of CONTAM and WUFI are −2.28%, −100.99% and −8.07% different from those simulated by the CONTAM, respectively.

- The average percentage differences of indoor relative humidity (RH) and predicted mean vote (PMV) with an acceptable level of ASHRAE Standard 160 and 55 simulated

by the coupled model of CONTAM and WUFI are 0.09% and 12.5 % different from those simulated by WUFI, respectively.

- The average percentage of dissatisfied (PPD) simulated by the coupled model of CONTAM and WUFI is 2.13 % different from the one simulated by WUFI based on ASHRAE Standard 55.

In the same assumption of a three-story house with an effective leakage area of 0.3 m^2 and exhaust fan flow rate of 24 L/s in switch on mode for Vancouver, the following discussions can be considered:

- The average percentage differences of indoor CO_2, indoor $PM_{2.5}$ and indoor VOCs concentrations with an acceptable level of ASHRAE Standard 62.1, simulated by the coupled model of CONTAM and WUFI are −2.45%, −106% and −8.83% different from those simulated by the CONTAM, respectively.

- The average percentage differences of indoor relative humidity (RH) and predicted mean vote (PMV) with an acceptable level of ASHRAE Standard 160 and 55 simulated by the coupled model of CONTAM and WUFI are −0.83% and 2.97 % different from those simulated by WUFI, respectively.

- The average percentage of dissatisfied (PPD) simulated by the coupled model of CONTAM and WUFI is 0.69 % different from the one simulated by WUFI based on ASHRAE Standard 55.

In the same assumption of a three-story house with an effective leakage area of 0.3 m^2 and exhaust fan flow rate of 24 L/s in switch on mode for Miami, the following discussions can be considered:

- The average percentage differences of indoor CO_2, indoor $PM_{2.5}$ and indoor VOCs concentrations with an acceptable level of ASHRAE Standard 62.1, simulated by the coupled model of CONTAM and WUFI are −3.2%, −106.06% and −8.89% different from those simulated by the CONTAM, respectively.

- The average percentage differences of indoor relative humidity (RH) and predicted mean vote (PMV) with an acceptable level of ASHRAE Standard 160 and 55 simulated by the coupled model of CONTAM and WUFI are −0.26% and 0.35 % different from those simulated by WUFI, respectively.

- The average predicted percentage of dissatisfied (PPD) simulated by the coupled model of CONTAM and WUFI is −0.09 % different from the one simulated by WUFI based on ASHRAE Standard 55.

Above, the differences of indoor CO_2, indoor $PM_{2.5}$ and VOCs, indoor relative humidity (RH), predicted percentage of dissatisfied (PPD) and predicted mean vote (PMV), simulated by coupled and single models of CONTAM and WUFI have been presented under the same assumption and the same climate conditions in the cities of Montreal, Vancouver and Miami. The reason for these differences is the result of the combination mechanism of CONTAM and WUFI shown in Figure 4.1. In this mechanism, airflow control variables are exchanged between CONTAM and WUFI, and this exchange leads to corrections of control variables. Average daily paths and ducts airflows simulated by CONTAM are used as natural (infiltration) and mechanical ventilation in WUFI, and then average hourly natural and mechanical ventilation airflows simulated by WUFI are used as effective leakage area (ELA) and design fan flow rate in CONTAM. This cyclic loop of exchange of airflow control variables leads to the fact that the simulation results of coupled models of CONTAM and WUFI are different from single models. However, to evaluate the accuracy of the results simulated by the coupled model in comparison with single models, it is necessary to combine all three EnergyPlus, CONTAM and WUFI models and then evaluate and analyze the

simulation results of this fully coupled model with single models in the same assumptions and same climate conditions. Therefore, this analysis has been followed in the third phase.

In the third phase according to Figure 6.1, based on the feasibility of combining EnergyPlus and CONTAM in phase 1 and the feasibility of combining CONTAM and WUFI in phase 2, the combination of EnergyPlus, CONTAM and WUFI was developed as a fully combined model. The combination mechanism of EnergyPlus, CONTAM and WUFI has been presented in Figures 5.1 and 6.2. The details of the fully combined model development were described in Chapter 5. According to Figure 6.1, after developing the combined model based on the combination of EnergyPlus, CONTAM and WUFI, model verification was performed. The results simulated by the combined model under the same assumptions and the same climate conditions were compared with the results simulated by the single models of EnergyPlus, CONTAM and WUFI. For this purpose, according to Figure 6.1, four scenarios were defined.

The differences between scenarios are:

1. The airtight fan-off scenario is a case of three-story house with an effective leakage area of 0.04 m^2 and exhaust fan flow rate of 24 L/s in switch off mode.

2. The airtight fan-on scenario is a case of three-story house with an effective leakage area of 0.04 m^2 and exhaust fan flow rate of 24 L/s in switch on mode.

3. The leaky fan-off scenario is a case of three-story house with an effective leakage area of 0.3 m^2 and exhaust fan flow rate of 24 L/s in switch off mode.

4. The leaky fan-on scenario is a case of three-story house with an effective leakage area of 0.3 m^2 and exhaust fan flow rate of 24 L/s in switch on mode.

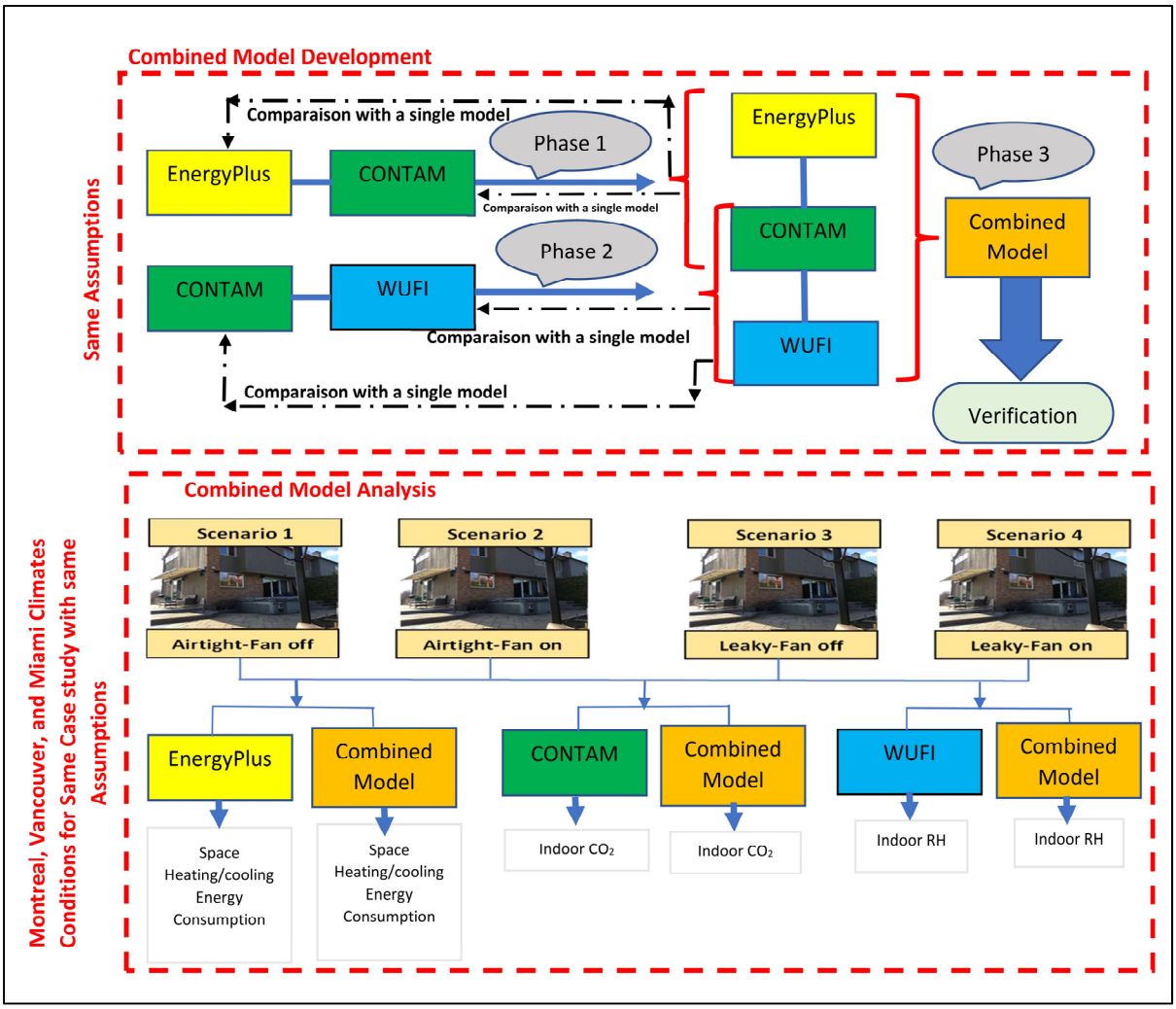

Figure 6.1 Overview of the combined model development phases based on the research methodology

In the same conditions, space heating/cooling energy consumptions simulated by the combined model with heating/cooling energy consumptions simulated by EnergyPlus, indoor CO_2 concentrations simulated by the combined model with indoor CO_2 concentrations simulated by the CONTAM and indoor relative humidity (RH) simulated by the combined model with indoor relative humidity (RH) simulated by WUFI were compared according to Figure 6.1.

To discuss the details related to the exchange of control variables between EnergyPlus, CONTAM and WUFI in the development of the fully combined model, Figure 6.2 was

presented. In Figure 6.2, EnergyPlus, CONTAM and WUFI was connected as energy, indoor air quality (IAQ) and moisture software by exchanging control variables in a complete cyclic loop from the beginning sub-model to the destination sub-model. The simulated control variables at the beginning sub-model were exchanged as input data variables to the destination sub-model so that the loop of all three sub-models was completed. In this case, the combined model of EnergyPlus, CONTAM and WUFI was created.

According to Figures 5.1 and 6.2, considering that CONTAM consists of two parts of ContamW as a graphic interface with viewing simulation results capability, and ContamX as the simulator. ContamW by producing a project (PRJ) file, which includes all the data related to temperatures, airflows, geometry and other control variables, was first converted to input data (IDF) file and ContamFMU.fmu files with the help of CONTAM3DExporter tool. As shown in Figures 5.1 and 6.1, ContamFMU.fmu was a compressed zipped file that includes a variable exchange file (VEF), extensible markup language (XML) and ContamFMU.dll. Considering that in Chapters 3 and 5, the co-simulation mechanism between CONTAM and EnergyPlus was described in detail through the functional mock-up interface method, therefore the control variables of temperatures and airflows are exchanged between ContamX and EnergyPlus, and then the output of the simulated coupled model of CONTAM and EnergyPlus as shown in Figure 6.2 were used as WUFI input data. At this stage, average daily paths and ducts airflows, space heating/cooling flow and heating/cooling temperatures simulated by the coupled model of EnergyPlus and CONTAM were replaced by natural (infiltration) and mechanical ventilation, space heating/cooling capacities and maximum/minimum temperatures, input data of WUFI, respectively as comma-separated values (CSV) file.

According to Figures 5.1 and 6.2, the IDF file created by the CONTAM3DExporter tool includes geometry and airflows variables such as infiltration, interzone mixing flows, outdoor air mixer, HVAC airflow and other variables required in co-simulation between CONTAM and EnergyPlus. The IDF file can be viewed and edited in SketchUp through OpenStudio SketchUp Plug-in before using it in EnergyPlus. Also, this edited IDF file can be converted to

WPS (WUFI Passive-SketchUp) file through WUFI SketchUp's Plug-in in SketchUp and then can be used as geometry input data in WUFI.

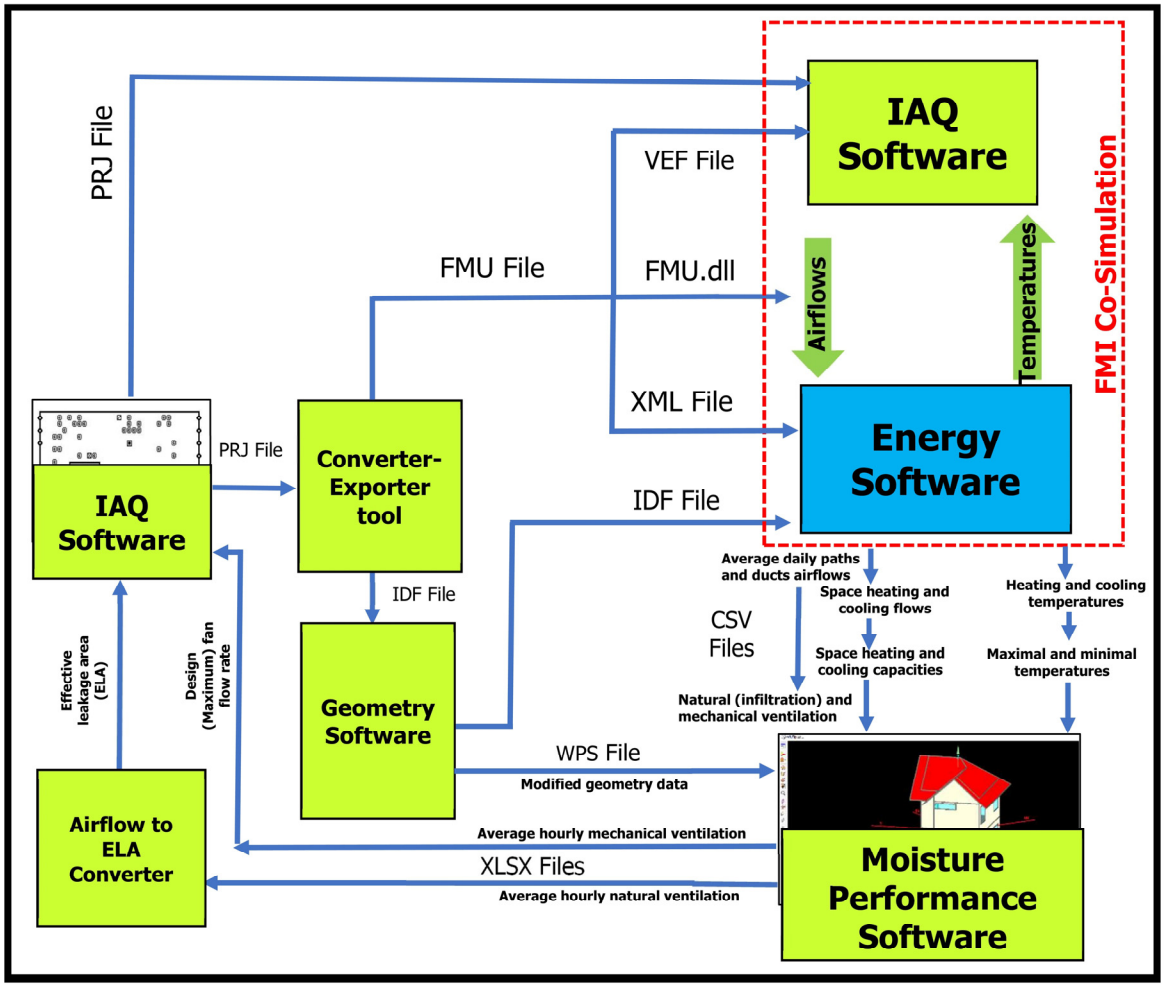

Figure 6.2 Fully combined model methodology approach on connections of energy, indoor air quality and moisture performance software by exchanging control variables

In the next step, average hourly natural and mechanical ventilation, simulated by WUFI replaced by CONTAM's effective leakage area (ELA) and design (maximum) fan flow rate input data as XLSX file, respectively. Average hourly natural ventilation was converted to a new effective leakage area by ELA converter before use in CONTAM. Finally, the ContamW was connected by the project (PRJ) to ContamX, and in this last step the whole cyclic loop connections of EnergyPlus, CONTAM WUFI were completed.

The interconnections between EnergyPlus, CONTAM and WUFI were completed in a cyclic loop according to Figure 6.2, so it can be concluded that this new model is the fully combined model. Therefore, this interconnections for EnergyPlus, CONTAM and WUFI with the control variables of temperatures, airflows and space heating/cooling flows were iterated enough to predict the optimum scenarios in each of the fields of energy, indoor air quality and moisture performance.

Equations 5.4, 5.5 and 5.6 described in Chapter 5 as energy, contaminant, and moisture balances, are the governing equations of EnergyPlus, CONTAM and WUFI sub-models, respectively. If the airflow control variables are exchanged between EnergyPlus, CONTAM and WUFI as a complete cyclic loop, it can be concluded that energy, contamination, and moisture balances are solved based on the same airflow variables. Therefore, by continuous iterations exchanging airflows input data values between the beginnings to the destination sub-models, the optimum scenario based on ASHRAE Standard criteria was created.

The exchange of control variables between sub-models of EnergyPlus, CONTAM and WUFI was iterated as a cyclic loop until the minimum percentage differences of hourly space heating/cooling energy consumption, daily indoor CO_2 concentration and hourly relative humidity (RH) with an acceptable level of ASHRAE Standards 90.1, 62.1 and 160, respectively, are satisfied for defined scenarios. Then, the scenarios with minimum average percentage differences of hourly space heating/cooling energy consumption, daily indoor CO_2 concentration and hourly relative humidity (RH) with acceptable levels of ASHRAE Standards 90.1, 62.1 and 160 were selected as the optimum scenarios.

6.2 Discussion of the verification method

As explained in Chapters 4 and 5, the paired sample t-test method was used in the verification of this combined model for this reason because with the help of this method, it was possible to accurately evaluate whether the actual and simulated results had the significant differences or not. Theses significant differences can be validated based on statistical criteria. Therefore, if

the combined model was not properly developed or its accuracy was low, these significant differences between the simulated results and the actual values were higher than the permissible limit.

Considering that many researchers had used paired sample t-test method with a high citation in their research work in verification of simulated models, such as Zhu (2006), Balci (1998), Kleijnen (1995), Park & Qi (2005) and Sargent (2010), so this method can be valid for this research.

Another important reason was that in paired sample t-test method, the significant differences between actual and simulated results were tested twice in two procedures, and this advantage made its results more valid.

Details related to the accuracy, and choosing simulated samples and measured actual data, location and days were discussed for a fully combined model based on the verification method presented in Chapter 5.

Considering that, the innovation of the fully combined model was the possibility of simulating energy, indoor air quality and moisture performance measures in a combined method, therefore, daily space heating energy consumption, daily indoor CO_2 concentration and hourly relative humidity (RH) were chosen as simulated and actual measured data samples. To properly analyze simulated data with actual measured data accurately through paired sample t-test, these samples data were selected for the 15^{th} days of the months in 2020.

Actual measured data for daily space heating energy consumptions, daily indoor CO_2 concentrations and hourly relative humidity (RH) respectively were measured by the plug-in energy monitor, CO_2 meter monitor and humidity meter monitor for a real case of a three-story house with the area of 110 m^2, the volume of 329 m^3, floor to floor height of 3 m, leakage areas of 0.3 m^2 with exhaust fan airflow rate of 24 L/s located in Montreal city.

In the next step daily space heating energy consumptions, daily indoor CO_2 concentrations and hourly relative humidity (RH) have been simulated by combined model for this real case.

Therefore, it can be concluded that the reason for choosing the location of Montreal with the desired case is limited to real conditions.

The values of simulated and actual measured data samples for daily space heating energy consumption, daily indoor CO_2 concentration and hourly relative humidity (RH) respectively were presented in Tables 5.1, 5.2 and 5.3.

According to the criteria of the paired sample t-test, all simulated samples were validated in comparison with the actual measured data samples in both steps, so due to this advantage of this method, it can be concluded that there are no significant differences between simulated and actual data samples and can verify the combined model with the high accuracy.

6.3 Discussion of the comparison approach for combined and single models results

Figure 6.3 shows the comparison mechanism of the simulated results between the combined model with the single models of EnergyPlus, CONTAM and WUFI.

In the field of energy, the combined model and EnergyPlus simulated hourly space heating/cooling energy consumption measures. In the field of indoor air quality, the combined model and CONTAM simulated daily indoor CO_2 concentrations. In the field of moisture performance, the combined model and WUFI simulated indoor relative humidity (RH).
To building performance evaluation of the simulated results by the combined model and single models of EnergyPlus, CONTAM and WUFI into an analytical relationship as the equation presented in Figure 6.3, percentage differences of simulated results with an acceptable level of ASHRAE Standards were calculated.

ASHRAE Standard 90.1 was used for hourly space heating/cooling energy consumptions simulated by the combined model and EnergyPlus as energy performance criteria. In ASHRAE Standard 90.1 the acceptable level of hourly space heating/cooling energy consumptions should be less than 1.72 kW for the case study. Therefore, percentage differences of hourly space heating/cooling energy consumptions simulated by the combined model and EnergyPlus were calculated by Equation (5.23).

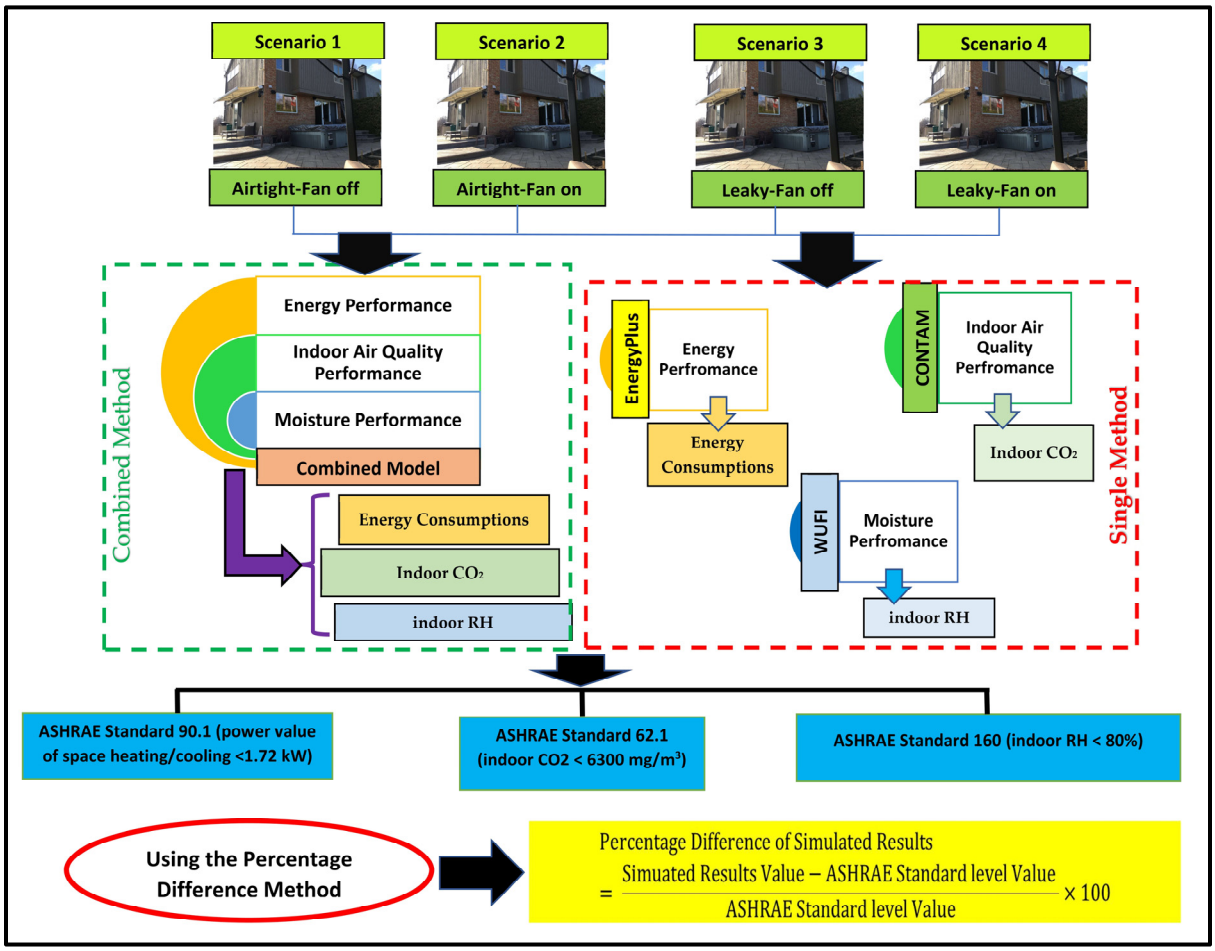

Figure 6.3 Approach for comparing results of the fully combined model and single model

ASHRAE Standard 62.1 was used for daily indoor CO_2 concentrations simulated by the combined model and CONTAM as indoor air quality performance criteria. In ASHRAE Standard 62.1 the acceptable level of indoor CO_2 concentration should be less than 52.32 ×

10−4 kg/kg for the case study. So, percentage differences in daily indoor CO_2 concentrations simulated by the combined model and CONTAM were calculated by Equation (5.24).

ASHRAE Standard 160 was used for hourly relative humidity (RH) simulated by the combined model and WUFI as moisture performance criteria. In ASHRAE Standard 160 the acceptable level of hourly relative humidity (RH) is less than 80% for the case study of this research. Percentage differences of hourly relative humidity (RH) simulated by the combined model and WUFI were calculated by Equation (5.25).

According to the presented approach in Figure 6.3 and Equations (5.23) to (5.25) for calculating the percentage differences of hourly space heating/cooling energy consumptions, daily indoor CO_2 concentrations and hourly relative humidity (RH) with acceptable levels of ASHRAE Standards 90.1, 62.1 and 160, respectively, it is possible to compare the performances of the energy, indoor air quality and moisture results obtained by the combined and single models.

6.4 Discussion of the optimal scenarios selections and comparisons in the combined and single models

The accuracy of the combined model verification was discussed, and it was concluded that the reason that there were no significant differences between the values of simulated data and actual measured data was due to the exchange of control variables of airflows, temperatures, and heating/cooling flows in a cyclic loop between sub-models. Therefore, the optimal scenarios can be predicted as the advantages of the combined model with high precision by iteration possibility of exchanging control variables. In this section, we can discuss the differences between the optimal scenarios selected through the combined model and the optimal scenarios selected through the single models.

The selected optimal scenarios of the results simulated by the combined model have been compared to the selected optimal scenarios of the results simulated by single models through Figures 6.4 to 6.6.

The results obtained by the combined model and single models have been shown as the average percentages differences of hourly space heating/cooling energy consumptions, daily indoor CO_2 concentrations and hourly relative humidity (RH) with acceptable levels of ASHRAE Standards 90.1, 62.1 and 160, for four scenarios, in Figures 6.4, 6.5 and 6.6 respectively, and then the minimum values of average percentage differences are selected as the optimal scenarios.

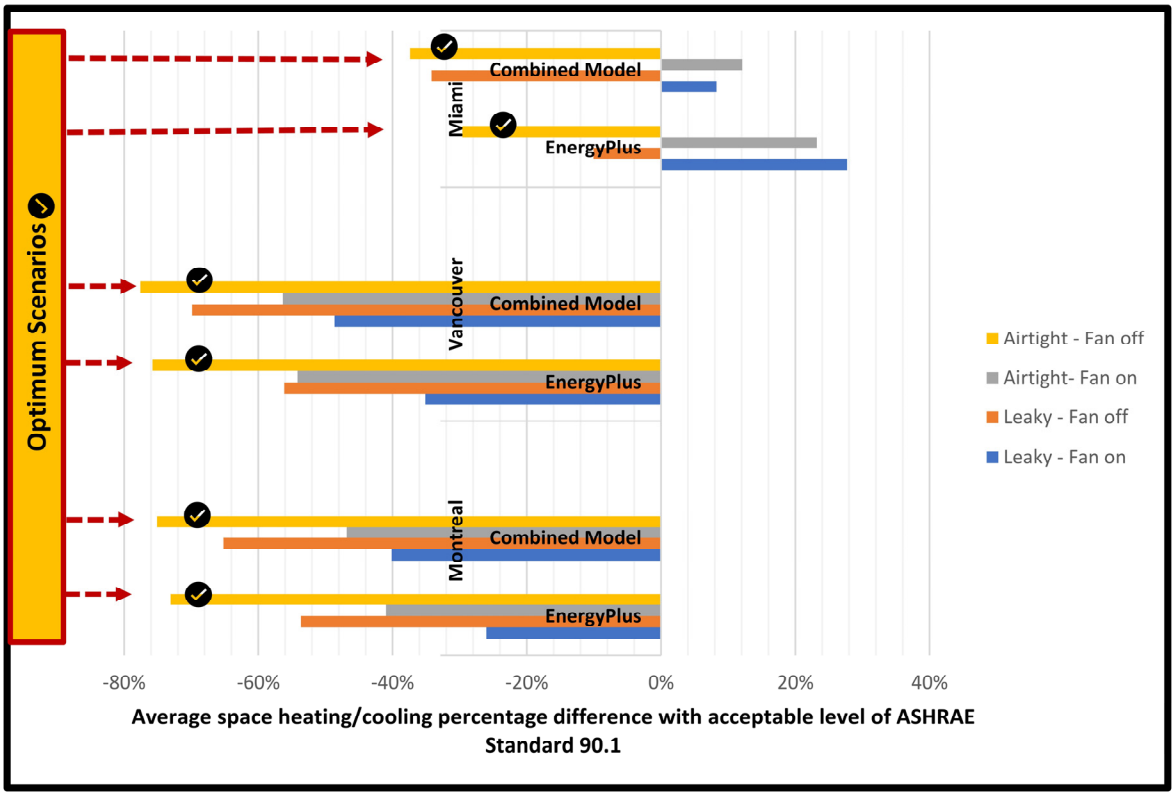

Figure 6.4 Comparison of the optimal scenarios predicted by the fully combined model and EnergyPlus based on average percentage differences of hourly space heating/cooling energy consumption with acceptable level of ASHRAE Standard 90.1 in Montreal, Vancouver, and Miami

In Figure 6.4, the average percentage differences of hourly space heating/cooling energy consumptions with an acceptable level of ASHRAE Standard 90.1, simulated by the combined

model have been compared with EnergyPlus for four scenarios, in Montreal, Vancouver and Miami.

According to Figure 6.4, the scenario with an effective leakage area of 0.04 m^2 and exhaust fan flow rate of 0 L/s (airtight fan-off) has the minimum values of percentage differences with an acceptable level of ASHRAE Standard 90.1 as the optimum scenario. However, the optimum scenario values predicted by the combined model are −2.03%, −1.82% and −7.78% different from the optimum scenarios predicted by EnergyPlus for Montreal, Vancouver and Miami, respectively.

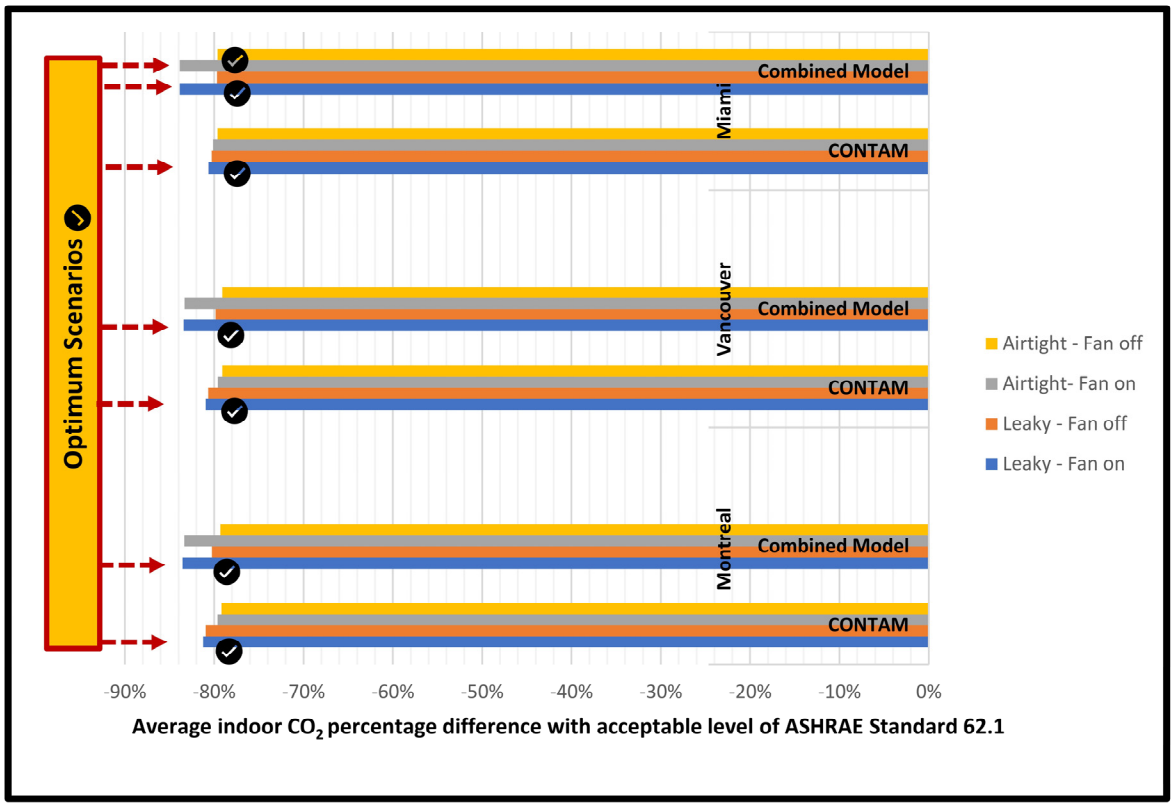

Figure 6.5 Comparison of the optimal scenarios predicted by the fully combined model and CONTAM based on average percentage differences of daily indoor CO_2 concentration with an acceptable level of ASHRAE Standard 62.1 in Montreal, Vancouver, and Miami

The average percentage differences in daily indoor CO_2 concentrations with an acceptable level of ASHRAE Standard 62.1, simulated by the combined model, are compared with CONTAM for four scenarios, in Montreal, Vancouver and Miami according to Figure 6.5.

The scenario with an effective leakage area of 0.3 m^2 and an exhaust fan flow rate of 24 L/s (leaky fan-on) has the minimum values of percentage differences with an acceptable level of ASHRAE Standard 62.1 as the optimum scenario for CONTAM and combined model in Montreal and Vancouver. The optimum scenario values predicted by the combined model, are −2.28% and −2.46% different from the optimum scenario predicted by CONTAM in Montreal and Vancouver, respectively.

The scenario with an effective leakage area of 0.3 m^2 and an exhaust fan flow rate of 24 L/s (leaky fan on) has the minimum values of percentage differences with an acceptable level of ASHRAE Standard 62.1 as the optimum scenario for CONTAM in Miami. In the combined model the two scenarios with an effective leakage area of 0.04 m^2 or 0.3 m^2 and exhaust fan flow rate of 24 L/s (airtight fan-on and leaky fan-on) have the same minimum values of percentage differences with an acceptable level of ASHRAE Standard 62.1 as optimum scenarios in Miami. The optimum scenarios values predicted by the combined model, are −3.22% different from the optimum scenario predicted by CONTAM.

In Figure 6.6, the average percentage differences of hourly relative humidity (RH) with an acceptable level of ASHRAE Standard 160, simulated by a combined model have been compared with WUFI for four scenarios, in Montreal, Vancouver and Miami.

According to Figure 6.6, the scenario with an effective leakage area of 0.3 m^2 and an exhaust fan flow rate of 24 L/s (leaky fan-on) has the minimum values of percentage differences with an acceptable level of ASHRAE Standard 160 as the optimum scenario for WUFI in Montreal, Vancouver, and Miami. But, in the combined model the scenario with an effective leakage area of 0.04 m^2 and exhaust fan flow rate of 24 L/s (airtight fan-on) has the minimum value of percentage difference with an acceptable level of ASHRAE Standard 160 as the optimum scenario in Montreal. The scenario with an effective leakage area of 0.04 m^2 and exhaust fan

flow rate of 0 L/s (airtight fan-off) in the combined model has the minimum values of percentage differences with an acceptable level of ASHRAE Standard 160 as the optimum scenario for the combined model in Vancouver, Miami. The optimum scenarios values predicted by the combined model, are 54.76%, 47.64% and −5.54 different from the optimum scenario predicted by WUFI in Montreal, Vancouver and Miami.

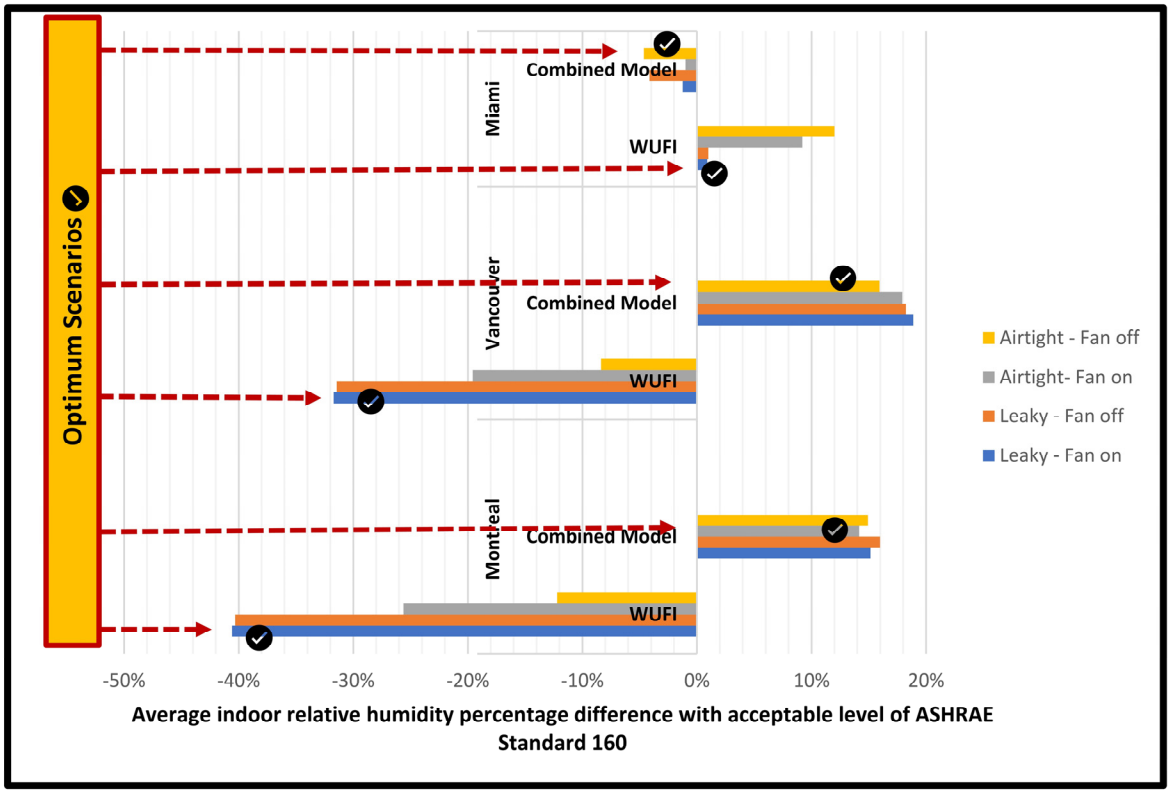

Figure 6.6 Comparison of the optimal scenarios predicted by the fully combined model and WUFI based on average percentage differences of hourly relative humidity (RH) with an acceptable level of ASHRAE Standard 160 in Montreal, Vancouver, and Miami

CONCLUSION

The main purpose of the Ph.D. program is a fully combined model development based on a combination of energy-indoor air quality and moisture models for the whole building's performance. Achieving this main goal in three phases of Ph.D. is performed with the following contributions.

- In the first phase, the feasibility of combining EnergyPlus and CONTAM has been evaluated and analyzed using the co-simulation method. The contribution of this research is the paper entitled: “Assessing the Energy and Indoor Air Quality Performance for a Three-Story Building Using an Integrated Model, Part One: The Need for Integration”, which was extracted.

- In the second phase of this research, the feasibility of combining CONTAM with WUFI was evaluated and analyzed using the co-simulation method. Finally, the paper entitled: “Assessing the Energy, Indoor Air Quality, and Moisture Performance for a Three-Story Building Using an Integrated Model, Part Two: Combination the Indoor Air Quality, Moisture, and Thermal Comfort”, was extracted.

- In the final phase, the combination of all three EnergyPlus, CONTAM and WUFI was performed by co-simulation method and using the experiences obtained from the results of the previous two phases and the final paper entitled: “Assessing the Energy, Indoor Air Quality, and Moisture Performance for a Three-Story Building Using an Integrated Model, Part Three: Development of Integrated Model and Applications”, was extracted.

In the feasibility and analysis of the combination of different sub-models of EnergyPlus, CONTAM and WUFI in the three phases, a three-story house was assumed as a case study. The development of different parts of the combined model in three different cold-humid,

medium-humid, and hot-humid climatic conditions was analyzed for Montreal, Vancouver and Miami, respectively. The general conclusions that can be described from this Ph.D. program include the followings:

- In the first phase of this research, the co-simulation method for coupling of EnergyPlus-CONTAM model was developed based on Dols & Polidoro (2015) method.

- Because the EnergyPlus-CONTAM coupled model has been validated by Dols & Polidoro (2015) method, and the accuracy of the coupled model was verified.

- To better analyze the capabilities of the coupled model compared to the single models, three scenarios have been defined. These scenarios include: (1) airtight building as energy efficient, (2) building with the exhaust fan as indoor air quality efficient and, (3) building with airtight, exhaust fan and upgraded filters as both energy and indoor air quality efficient.

coupled

- EnergyPlus and CONTAM single molds were used to simulate energy efficiency and indoor air quality measures for the baseline, scenario 1 and scenario 2.

- Given that Scenario 3 defined as a combination of energy efficiency and indoor air quality criteria, energy and indoor air quality measures were simulated once by both coupled and single models, and their results were compared with each other.

- Air change rates, indoor particle (PM_5) concentrations, indoor CO_2 concentrations and indoor VOCs concentrations have been assumed as measures of indoor air quality as well as electrical and gas energy consumptions as energy measures.

- Therefore, in scenario 3, the results of energy consumptions and air change rates simulated by single models of EnergyPlus and CONTAM, respectively, were compared with the results of energy consumptions and air exchange rates simulated by the coupled model and their differences were analyzed.

- Since in the coupled model the airflows and temperatures control variables are exchanged and modified between both sub-models of EnergyPlus and CONTAM due to the co-simulation mechanism, the necessity of replacing the coupled model instead of single models is concluded.

In the second phase of this research, a coupled model of CONTAM with WUFI was developed using the co-simulation method and also the following conclusions have been extracted**:**

- The main purpose of developing the coupled model of CONTAM-WUFI in this part of the research was to combine indoor air quality, moisture and thermal comfort with high accuracy.

- The exchange of airflows along with the temperatures variables between all three equations of energy, moisture and contaminant balances lead to a coupled solution in accurate predicting and improvement of the results according to ASHRAE 62.1, 160 and 55 standards.

- Accuracy of the coupled model of CONTAM-WUFI has been verified in two parts of 1- paired samples 'differences and 2- paired samples' correlations based on comparison of simulated and actual data samples of daily indoor CO_2 concentrations and indoor relative humidity.

- To analyze the accuracy of the predicted results of the coupled model compared to the single models, four scenarios of airtight fan-off, airtight fan-on, leaky fan-off and leaky fan-on were defined. So that the simulated results of indoor air quality, moisture

performance and thermal comfort measures by the coupled model of CONTAM-WUFI in different situations of the case study can be compared with the simulated results of single models of CONTAM and WUFI.

- In coupled model of CONTAM-WUFI all three indoor air quality, moisture performance and thermal comfort measures seamlessly were simulated but in the single models, indoor air quality by CONTAM and moisture performance with thermal comfort by WUFI were simulated.

- Indoor CO_2 concentrations, indoor $PM_{2.5}$ concentrations, indoor VOCs concentrations as indoor air quality measures, indoor relative humidity (RH) as moisture performance measures as well as predicted percentage of dissatisfied (PPD) and predicted mean vote (PMV) as thermal comfort measures were simulated by coupled and single models.

- For both of coupled and single models, the percentage differences of indoor CO_2, $PM_{2.5}$ and VOCs concentrations with an acceptable level of ASHRAE Standard 62.1, indoor relative humidity (RH) with an acceptable level of ASHRAE Standard 160, predicted percentage of dissatisfied (PPD) and predicted mean vote (PMV) with an acceptable level of ASHRAE Standard 55 were calculated.

- The simulated results of coupled and single models were different in the optimal scenarios.

- The reason for the differences in simulated results of indoor CO_2, indoor $PM_{2.5}$ and indoor VOCs between the coupled model and CONTAM was that in the coupled model, the effective leakage rates and exhaust fan data were defined as airflows input data by user but in the single models, airflows were exchanged by using the co-simulation mechanism.

- The reason for the difference in the simulated result of indoor relative humidity (RH) between the coupled model and WUFI was that the infiltration and mechanical ventilation were defined as airflows input data by user, while in the coupled model, airflows due to co-simulation mechanisms were exchanged.

- The reason for the difference in simulated results of the percentage of dissatisfied (PPD) and indoor predicted mean vote (PMV) between the coupled model and WUFI, was that the infiltration rate was defined as airflow input data in WUFI by user but the airflow in the coupled model was exchanged by the co-simulation mechanism.

- Considering the differences between the simulation results of the coupled and single models and also verification of the coupled model, it can be concluded that combination of CONTAM and WUFI leads to an increase the accuracy of simulated results. For predicting the real building performance, it is necessary to combine all three energy, indoor air quality and moisture performance tools.

The third phase was performed as the final phase based on the results and experiences gained from other previous phases, and its general conclusions include the following:

- In the second phase a fully combined model has been developed.

- Comparing the simulation results of EnergyPlus-CONTAM coupled model and CONTAM-WUFI coupled model, there was the necessity to develop a fully combined model of EnergyPlus, CONTAM and WUFI .

- In the fully combined model the three equations of energy, moisture and contaminant balances were solved in a combined method by exchanging airflows and temperatures control variables.

- The accuracy of the fully combined model was verified by paired sample t-test method.

- An important point in the development of a fully combined model was that due to the exchange of temperatures, airflows, and heating-cooling flows between all three sub-models of EnergyPlus, CONTAM and WUFI.

- To evaluate the accuracy and capability of the fully combined model compared to single models, four scenarios of airtight fan-off, airtight fan-on, leaky fan-off, and leaky fan-on were defined for the case of a three-story house.

- The values of hourly space heating/cooling energy consumptions, daily indoor CO_2 concentrations, and hourly indoor relative humidity (RH) were assumed as measures of energy, indoor air quality and moisture performance, respectively for the fully combined and single models.

- The most important innovation of this research is the possibility of simulating energy, indoor air quality and moisture performance measures in a combined method for any type of building. Therefore, the simulation results of the combined model with single models are compared and analyzed with each other.

- Percentage differences of simulated results values of hourly space heating/cooling energy consumptions, daily indoor CO_2 concentrations, and hourly indoor relative humidity concentrations with acceptable levels of ASHRAE Standard 90.1, 62.1 and 160 for all scenarios have been evaluated by the fully combined model compared to single models.

- The results simulated by the fully combined model was different from the single models due to the following reasons:

    - In EnergyPlus, the values of infiltration and design of air-handling system airflows were defined as airflow input data by the user, while in the fully

combined model, the airflows were exchanged by the combination mechanism for EnergyPlus, CONTAM and WUFI.

- In CONTAM, the effective leakage area and exhaust fan airflow values as airflow input data, junction temperature, and default zone temperature as temperature input data were defined by the user, but in the fully combined model airflows and temperatures were exchanged based on the combination mechanism for EnegryPlus, CONTAM and WUFI.

- In WUFI, the values of infiltration and mechanical ventilation as airflows input data, minimum /maximum zone temperatures as temperatures input data and space heating/cooling flows input data were defined by the user, but airflow, temperatures and heating/cooling flows were exchanged by the combination mechanism of EnergyPlus, CONTAM and WUFI.

The main goal of this research was to develop a combined model that predicts energy efficiency, indoor air quality and moisture performance in a combined approach with high accuracy. The result values simulated by the combined model method were different from the results values simulated by the single model methods. Because the accuracy of the combined model was verified, it can be concluded that the differences between the results values simulated by the combined and single models are due to the accuracy of the combined model. In the combined model method, all three sub-models of EnergyPlus, CONTAM and WUFI, were connected in a cyclic loop by exchanging the control variables of airflows, temperatures and heating/cooling flow, and the input data of each sub-model was replaced by the simulated output data of the previous sub-model. In the single model method, the input data was defined by the user. Using simulated data by the primary sub-model as input data for the next connected sub-model can prove the advantage of validating the input data to each sub-models and the accuracy of the combined model. Also, in the combined model, it is possible to evaluate different scenarios based on ASHRAE Standard criteria by values changing the control variables in a combined loop with iterations.

In the combined model method, due to the exchange of airflows, temperatures and heating/cooling flows control variables between EnergyPlus, CONTAM and WUFI sub-models in a combined loop, the iteration can continue if the ASHRAE Standards 90.1, 62.1 and 160, are satisfied for simulated results in different scenarios. The optimal scenario can be predicted based on choosing the minimum average percentages of hourly space heating/cooling energy consumption, daily indoor CO_2 concentration and hourly relative humidity (RH) with acceptable levels of ASHRAE Standards 90.1, 62.1 and 160, respectively. While in the single model method, there is no connection mechanism between EnergyPlus, CONTAM and WUFI by exchanging control variables. The airflows, temperatures and heating/cooling flows input data are used to single models independently by the user's definition. Therefore, in the single model method, for different scenarios, there is no potential to minimize the percentage differences of simulated results of energy, indoor air quality and moisture performance measures with an acceptable level of ASHRAE Standards 90.1, 62.1 and 160, respectively. The results simulated by the single model's method for each scenario are calculated based on the initial assumptions, and it is not possible to change the control variables with the iteration approach until the ASHRAE Standard criteria are satisfied in a combined loop. Also, the optimal scenarios in a single model's method models are predicted independently.

The limitation considered in this research for the combined model is that the variety of selected scenarios is only limited to the selection of the envelope for the case of a three-story house with values of effective leakage areas of 0.04 m^2 or 0.3 m^2 and exhaust fan with an airflow rate of 24 L/s in two positions of "on or off". This limitation for the combined model has led to predict the different optimal scenarios for each field of energy, indoor air quality and moisture performance criteria a combined model. But in this combined model with continuous iterations of different airflows input data variable values and creation of various scenarios based on the other building performance elements such as replacement of old active and passive systems with high-performance technologies, such as insulation, installation of double-glazed windows, high-performance HVAC systems with high-performance filters, renewable energy systems like solar systems and geothermal systems, etc., can increase the variety of the

proposed scenarios so that it can be predicted the unique optimized scenario for the whole energy, indoor air quality, and moisture performance criteria. These practical goals can be proposed in future research works.

Given that the results of this analysis have been performed in three different climatic conditions of Montreal, Vancouver and Miami, it can be concluded that the fully combined model using the co-simulation method based on the combination mechanism of EnergyPlus, CONTAM and WUFI can be used as a benchmark for energy efficiency, indoor air quality and moisture performance areas. So, this fully combined model can replace the existing single models for all different climate situations with realistic results.

LIST OF BIBLIOGRAPHICAL REFERENCES

Abdalla, T. e., & Chengzhi, P. (2021). Evaluation of housing stock indoor air quality models: A review of data requirements and model performance. *Journal of Building Engineering*, 102846.

Adams, E., Sgamboti, C., Sherber, M., & Thompson, J. (1993). Simulations of indoor air quality and comfort in multi-zone buildings. *Proceedings of the Indoor Air, Helsinki, Finland*, 4-8.

Adesanya, M. A., Na, W.-H., Rabiu, A., Ogunlowo, Q. O., Akpenpuun, T. D., Rasheed, A., . . . Lee, H.-W. (2022). TRNSYS Simulation and Experimental Validation of Internal Temperature and Heating Demand in a Glass Greenhouse. *Sustainability, 14*(14), 8283. Retrieved from https://www.mdpi.com/2071-1050/14/14/8283

Ahmed, T., Kumar, P., & Mottet, L. (2021). Natural ventilation in warm climates: The challenges of thermal comfort, heatwave resilience and indoor air quality. *Renewable and Sustainable Energy Reviews, 138*, 110669.

Alonso, M. J., Dols, W. S., & Mathisen, H. (2022). Using Co-simulation between EnergyPlus and CONTAM to evaluate recirculation-based, demand-controlled ventilation strategies in an office building. *Building and environment, 211*, 108737.

Amani, N., Sabamehr, A., & Palmero Iglesias, L. M. (2022). Review on Energy Efficiency using the Ecotect Simulation Software for Residential Building Sector. *Iranian (Iranica) Journal of Energy & Environment, 13*(3), 284-294.

Angel, W. L. (2012). *HVAC design sourcebook*. McGraw-Hill.

Ansari, A., & Patil, K. (2021). Calibration of EnergyPlus Building Simulation Model Using Existing Field Measurements. *Journal of Architectural Engineering, 27*(4), 06021004.

Antretter, F., Künzel, H., Winkler, M., Pazold, M., Radon, J., Kokolsky, C., & Stadler, S. (2018). WUFI®Plus, Fundamentals.

Ardente, F., Beccali, M., Cellura, M., & Mistretta, M. (2011). Energy and environmental benefits in public buildings as a result of retrofit actions. *Renewable and Sustainable Energy Reviews, 15*(1), 460-470.

ASHRAE. (2016a). *ANSI/ASHRAE Standard 160*. 1791 Tullie Circle NE, Atlanta, GA 30329, United States.

ASHRAE. (2016b). *Standard 62.2. Ventilation and Acceptable Indoor Air Quality in Residential Buildings (ANSI Approved)*. American Society of Heating, Refrigerating, and Air-Conditioning Engineers: Atlanta, GA, USA.

ASHRAE. (2017a). *ANSI/ASHRAE Standard 55*. 1791 Tullie Circle NE, Atlanta, GA 30329, United States.

ASHRAE. (2017b). *Fundamentals Handbook. American Society of Heating, Refrigerating, and Air-Conditioning Engineers*.

ASHRAE. (2019a). *ANSI/ASHRAE Standard 62.1*. 1791 Tullie Circle NE, Atlanta, GA 30329, United States.

ASHRAE. (2019b). *ANSI/ASHRAE/IES Standard 90.1*. 1791 Tullie Circle NE, Atlanta, GA 30329, United States.

Asphaug, S. K., Andenæs, E., Geving, S., Time, B., & Kvande, T. (2022). Moisture-resilient performance of concrete basement walls–Numerical simulations of the effect of outward drying. *Building and environment, 222*, 109393.

Attia, S. (2011). State of the art of existing early design simulation tools for net zero energy buildings: a comparison of ten tools.

Badura, A., Martina, I., & Müller, B. (2022). Adaptive Envelopes for Better Energy Efficiency and Enhanced Indoor Thermal Comfort. Dans *CLIMA 2022 conference*.

Bahadori-Jahromi, A., Salem, R., Mylona, A., Hasan, A. U., & Zhang, H. (2022). The Effect of Occupants’ Behavior on the Building Performance Gap: UK Residential Case Studies. *Sustainability, 14*(3), 1362. Retrieved from https://www.mdpi.com/2071-1050/14/3/1362

Bahramian, F., Akbari, A., Nabavi, M., Esfandi, S., Naeiji, E., & Issakhov, A. (2021). Design and tri-objective optimization of an energy plant integrated with near-zero energy building including energy storage: An application of dynamic simulation. *Sustainable Energy Technologies and Assessments, 47*, 101419.

Bai, Z., Wang, Z., Zhu, T., & Zhang, J. J. (2003). Developing indoor air quality related standards in China. *Journal of Asian Architecture and Building Engineering, 2*(1), 55-60.

Balci, O. (1998). Verification, validation, and testing. *Handbook of simulation, 10*(8), 335-393.

Banfill, P. (2021). Hygrothermal simulation of building performance: data for Scottish masonry materials. *Materials and Structures, 54*(4), 1-20.

Barbosa, R. M., & Mendes, N. (2008). Combined simulation of central HVAC systems with a whole-building hygrothermal model. *Energy and Buildings, 40*(3), 276-288.

Berger, J., Guernouti, S., Woloszyn, M., & Buhe, C. (2015). Factors governing the development of moisture disorders for integration into building performance simulation. *Journal of Building Engineering, 3*, 1-15.

Blomsterberg, A., Carlsson, T., & Svensson, C. (1996). Multi-zone calculations and measurements of air flows in dwellings. Dans *DOCUMENT-AIR INFILTRATION CENTRE AIC PROC* (pp. 429-444).

Borkowska, A. (2021). *Influence of the amount of fresh air supplied by the mechanical ventilation system on the indoor air quality in the room* (Zakład Klimatyzacji i Ogrzewnictwa).

Brambilla, A., & Sangiorgio, A. (2020). Mold growth in energy efficient buildings: Causes, health implications and strategies to mitigate the risk. *Renewable and Sustainable Energy Reviews, 132*, 110093.

Brambley, M. R., Haves, P., McDonald, S. C., Torcellini, P., Hansen, D. G., Holmberg, D., & Roth, K. (2005). *Advanced sensors and controls for building applications: Market assessment and potential R&D pathways*. Pacific Northwest National Lab.(PNNL), Richland, WA (United States).

Brito, J., Silva, J., Teixeira, J., & Teixeira, S. (2021). Energy Performance of a Service Building: Comparison Between EnergyPlus and TRACE700. Dans *International Conference on Computational Science and Its Applications* (pp. 364-375). Springer.

Burhenne, S., Radon, J., Pazold, M., Herkel, S., & Antretter, F. (2011). Integration of HVAC models into a hygrothermal whole building simulation tool. Dans *Proceedings of Building Simulation 2011: 12th Conference of International Building Performance Simulation Association, Sydney, Australia*.

Burhenne, S., Wystrcil, D., Elci, M., Narmsara, S., & Herkel, S. (2013). Building performance simulation using Modelica: Analysis of the current state and application areas. Dans *13th International Conference of the International Building Performance Simulation Association*.

Cai, W., Wu, Y., Zhong, Y., & Ren, H. (2009). China building energy consumption: situation, challenges and corresponding measures. *Energy policy, 37*(6), 2054-2059.

Canada, E. C. C. (2018). *Canadian Environmental Sustainability Indicators Air quality*. Retrieved from

https://www.canada.ca/content/dam/eccc/documents/pdf/cesindicators/air-quality/air-quality-en.pdf

Cao, Z., Yang, Y., Lu, J., & Zhang, C. (2011). Atmospheric particle characterization, distribution, and deposition in Xi'an, Shaanxi Province, Central China. *Environmental Pollution, 159*(2), 577-584.

Chan, W. R., Price, P. N., Sohn, M. D., & Gadgil, A. J. (2003a). Analysis of US residential air leakage database. *Lawrence Berkeley National Laboratory*. Retrieved from https://escholarship.org/content/qt6pk6r4gs/qt6pk6r4gs.pdf

Chan, W. R., Price, P. N., Sohn, M. D., & Gadgil, A. J. (2003b). *Analysis of US residential air leakage database*. Lawrence Berkeley National Lab.(LBNL), Berkeley, CA (United States).

Chang, S. J., Kang, Y., Wi, S., Jeong, S.-G., & Kim, S. (2017). Hygrothermal performance improvement of the Korean wood frame walls using macro-packed phase change materials (MPPCM). *Applied Thermal Engineering, 114*, 457-465.

Chang, S. J., Wi, S., Kang, S. G., & Kim, S. (2020). Moisture risk assessment of cross-laminated timber walls: Perspectives on climate conditions and water vapor resistance performance of building materials. *Building and environment, 168*, 106502.

Chen, L., Zheng, X., Yang, J., & Yoon, J. H. (2021). Impact of BIPV windows on building energy consumption in street canyons: Model development and validation. *Energy and Buildings, 249*, 111207.

Chen, Q. (2009). Ventilation performance prediction for buildings: A method overview and recent applications. *Building and environment, 44*(4), 848-858.

Chen, Y., Gu, L., & Zhang, J. (2015). EnergyPlus and CHAMPS-Multizone co-simulation for energy and indoor air quality analysis. Dans *Building Simulation* (Vol. 8, pp. 371-380). Springer.

Chidiac, S., Catania, E., Morofsky, E., & Foo, S. (2011). Effectiveness of single and multiple energy retrofit measures on the energy consumption of office buildings. *Energy, 36*(8), 5037-5052.

Cho, H., Cabrera, D., Sardy, S., Kilchherr, R., Yilmaz, S., & Patel, M. K. (2021). Evaluation of performance of energy efficient hybrid ventilation system and analysis of occupants' behavior to control windows. *Building and environment, 188*, 107434.

Chung, D., Wen, J., & Lo, L. J. (2020). Development and verification of the open source platform, HAM-Tools, for hygrothermal performance simulation of buildings using a stochastic approach. Dans *Building simulation* (Vol. 13, pp. 497-514). Springer.

Clark, J. D., Walker, I. S., Less, B. D., Dutton, S. M., Li, X., & Sherman, M. H. (2019). Energy Savings Estimates for Occupancy and Temperature-based Smart Ventilation Control Approaches in Single-family California Homes. *ASHRAE Transactions, 125*.

Clarke, J. (2007). *Energy simulation in building design*. Routledge.

ClimaTemps.com. (2019). Retrieved from Average Weather and Climate guide with graphs and analysis of average temperatures, rainfall, sunlight hours, relative humidity, windspeeds etc. (climatemps.com)

Contam3DExport (Version 3.4.0.0). (2020). 100 Bureau Drive, Gaithersburg, MD 20899, 301-975-2000: National Institute of Standards and Technology (NIST).

CONTAM 3.2 (Version Ver. 3.2.0.2). (2016). United States: National Institute of Standards and Technology Engineering Laboratory.

CONTAM 3.2. (2021). National Institute of Standards and Technology (NIST). Retrieved from https://www.nist.gov/el/energy-and-environment-division-73200/nist-multizone-modeling/download-contam

CONTAM Utilities - CONTAM Weather File Creator (Version Version: 1.1). (2014): National Institute of Standards and Technology (NIST). Retrieved from https://pages.nist.gov/CONTAM-apps/software/WEATHERprogram.htm

Cornick, S., Maref, W., Abdulghani, K., & van Reenen, D. (2003). 1-D hygIRC: a simulation tool for modeling heat, air and moisture movement in exterior walls. *National Research Council, Kanada, NRCC-46896*.

Cornick, S., Maref, W., & Tariku, F. (2009). Verification and validation: establishing confidence in hygrothermal tools.

Costanzo, V., & Donn, M. (2017). Thermal and visual comfort assessment of natural ventilated office buildings in Europe and North America. *Energy and Buildings, 140*, 210-223.

Craig, D., Richard, S., & Gniffin, B. Finding System-Required Airflow. Repéré le Jan 27 à https://www.contractingbusiness.com/archive/article/20863033/finding-systemrequired-airflow

Crawley, D. B., Hand, J. W., Kummert, M., & Griffith, B. T. (2008). Contrasting the capabilities of building energy performance simulation programs. *Building and environment, 43*(4), 661-673.

Crawley, D. B., Lawrie, L. K., Winkelmann, F. C., Buhl, W. F., Huang, Y. J., Pedersen, C. O., . . . Witte, M. J. (2001). EnergyPlus: creating a new-generation building energy simulation program. *Energy and Buildings, 33*(4), 319-331.

D'Amico, A., Pini, A., Zazzini, S., D'Alessandro, D., Leuzzi, G., & Currà, E. (2021). Modelling VOC emissions from building materials for healthy building design. *Sustainability, 13*(1), 184.

Dassault Systèmes AB. (2016). Dymola. *Dynamic Modeling Laboratory. Dymola Release notes, Lund, Sweden*.

Defo, M., Lacasse, M., & Laouadi, A. (2022). A comparison of hygrothermal simulation results derived from four simulation tools. *Journal of Building Physics, 45*(4), 432-456.

Delgado, J., Ramos, N. M., Barreira, E., & De Freitas, V. P. (2010). A critical review of hygrothermal models used in porous building materials. *Journal of Porous Media, 13*(3).

Details:Physics-Wufiwiki. (2020). Retrieved from https://www.wufi-wiki.com/mediawiki/index.php/Details:Physics

Ding, C., & Zhou, N. (2020). Using residential and office building archetypes for energy efficiency building solutions in an urban scale: A China case study. *Energies, 13*(12), 3210.

Division of Air Resource Management, F. D. o. E. P. 2019 Design Values for Fine Particulate Matter, PM2.5. Retrieved from https://floridadep.gov/sites/default/files/2019-PM2.5%20Design%20Values-Update.pdf

Dols, W. S. (2001). A tool for modeling airflow & contaminant transport. *ASHRAE Journal, 43*(3), 35-43.

Dols, W. S., Dols, W. S., & Polidoro, B. J. (2015). CONTAM User Guide and Program Documentation: Version 3.2.

Dols, W. S., Emmerich, S. J., & Polidoro, B. J. (2016). Coupling the multizone airflow and contaminant transport software CONTAM with EnergyPlus using co-simulation. Dans *Building simulation* (Vol. 9, pp. 469-479). Springer.

Dols, W. S., Milando, C. W., Ng, L., Emmerich, S. J., & Teo, J. (2021). On the Benefits of Whole-building IAQ, Ventilation, Infiltration, and Energy Analysis Using Co-

simulation between CONTAM and EnergyPlus. Dans *Journal of Physics: Conference Series* (Vol. 2069, pp. 012183). IOP Publishing.

Dols, W. S., & Underhill, L. J. (2018). *Cross-platform, Public Domain Simulation Tools for Performing Parametric IAQ and Energy Analysis* (National Institute of Standards and Technology).

Doty, S. (2009). Building Operations: Balancing Energy Efficiency with Indoor Air Quality. *Energy Engineering, 106*(4), 31-52.

Du, C., Li, B., & Yu, W. (2021). Indoor mold exposure: characteristics, influences and corresponding associations with built environment—a review. *Journal of Building Engineering, 35*, 101983.

e Silva, A. C. P. S., & Calili, R. F. (2021). New building simulation method to measure the impact of window-integrated organic photovoltaic cells on energy demand. *Energy and Buildings, 252*, 111490.

Elbayoumi, M., Ramli, N. A., Yusof, N. F. F. M., Yahaya, A. S. B., Al Madhoun, W., & Ul-Saufie, A. Z. (2014). Multivariate methods for indoor PM10 and PM2. 5 modelling in naturally ventilated schools buildings. *Atmospheric Environment, 94*, 11-21.

Elzafraney, M., Soroushian, P., & Deru, M. (2005). Development of energy-efficient concrete buildings using recycled plastic aggregates. *Journal of Architectural Engineering, 11*(4), 122-130.

Emil, F., & Diab, A. (2021). Energy rationalization for an educational building in Egypt: Towards a zero energy building. *Journal of Building Engineering, 44*, 103247.

Emmerich, S. J. (2001). Validation of multizone IAQ modeling of residential-scale buildings: a review. *Transactions-American Society of Heating Refrigerating and Air Conditioning Engineers, 107*(2), 619-628.

Emmerich, S. J., Howard-Reed, C., & Gupte, A. (2005). *Modeling the IAQ impact of HHI interventions in inner-city housing*. US Department of Commerce, National Institute of Standards and Technology.

EnergyPlus. (2020). Weather Data Sources. Retrieved from https://energyplus.net/weather

EnergyPlus. (2021). 9.5. 0. *US Department of Energy's (DOE) Building Technologies Office (BTO): Washington, DC, USA*.

Fan, Y., & Ito, K. (2014). Optimization of indoor environmental quality and ventilation load in office space by multilevel coupling of building energy simulation and

computational fluid dynamics. Dans *Building Simulation* (Vol. 7, pp. 649-659). Springer.

Fanger, P. O. (1970). Thermal comfort. Analysis and applications in environmental engineering. *Thermal comfort. Analysis and applications in environmental engineering.*

Fayad, F. A., Maref, W., & Awad, M. M. (2021). Review of white roofing materials and emerging economies with focus on energy performance cost-benefit, maintenance, and consumer indifference. *Sustainability, 13*(17), 9967.

Federal, R. (2008). Agenda for Net-Zero Energy, High-Performance Green Buildings: National Science and Technology Council, October.

Fedorik, F., Alitalo, S., Savolainen, J.-P., Räinä, I., & Illikainen, K. (2021). Analysis of hygrothermal performance of low-energy house in Nordic climate. *Journal of Building Physics*, 1744259120984187. doi: 10.1177/1744259120984187. Retrieved from https://doi.org/10.1177/1744259120984187

Fedorik, F., Malaska, M., Hannila, R., & Haapala, A. (2015). Improving the thermal performance of concrete-sandwich envelopes in relation to the moisture behavior of building structures in boreal conditions. *Energy and Buildings, 107*, 226-233.

Feijó-Muñoz, J., Poza-Casado, I., González-Lezcano, R. A., Pardal, C., Echarri, V., Assiego de Larriva, R., . . . José, V. (2018). Methodology for the study of the envelope airtightness of residential buildings in Spain: A case study. *Energies, 11*(4), 704.

Feng, G., Wang, G., Li, Q., Zhang, Y., & Li, H. (2022). Investigation of a solar heating system assisted by coupling with electromagnetic heating unit and phase change energy storage tank: Towards sustainable rural buildings in northern China. *Sustainable Cities and Society, 80*, 103449. doi: https://doi.org/10.1016/j.scs.2021.103449. Retrieved from https://www.sciencedirect.com/science/article/pii/S2210670721007228

Ferdyn-Grygierek, J., Grygierek, K., Gumińska, A., Krawiec, P., Oćwieja, A., Poloczek, R., . . . Żukowska-Tejsen, D. (2021). Passive Cooling Solutions to Improve Thermal Comfort in Polish Dwellings. *Energies, 14*(12), 3648.

Feustel, H. E. (1999). COMIS—an international multizone air-flow and contaminant transport model. *Energy and Buildings, 30*(1), 3-18. doi: https://doi.org/10.1016/S0378-7788(98)00043-7. Retrieved from https://www.sciencedirect.com/science/article/pii/S0378778898000437

Feustel, H. E., & Dieris, J. (1992). A survey of airflow models for multizone structures. *Energy and Buildings, 18*(2), 79-100.

Fine, J. P., & Touchie, M. F. (2021). Evaluating ventilation system retrofits for high-rise residential buildings using a CONTAM model. *Building and environment, 205*, 108292.

Freire, R. Z., Abadie, M. O., & Mendes, N. (2009). Integration of natural ventilation models in the hygrothermal and energy simulation program PowerDomus. Dans *Proceedings of the 11th international building performance simulation association conference* (pp. 1037-1044).

Fu, H., Ding, Y., Li, M., Cao, Y., Xie, W., & Wang, Z. (2021). Research and simulation analysis of thermal performance and hygrothermal behavior of timber-framed walls with different external thermal insulation layer: Cork board and anticorrosive pine plate. *Journal of Building Physics, 45*(2), 180-208.

Fumo, N., Mago, P., & Luck, R. (2010). Methodology to estimate building energy consumption using EnergyPlus Benchmark Models. *Energy and Buildings, 42*(12), 2331-2337.

Gan, V. J., Wang, B., Chan, C. M., Weerasuriya, A. U., & Cheng, J. C. (2022). Physics-based, data-driven approach for predicting natural ventilation of residential high-rise buildings. Dans *Building Simulation* (Vol. 15, pp. 129-148). Springer.

Gao, N., Zhang, H., & Niu, J. (2007). Investigating indoor air quality and thermal comfort using a numerical thermal manikin. *Indoor and built environment, 16*(1), 7-17.

Ghazaryan, T., & Tariku, F. (2021). Hygrothermal performance assessment of split insulated cork wall assemblies under various moisture load conditions. Dans *Journal of Physics: Conference Series* (Vol. 2069, pp. 012031). IOP Publishing.

Gholami, M., Barbaresi, A., Tassinari, P., Bovo, M., & Torreggiani, D. (2020). A comparison of energy and thermal performance of rooftop greenhouses and green roofs in mediterranean climate: A hygrothermal assessment in wufi. *Energies, 13*(8), 2030.

Golić, K., Kosorić, V., & Furundžić, A. K. (2011). General model of solar water heating system integration in residential building refurbishment—Potential energy savings and environmental impact. *Renewable and Sustainable Energy Reviews, 15*(3), 1533-1544. doi: https://doi.org/10.1016/j.rser.2010.11.052. Retrieved from https://www.sciencedirect.com/science/article/pii/S1364032110004211

Gowri, K., Winiarski, D. W., & Jarnagin, R. E. (2009). *Infiltration modeling guidelines for commercial building energy analysis*. Pacific Northwest National Lab.(PNNL), Richland, WA (United States).

Grillone, B., Mor, G., Danov, S., Cipriano, J., & Sumper, A. (2021). A data-driven methodology for enhanced measurement and verification of energy efficiency savings in commercial buildings. *Applied Energy, 301*, 117502.

Grubler, A., Wilson, C., Bento, N., Boza-Kiss, B., Krey, V., McCollum, D. L., . . . De Stercke, S. (2018). A low energy demand scenario for meeting the 1.5 C target and sustainable development goals without negative emission technologies. *Nature energy, 3*(6), 515-527.

Haghighat, F., Donnini, G., & D'Addario, R. (1992). Relationship between occupant discomfort as perceived and as measured objectively. *Indoor Environment, 1*(2), 112-118.

Haghighat, F., & Megri, A. C. (1996). A comprehensive validation of two airflow models—COMIS and CONTAM. *Indoor Air, 6*(4), 278-288.

Haghighat, F., & Rao, J. (1991). Computer-aided building ventilation system design—a system-theoretic approach. *Energy and Buildings, 17*(2), 147-155.

He, L. (2021). A Review: Green Roof Based on the Waterfront in Hot Summer as Well as Cold Winter Zone Via Energyplus. *Available at SSRN 3917468*.

Heibati, S., Maref, W., & Saber, H. H. (2019). Assessing the energy and indoor air quality performance for a three-story building using an integrated model, part one: the need for integration. *Energies, 12*(24), 4775.

Heibati, S., Maref, W., & Saber, H. H. (2021a). Assessing the Energy, Indoor Air Quality, and Moisture Performance for a Three-Story Building Using an Integrated Model, Part Three: Development of Integrated Model and Applications. *Energies, 14*(18), 5648.

Heibati, S., Maref, W., & Saber, H. H. (2021b). Assessing the Energy, Indoor Air Quality, and Moisture Performance for a Three-Story Building Using an Integrated Model, Part Two: Integrating the Indoor Air Quality, Moisture, and Thermal Comfort. *Energies, 14*(16), 4915. Retrieved from https://www.mdpi.com/1996-1073/14/16/4915

Heibati, S., Maref, W., & Saber, H. H. (2021c). Developing a model for predicting optimum daily tilt angle of a PV solar system at different geometric, physical and dynamic parameters. *Advances in Building Energy Research, 15*(2), 179-198.

Heibati, S. M., & Atabi, F. (2013). Integrated dynamic modeling for energy optimization in the building: Part 2: An application of the model to analysis of XYZ building. *Journal of Building Physics, 37*(2), 153-169.

Heibati, S. M., Atabi, F., Khalajiassadi, M., & Emamzadeh, A. (2013). Integrated dynamic modeling for energy optimization in the building: Part 1: The development of the model. *Journal of Building Physics, 37*(1), 28-54.

Hejazi, B., Sakiyama, N. R., Frick, J., & Garrecht, H. (2019). Hygrothermal simulations comparative study: assessment of different materials using WUFI and DELPHIN software. Dans *Proceedings of the 16th IBPSA International Conference, Rome, Italy* (pp. 2-4).

Hestnes, A. G., & Kofoed, N. U. (2002). Effective retrofitting scenarios for energy efficiency and comfort: results of the design and evaluation activities within the OFFICE project. *Building and environment, 37*(6), 569-574.

Ho, D. X., Kim, K.-H., Ryeul Sohn, J., Hee Oh, Y., & Ahn, J.-W. (2011). Emission rates of volatile organic compounds released from newly produced household furniture products using a large-scale chamber testing method. *TheScientificWorldJournal, 11*.

Howard-Reed, C., Wallace, L. A., & Emmerich, S. J. (2003). Effect of ventilation systems and air filters on decay rates of particles produced by indoor sources in an occupied townhouse. *Atmospheric Environment, 37*(38), 5295-5306.

Hunter-Sellars, E., Tee, J., Parkin, I. P., & Williams, D. R. (2020). Adsorption of volatile organic compounds by industrial porous materials: Impact of relative humidity. *Microporous and Mesoporous Materials, 298*, 110090.

IBM SPSS Statistics. (2021). 1 New Orchard Road, Armonk, New York 10504-1722, United States. doi: https://www.ibm.com/account/reg/us-en/signup?formid=urx-19774. Retrieved from https://www.ibm.com/account/reg/us-en/signup?formid=urx-19774

Ibrahim, M., Sayegh, H., Bianco, L., & Wurtz, E. (2019). Hygrothermal performance of novel internal and external super-insulating systems: In-situ experimental study and 1D/2D numerical modeling. *Applied Thermal Engineering, 150*, 1306-1327.

IEA. (2021). *World Energy Model Documentation*. Retrieved from https://iea.blob.core.windows.net/assets/8971c3c8-2664-4578-89ce-3166bc98c2e4/WEM_Documentation_WEO2021.pdf

Iwaro, J., & Mwasha, A. (2010). A review of building energy regulation and policy for energy conservation in developing countries. *Energy policy, 38*(12), 7744-7755.

Jain, N., Burman, E., Robertson, C., Stamp, S., Shrubsole, C., Aletta, F., . . . Raynham, P. (2020). Building performance evaluation: Balancing energy and indoor environmental quality in a UK school building. *Building Services Engineering Research and Technology, 41*(3), 343-360.

Jiang, S. S. S., Hao, J. L., & De Carli, J. N. (2021). Hygrothermal and mechanical performance of sustainable concrete: A simulated comparison of mix designs. *Journal of Building Engineering, 34*, 101859.

Jin, Z., Wu, Y., Li, B., & Gao, Y. (2009). Energy efficiency supervision strategy selection of Chinese large-scale public buildings. *Energy policy, 37*(6), 2066-2072.

Jirgensone, B. (2022). Mitruma un siltuma pārneses modelēšana ēku norobežojošās konstrukcijās un iekštelpās.

Kang, Y., & Kim, S. (2021). Evaluation of Indoor Hygrothermal Performance with the Heat and Moisture Transport in Walls. *Available at SSRN 4047762*.

Kazemi, M., & Courard, L. (2021). Modelling hygrothermal conditions of unsaturated substrate and drainage layers for the thermal resistance assessment of green roof: Effect of coarse recycled materials. *Energy and Buildings, 250*, 111315.

Kim, Y. K., Bande, L., Tabet Aoul, K. A., & Altan, H. (2021). Dynamic Energy Performance Gap Analysis of a University Building: Case Studies at UAE University Campus, UAE. *Sustainability, 13*(1), 120. Retrieved from https://www.mdpi.com/2071-1050/13/1/120

Kleijnen, J. P. (1995). Verification and validation of simulation models. *European journal of operational research, 82*(1), 145-162.

Kolokotsa, D., Tsiavos, D., Stavrakakis, G., Kalaitzakis, K., & Antonidakis, E. (2001). Advanced fuzzy logic controllers design and evaluation for buildings' occupants thermal–visual comfort and indoor air quality satisfaction. *Energy and Buildings, 33*(6), 531-543.

Künzel, H. M. (1995). Simultaneous heat and moisture transport in building components. *One-and two-dimensional calculation using simple parameters. IRB-Verlag Stuttgart, 65*.

Kusiak, A. (1988). Artificial intelligence and CIM systems. *Artificial Intelligence Applications for CIM; Kusiak, A., Ed.; IFS Publications: Bedford, UK*, 1-30.

Kusuda, T. (1999). Early history and future prospects of building system simulation. Dans *Proceedings of Building Simulation* (Vol. 99, pp. 3-15).

Lacasse, M. A., Saber, H. H., Maref, W., Ganapathy, G., Plescia, S., & Parekh, A. (2016). Field evaluation of thermal and moisture response of highly insulated wood-frame walls. Dans *The 13th International Conference on Thermal Performance of the Exterior Envelopes of Whole, Buildings XIII, held in Clearwater, Florida, USA*.

Le, A. D. T., Zhang, J. S., Liu, Z., Samri, D., & Langlet, T. (2020). Modeling the similarity and the potential of toluene and moisture buffering capacities of hemp concrete on IAQ and thermal comfort. *Building and environment*, 107455.

Lengsfeld, K., & Holm, A. (2007). Development and validation of the hygrothermal indoor climate simulation software WUFI {sup registered}-Plus; Entwicklung und Validierung einer hygrothermischen Raumklima-Simulationssoftware WUFI {sup registered}-Plus. *Bauphysik, 29*.

Li, B., & Yao, R. (2009). Urbanisation and its impact on building energy consumption and efficiency in China. *Renewable Energy, 34*(9), 1994-1998.

Li, H. (2002). *Validation of three multi-zone airflow models* (Concordia University).

Libralato, M., De Angelis, A., Tornello, G., Saro, O., D'Agaro, P., & Cortella, G. (2021). Evaluation of Multiyear Weather Data Effects on Hygrothermal Building Energy Simulations Using WUFI Plus. *Energies, 14*(21), 7157.

Lim, H., Seo, J., Song, D., Yoon, S., & Kim, J. (2020). Interaction analysis of countermeasures for the stack effect in a high-rise office building. *Building and environment, 168*, 106530.

Liu, M., Wittchen, K. B., & Heiselberg, P. K. (2014). Development of a simplified method for intelligent glazed façade design under different control strategies and verified by building simulation tool BSim. *Building and environment, 74*, 31-38. doi: https://doi.org/10.1016/j.buildenv.2014.01.003. Retrieved from https://www.sciencedirect.com/science/article/pii/S0360132314000067

Lv, Y., Liang, J., Wang, B., Zhang, X., Yuan, W., Li, Y., & Xie, J. (2020). Effect of heat and moisture transfer on the growth of mold on the inner surface of walls: A case study in Dalian of China. Dans *Building Simulation* (Vol. 13, pp. 1269-1279). Springer.

Ma, N., Aviv, D., Guo, H., & Braham, W. W. (2021). Measuring the right factors: A review of variables and models for thermal comfort and indoor air quality. *Renewable and Sustainable Energy Reviews, 135*, 110436.

Ma, R., Wang, T., Wang, Y., & Chen, J. (2021). Tuning urban microclimate: A morpho-patch approach for multi-scale building group energy simulation. *Sustainable Cities and Society*, 103516.

Maref, W., Lacasse, M., & Rousseau, M. (2006). Experimental Tests To Assess Hygrothermal Performance of Building Envelope Systems. *3rd International Building Physics Conference, August 27-31*. (IRC-ORAL-740)

Maref, W., & Lacasse, M. (2010). Drying response of wood-frame construction: Laboratory and modeling. ASTM International.

Maref, W., Lacasse, M.A., "Drying response of wood-frame construction: laboratory and modelling," Journal of ASTM International (JAI), 7, (1), Second Symposium on Heat-Air-Moisture Transport: Measurements and Implications in Buildings (Vancouver, B.C., April 19, 2009), pp. 1-12, January 1, 2010 (Paper ID JAI2102067) (NRCC-53231)

Maref, W., Booth, D. G., Lacasse, M., & Nicholls, M. (2002). Drying Experiment of Wood-Frame Wall Assemblies Performed in the Climatic Chamber EEEF, NRC, Institute for Research in Construction. Research Report, pp. 42, October 18, 2002 (RR-105).

Maref, W., Cornick, S., Abdulghani, K., & van Reenen, D. (2004). An Advanced hygrothermal design tool 1-D hygIRC. Proceedings of eSim 2004, 10-11. (Vancouver, B.C., 2004-06-09), pp. 1-6, (NRCC-46902)

Maref, W., Lacasse, M., & Booth, D. (2004). Large-scale laboratory measurements and benchmarking of an advanced hygrothermal model. NRC, Institute for Research in Construction*., NRCC-46784*.

Maref, W., Lacasse, M., Kumaran, M. K., & Swinton, M. C. (2002). Benchmarking of the advanced hygrothermal model hyg*I*rc with mid scale experiments. Proceedings of eSim 2002, September 11th - 13th, 2002 (Montreal-University of Concordia) pp. 171-176, October 01, 2002 (NRCC-43970).

Maref, W., Lacasse, M. A., & Booth, D. (2002). *Benchmarking of IRC's Advanced Hygrothermal Model-hygIRC Using Mid-and Large-scale Experiments*. NRC, Institute for Research in Construction. Technical Report, T7-09.

Maref, W., Lacasse, M. A., & Krouglicof, N. (2001). A Precision weighing system for helping assess the hygrothermal response of full-scale wall assemblies. Proceedings of Performance of Exterior Envelopes of whole Building VIII- Integration of Building Envelopes, December 2-6, 2001, Clearwater Beach, FL (USA).

Maref, W., Van Den Bossche, N., Armstrong, M., Lacasse, M., Elmahdy, H., & Glazer, R. (2011). Laboratory tests of window-wall interface details to evaluate the risk of condensation on windows. Journal of Testing and Evaluation, 39(4), 562-575.

Maref, W., Van Den Bossche, N., Armstrong, M., Lacasse, M., Elmahdy, H., & Glazer, R. (2012). Condensation risk assessment on box windows: the effect of the window–wall interface. Journal of Building Physics, 36(1), 35-56.

Maref, W., Tariku, F., Di Lenardo, B., & Gatland, S. (2009). Hygrothermal performance of exterior wall systems using an innovative vapor retarder in Canadian climate. Dans 4th International Building Physics Conference, Istanbul, Turkey, June. 15 (Vol. 18).

Mckeen, P., & Liao, Z. (2021). The influence of airtightness on contaminant spread in MURBs in cold climates. Dans Building Simulation (pp. 1-16). Springer.

McPherson-Hathaway, B. (2021). COMPARING BEOPT (EnergyPlus) ENERGY PREDICTIONS TO MEASURED CIRCUIT LEVEL ENERGY CONSUMPTION OF 12 SIMILAR SMALL ENERGY-EFFICIENT SINGLE-FAMILY RESIDENCES.

Megahed, N. A., & Ghoneim, E. M. (2021). Indoor Air Quality: Rethinking rules of building design strategies in post-pandemic architecture. Environmental Research, 193, 110471. doi: https://doi.org/10.1016/j.envres.2020.110471. Retrieved from https://www.sciencedirect.com/science/article/pii/S0013935120313682

Meklin, T., Hyvärinen, A., Toivola, M., Reponen, T., Koponen, V., Husman, T., . . . Nevalainen, A. (2003). Effect of building frame and moisture damage on microbiological indoor air quality in school buildings. Aiha Journal, 64(1), 108-116.

Mendes, N., Winkelmann, F., Lamberts, R., & Philippi, P. C. (2003). Moisture effects on conduction loads. Energy and Buildings, 35(7), 631-644.

Miami, Florida Climate & Temperature. (2021). Retrieved from http://www.miami.climatemps.com/index.php

Michael Bluejay, I. (2022). Methods of sizing HVAC equipment. Retrieved from https://michaelbluejay.com/electricity/hvac-sizing.html

MODELICA. (2017). Functional Mock-up Interface for Co-Simulation. MODELICA Association Project FMI.

Mokhtari, R., & Jahangir, M. H. (2021). The effect of occupant distribution on energy consumption and COVID-19 infection in buildings: A case study of university building. Building and environment, 190, 107561.

Montreal, Quebec Climate & Temperature (2021). Retrieved from http://www.montreal.climatemps.com/index.php

Moon, H. J. (2005). Assessing mold risks in buildings under uncertainty. Georgia Institute of Technology.

Moon, H. J., Ryu, S. H., & Kim, J. T. (2014). The effect of moisture transportation on energy efficiency and IAQ in residential buildings. Energy and Buildings, 75, 439-446.

Morton, J., Pyo, C., & Choi, B. (1992). Interfacing computer-assisted drafting and design with the building loads analysis and system thermodynamics (BLAST) program. Final report. Army Construction Engineering Research Lab., Champaign, IL (United States).

Moschetti, R., & Carlucci, S. (2017). The impact of design ventilation rates on the indoor air quality in residential buildings: an Italian case study. Indoor and built environment, 26(10), 1397-1419.

Motherway, B. (2017). Energy Efficiency 2017. OEVD/IEA.

Moujalled, B., Aït Oumériane, Y., Moissette, S., Bart, M., Lanos, C., & Samri, D. (2018). Experimental and numerical evaluation of the hygrothermal performance of a hemp lime concrete building: A long term case study. Building and environment, 136, 11-27. doi: https://doi.org/10.1016/j.buildenv.2018.03.025. Retrieved from http://www.sciencedirect.com/science/article/pii/S0360132318301549

Muhammad, A., & Karinka, S. (2022). Comparative energy analysis of a laboratory building with different materials using eQUEST simulation software. Materials Today: Proceedings, 52, 2160-2165. doi: https://doi.org/10.1016/j.matpr.2022.01.187. Retrieved from https://www.sciencedirect.com/science/article/pii/S2214785322002206

Mundt-Petersen, S. O., & Harderup, L.-E. (2015). Predicting hygrothermal performance in cold roofs using a 1D transient heat and moisture calculation tool. Building and environment, 90, 215-231.

Myatt, T. (2015). Volatile organic compounds in the home: sources, health implications, and solutions: HONEYWELL.

Nadeem, T. B., Ahmed, A., Naqvi, A. A., Saad, M., Abbasi, A. A., Arshad, S. M. U., & Ahmed, F. (2022). Designing of Heating, Ventilation, and Air Conditioning (HVAC) System for Workshop Building in Hot and Humid Climatic Zone Using CLTD Method and HAP Analysis: A Comparison. Arabian Journal for Science and Engineering, 1-23.

Neto, A. H., & Fiorelli, F. A. S. (2008). Comparison between detailed model simulation and artificial neural network for forecasting building energy consumption. Energy and Buildings, 40(12), 2169-2176.

Ng, L. C., Dols, W. S., & Emmerich, S. J. (2021). Evaluating potential benefits of air barriers in commercial buildings using NIST infiltration correlations in EnergyPlus. Building and environment, 196, 107783.

Ng, L. C., Musser, A., Persily, A. K., & Emmerich, S. J. (2013). Multizone airflow models for calculating infiltration rates in commercial reference buildings. Energy and Buildings, 58, 11-18.

Ng, L. C., Quiles, N. O., Dols, W. S., & Emmerich, S. J. (2018). Weather correlations to calculate infiltration rates for US commercial building energy models. Building and environment, 127, 47-57.

Nouidui, T., Wetter, M., & Zuo, W. (2014). Functional mock-up unit for co-simulation import in EnergyPlus. Journal of Building Performance Simulation, 7(3), 192-202.

NREL. (2019). OpenStudio Version 2.8.0. Retrieved from https://www.openstudio.net

Nusser, B., & Teibinger, M. (2012). Coupled Heat and Moisture Transfer in Building Components-Implementing WUFI Approaches in COMSOL Multiphysics. Dans Proceedings of the COMSOL Users Conference 2012 Milan.

OpenStudio (Version 3.1.0). (2021). U.S. Department of Energy, Office of Energy Efficiency and Renewable Energy: National Renewable Energy Laboratory (NREL).

Park, B., & Qi, H. (2005). Development and Evaluation of a Procedure for the Calibration of Simulation Models. Transportation Research Record, 1934(1), 208-217.

Pazold, M., Burhenne, S., Radon, J., Herkel, S., & Antretter, F. (2012). Integration of Modelica models into an existing simulation software using FMI for Co-Simulation. Dans Proceedings of the 9th International MODELICA Conference; September 3-5; 2012; Munich; Germany (pp. 949-954). Linköping University Electronic Press.

Pekdogan, T., Tokuç, A., Ezan, M. A., & Başaran, T. (2021). Experimental investigation of a decentralized heat recovery ventilation system. Journal of Building Engineering, 35, 102009.

Persily, A. K. (1998). A modeling study of ventilation, IAQ and energy impacts of residential mechanical ventilation.

Persily, A. K., & Emmerich, S. J. (2012). Indoor air quality in sustainable, energy efficient buildings. HVAC&R Research, 18(1-2), 4-20.

Plathner, P., & Ross, D. (2003). The Effect of Sorption on Airborne Moisture Movement in Dwellings. International Journal of Ventilation, 1(3), 201-208. doi: 10.1080/14733315.2003.11683635. Retrieved from https://doi.org/10.1080/14733315.2003.11683635

Plathner, P., & Woloszyn, M. (2002). Interzonal air and moisture transport in a test house: experiment and modelling. Building and environment, 37(2), 189-199.

Policy, I. E. A. D. o. S. E. (2013). Transition to sustainable buildings: strategies and opportunities to 2050. Organization for Economic.

Promis, G., Dutra, L. F., Douzane, O., Le, A. T., & Langlet, T. (2019). Temperature-dependent sorption models for mass transfer throughout bio-based building materials. Construction and Building Materials, 197, 513-525.

Provata, E., & Kolokotsa, D. ENERGY SAVING AND INDOOR AIR QUALITY IN OFFICE BUILDINGS.

Qi, D., Cheng, J., Katal, A., Wang, L., & Athienitis, A. (2020). Multizone modelling of a hybrid ventilated high-rise building based on full-scale measurements for predictive control. Indoor and built environment, 29(4), 496-507.

Rabani, M., Bayera Madessa, H., & Nord, N. (2021). Building Retrofitting through Coupling of Building Energy Simulation-Optimization Tool with CFD and Daylight Programs. Energies, 14(8), 2180.

Rahman, M., Rasul, M., & Khan, M. (2006). Buildings energy simulation using energy express: a case study on sub-tropical Central Queensland University (CQU) buildings.

Ratnasari, L. D., MT, S. S. S., & MT, E. S. S. (2020). Evaluation of energy consumption with energyplus simulation in office existing buildings. Dans AIP Conference Proceedings (Vol. 2296, pp. 020031). AIP Publishing LLC.

Reyna, J. L., & Chester, M. V. (2017). Energy efficiency to reduce residential electricity and natural gas use under climate change. Nature communications, 8(1), 1-12.

Rode, C., Grunewald, J., Liu, Z., Qin, M., & Zhang, J. (2020). Models for residential indoor pollution loads due to material emissions under dynamic temperature and humidity conditions. Dans E3S Web of Conferences (Vol. 172, pp. 11002). EDP Sciences.

Roman, N. D., Bre, F., Fachinotti, V. D., & Lamberts, R. (2020). Application and characterization of metamodels based on artificial neural networks for building performance simulation: A systematic review. Energy and Buildings, 217, 109972.

Roseme, G. (1980). Residential ventilation with heat recovery: improving indoor air quality and saving energy.

Roulet, C.-A., Fürbringer, J.-M., & Romano, B. (1996). Evaluation of the Multizone Air Flow Simulation Code COMIS.

Saber, H. H. (2022). Hygrothermal performance of cool roofs with reflective coating material subjected to hot, humid and dusty climate. Journal of Building Physics, 45(4), 457-481.

Saber, H. H., Hajiah, A. E., & Maref, W. (2020). Impact of reflective roofs on the overall energy savings of whole buildings. E3S Web Conf., 172, 25008. Retrieved from https://doi.org/10.1051/e3sconf/202017225008

Saber, H. H., Lacasse, M. A., & Moore, T. V. (2017). Hygrothermal performance assessment of stucco-clad wood frame walls having vented and ventilated drainage cavities. ASTM International.

Saber, H. H., & Maref, W. (2015). Risk of condensation and mold growth in wood-frame wall systems with different exterior insulations. Dans Building Enclosure Science & Technology Conference (BEST4 Conference), held in April (pp. 12-15).

Saber, H. H., & Maref, W. (2019). Energy Performance of Cool Roofs Followed by Development of Practical Design Tool. Frontiers in Energy Research, 7. doi: 10.3389/fenrg.2019.00122. Retrieved from https://www.frontiersin.org/article/10.3389/fenrg.2019.00122

Saber, H. H., & Maref, W. (2019). Energy performance of cool roofs followed by development of practical design tool. Frontiers in Energy Research, 122.

Saber, H. H., Maref, W., Elmahdy, H., Swinton, M. C., & Glazer, R. (2012). 3D heat and air transport model for predicting the thermal resistances of insulated wall assemblies. Journal of Building Performance Simulation, 5(2), 75-91.

Saber, H. H., Maref, W., & Hajiah, A. E. (2019). Hygrothermal Performance of Cool Roofs Subjected to Saudi Climates. Frontiers in Energy Research, 7. doi: 10.3389/fenrg.2019.00039. Retrieved from https://www.frontiersin.org/article/10.3389/fenrg.2019.00039

Saber, H. H., Maref, W., & Hajiah, A. E. (2019). Hygrothermal performance of cool roofs subjected to saudi climates. Frontiers in Energy Research, 7, 39.

Saber, H. H., Maref, W., Swinton, M. C., & St-Onge, C. (2011). Thermal analysis of above-grade wall assembly with low emissivity materials and furred airspace. Building and environment, 46(7), 1403-1414.

Saber, H. H., Swinton, M. C., Kalinger, P., & Paroli, R. M. (2012). Long-term hygrothermal performance of white and black roofs in North American climates. Building and environment, 50, 141-154.

Sargent, R. G. (2010). Verification and validation of simulation models. Dans Proceedings of the 2010 winter simulation conference (pp. 166-183). IEEE.

Sarkar, A., & Bardhan, R. (2020). Improved indoor environment through optimised ventilator and furniture positioning: A case of slum rehabilitation housing, Mumbai, India. Frontiers of Architectural Research, 9(2), 350-369. doi: https://doi.org/10.1016/j.foar.2019.12.001. Retrieved from https://www.sciencedirect.com/science/article/pii/S2095263519300937

Schiavon, S., Hoyt, T., & Piccioli, A. (2014). Web application for thermal comfort visualization and calculation according to ASHRAE Standard 55. Dans Building Simulation (Vol. 7, pp. 321-334). Springer.

Schiffer, H.-W., Kober, T., & Panos, E. (2018). World energy council's global energy scenarios to 2060. Zeitschrift für Energiewirtschaft, 42(2), 91-102.

Schweiker, M. (2016). comf: An R Package for Thermal Comfort Studies. R J., 8(2), 341.

SeppĘnen, O. (2008). Ventilation strategies for good indoor air quality and energy efficiency. International Journal of Ventilation, 6(4), 297-306.

Shen, J., Krietemeyer, B., Bartosh, A., Gao, Z., & Zhang, J. (2021). Green Design Studio: a modular-based approach for high-performance building design. Dans Building Simulation (Vol. 14, pp. 241-268). Springer.

Sherman, M. H., & Dickerhoff, D. J. (1998). Air-tightness of US dwellings. Transactions-American Society of Heating Refrigerating and Air Conditioning Engineers, 104, 1359-1367.

Shirzadi, M., Mirzaei, P. A., & Naghashzadegan, M. (2018). Development of an adaptive discharge coefficient to improve the accuracy of cross-ventilation airflow calculation in building energy simulation tools. Building and environment, 127, 277-290.

Shrestha, P., DeGraw, J. W., Zhang, M., & Liu, X. (2021). Multizonal modeling of SARS-CoV-2 aerosol dispersion in a virtual office building. Building and environment, 206, 108347.

Shrestha, P. M., & DeGraw, J. W. (2021). Air Return Strategies and Airborne SARS-CoV-2. Engineering Challenges and Opportunities: Post COVID-19.

Silva, A. S., & Ghisi, E. (2014). Uncertainty analysis of user behavior and physical parameters in residential building performance simulation. Energy and Buildings, 76, 381-391.

Singh, G., & Das, R. (2021). Energy Saving Assessment of Triple-Hybrid Vapor Absorption Building Cooling System Under Hot-Dry Climate. Dans ASME Power Conference (Vol. 85109, pp. V001T009A005). American Society of Mechanical Engineers.

Smargiassi, A., Baldwin, M., Pilger, C., Dugandzic, R., & Brauer, M. (2005). Small-scale spatial variability of particle concentrations and traffic levels in Montreal: a pilot study. Science of the Total Environment, 338(3), 243-251.

Soebarto, V. I., & Degelman, L. O. (1998). Energy Analysis Software as A Design Tool in Architectural Design Studio Projects.

Sowa, J., & Mijakowski, M. (2020). Humidity-Sensitive, Demand-Controlled Ventilation Applied to Multiunit Residential Building—Performance and Energy Consumption in Dfb Continental Climate. Energies, 13(24), 6669.

Stadler, M., Firestone, R., Curtil, D., & Marnay, C. (2006). On-site generation simulation with energyplus for commercialbuildings. Lawrence Berkeley National Lab.(LBNL), Berkeley, CA (United States).

Stamp, S., Burman, E., Shrubsole, C., Chatzidiakou, L., Mumovic, D., & Davies, M. (2021). Seasonal variations and the influence of ventilation rates on IAQ: A case study of five low-energy London apartments. Indoor and built environment, 1420326X211017175.

The Sustainable Development Goals Report (SDGs) (2016). New York. Retrieved from https://unstats.un.org/sdgs/report/2016/The%20Sustainable%20Development%20Goals%20Report%202016.pdf

Tagliabue, L. C., Cecconi, F. R., Rinaldi, S., & Ciribini, A. L. C. (2021). Data driven indoor air quality prediction in educational facilities based on IoT network. Energy and Buildings, 236, 110782.

Tahmasebinia, F., Jiang, R., Sepasgozar, S., Wei, J., Ding, Y., & Ma, H. (2022). Implementation of BIM Energy Analysis and Monte Carlo Simulation for Estimating Building Energy Performance Based on Regression Approach: A Case Study. Buildings, 12(4), 449. Retrieved from https://www.mdpi.com/2075-5309/12/4/449

Tariku, F. (2008). Whole building heat and moisture analysis (Concordia University).

Tariku, F., Maref, W., Di Lenardo, B., & Gatland, S. (2009). Hygrothermal performance of RH-dependent vapor retarder in Canadian coastal climate. Dans 12th Canadian Conference of Building Science and Technology, Montreal, QC.

Tartarini, F., & Schiavon, S. (2020). pythermalcomfort: A Python package for thermal comfort research. SoftwareX, 12, 100578.

Thörn, Å. (1998). The sick building syndrome: a diagnostic dilemma. Social science & medicine, 47(9), 1307-1312.

Tian, X., Fine, J., & Touchie, M. (2020). Analysis of alternative ventilation strategies for existing multi-family buildings using CONTAM simulation software. Dans E3S Web of Conferences (Vol. 172, pp. 09004). EDP Sciences.

Travers, M. J., Higbee, C., & Hyland, A. (2007). Vancouver island outdoor smoking area air monitoring study 2007. Buffalo, New York: Roswell Park Cancer Institute.

Trofimova, P., Cheshmehzangi, A., Deng, W., & Hancock, C. (2021). Post-occupancy evaluation of indoor air quality and thermal performance in a zero carbon building. Sustainability, 13(2), 667.

Tuomaala, P. (1993). New building air flow simulation model: Theoretical basis. Building Services Engineering Research and Technology, 14(4), 151-157.

Underhill, L. J., Dols, W. S., Lee, S. K., Fabian, M. P., & Levy, J. I. (2020). Quantifying the impact of housing interventions on indoor air quality and energy consumption using coupled simulation models. Journal of exposure science & environmental epidemiology, 30(3), 436-447.

U.S. Department of Energy. (2021). EnergyPlus™ Version 9.5.0 Documentation, Engineering Reference. Retrieved from EnergyPlus Essentials

Vancouver, British Columbia Climate & Temperature. (2021). Retrieved from http://www.vancouver.climatemps.com/index.php

Vyas, Y., Johns, D., Richman, R., & Liao, Z. (2023). Developing a novel 1D-HAM numerical modelling tool for assessing the hygrothermal properties of cross-laminated timber (CLT) including adhesive layers. Dans Canadian Society of Civil Engineering Annual Conference (pp. 429-442). Springer.

Walker, I., Clark, J., Less, B., Dutton, S., Li, X., & Sherman, M. (2021). Energy Savings Estimates for Occupancy-and Temperature-based Smart Ventilation Control Approaches in Single-family California Homes.

Walker, I., Less, B., Lorenzetti, D., & Sohn, M. (2021). Development of advanced smart ventilation controls for residential applications. Energies, 14(17), 5257.

Walker, R., Hayes, S., & White, M. (1996). How effective is natural ventilation? A study of local mean age of air by modelling and measurement. Dans DOCUMENT-AIR INFILTRATION CENTRE AIC PROC (pp. 27-40).

Wallace, L. A., Emmerich, S. J., & Howard-Reed, C. (2004). Source strengths of ultrafine and fine particles due to cooking with a gas stove. Environmental Science & Technology, 38(8), 2304-2311.

Walton, G., & Dols, W. S. (2006). CONTAM 2.4 user guide and program documentation.

Walton, G. N. (1989). Airflow network models for element based building airflow modeling. ASHRAE Transactions, 95(2), 611-620.

Wang, L., Defo, M., Xiao, Z., Ge, H., & Lacasse, M. A. (2021). Stochastic Simulation of Mold Growth Performance of Wood-Frame Building Envelopes under Climate Change: Risk Assessment and Error Estimation. Buildings, 11(8), 333.

Wang, L., & Wong, N. H. (2008). Coupled simulations for naturally ventilated residential buildings. Automation in Construction, 17(4), 386-398.

Wang, L. L., & Chen, Q. (2008). Evaluation of some assumptions used in multizone airflow network models. Building and environment, 43(10), 1671-1677.

Wang, L. L., Dols, W. S., & Chen, Q. (2010). An Introduction to the CFD Capabilities in CONTAM 3.0. Proceedings of SimBuild, 4(1), 490-496.

Wang, X., Feng, W., Cai, W., Ren, H., Ding, C., & Zhou, N. (2019). Do residential building energy efficiency standards reduce energy consumption in China?–A data-driven method to validate the actual performance of building energy efficiency standards. Energy policy, 131, 82-98.

Wieprzkowicz, A., Heim, D., & Knera, D. (2022). Coupled Model of Heat and Power Flow in Unventilated PV/PCM Wall-Validation in a Component Scale. Applied Sciences, 12(15), 7764. Retrieved from https://www.mdpi.com/2076-3417/12/15/7764

Winkler, J., Munk, J., & Woods, J. (2018). Effect of occupant behavior and air-conditioner controls on humidity in typical and high-efficiency homes. Energy and Buildings, 165, 364-378.

Wolkoff, P. (2018). Indoor air humidity, air quality, and health–An overview. International journal of hygiene and environmental health, 221(3), 376-390.

Woloszyn, M., Kalamees, T., Abadie, M. O., Steeman, M., & Kalagasidis, A. S. (2009). The effect of combining a relative-humidity-sensitive ventilation system with the moisture-buffering capacity of materials on indoor climate and energy efficiency of buildings. Building and environment, 44(3), 515-524.

WUFI® Plus (Version Ver.3.2.0.1). (2021). Germany: Fraunhofer Institute for building physics.

Xing, Y., Hewitt, N., & Griffiths, P. (2011). Zero carbon buildings refurbishment—A Hierarchical pathway. Renewable and Sustainable Energy Reviews, 15(6), 3229-3236. doi: https://doi.org/10.1016/j.rser.2011.04.020. Retrieved from https://www.sciencedirect.com/science/article/pii/S1364032111001572

Yaşar, Y., & Kalfa, S. M. (2012). The effects of window alternatives on energy efficiency and building economy in high-rise residential buildings in moderate to humid climates. Energy conversion and management, 64, 170-181.

Yu, J., Kang, Y., & Zhai, Z. J. (2020). Advances in research for underground buildings: Energy, thermal comfort and indoor air quality. Energy and Buildings, 215, 109916.

Zender–Swiercz, E. (2021). Assessment of Indoor Air Parameters in Building Equipped with Decentralised Façade Ventilation Device. Energies 2021, 14, 1176: s Note: MDPI stays neutral with regard to jurisdictional claims in published ….

Zhang, F., de Dear, R., & Hancock, P. (2019). Effects of moderate thermal environments on cognitive performance: A multidisciplinary review. Applied Energy, 236, 760-777.

Zhang, J. (2020). Research on building energy efficiency based on energyplus software. Dans IOP Conference Series: Earth and Environmental Science (Vol. 432, pp. 012013). IOP Publishing.

Zhang, J., Bai, Z., Chang, V. W., & Ding, X. (2011). Balancing BEC and IAQ in civil buildings during rapid urbanization in China: Regulation, interplay and collaboration. Energy policy, 39(10), 5778-5790.

Zhang, Y., Diao, R., Lei, X., Wang, Z., & Zheng, Y. (2021). Research on improving the effectiveness of building energy saving by enclosure structure. Dans Second IYSF Academic Symposium on Artificial Intelligence and Computer Engineering (Vol. 12079, pp. 711-718). SPIE.

Zhongming, Z., Wangqiang, Z., & Wei, L. (2018). Market Report Series: Energy Efficiency 2018.

Zhou, N., Khanna, N., Feng, W., Ke, J., & Levine, M. (2018). Scenarios of energy efficiency and CO 2 emissions reduction potential in the buildings sector in China to year 2050. Nature energy, 3(11), 978-984.

Zhu, Y. (2006). Applying computer-based simulation to energy auditing: A case study. Energy and Buildings, 38(5), 421-428.

Zu, K., Qin, M., Rode, C., & Libralato, M. (2020). Development of a moisture buffer value model (MBM) for indoor moisture prediction. Applied Thermal Engineering, 171, 115096.